Silica and boron nitride supported molybdenum and vanadium oxide catalysts for alkane oxidation.

PhD Thesis

Mr Ashleigh J.J. Pollard BSc. (Hons)

Chemistry Department

Cardiff University

ProQuest LLC
789 East Eisenhower Parkway
P.O. Box 1346
Ann Arbor, MI 48106-1346

Summary

A range of silica supported molybdenum catalysts and vanadium catalysts have been prepared and tested for alkane oxidation. Further vanadium catalysts supported on boron nitride have also been prepared and tested for alkane oxidation. The silica supported molybdenum oxide catalysts demonstrated appreciable activity for propane total oxidation to carbon oxides with some trace acrolein. The silica supported vanadium catalysts were also active for propane oxidation, and although the major product was carbon dioxide, higher selectivity to acrolein was observed when compared to the silica supported molybdenum catalysts. The use of boron nitride as a support significantly increased the selectivity towards acrolein and other selective oxidation products like acrylic acid. These results lead to the catalysts being tested for propene oxidation, which produced similar results that showed the boron nitride supported vanadium catalysts were more selective than the silica supported catalysts for acrolein. Further tests were carried out on methane and ethane, which produced mostly carbon oxides as a result. The effect of co-feeding water was also tested when performing propane oxidation with the presence of water effecting the selectivity and activity of the catalysts. Some catalyst's activity was suppressed with increased selectivity to acrolein and other catalysts activity was promoted which led to total oxidation to carbon oxides. This study aim is to compare and contrast the different catalysts produced and give evidence about how the use and development of a hydrophobic support may lead to better catalyst design in the future.

Abstract

The direct selective oxidation of alkanes by heterogeneous catalysts to commercially viable products has been researched for many years. Most work has centred on the difficult transformation from methane into methanol and formaldehyde. Two of the most studied systems have been molybdenum and vanadium oxides supported on silica. This study has focused on and investigated the oxidation of propane with molecular oxygen using silica supported molybdenum oxide and vanadium catalysts. Acrolein was the major selective oxidative product seen with CO_2 being the most predominant product of all. Further catalysts have been developed using vanadium oxide, which was found to be more selective than the molybdenum oxide catalysts, that were supported on boron nitride giving much improved selectivities to oxygenates, in particular acrolein and improved conversions when comparing them to their silica supported counterparts. These catalysts were also tested for the effect of co-feeding water when oxidising propane giving some interesting differences when comparing the activation and selectivities of the two different conditions. From the results obtained during propane oxidation, propene was also studied in depth to try and help understand the mechanism of the reaction. Two further alkanes have been studied, methane and ethane but these mainly gave combustion products. Catalysts have been characterised by a range of techniques including BET, powder XRD, Raman and TPR and these will be presented and discussed. Further characterisation was carried out using *in situ* Raman on molybdenum oxide systems, with and without the presence of water, which will also be presented. In this study the catalytic results obtained will be discussed, and the comparison and differences between the two different supported systems will be investigated giving evidence how using a hydrophobic support may lead to better catalyst design in the future.

Abstract (micro)

This study investigated the oxidation of propane with molecular oxygen using silica supported molybdenum and vanadium catalysts. Acrolein was the major selective oxidative product seen, with CO_2 being the most predominant product of all. Further catalysts have been developed using vanadium supported on boron nitride which gave much improved selectivities to oxygenates, in particular acrolein and improved conversions when comparing them to their silica supported counterparts. The catalysts were also tested for the effect of co-feeding water with the reactants when oxidising propane, giving some interesting differences when comparing the activation and selectivities of the two different conditions. Propene was also studied in depth to try and help understand the mechanism of propane oxidation as well as methane and ethane as a comparison to other alkanes. The catalysts developed have been characterised using a wide range of techniques. This study aims to compare and contrast the different catalysts produced and give evidence about how the use and development of a hydrophobic support may lead to better catalyst design in the future.

Acknowledgements

I would like to thank my supervisor Dr. Stuart H. Taylor for showing faith in me at the beginning of these 3 years and for the continuous support, advice and helpful knowledge that you have given me.

Thanks to my Mum, Dad, sister Sarah, Nan, Grandad and Keiron for their continued love and support over my last 8 or so years here in Cardiff and especially at times in a financial way. I know I would have not got through the undergraduate days let alone postgraduate without you.

Thank you to all the people I have become friends with from the GJH catalysis group and to those who have helped me over the 3 years. Special mention to Charles (who put up living with me for 5 years), Tanner, Dave, Mike, Trev, Mel, Luisa, Toni, John, Owain and Chris J. Extra special thanks to Mary-Lou who took time out to teach me in the beginning how to use the funny looking machines you'll read about in chapter 3.

Thank you to all the friends I have made over the past 8 years in my time at Cardiff. From chemistry, Bitch, Simon, Dee, fat John, Will and Chris C. along with a whole host of others from students, staff and technicians from the department over the years. From uni and normal life I would like to thank Anna, Clare, Jo, Big Si, Amanda and Al and Eoin. Finally a big hello and thanks to all my friends from The George pub I have made in the 2 and a half years I have spent working and occasionally socialising there. Special mention to Mikey who's made the time knowing him an experience. Clare, Jo Jo, James G, James I, Mills, Steve to name a few staff. Hello to the other staff (sorry) and to the locals especially Clive in the night and Andrew in the day.

Thank you to anyone else who believes that they have been missed out, I apologise but I am limited by space. Let me know and I will tell you if it was a mistake.

The final thank you is for Magdalena, my girlfriend who has been by my side through the last 2 years and has helped me out in so many obvious ways and many more that I probably don't realise. I love you loads and look forward to spending the rest of my life with you. I would like to tell you I love in German but Entschuldigung, aber mein, Deutsch ist nicht sehr gut.

Abbreviations

AMH = Ammonium hetpamolybdate

AMV = Ammonium metavandadate

V_{acac} = Vanadyl acetylacetonate

BN = Boron nitride

GHSV = Gas Hourly Space Velocity

GC = Gas chromatograph

TCD = Thermal Conductivity Detector

FID = Flame Ionisation Detector

HC = Hydrocarbon

BET = Brunauer Emmett Teller

XRD = X-ray diffraction

TPR = Temperature programmed reduction

TPO = Temperature programmed oxidation

SEM = Scanning Electron microscopy

M.S. = Mass spectrometer

Silica and boron nitride supported molybdenum and vanadium oxide catalysts for alkane oxidation

Chapter 1: Introduction.

Chapter 2: Experimental.

Chapter 3: Characterisation of catalysts.

Chapter 4: Silica and boron nitride supported molybdenum and vanadium oxide catalysts for propane and propene oxidation.

Chapter 5: Silica and boron nitride supported molybdenum and vanadium oxide catalysts for propane oxidation with and without the presence of water.

Chapter 6: Silica and boron nitride supported molybdenum and vanadium oxide catalysts for methane and ethane oxidation.

Chapter 1: Introduction.

1.1: What is catalysis?

As early as the nineteenth century it was noticed that some chemical reactions were affected by trace amounts of substances that were not consumed in the reaction. The first attempt to define this phenomenon was made in 1836 by J. J. Berzelius who wrote:

"I shall therefore call it the *catalytic power* of substances, and the decomposition by means of this power *catalysis*, just as we use the word analysis to denote the separation of the component parts of bodies by means of ordinary chemical forces. Catalytic power actually means that substances are able to awake affinities which are asleep at this temperature by their mere presence and not by their own affinity."

The word catalysis comes from *cata* meaning down and *lysein* meaning break or split in Greek, i.e. catalysts break down the forces which inhibit the reaction of molecules. Today's definition is a *catalyst is a substance that increases the rate at which a chemical system approaches equilibrium, without being consumed in the process.* [1]

1.2: Basic principles of catalysis

The main effect a catalyst has on a chemical reaction is to increase its rate i.e. to increase the rate coefficient. This can be looked at in two ways:

1.2.1: Collision theory

In collision theory the rate coefficient k is shown as:

$$k = PZ \exp(-E / RT)$$

Where P is the steric factor, Z the collision frequency, E is the activation energy, R the gas constant and T the temperature.

For a simple molecular transformation ($A \rightarrow B$) where the slow step is the adsorption of the reactant, the collision frequency is the number of collisions between reactant molecules and the catalytic sites per unit time. The number of catalytic sites will be smaller so the number of relevant collisions will be much smaller (by a factor of 10^{12}) than the number of collisions between reactants only. This figure is relevant to the uncatalysed reaction but irrelevant to the catalysed reaction. For the catalysed reaction to compete its exponential term must be 10^{12} times larger which means its activation energy must be about 65 kJ mol^{-1} less. This only makes the two equal so for a catalysed reaction to be efficient an activation energy around 100 kJ mol^{-1} less is required.

1.2.2: Absolute rate theory

In absolute rate theory the rate coefficient is shown as:

$$k = \kappa T / h * \exp(-\Delta G^{\neq} / RT)$$

Where K is the Boltzmann constant, $\Delta G^{\neq}$ is Gibbs free energy of activation and h is Planck's constant. The catalyst decreases the free energy of activation that is made up of entropy and an enthalpy of activation. In a catalysed reaction the entropy is lower due loss of translational freedom as the reactant is immobilised on the catalyst surface. This means there must be a decrease in enthalpy of activation or more so to make the catalyst efficient.

So for both theories a decrease in the activation energy is required for the catalysed reaction when compared to the uncatalysed reaction.

1.3: Catalysis and thermodynamics

For all reactions the laws of thermodynamics require that the position of equilibrium attained is the same whether a catalyst is present or not. There cannot be two different positions of equilibrium giving two different free energy changes coexisting when you compare a reaction in the presence and without a catalyst. Thermodynamics is the difference between the initial and final states and not whether a catalyst was used to make the change happen. Another important aspect is that a catalyst can only increase the rate of a reaction that is thermodynamically feasible not one that would be impossible with or without the presence of the catalyst. In this study the reaction of propane or propene to oxidative products like acetone and acrolein as well as greater oxidation products like CO and CO_2 are all thermodynamically feasible. All of this means that a catalysed reaction proceeds by a new and more energetically favourable pathway.

1.4: Types of catalysis

The same rules apply for all forms of catalysis. There are two main types of catalytic systems:

- 1: Homogeneous catalysis. The catalyst is of the same phase as the reactants, i.e. both are in the gas phase or both are in the liquid phase.

- 2: Heterogeneous catalysis. Here a phase boundary separates the catalyst from the reactants. This leads to a number of possibilities of combinations of gas, liquid and solid phases.

This study uses heterogeneous catalysis where reactant gas molecules (e.g. propane and oxygen) are passed over solid catalysts, e.g. MoO_3/ SiO_2.

This leads to the question why are we trying to selectively oxidise alkanes and alkenes with molecular oxygen or other known oxidants like ozone and nitrous oxide over metal oxide catalysts.

1.5: The petrochemical industry

In the modern petrochemical industry a great deal of products are derived from crude oil, which has replaced the use of coal since World War 2 due to the easier way it can be transformed into more useful products. Crude oil first undergoes separated into a

volatile fraction and a non-volatile 'residual oil'. The volatile section is fractionally distilled giving the following fractions in order of volatility: (1) C_1-C_4 hydrocarbons, (2) light gasoline, (3) heavy gasoline or naphtha, (4) kerosene, and (5) light gas oil. These intermediates can undergo steam cracking and reforming to give a wide range of products like light alkenes such as ethene and propene, which can be turned into more useful products like plastics and chemicals. The lighter fraction (1) is used as fuels for cars and aircraft with the heavier fraction (5) used as lubricating oils and greases. There are some very important industrial reactions for alkenes and alkanes and fig 1.5 shows some of the important reactions that involve propene into more beneficial products.

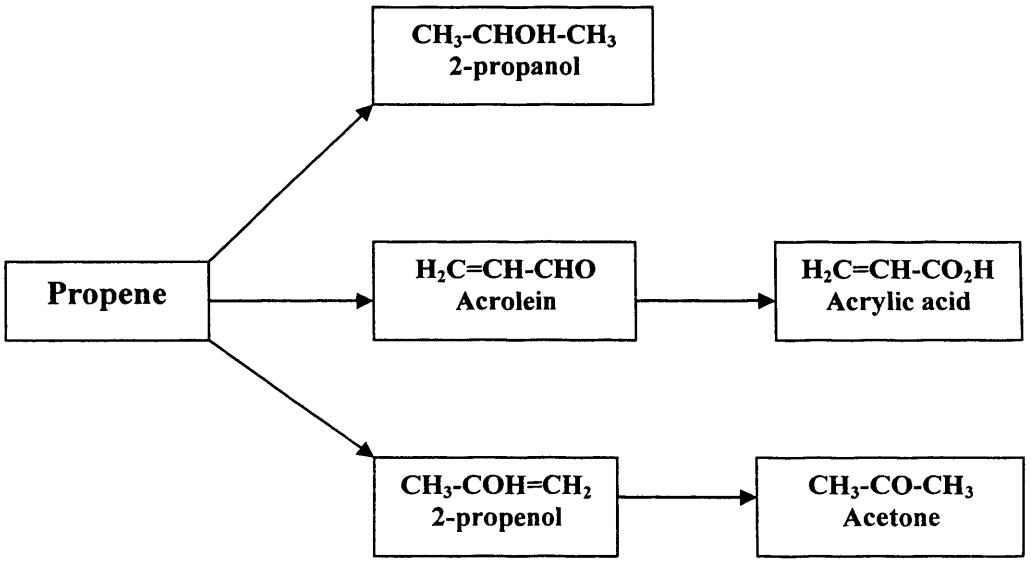

Fig. 1.5: Some important reactions of propene performed in industry [2].

The direct conversion of light alkanes and alkenes into useful oxygenated products has been the subject of extensive research for many years. The development of

catalysts to do this cheaply and efficiently by heterogeneous catalysis would be a major benefit to the world. This is especially so for alkanes as the only worldwide industry process used today generally is the cyclic conversion of n-butane to maleic anhydride using a vanadium, phosphorus and oxygen (VPO) catalyst. One of the biggest areas of research has centred on the conversion of natural gas (mainly CH_4) into methanol and this has involved research into a wide variety of catalysts and conditions covered later in this chapter. One reason for the interest is that natural gas is widely available all over the world and its current main uses are in the synthesis of ammonia and methanol. The methanol synthesis is not a direct conversion via heterogeneous catalysis and is produced by steam reforming of methane shown in figure 1.5.1.

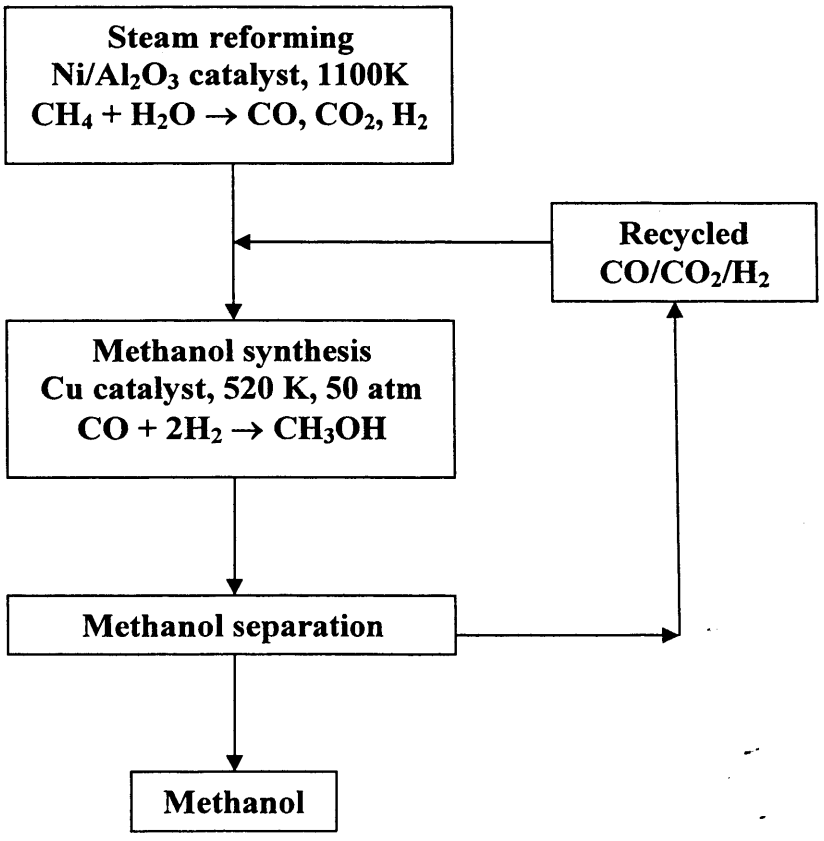

Fig. 1.5.1: The process involved when steam reforming natural gas to methanol [2].

In this process the gas is heated to high temperatures and is passed through a reactor containing a nickel supported on alumina catalyst. This is heated to over 1000 K by burning gas on the outside of the reactor tube. The resulting reaction is the oxidation of methane by steam to give primarily CO and H_2. Further oxidation reactions also take place to produce CO_2 as the major product in this entire process. The presence of CO_2 does yield further H_2 and this is known as the gas shift reaction and is shown in equation 1.5.

$$CO + H_2O \rightleftharpoons CO_2 + H_2$$

Equation 1.5: Water gas shift reaction.

Much research has been carried out to develop a catalyst that would convert methane to methanol in a single step process. The research aims to lower the high temperatures and pressures required and to make the methanol the most selective product. This process if successful could lower the production costs of making methanol, which is an important chemical and used worldwide, if a suitable catalyst could be developed. This can be extended to a much greater range of selectively oxygenated products that could be produced from longer alkanes that a catalyst reaction would give cheaply and efficiently.

1.6: This study

Most research carried out on alkanes in the previous years has centred on the conversion of methane to methanol and to a lesser extent formaldehyde via

heterogeneous catalysis trying to selectively oxidise the alkane. This study aims to continue this research but expand to include ethane and propane as there is not a great deal of literature available concerning the research of these alkanes. By doing this it could be hoped to investigate the differences in alkane chain length and the various C-H bonds which show the potential for selective oxidation. The objective would be to compare the primary and secondary carbons present probing the regio-selectivity of the different alkanes and their thermodynamically feasible oxygenated products. This will be extended to propene due to the greater amount of research carried out upon it. Theses studies will involve microreactor testing and full characterisation of the catalysts produced.

Early research involved the use of methane and the identification of suitable catalysts for the oxidation process. This work led on to the frequent study into the use of molybdenum and vanadium oxides as catalysts, although it was discovered that a variety of oxide catalysts were potential candidates for these reactions. Further study into the chemistry behind the reaction mechanism of methane took place and the work suggested that this involved the rapid formation of gas-phase methyl radicals via the interaction of methane with the oxide surface as well as activated oxygen on the surface also being involved. It is known at present that heterogeneous catalysis reactions involving methane are dominated by gas phase chemistry of the methyl radical and that butane is principally a surface process. It is suspected that both ethane and propane could be a mixture of gas phase and surface phase for their respective oxidative processes, but this will be looked at further both experimentally and theoretically.

The aim of the study will be centred on the conversion of these light alkanes to their respective oxidative products, the nature of the reaction, intrinsically looking mechanisms and the appropriate phases involved. The majority of the work carried out will be on propane as there are few studies concentrating on this alkane as most work has centred on methane. This will be expanded to include propene, which might give us an idea about the chemistry involved in the oxidation of propane as acrolein, the propene aldehyde, is often seen as one of the major partial oxidation product in propane studies. The study will concentrate less on methane because it has been already widely studied and will also include ethane oxidation.

1.7: Literature review

1.7.1: Early work.

The partial oxidation of methane has attracted varying amounts of interest over the past years. At the beginning of the century one of the first patents was awarded in 1905 to Lance and Elworthy [3] who claimed that by oxidising methane with hydrogen peroxide in the presence of ferrous sulphate, that methanol, formaldehyde and formic acid were produced. More work followed over the next few years mainly focusing on the study of high-pressure combustion systems for methane with the onset of these high pressures systems producing the first detection of methanol as either a reaction intermediate or as a final product was discovered. These though were non-catalysed reactions and probably occurred by a radical chain mechanism involving the reactor walls. As these temperatures were increased the reaction went more characteristic of a homogeneous reaction.

Experimental work by Wiezevitch and Frolich [4] showed that various mixtures of natural gas up to 99% methane could be oxidised at elevated pressure when in contact with catalytic surfaces. Following this Boomer and Broughton [5] carried out experiments using oxygen and natural gas mixtures of around 7.3 to 7.5% oxygen. Their results identified some important factors. Firstly the yield of methanol was found to be high when the concentration of the oxygen was kept low. Increasing the flow rates increased the yield of useful products but had little effect on the conversion of carbon. An increase in pressure caused the increase in the conversion of natural gas to the various products.

1.7.2: Catalyst design.

Dowden et al. used the selective oxidation of methane to formaldehyde as a case study in catalyst design [6] stating that the functions of the catalyst were dehydrogenation and oxygen insertion aswell as a hydration function to suppress total oxidation to unfavourable products. A scheme was suggested in figure 1.7.2.1 that in order to prevent total oxidation, the dehydrogenation of intermediate methyl or methylene groups should be suppressed with respect to their migration. The formation of intermediate methyl groups is preferential over methylene, which would be more firmly bound to the surface so more susceptible to further dehydrogenation. This indicated that an oxide was preferable to a metal catalyst preventing methylene formation. It was also stated that the surface to methyl bond should be made weaker than the surface to oxygen bond to favour methyl migration so its rate can compete

with that of the reaction of the groups with gas-phase oxygen. From this it was proposed that a relatively weak dehydrogenation function be required (to possess d^0, d^1, d^5, d^{10} or possibly d^4 configuration) in conjunction with an n-type oxide oxygen insertion function (V_2O_5 and MoO_3 as examples). They also suggested that the catalyst should consist of only one crystallographic phase to allow rapid migration of reaction intermediates. To prevent over oxidation of the product, it was proposed that a hydration function, which would increase the production of methanol relative to formaldehyde, should be incorporated into the catalyst. This would generate a methylene diol which was stated to be resistant to oxidation by one electron oxidants in aqueous solution with V^{5+} and Mo^{6+} recommended for oxygen insertion and V^{5+} recommended for dehydrogenation.

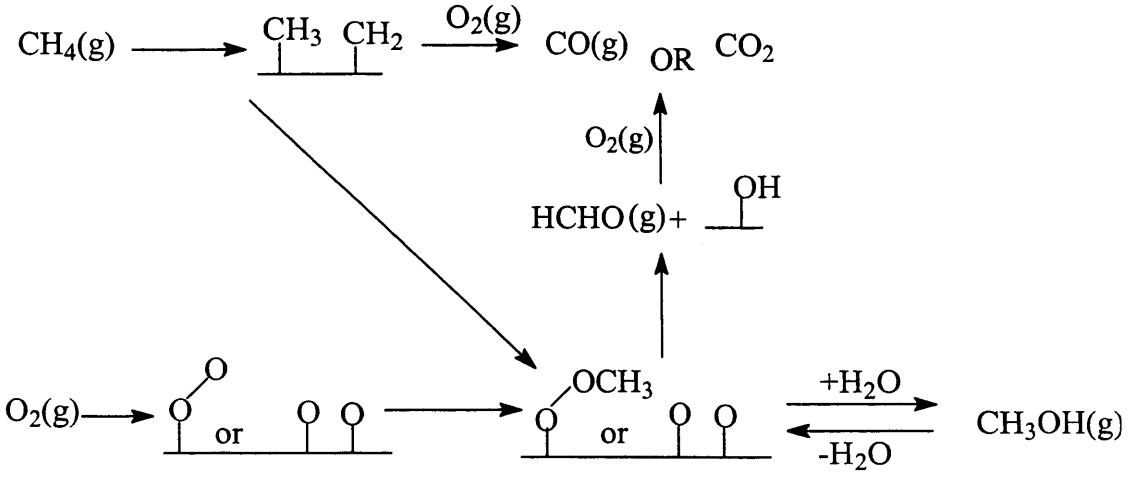

Figure 1.7.2.1: Surface scheme for the design of methane oxidation catalysts [6]

Talyor et al. [7] aimed to identify the types of materials over which methanol possesses the required degree of stability, instead of going to combustion after the harsh conditions are required to activate it. This differed from a lot of studies that

centred on the conversion of methane to formaldehyde, not the stability of methanol. A wide range of oxides were used, 33 in total with a gas stream containing methanol, oxygen and helium to dilute. Nb_2O_5, Ta_2O_5 and WO_3 gave high selectivity to oxygenated products at all levels of methanol conversion. These products were dimethyl ether and formaldehyde. At lower temperatures dimethyl ether was the main product but with increasing temperature increased the selectivity of formaldehyde and carbon oxides.

When comparing the oxides of V_2O_5, Nb_2O_5 and Ta_2O_5 they are closely related in the periodic table and would be expected to behave in a similar way. Vanadium oxide gave a different result with a high selectivity to HCHO only at low levels of conversion when compared to the other oxides which gave high selectivity to oxygenated products at all levels of methanol conversion. MoO_3 showed a methanol conversion from zero at 300°C to around 90% at 500°C. Methanol was exceptionally stable over Sb_2O_3 with the conversion being extremely low throughout the temperature range investigated. Between 250-400°C dimethyl ether was the exclusive product with its selectivity decreasing above 450°C and reached zero at 500°C. Above 450°C HCHO was produced with some selectivity to carbon monoxide noted above 500°C.

It was found that conversion was best over WO_3 lying in the range of 90-100% between 400-500°C. The yield of carbon oxides for MoO_3 was zero below 400°C increasing to 0.5% at 450°C and 2.5% at 500°C. The others all had higher carbon oxide yields. The stability of the product was identified as a major problem when looking at the partial oxidation of methane to methanol. The study concluded that only on Sb_2O_3 was methanol stable with other materials showing some stability for

HCHO and dimethyl ether with MoO_3 showing particularly good stability for HCHO. Work carried out on a 5% Mo catalyst showed similar results as bulk MoO_3 for methanol oxidation. The group concluded whether HCHO is formed via a methanol intermediate from sequential oxidation or via a direct route. It was generally seen that any methanol made from the oxidation of methane would be rapidly converted before diffusing out of the catalyst bed. It was proposed that contact times may be of value or the addition of water could be employed to preserve methanol by quenching gas-phase reactions.

1.7.3: Reaction kinetics and mechanism.

Khan and Somorjai [8] reproduced the results of Liu et al's [36] who proposed a reaction scheme for methane oxidation using N_2O as the oxidant but Khan's examination of the kinetics showed some important differences. They were able to specify rate equations for both the formation of methanol and formaldehyde. For methanol it was found the rate of formation was approximately first order with respect to methane and water and zero order with respect to nitrous oxide. For formaldehyde the kinetic rates were found to be zero order with respect to all reactants. This showed that methanol and formaldehyde were formed simultaneously from the same intermediate by two independent pathways. Above 540°C the activation energies for methanol and formaldehyde can be seen as almost identical, this implies that the formation of formaldehyde is by the sequential oxidation of methanol.

A study by Banares et al. [9] using $^{18}O_2$ isotope tracer techniques suggested that oxygen in the formaldehyde molecule originated from lattice oxygen of the support. It was also suggested that reoxidation of the catalyst took place via a Mars-van Krevelen mechanism. But another study by Mauti and Mims [10] employing isotope exchange and steady-state oxygen isotope transient techniques concluded that due to the substantial and rapid exchange of oxygen between products and the catalyst that no information could be found about how the mechanism proceeds. They discovered that HCHO was a stable product even after participating in this multiple exchange process. It was proposed in figure 1.7.3.1 that the exchange might take place via the terminal Mo=O site forming an irreversible acetal species but it is clear that exchange is due to the molybdenum phase which utilises lattice oxygen from the support.

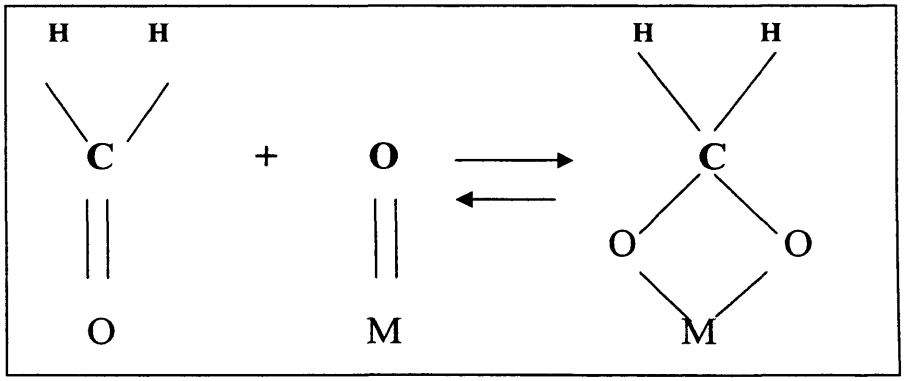

Figure 1.7.3.1: Surface acetal formation on MoO_3 based catalyst [10]

Information on the mechanism of the reaction was carried out by Kartheuser et al. [11] using a transient kinetics temporal analysis of products (TAP) reactor. It was shown that oxygen interacted with the catalyst to produce a species with active lifetimes between 5-60 seconds. The interaction of methane with the surface was very

weak, exhibiting short lifetimes and the surface oxygen species activated the methane molecule. From here the radicals reacted with the catalyst extracting lattice oxygen, which was then incorporated into the formaldehyde molecule shown by the following scheme:

$$CH_4 + O^-_{n(ads)} \rightarrow CH_3\cdot + OH(s)$$

$$CH_3\cdot + {}^{16}O_{(latt)} \rightarrow CH^{16}OH + H\cdot$$

1.7.4: Silica as a support.

Silica has been the most widely studied support. Various silicas have been looked at and there contribution to catalyst activity. Kastanas et al. [12] reported the production of formaldehyde, C_2, CO and CO_2 in the presence of a range of silica compounds including silicic acid, Cab-O-Sil and Ludox silica gel using oxygen at elevated pressures. Here it was suggested that formaldehyde production was a gas phase process because the activation energy of its formation was independent of the catalyst used.

Parmaliana et al. [13] emphasised the role of silica in selective oxidation. Using a batch reactor with external recycle they compared the activities of various silicas. Results showed that as well as the preparation method, the pre-treatment conditions and sodium content exerted an influence on catalytic performance. Silicas prepared by precipitation were found to be the most active, with extrusion or sol gel being intermediate and fumed silicas being the least active. The addition of sodium to

levels higher than normally found in silica was found to have negative effects, whilst acid washing to remove the sodium didn't enhance performance. The group drew attention to the importance of considering the background activity of silica for supported catalysts. Vanadium oxide catalysts enhanced the activity of both fumed and precipitated silicas whilst molybdenum oxide only enhanced fumed and decreased the activity of the precipitated. In a temperature programmed reaction the temperature for the onset of formaldehyde production was significantly lower for SiO_2 than for supported MoO_3. Vanadium oxide though was observed to reduce the onset temperature and increase the quantity of formaldehyde produced up to 650°C compared to bare silica.

An investigation into the reaction mechanism of formaldehyde formation over silica catalysts in the range of 630-780°C temperature range by Sun et al. [14] proposed that HCHO is formed by a surface reaction rather than gas-phase radical reactions. Both formaldehyde and C_2 hydrocarbons were primary products both having different reaction pathways due to the apparent activation energies determined for total methane conversion. The mechanism they proposed in Figure 1.7.4.1 suggested that methane dissociates on a siloxane bridge and is chemisorbed as two possible intermediates, one of which decomposes to generate formaldehyde, whilst the other releases methyl radicals which couple in the gas phase to form ethane.

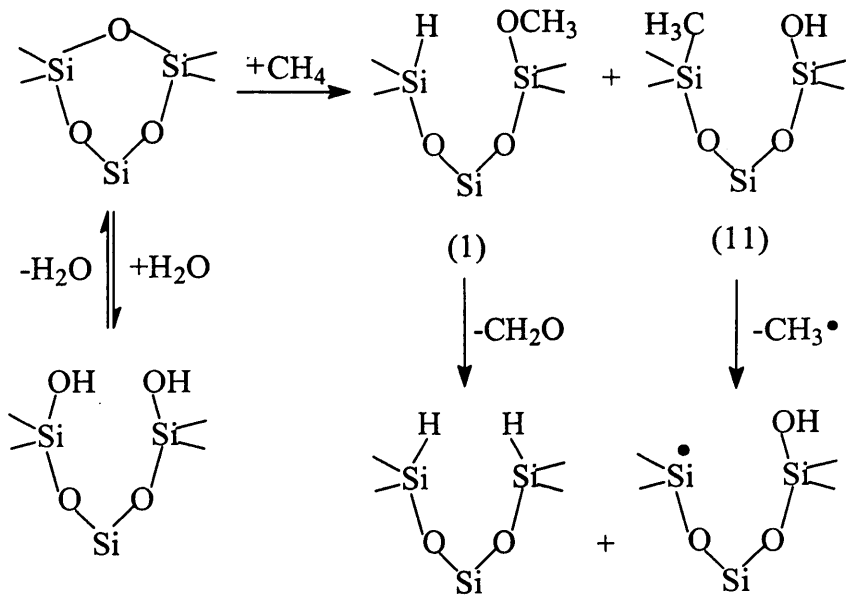

Figure 1.7.4.1: Schematic mechanism for methane oxidation over SiO_2 catalyst [14]

Parmaliana et al. [15] in another paper looked at the nature of active sites of silica based oxide catalysts for methane partial oxidation to formaldehyde. They analysed three distinct theoretical models proposed to describe the working mechanism of the catalysts:

- 1:) Langmuir-Hinshelwood model or concerted mechanism.
- 2:) Mars-van Krevelen model or redox mechanism
- 3:) Heterogeneous-homogeneous model or surface assisted gas-phase reaction mechanism.

Using pulse reaction tests in the presence or absence of O_2 they discovered that the oxidation reaction proceeds in the presence of gas-phase oxygen with only a small amount of reaction product being detected in the absence of gas-phase oxygen at the highest temperature on V_2O_5/SiO_2 catalyst. As the reaction rates in the mixture of

reactant and in separate steps differ this data excludes the participation of lattice oxygen in the partial oxidation of methane via a two step redox mechanism as the main reaction pathway proving the occurrence of a concerted mechanism. They stated that O_2 in the gas-phase is more active than lattice O_2 ions ($O^{2-}_{(l)}$) are involved in the reaction. These active species are made with gas-phase O_2 interacting with the reduced sites of the catalyst surface. The number of specific reduced sites having the capability to activate gas-phase O_2 and stabilise surface active O_2 species $(O)_s^*$ governs the catalytic behaviour of silica supported oxide catalysts in methane partial oxidation.

The statement was supported by the straight correlation between density of reduced sites and STY_{HCHO} of different supported oxide catalysts. They then went on to examine the activation of the hydrocarbon molecule with this occurring on acidic sites of the oxide surface. Although the acidic properties differ for MoO_3 and V_2O_5 it was argued that for all catalysts with a suitable extent of CH_4 activation a change in the acidity doesn't have any effect on catalyst activity. A reaction pathway was proposed in figure 1.7.4.2 where P refers to products of HCHO and CO_2 and L and RS represent the specific centres for CH_4 activation and reduced sites for oxygen.

$$CH_4 + (CH_4)_S^* + (O)_S \longrightarrow (P)_S^* \longrightarrow P + L + RS$$

$$\uparrow$$

$$RS + O_{2(g)} \text{ or } O_{2(s)}$$

Figure 1.7.4.2: Reaction pathway for the partial oxidation of methane. [15]

1.7.5: Supported MoO_3 catalysts.

Work was carried out by Spencer [16] looking at the partial oxidation of methane using molecular oxygen over a MoO_3/silica supported catalyst. The major products of this were HCHO, CO and CO_2 with only trace amounts of CH_3OH and H_2. At low conversions HCHO was produced with a selectivity of 71% with the best catalyst being MoO_3 Cab-O-Sil prepared by physical milling of the components with catalysts prepared by impregnation active but less selective. Also looked at were the effects of impurities, which showed that sodium levels as low as 300 ppm had an effect of the conversion and selectivity.

Spencer et al. later showed by kinetic analysis [17] that sodium lowers the direct oxidation of CH_4 to HCHO and CO_2 whilst promoting the further oxidation of HCHO to CO. A reaction pathway was proposed in figure 1.7.5.1 showing that the initial CH_4 activation took place on a Mo-O_3 species generated thermally at the temperature of the reaction as Mo(V) is important in several steps of the mechanism.

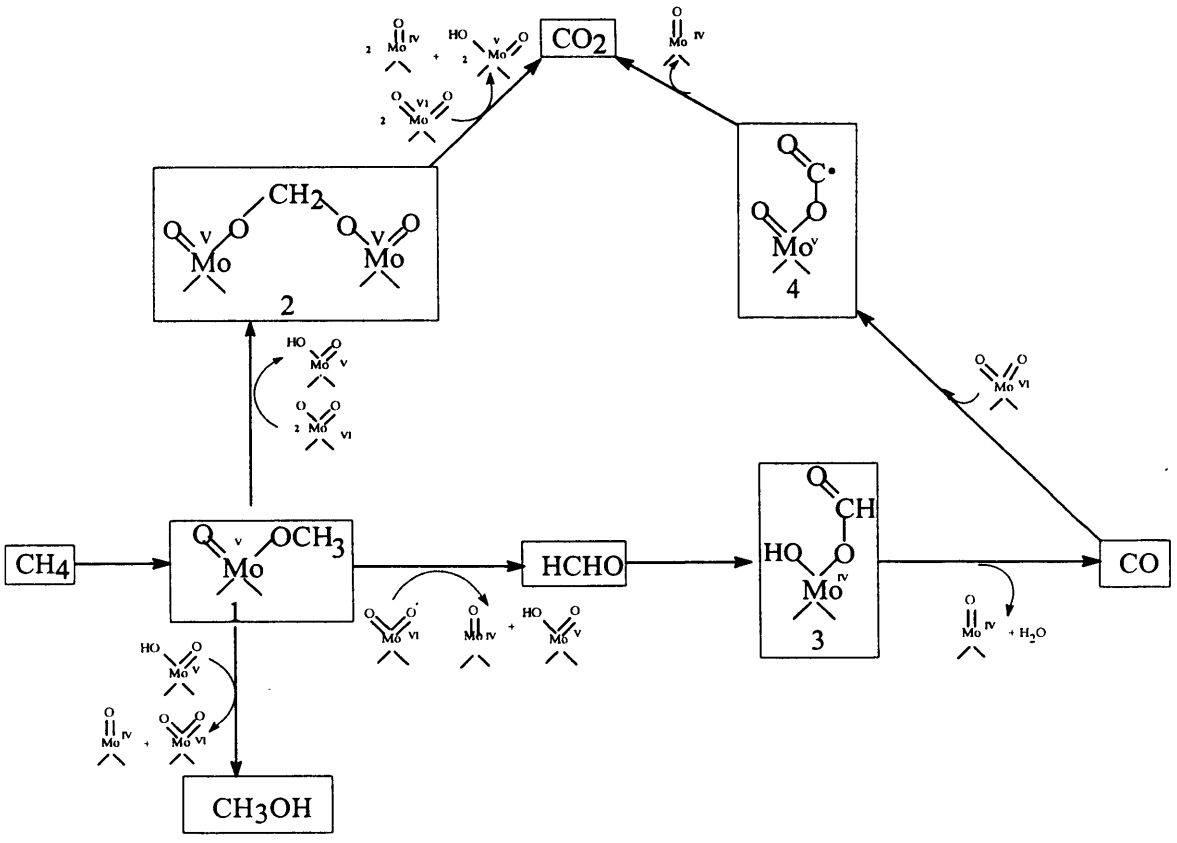

Figure 1.7.5.1: Schematic mechanism for methane oxidation over a supported MoO_3 catalyst [17]

Work by Hodnett et al. [18] using a 2% Mo catalyst on an untreated support showed 100% selectivity to HCHO at 500°C and increased Mo loading resulted in a marked decrease in the HCHO selectivity.

Another study by Barbaux et al. [19] centred comparing a range of supported Mo catalysts and correlating the results with catalytic activity. They discovered three types of molybdenum species, which were dependent on the Mo content of the catalyst. Loadings in the range of 1-5% showed a uniformly distributed phase, which interacted strongly with the support and identified it as silicomolybdic acid (SMA). From loading of 5-10% they discovered a polymolybdate species which appeared to

cover the SMA but not the support. At loading higher than 10%, SMA was no longer detected and crystalline MoO_3 was identified distributed over the polymolybdate phase.

Another report at the same time found slightly different results with Smith et al. [20] investigating the nature of the surface species for MoO_3/SiO_2 catalysts identifying three species. This time below 2% loading a silicomolybdic species was present which was characterised by using Raman spectroscopy and TPR, which was never found by Barares et al [21] who prepared catalysts in the same manner. Increased loading brought a surface co-ordinated polymeric molybdate and above 3.5% loading crystalline MoO_3 was detected with the polymolybdate species coexisting up to the highest loading analysed at 9.8%. Loading of the Mo catalysts affected their behaviour with a large decrease in CH_4 conversion above 5%, which corresponded with large amounts of crystalline MoO_3. The lowest loaded catalyst at 0.5% was the best catalyst discovered as it had the most dispersed silicomolybdic phase. It was proposed that the silicomolybdic species has terminal Mo=O sites which are responsible for the selective oxidation of methane the HCHO. With increased loading there is an increase in Mo-O-Mo bridging sites which are the expense of the terminal Mo=O, which corresponds to a decrease in the production of HCHO and an increase in non-selective oxidation products. Although generally the species at the higher loadings are generally agreed the phases present at lower loadings are still uncertain.

Work by Ozkan and Smith [22] looked at unsupported MoO_3 catalysts with differing amounts of basal (010) denoted MoO_3-R and side (100) denoted MoO_3-C plane areas exposed. Their study on MoO_3 resulted in the knowledge that if MoO_3-C is

preferential, which happens to expose the greater area, this shows twice as much selectivity for HCHO than the MoO_3-R. This is true for any oxygen concentration and conversion ranges used, although increasing the oxidant levels increased the relative amounts of CO_x. Investigation into the oxidation of HCHO indicated it was less stable over the MoO_3-R when compared to the MoO_3-C catalysts. From this they proposed that Mo=O sites residing mainly on the side planes are active in selective oxidation, while the Mo-O-Mo bridging sites mainly on the basal plane contribute to the complete and sequential oxidation reactions, similar to the proposed supported oxide. In situ laser Raman, TPR and $^{18}O_2$ labelling studies they claim demonstrated that the reoxidation of the Mo-O-Mo sites takes place via-gas phase oxygen whilst the reoxidation of the Mo=O sites seemed to occur via diffusion of bulk oxygen.

The preparation methods of the molybdenum oxide based catalysts have been found to be very important especially the pH of the impregnating heptamolybdate solution.

The Mo species present in solution is dependent on the equilibrium:

$$7MoO_4^{2-} + 8H^+ \Leftrightarrow Mo_7O_{24}^{6-} + 4H_2O$$

At pH 6, $Mo_7O_{24}^{6-}$ is predominant with the Mo in an octahedral environment, whilst MoO_4 tetrahedral are formed at pH 11. At solutions of pH 1 hydrated polymeric oxyanions are present with the octahedral Mo environment predominating. The pH also affects the net surface charge of the support.

Ismail et al. [23] identified the Mo species present on the silica support for 8% loaded Mo catalyst at varying pH and calcination temperatures. At pH 6, MoO_3 islands and particles were present with the Mo tetrahedrally and octahedrally co-ordinated. MoO_3 was again detected at pH 11 but at pH 1 a highly dispersed silicomolybdate $SiMoO_x$ phase was detected.

In more recent years the most widely studied catalysts for the partial oxidation of methane have been based on molybdenum trioxide. One of the first patents was by Dowden and Walker [24] who developed a variety of multi-component oxides of molybdenum. They also found it an advantage to support the catalyst using for example alumina and silica. They reacted mixtures of methane and oxygen at around 50 bar and between 130-500 °C and obtained high selectivities in several of them.

1.7.6: Supported V_2O_5 catalysts.

One study by Hodnett et al. [25] investigated a range of catalysts including cobalt, iron, silver, vanadium and chromium of 2% loading. Only vanadium exhibited selectivity towards HCHO although all did with the addition of molybdenum. This was significant for vanadium as the Mo increased conversion whilst depressed HCHO selectivity which resulted in increased production of HCHO. It was evident that conversion depended on methane partial pressure. Work done on a 7% loaded Mo catalyst using both O_2 and N_2O found it difficult to identify which oxidant is more suitable to the reaction, but it was clear that a difference does exist.

It was also shown by Khan and Somorjai [26] that silica supported vanadium pentoxide is also a suitable catalyst for the partial oxidation reaction with good selectivity. One general point about the catalysts was that the V_2O_5-SiO_2 catalyst was found to be more active for the production of methanol than the MoO_3-SiO_2 catalyst, but the product selectivity was generally poorer.

Catalysts based on vanadium oxide have been extensively studied for the partial oxidation reaction of methane. Spencer and Pereira [27] discovered that V_2O_5 supported on silica formed HCHO when molecular oxygen was used. Reactions had low conversions but high selectivity for HCHO with even trace amounts of CH_3OH under the same conditions. The general scheme form the reaction pathway was that HCHO was formed directly from methane but this was then oxidised to CO and then CO_2 in a sequential manner:

$$CH_4 + O_2 \rightarrow HCHO \rightarrow CO \rightarrow CO_2$$

1.7.7: Comparison of Mo and V catalysts.

Comparison with molybdenum oxide catalysts showed that the vanadium based was more active. The study by Hodnett et al. [25] discovered that yields of HCHO under both methane rich and lean conditions depends on vanadium loading. The optimum loadings were between 1-4% whilst the selectivity was essentially constant. TPR measurements demonstrated that the lower loaded catalysts were easier to re-oxidise than the higher loadings. It was suggested that catalysts with loading greater than 4%

were less active due to the catalyst not being able to re-oxidise itself quickly enough, while catalysts below 1% didn't have enough extractable oxygen.

The effects of loading in molybdenum and vanadium supported silica catalysts were investigated by Miceli et al. [28]. They prepared loadings in the range of 0.2-4.0 Wt % for molybdenum oxide and 0.2-5.3 Wt % for vanadium oxide. They found that specific reaction rates decreased steadily with increased molybdenum loading compared to bare silica but the opposite was seen for vanadium oxide. Increasing the loading of molybdenum enhanced HCHO selectivity while it was suppressed by the further addition of vanadium oxide. In both cases the addition of the metal oxides promoted combustion to CO_x. A model of the surface was proposed in which SiO_2 exposes two kinds of site, one that is a reduced site capable of activating O_2 and the other being strained siloxane bridges which are effective for activating CH_4. Addition of MoO_3 partially masks the active reduced sites producing the detrimental effect whilst the addition of V_2O_5 may also partially mask the same sites but it consequently creates new sites which are also active.

Comparing molybdenum and vanadium it was discovered that the vanadium material exhibits higher activity, whilst the molybdenum shows better selectivity. But it was unclear about the precise nature of the active sites for the activation of methane.

Parmaliana et al. [29] investigated the performance of a series of silica supported MoO_3 (2-7 wt.) and V_2O_5 (2-20 Wt %) catalysts looking at the partial oxidation of methane to formaldehyde and the oxidative dehydrogenation of propane to propene. They discovered that V_2O_5 acts as a promoter to the reactivity of the SiO_2 that allows the stabilisation of a higher density of reduced sites owing to its easier reducibility for

both reactions. Whilst the MoO_3 generally had a negative effect on the catalytic functionality of the SiO_2 surface due to it being essentially unreducible under the reaction conditions. The MoO_3 depresses the activity of the silica because of a negative physical effect linked to the partial coverage of the silica surfaces own active sites. The MoO_3 did act as a promoter for the methane reaction at T>650°C and it is also affected by the type of silica it is supported on. They concluded that a direct relationship between the density of the reduced sites of low-medium loaded silica based oxide catalysts and the reaction rate in both reactions does exist. This suggests that there is an occurrence of a concerted reaction mechanism involving the activation of gas-phase O_2 on the reduced sites of the catalyst surface.

Parmaliana et al. [30] investigated the partial oxidation of methane to formaldehyde with molecular oxygen on bare silica and supported MoO_3 and V_2O_5 catalysts between 550-650°C. Precipitated silica was found to more active than fumed silica but the incorporation of molybdena depresses the STY_{HCHO} value for precipitated silica but enhances the STY_{HCHO} values for fumed. In contrast the addition of vanadia to both silicas leads to higher STY_{HCHO} values in both silicas.

Using a technique of continuous scanning of the reaction mixture with a quadrupole M. S. they ruled out the participation of lattice oxygen in the main reaction pathway. They closely looked at the density of reduced sites and the catalytic activity of silica-based oxide systems. They found as previously stated the addition of MoO_3 causes a decrease in both the catalytic activity and the density of reduced sites of the unprompted precipitated SiO_2 surface.

The different effect when using V_2O_5 can be put down to both partially masking active sites of the precipitated silica surface but the vanadium generates its own reduced sites which are able to activate gas-phase oxygen. It was proposed that because of a strong interaction pathway between MoO_3 and SiO_2 and the formation of hardly reducible $SiMoO_4$ species [30] assists in the inability of the silica-supported MoO_3 to assist in the formation and stabilisation of its own reduced sites. Further argument involves that the strong interaction is due to electron transfer between Mo ions and the silica support, which negatively effects the concentration of the reduced sites on the SiO_2 surface. For fumed silica the interaction between MoO_3 and the inert surface could allow the stabilisation of reduced sites on the supported MoO_3 patches which accounts for the promoting effect. They stated that the promoting effect of the V_2O_5 even at different loading on both silicas is the consequence of weak interactions. On the surface the Mo ions exist in octahedral co-ordination [30] which assists in the stabilisation of the highest oxidation state Mo^{VI} while for V_2O_5 it is claimed that V ions form surface with lower co-ordination number which assists in the stabilisation of lower oxidation states [30].

A further study by Parmaliana et al. [31] looked at the direct relationship of loading of the catalysts and the reaction mechanism. They had already stated that at low loadings the mechanism for the partial oxidation of methane goes via a concerted mechanism. But using various techniques they proposed that on higher loadings up to bulk molybdenum and vanadium oxide the reaction goes via a redox mechanism with the reaction rate dropping off dramatically. The active centres for oxygen activation on low and medium loaded V_2O_5/SiO_2 catalysts could be V ions with low co-ordination number stabilised on the silica surface. This leads to these sites producing

the formation of partially reduced very active surface oxygen species, which participate in the reaction instead to undergo a reduction up to lattice ions.
Loadings higher than 5% imply the formation of surface vanadia clusters as crystals of bulk V_2O_5 causing the gradual decrease of low co-ordinated V centres concomitant enhancement in the amounts of 'extractable' lattice oxygen. They concluded that the highly loaded vanadium catalysts going via the redox mechanism lead to the formation of CO_x whilst the concerted mechanism leads to the formation of HCHO as the primary product.

Results for molybdenum based catalysts were very similar with the catalysts being very inactive up to 650°C with any interaction between CH_4 and the catalyst surface being hindered. It was therefore concluded that on medium loaded catalyst, methane partial oxidation proceeds according to the surface mechanism implying the activation of gas-phase oxygen with high loaded catalysts exhibiting low activity due to the redox mechanism, which isn't effective.

They looked at the density of reduced sites and the oxygen pathway. The activity of the vanadium catalysts reaches maximum on 5% loading while the density of reduced sites increases up to 20 Wt % loading where it levels off. The higher density of reduced sites on higher loadings favours a rapid incorporation of surface oxygen species into the lattice. As this lattice oxygen is much less reactive than the surface oxygen species the reaction rate of the methane partial oxidation proceeding via the redox mechanism is much lower than for the concerted mechanism. This means there is no relationship between the density of reduced states and catalytic activity for the higher loaded catalysts. The same can be said for the molybdenum oxide catalysts

proceeding via a surface mechanism for lower loadings going to a less effective redox mechanism for the higher loadings.

Parmaliana and Arena [32] investigated the working mechanism of oxide catalysts in the partial oxidation of methane to formaldehyde using temperature programmed analysis. It was discovered that the addition of vanadium to silica promoted the formation of HCHO at lower temperatures, (450-470°C) than for bare silica (480°C). The opposite effect was seen in molybdenum oxide with an increase in the formation of HCHO temperature to (490-530°) when compared to bare silica. At temperatures immediately higher than the HCHO formation all the systems catalyse CO and at temperatures higher than CO formation CO_2 was detected. Bare silica was shown to exhibit a considerable specific surface activity (SSA, $nmol_{CH4}$ s^{-1} m^{-2}) with the addition of vanadium oxide markedly enhancing the surface activity at any temperature.

In contrast, molybdenum oxide was found to exert a negative effect on the SSA at temperatures below 650°C and a promotive effect on silica above 700°C. The subsequent formation of CO at a slightly higher temperature than HCHO was assigned to the sequential oxidation of HCHO with the CO going on to form CO_2 in the same manner. The optimum loading of vanadium was reported to be 1-8%, which ensured the best selectivity and activity. This was put down to a more effective reduction-oxidation cycle of V^{5+} to V^4/V^{3+} associated with the presence of tetrahedral vanadate species on the silica surface. At higher loadings V_2O_5 crystallites were present which depress the formation of partial oxidation products giving a much higher selectivity for CO_2. For the molybdenum oxide lower loadings acted similar to

bare silica with optimum loading a 7%. Here it was found that HCHO selectivity can be related to the with the catalytic functionality of Mo=O sites of MoO_3 crystallites which are less active and more selective than "Mo-O-Mo" bridging sites of dispersed Mo species.

Arena et al. [33] investigated the redox properties of V_2O_5 and MoO_3 on silica and titanium oxides using temperature programmed reduction (TPR) with H_2 and CH_4 and high temperature oxygen chemisorption (HTOC). It was discovered that the most effective reaction mechanism leading to the primary formation of HCHO implies the direct participation of gas-phase oxygen with bulk-lattice oxygen ions in the process of product formation lead to mainly CO_x. This was investigated using H_2-TPR where it was discovered that increasing the loadings of MoO_3 enhances the reduction rate of the system at temperatures below 800°C. TPR profiles contained two overlapping peaks accounting for the step-wise:

$$Mo^{VI} \rightarrow Mo^{IV} \rightarrow Mo^{0} = \text{reduction of } MoO_3 \text{ to } Mo^{0}.$$

For V_2O_5 lower loadings contain a sharp reduction peak with the increased loading not affecting the reduction pattern. Above 10% loading the reduction pattern was found to shift to a higher temperature with new smaller peaks forming. The bulk vanadium oxide contained two very sharp, overlapping with a further similar third peak. The relative intensities were put down to the sequential reduction path of:

$$V_2O_5 \rightarrow V_6O_{13} \rightarrow VO_2 \rightarrow V_2O_3$$

For HTOC experiments increased loading resulted in a greater oxygen uptake, with the vanadium oxide catalysts supported on silica catalysts requiring more oxygen than the equivalently loaded molybdenum oxide catalysts. Using CH_4-TPR molybdenum oxide catalysts supported on silica show very low reactivity towards CH_4 compared to bare silica at temperatures below 650°C. At temperatures above 650°C there is a substantial increase in the rate of formation of oxygenated products like HCHO, CO and CO_2 with carbon deposits being discovered above 700°C. For vanadium oxide catalysts it was discovered that they exhibit a high reactivity to CH_4 with lattice oxygen consumption found below 500°C with HCHO being the primary product of the reaction. Above 500°C a drop in the rate of HCHO formation occurs and CO_2 was detected with CO and C_2 products being the primary products above 650°C. The relative concentration of isolated molybdenum and vanadium species as well as crystallite molybdenum and vanadium species controls the catalytic patterns in methane partial oxidation.

For the low-medium loaded catalysts the different effects of MoO_3 and V_2O_5 promoters on the functionality of the silica support at temperatures lower than 650°C was found to be consequence of the different reducibility patterns of the two isolated species. Crystalline vanadium oxide in catalysts above 10% loading was found to shift the reaction mechanism from surface to a redox mechanism resulting in a lower effectiveness in terms of activity and HCHO selectivity. It was concluded that the most effective reaction pathway of methane partial oxidation on silica oxide based

catalysts involved the direct participation of gas-phase oxygen activated on the surface reduced site.

1.7.8: The role of the oxidant.

Barbaux et al. [19] carried out microreactor studies beginning with 1-5% Mo catalysts at 597°C using N_2O and discovered HCHO was the major product. They linked formaldehyde selectivity directly to the concentration of SMA present in the catalyst. Co-feeding H_2O with the reactants enhanced HCHO selectivity and depressed CH_4 conversion with no methanol being detected under these conditions. They discovered that loadings above 5% were not active for HCHO production and changing N_2O for O_2 produced CO_x over all catalyst systems.

The influence of the oxidant involved using different molybdenum loadings and silica as a support was investigated by Banares et al. [21]. They made a range of MoO_3 Wt % loadings from 0.3 to 16.2% and from here they found that trends in product distribution with increased contact time using O_2 were very similar to that shown by N_2O but still significant differences in activity and selectivity were present. They found that when using N_2O the conversion was considerably lower than when O_2 was used under the same conditions. Molecular oxygen had a greater selectivity towards HCHO with decreased CO_x selectivity relative to that of N_2O. This has been put down to the oxidising power of the two gases with O_2 being a more powerful oxidising agent than N_2O.

This is believed that to effect the mechanism of the overall reaction as the proposed reaction is a Mars-van Krevelan mechanism with lattice oxygen in the support exchanging with gas phase oxygen. It's believed that N_2O isn't powerful enough to reoxidise the support which resulted in the catalysts becoming blue in colour, indicative of partially reduced MoO_3 and the presence of MoO_2 in powder XRD patterns supported this view. At around the loading of 1 Mo nm^{-2} spectroscopy like Raman, XPS and XRD show a Mo species interacting strongly with the surrounding silica surface. Below this level it was noted that a highly dispersed molybdate phase was present and above that crystalline MoO_3 was discovered while suggesting that a polymolybdate species was also present.

Another study by Chen and Wilcox [34] investigated the vanadium system under different reaction conditions. TPR indicated that a single vanadium species was present throughout the catalysts with loadings of between 1-8% with no well-defined phases of vanadium being identified by XRD. Using feeds that contained CH_4/N_2O, O_2, H_2O = 25/65: 2: 8 they discovered that the main reaction products were methanol, CO and CO_2 with HCHO being formed but at levels too low for their detection methods. Methane conversion was increased when N_2O was the sole oxidant involved and decreased for O_2 demonstrating that N_2O was the more active oxidant. It was suggested that the greater loadings of vanadium offer an explanation in the decrease in methanol selectivity with the higher loadings with more active oxygen being responsible for combustion reactions.

Other work also looked at the oxidant used in the reaction. All the previous work had centred on the use of oxygen but studies involving the use of nitrous oxide instead were carried out by various research groups. One group Liu et al. [35] published in

1982 a paper using nitrous oxide using methane at 1 bar and 1.7% Mo and SiO_2 catalyst. At 560°C they achieved a good selectivity towards methanol and formaldehyde and a conversion rate of 8.1%. They also discovered that the addition of steam to the system increased selectivity towards methanol by inhibiting the further oxidation of methanol although these results were later unable to be reproduced by the same group in 1984 [36]. They developed a rate law of the form:

$$d\,[CH_4]\,dt = -k\,[N_2O]^1\,[CH_4]^0$$

They were the first to consider the mechanism and the kinetics of the catalytic partial oxidation of methane to methanol. The Arrhenius plot of the rate of conversion of CH_4 was linear over a temperature range of 550-594°C giving an activation energy of 176 $^{+}$- 8 KJ mol^{-1}. They proposed a mechanism for both the selective and non-selective oxidation of methane. They used ESR spectroscopy to show that if O^{2-} instead of O^{-} was the product of the surface decomposition of N_2O, then the total oxidation process was preferred. It was concluded that the more reactive O^{-} species is responsible for the initiation of the selective oxidation cycle and this species was formed by the interaction of N_2O with the surface Mo(v) species.

They also proved the existence of $CH_3^{\cdot}$ radicals and IR spectroscopy showed the presence of $CH_30^{\cdot}$ at the surface of the catalyst. Combining these observations the following reaction mechanism was proposed for the partial oxidation of methane:

$$Mo(v) + N_2O \rightarrow Mo(VI)O^{-} + N_2$$

$$Mo(VI)O^{-} + CH_4 \rightarrow Mo(VI)OH^{-} + CH_3\cdot$$

$$Mo(VI)O^{2-} + CH_3\cdot \rightarrow Mo(v)OCH_3^-$$

$$Mo(v)OCH_3^- + H_2O \rightarrow Mo(V)OH^- + CH_3OH$$

$$Mo(VI)OH^- + Mo(V)OH^- \rightarrow Mo(V) + Mo(VI)O^{2-} + H_2O$$

Studies on molybdenum and vanadium oxides have used both oxygen and nitrous oxide as oxidants although molecular oxygen would be cheaper to use from a commercial point of view. Using both oxidants several studies have tried to identify the reaction pathways for the selective oxidation of methane. Khan and Somorjai [8] used N_2O and H_2O and Spencer et al. [16] stated that MoO_3-SiO_2 catalyst with O_2 generates the primary products of HCHO and CO_2 via parallel reaction pathways with a common activation step:

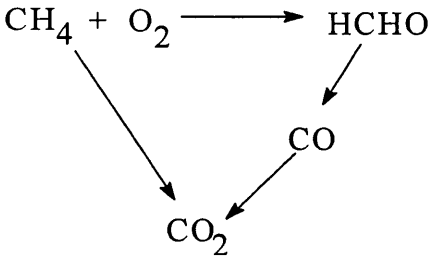

With CO being produced by the further oxidation of HCHO which is then subsequently oxidised to CO_2. Vanadium's pathway is the sequential oxidation through to CO_2.

Banares et al. [21] investigated oxidation using nitrous oxide and comparing it to molecular oxygen. Again the selective oxidation of methane using N_2O yielded HCHO, CO, and CO_2 as primary products with trends in the conversions and product

distribution at different temperatures etc. the same for molecular oxygen. But differences were discovered in both activity and selectivity with methane and oxidant conversions lower, but at the same level of methane conversion and reaction temperature HCHO selectivity is much lower than that in the presence of molecular oxygen. Varying the loading of the molybdenum oxide catalysts followed almost the same profile as molecular oxygen. They stated that the use of nitrous oxide instead of molecular oxygen resulted in the catalyst being reduced and different form of molybdenum oxide was found characterised by a blue colour. This is because the role of the oxidant was to re-oxide the lattice but when using N_2O, its lower oxidising power wasn't capable of this.

Banares et al. [37] investigated the role of NO concentration in the feed in the conversion of methane on very low-area silica supported vanadium oxide catalysts. It was stated that a large increase of methane conversion occurred upon the addition of NO. The low activity in the absence of NO was due to the lack of any source of radicals since the catalysts used had very low BET surface areas and no $CH_4 + O_2$ mixing volume is provided. The small amount of NO that was added to the feed stream giving an increased methane conversion was put down to the chain propagation of radical reactions with the conversion of O_2 increasing parallel. Also the product distribution changes with NO shifting the selectivity towards oxygen insertion with C_1-oxygenates increasing continuously with NO concentration. The yield of HCHO showed little change with NO concentration but the yield of methanol increased. The paper reports that the group Lunsford et al. observed that HCHO could originate from the degradation of methanol or both could have a common intermediate.

Banares et al [37] stated that methanol and formaldehyde must follow a parallel route for a given reaction temperature as the production of methanol increases faster than that of formaldehyde. Thus NO appears to promote the production of methanol from an intermediate common to HCHO thus establishing the relevance of NO concentration in the reaction for the production of C_1-oxygenates. The non-selective CO_x products are essentially constituted by CO (>90%) with deep oxidation CO_2 low. Carbon oxide production increased significantly with NO concentration up to 0.14% reactants then remaining constant with C_2 hydrocarbons passing through a maximum at 0.03% NO with only at very low concentrations does the coupling of methane become significant and with increased NO this decreases fast. The addition of NO alters the equilibrium towards oxygen-containing products at high concentration whilst some coupling occurs at very low concentrations.

1.8: Ethane oxidation.

All the carbon atoms in ethane are primary and are protected by a tetrahedral arrangement of C-H bonds with the C-H bond energy highest for primary carbons which makes itself and methane less reactive than larger alkanes. The C-H bonds are more exposed than the C-C bond present and it is expected that the cleavage of the C-H bond is the first transformation when trying to oxidise ethane and other short chain alkanes. A review by Batiot and Hodnett [38] reported that the oxidative dehydrogenation of ethane to ethene is expected to be highly selective with yields up to 60 %.

The terminal metal-oxygen double bond has been proposed as the active site for the selective oxidation of hydrocarbons by Busca and Centi [39]. This goes against evidence by Haber et al. [40] who suggests that interaction with the hydrocarbon is more favourable with a bridging oxygen than a terminal one for vanadium clusters. The study indicated that the terminal V=O bond does not appear to be involved in the catalytic oxidation of ethane. The oxygen bridging species on the surface of vanadium oxide to the support might play a role in catalyst activity.

Mendelovici et al [46] showed that if molecular oxygen is used ethane activity is very low and a certain activity is only seen at certain temperatures. In contrast, molybdenum oxide species are visibly oxidised which was not the case when N_2O was used as an oxidant. They concluded that a completely oxidised MoO_3/SiO_2 catalyst is not active for the oxidation of ethane.

Changing the support changes the V-O-S bond and this changes the catalytic performance in the sequence $TiO_2 > ZrO_2 > Al_2O_3 > Nb_2O_5 > SiO_2$ was reported by Banares et al for ethane oxidation [41]. The nature of the V-O-S bond appears to be critical for ethane oxidation with the activity of the catalysts being close to the reproducibility of the vanadium species on the supports.

The effect of the acidity of the support in ethane oxidation with molecular oxygen on various supported vanadium oxide catalysts has been investigated by Lé Bars et al. [42] with the activity decreasing with the lower number of acidic sites. This study had silica as the least active support compared to zeolites and phosphoric acid

supported compounds. All the catalysts produced carbon monoxide and ethene in similar levels of selectivity but the more active catalysts with acid sites were only active for the additional production of more carbon dioxide.

1.9: Propane and propene oxidation.

A review by Cavani and Trifiro [43] discussed some of the aspects that effect the selective oxidation of light alkanes. They discussed that one of the main problems concerned the reactivity of the product of partial oxidation, which is or can be higher than that of the reactant itself. Further non-selective oxidation under reaction conditions at which the reactant is activated makes it difficult to stop the reaction at he desired product. They stated that the only two heterogeneous catalysed reactions in advanced stages of development for propane were its conversion to either acrylonitrile or propene.

A study carried out by M. Ai [44] into the oxidation of propane to acrylic acid over V_2O_5-P_2O_5 based catalysts proposed that the oxidation of propane could proceed via the following reaction pathway:

Propane $\rightarrow$ Propene $\rightarrow$ Acrolein $\rightarrow$ Acrylic acid $\rightarrow$ $3CO_x$

Or

Propane $\rightarrow$ Propene $\rightarrow$ Propan-2-ol $\rightarrow$ Acetone $\rightarrow$ Acetic acid + CO_x $\rightarrow$ $3CO_x$

It was discovered that higher concentrations of oxygen and water vapour and a lower concentration of propane are favourable for obtaining a high yield of acrylic acid. It was also concluded that the yield of acrylic acid from propane is much lower than that of maleic anhydride from butane because:

a) Depression of the dehydrogenation of propan-2-ol is more difficult that for butan-2-ol.
b) Acrylic acid is much less stable than maleic anhydride.

A study by Stern and Grasselli [45] stated that acrolein was formed via propene when propane was used in the feed. When they used propene in the feed acrolein was observed as the major primary oxidation product. They proposed a reaction scheme that showed that propane was first oxidised to propene, which is further oxidised to acrolein. From here the acrolein can be further oxidised to acrylic acid but more preferentially acrolein was oxidised to carbon oxides.

1.10: References.

[1] G. C. Bond., Heterogeneous catalysis (2nd edition), Oxford University Press 1987.

[2] M. Bowker, The basis and applications of heterogeneous catalysis, Oxford University Press, 1998.

[3] Lance, D and Elworthy, E. G. 1906. Brit. Pat. 7,297.

[4] Wiezevich, P.J. and Frolich, P.K. Ind. Eng. Chem., **26** (1934) 267-276.

[5] Boomer, E.H. and Broughton, J.W., Can. J. Res., **15B** (1937) 375-382.

[6] Dowden, D.A., Schnell, C.R. and Walker, G.T., Proceedings of the 4th International Congress on Catalysts (Moscow). (1968). 201-215.

[7] Taylor, S.H., Hargreaves, J.S.J., Hutchings. G.J. and Joyner R.W. Appl. Catal. A: General **126** (1995) 287-296.

[8] Khan, M.M. and Somorjai, G.A., J. Catal. **94** (1985) 263-271.

[9] Banares, M.A., Rodriues-Ramos, I., Guerrero-Ruiz, A. and Fierro, J.L.G., Proceedings of the 10th International Congress on Catalysis., July 19-24, 1992, (Budapest)., 1131-1144.

[10] Mauti, R and Mimms, C.A., Catal. Lett., **21** (1993) 201-207.

[11] Karthueser, B., Hodnett, B.K., Zanthoff, H. and Baerns. M., Catal. Lett., **21** (1993) 209-214.

[12] Kastanas, G.N., Tsigdinos. G.A. and Schwank. J., Appl. Catal., **44**. (1998) 33-51.

[13] Parmaliana, A., Frusteri, F., Miscelli, D., Mezzapica, A. and Scurrell, M.S., Appl. Catal. **78**. (1991) L7-L12.

[14] Sun, Q., Herman, R.G. and Klier, K., Catal. Lett., **16** (1992) 251-261.

[15] Parmialana, A., Arena, F., Frusteri, F., Miceli, D. and Sokolovskii, V., Catal. Today, **24** (1995) 231-236.

[16] Spencer, N.D., J. Catal., **109** (1998) 187-195

[17] Spencer, N.D., Pereira. C.J., Grasselli, R.K., J. Catal., **126** (1990) 546-554.

[18] MacGiolla Coda. E., Kennedy, M., Mc Monagle. J.B. and Hodnett. B.K., Catal. Today, **6** (1990) 559-566.

[19] Barbaux, Y., Elamrani, A.R., Payen E., Gengembre, L., Bonnelle, J.O. and Grzyboska, B., Appl. Catal., **44** (1988) 117-132.

[20] Smith, M.R., Zhang, L., Driscoll, S.A. and Ozkan, U.S., Catal. Lett., **19** (1993) 1-15.

[21] Banares, M.A., Fierro, J.L.G. and Moffat, J.B., 1993. J. Catal., **142** (1993) 406-417.

[22] Smith, M.R., and Ozkan, U.S., 1993. J. Catal., **141** (1993) 124-139.

[23] Ismail, H.M., Zaki, M.I., Bond, G.C. and Shukri, R., Appl. Catal., **72** (1991) L1-L12.

[24] Dowden, D.A. and Walker, G.T., 1971. Brit. Pat., 1,244,001.

[25] Kennedy, M., Sexton, A., Kartheuser, B., MacGiolla Coda, E., MacMonagle, J.B. and Hodnett, B.K., Catal. Today, **13** (1992) 447-454.

[26] Zhen, K.J., Khan, M.M., Lewis, K.B. and Somorjai, G.A., J. Catal., **94** (1985) 501-507.

[27] Spencer, N.D. and Pereira, C.J., J. Catal., **116** (1989) 339-406.

[28] Miceli, D., Arena, F., Parmaliana, A., Scurrell, M.S. and Sokolovskii, V., Catal. Lett., **18** (1993) 283-288.

[29] Parmaliana, A., Arena, F., Frusteri, F., Martra, G., Coluccia, S. and Sokolovskii, V., (1997) 347-356.

[30] Parmaliana, A., Sokolovskii, V., Miceli, D., Arena, F. and Giordano, N., J. Catal., **148**, (1994) 514-523.

[31] Parmaliana, A., Arena, F., Sokolovskii, V., Frusteri, F. and Giordano, N., Catal. Today, **28** (1996) 363-371.

[32] Parmaliana, A. and Arena, F., J. Catal., **167** (1997) 57-65.

[33] Arena., F., Frusteri, F., Martra, G., Coluccia, S., Parmaliana, A.J. Chem. Soc. Faraday Trans. **93** (1997) 3849.

[34] Chen, S.Y. and Wilcox, D., Ind. Eng. Chem. Res., **23** (1993) 584-587.

[35] Liu, R.S., Iwamoto, M. and Lunsford, J.H., J Chem. Soc. Chem. Commun., (1982) 78-79.

[36] Liu, H.F., Liu, R.S., Liew, K.Y., Johnson, R.E. and Lunsford, J.H., J. Am. Chem. Soc., **106** (1984) 4117-4121.

[37] Banares, M.A., Cardoso, J.H., Huchings, G.J., Correa Bueno, J.M. and Fierro, J.L.G., Catal. Lett., **56** (1998) 149-153.

[38] C. Batiot, B.K. Hodnett, Appl. Catal. A **137** (1996) 179.

[39] Busca, G., Centi, G., J. Am Chem. Soc. **111** (1989) 46.

[40] Haber, J, Derouane, E.G., Lemos, F., Riberiro, F. R., Guisnet, M., Catalytic Activation and Functionalisation of Light Alkanes. Advances and Challenges, NATO ASI Series, Kluwer Acaemic Publishers, Dordrecht, 1998.

[41] Banares, M.A., Gao, X., Fierro, J.L.G., Wachs, I.E., Third World Congress on Oxidation Catalysis, Stud. Surf. Sci. Catal., **110** (1997) 295.

[42] Le Bars, J., Auroux, A., Forissier, M., Vedrine, J.C., J. Catal. **162** (1996) 250.

[43] F. Cavani, F Trifiro, Catal Today. **36**, (1997) 431-439.

[44] Ai, M., Catal. Today., **13** (1992) 679.

[45] Stern, D.L., Grasselli, R.K., Third World Congress on Oxidation Catalysis, Stud. Surf. Sci. Catal. , **110** (1997) 357.

[46] Mendelovici, L., Lunsford, J.H., J. Catal. **94** (1985) 37.

[47] Harris, R.H., Boyd, V.J., Hutchings, G.J. and Taylor, S.H., Catal. Lett. **78** (2002) 369-372.

Chapter 2. Experimental Methods

2.1: Catalyst preparation.

2.1.1: Preparation of MoO_3 and V_2O_5 catalysts on silica.

MoO_3/SiO_2 and V_2O_5/SiO_2 catalysts used in these experiments were prepared by using an incipient wetness technique with 4.2 ml/g of distilled water required to wet the silica into a paste. Ammonium heptamolybdate tetrahydrate (+99%) (AHT) and ammonium metavandadate (99%) (AMV) were supplied by Aldrich. Fumed silica (99.8 %) (BET = 194 m^2/g) was supplied by BDH. A range of loadings was prepared by Wt % on 3g silica batches. Table 2.1 shows the amounts of starting material required to obtain the various loadings.

Table 2.1: Amount of AHM and AMV required (g) to prepare the various silica supported catalysts.

Wt % loading	g required of AHM	g required of AMV
2.5	0.1385	0.1723
3.5	0.1933	0.2412
5	0.2760	0.3445
6	0.3314	0.4135
7	0.3866	0.4824
10	0.5521	0.6889
15	0.8282	1.0338

Catalysts were prepared in a small evaporating dish by mixing the catalyst solution and the silica together into a paste. Loadings from 6 Wt % to 15 Wt % of V_2O_5/SiO_2

required gentle heating on a hotplate to acquire the AMV to fully dissolve. This paste was then dried in an oven for 16 hours at 100°C. The powder was then ground in a pestal and mortar for 15 minutes. The resulting finely ground powder was then calcined in air at 700°C for 4 hours in a fused silica boat at a ramp rate of 20°C per minute from ambient temperature. The calcined sample was then ground for a further 15 minutes before use.

2.1.2: Preparation of V_2O_5 catalysts on Boron nitride.

V_2O_5/BN catalysts used in these experiments were prepared using an incipient wetness technique with 3 ml/g of methanol required. Boron nitride (99%) (BET = 7 m^2/g) was supplied by Strem. Methanol was supplied by Fischer and vanadium(III) acetylacetonate (97%) by Aldrich. A range of loadings was prepared by Wt % on 3g of boron nitride. Table 2.1.2 shows the amount of Vacac required to be dissolved in 50ml of methanol because of the little amount of $V_{(acac)}$ required to make the Wt % loadings due to boron nitride's low surface area.

Table 2.1.2: Amount of $V_{(acac)}$ required to prepare the various loaded boron nitride vanadium catalysts.

Wt % loading	g required of Vacac per 50ml methanol
7	0.5867
21	1.7601
35	2.9335

The catalysts were prepared in a small evaporating dish with 9ml of the stock solution being added to 3g of BN. This paste was dried in an oven for 16 hours at 100°C. The

powder was then ground in a pestel and mortar before being calcined at 650°C in a fused silica boat in static air for 5 hours using a ramp rate of 15°C per minute from ambient temperature. The sample was then ground for 15 minutes again before use.

2.2.1: Catalyst testing.

Catalyst performance was evaluated in a fixed bed stainless steel microreactor and carried out on propane, propene, ethane and methane using molecular oxygen as an oxidant and helium as a dilutent in the ratio $C_xH_x/O_2/He$, 2/1/7. A gas hourly space velocity of $2400h^{-1}$ was used and gas flow rates were regulated electronically using thermal mass flow controllers positioned immediately after air filters to remove any particles present in the oxygen, hydrocarbon and helium cylinders. Pressure relief valves were also positioned before the filters.

Catalysts were pelleted to a uniform particle size in the range of 300-600μm with the catalyst bed being packed to a constant volume and supported between plugs of silica wool in a ½in. o.d. stainless steel tube. Reaction temperatures were determined by a thermocouple placed in the centre of the catalyst bed. A further filter was positioned after the catalyst bed before the sample loop to protect it from particles that may have been carried from the reactor bed.

Analysis was performed on-line using a Varian 3800 GC with a 2m packed molecular sieve 13X and a 2m packed Poropak Q column. The columns were valved in a series/by-pass configuration with analysis of the products carried out by a thermal conductivity detector (TCD) and a flame ionization detector (FID) in series. The

reactions were carried out in the stainless steel tube heated by an external carbolite tube furnace. For the analysis of the reactants and products the GC was firstly calibrated by injecting known amounts of each reagent separately. When the concentrations are changed of a particular reagent, different peak areas are obtained that correspond to the amount that was injected. A graph was then plotted of concentration verses peak area which results in a straight line. The gradient of this line gives the response factor (RF value) for the particular reagent tested and this figure is then used to calculate unknown peak areas obtained in future catalyst testing.

Alkane and alkene conversion was calculated by the difference between the inlet and outlet concentration. This was achieved by taking the initial value of the hydrocarbon (HC) measured at the start of the analysis before the light-off temperature and subtracting subsequent amounts of hydrocarbon obtained during the temperature range tested. The level of conversion by difference is calculated using the following formula:

$$((\text{HC in} - \text{HC out}) / \text{HC in}) * 100$$

Selectivities were determined by the proportion of products after correcting for the carbon number of the products. This is achieved by taking the value for one product at a particular temperature and dividing it by the total value of all products at the same temperature and is calculated using the following formula using acrolein as an example:

$$(\text{Amount of acrolein} / \text{Total amount of products including acrolein}) * 100$$

Carbon and oxygen balances were in the range of 97-103% for all reactions. The carbon balances were calculated at specific temperatures and included the total amount of carbon from the unreacted hydrocarbon and any products made, with the values for the products corrected for the number of carbons involved. Oxygen balances were calculated in a similar way. These were again at specific temperatures and included the amount of unreacted oxygen and the amount of oxygen required to make the various selective and non-selective oxygenated products.

Figure 2.2 shows the schematic representation of the reactor built for this study.

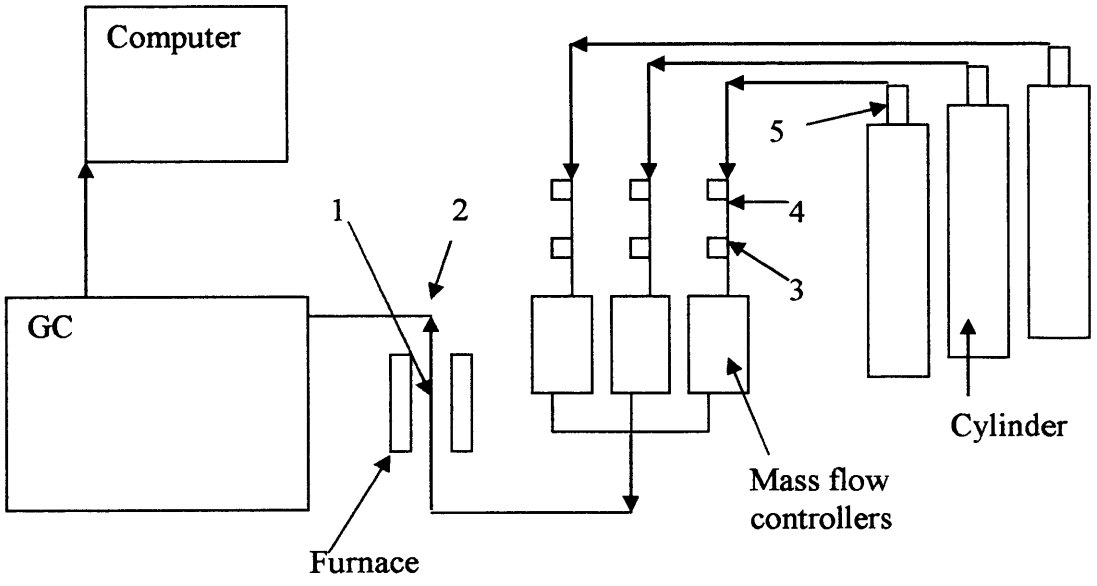

1: Reactor bed

2: Thermocouple placed in here to rest in reactor bed.

3: Filters

4: Pressure relief valves

5: Cylinder head

Figure 2.2.1.1: Schematic representation of the microreactor system used in this study.

Experiments were also carried out in which water was co-fed with the gas stream to assess whether water had any effect on selectivity and activity for the reactions. Water is thought to lower activity thus possibly producing more selective products. This was fed in with the alkane via a vessel in the line just after the mass flow controller. The water carrying alkane then joined the oxygen and helium lines before all were passed over the catalyst in the reaction bed. Figure 2.2.1 shows a small schematic of the vessel that was used in the same microreactor set up as shown in figure 2.2. For these reactions the water was at room temperature. By passing it through the alkane it was calculated that the feed would contain 10 % water.

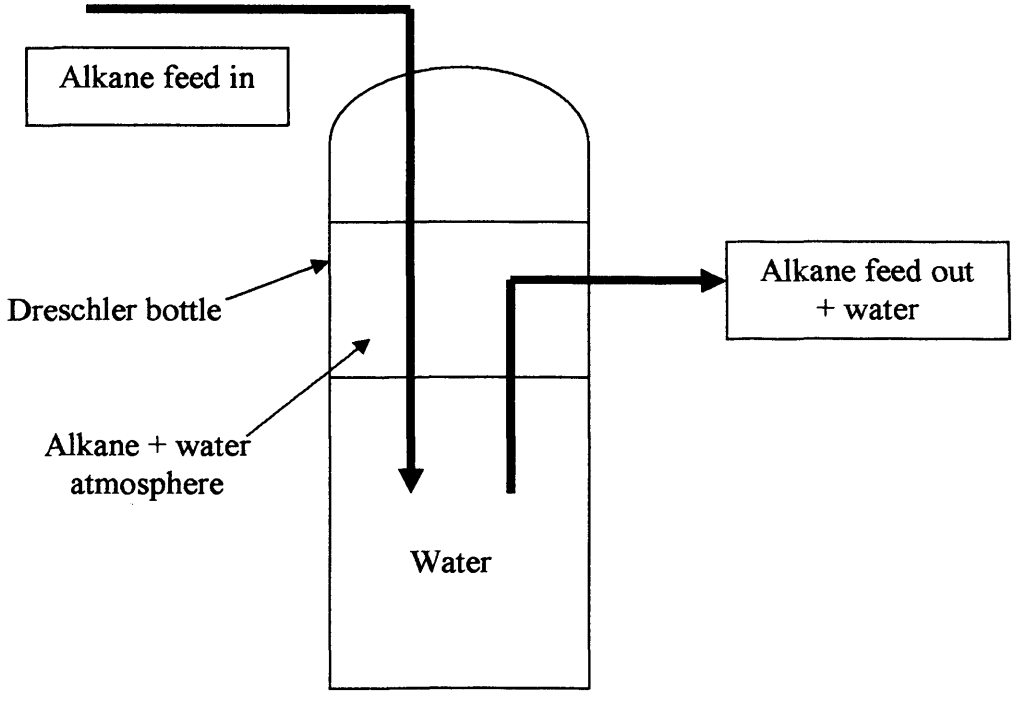

Figure 2.2.1.2: Apparatus for experiments investigating the effect of water.

2.2.2: Gas Chromatographic Analysis.

Gas chromatography is a form of chromatography in which the mobile phase is a gas and the stationary phase is either a solid or a liquid and this study gas-solid chromatography is the method used. The process relies on the interactions of the different gas molecules with the solid phase of the chromatography columns to separate out the components of the sample injected.

The samples were injected into the GC by using a 6-port valve heated to 200°C. For these studies a molecular sieve 13x column was used which is able to separate similar sized molecules like molecular oxygen, nitrogen and carbon monoxide. A Poropak Q column was used to separate the various alkanes and alkenes used in the study and also oxidation products like carbon dioxide or those products that were desired for example acrolein. On injection some components of the sample must not pass through the molecular sieve, like CO_2 because they become irreversibly adsorbed and deactivate the column. The molecular sieve column must be by-passed until these products have come through the Poropak Q.

The temperature of the column oven is also important for the separation of the components of the sample. Initial temperatures need to be low typically 35°C to enable the separation of products on the molecular sieve and other products of low molecular weight as these pass through the columns with ease. These temperatures need to be raised to typically 175°C to speed up the separation of higher molecular weight products like propane, acrolein and acrylic acid.

Table 2.2 shows a typical GC programme displaying valve switches, the heating rate for the separation of products and reactants for the reaction of propane over either MoO_3 or V_2O_5 supported silica catalysts performed in this study. The switching of valve 1 injects the sample from the sample loop and the switching of valve 2 controls the flow of the sample injected along the columns allowing components to be separated by either the molecular sieve or the Poropak Q.

Table 2.2.2.1: GC analysis programme for propane oxidation.

Time / min	Event	Effect	Temp (C)	Product (Min)
0.01	Switch valve 1	Sample injection	35	None
0.9	Switch valve 2	Poropak Q in series	35	CH_4 (1.4) CO_2 (2.7)
3.3	Switch Valve 2	Molecul. sieve back in series	35	O_2 (4.1) CO (5.0)
5.1	Temp. Ramp	Rate = 50°C min^{-1}	35 → 175	None
7.8	Switch valve 2	Poropak Q in series	175	Propane (8.2) Acrolein (10.5)
12.5	Switch valve 1	End Analysis	175 → 35	None

The reactants and products were detected using both a thermal conductivity detector (TCD) and a flame ionization detector (FID). The TCD is commonly used in hydrocarbon oxidation experiments and is ideal for the detection of CO_2 and CO. The

FID cannot detect these products as they are already combusted but this detector is ideal for the identification of hydrocarbons and selective oxidation products like acrolein. So it is very common as in this study to use the two together to analyse the sample injected.

The TCD works by detecting the difference in thermal conductivity of the reactants and products compared to the thermal conductivity of a pure carrier gas in this case helium. The TCD was maintained at 200°C with the internal filaments that do the detection an additional 50°C higher and the resulting difference in thermal conductivity recorded by computer. The FID works by ionising all the combustible hydrocarbons in a H_2 / O_2 flame. A collector filament is placed above the flame and measures the current from the ions. This current is then amplified electronically for the signal. The analysis gas used in this study was H_2 at 30ml min^{-1}, air at 300ml min^{-1} with helium from the TCD at 30ml min^{-1}.

2.3: Brunauer Emmett Teller (BET) adsorption.

2.3.1: Theory.

Catalyst surface areas have been measured by the physical adsorbents of N_2 gas using the Brunauer, Emmett and Teller method. The method is based on a theoretical model, which describes the adsorption of an inert gas (usually N2), onto a solid. The adsorption isotherm is measured with the monolayer capacity of the adsorbant required to give monolayer coverage hence surface area is directly proportional to monolayer capacity.

$$S.A. = Vm\ \sigma\ Na / M\ Vo$$

Where: Vo = molar vol. of gas

M = mass of sample

Vm = monolayer capacity

σ = Area of adsorbate

Na = Avagadros constant

Vm can be determined using the BET equation.

$$P / V(Po - P) = 1 / Vm\ C + (C-1)\ P / Vm\ C\ Po$$

Where: P = Pressure

Po = Saturated vapour pressure at T of determination

C = BET Constant

V = Volume in cm^3

If the gaseous uptake is measured in the range $0.05 < P / Po < 0.3$ the constant C and Vm can be obtained. From this the surface area of the sample can be calculated from the volume of gas required for monolayer coverage. The value for the absorbate N_2 is 0.162 nm^2 at 77K. The value of C is exponentially related to the heat of adsorption of the monolayer and is generally similar for materials like oxides and metals.

2.3.2: Experimental.

Surface area measurements were carried out using a micromeritics ASAP 2000 and a micromeritics gemini apparatus. Both systems were computer controlled. Samples were weighed accurately into the relevant glass sample tube, which was attached to the vacuum. Weights of around 0.2 to 0.4g were used to give accurate measurements. Samples were firstly degassed under vacuum to remove any contaminating physisorbed species. This procedure was done for around 4-5 hours. V_2O_5 / SiO_2 and V_2O_5 / BN samples where heated to 130°C during this process to remove any surface water but the MoO_3 / SiO_2 samples remained at room temperature. This was because the MoO_3 was partially reduced in the N_2 reducing atmosphere, which was shown by the white MoO_3/SiO_2 turning a pale blue. When cooled the dead volume of the apparatus was measured accurately by expansion of He from a known volume. The glass tube was immersed in liquid N_2 and the dead volume measured. Following this the He was pumped out and replaced with N_2. A known volume of N_2 was admitted to the sample at 77K and the pressure was determined. From the measurements an adsorption isotherm was constructed and the surface area derived from the isotherm using the BET equation.

2.4: Raman spectroscopy.

2.4.1: Theory.

Catalysts were characterised using Raman spectroscopy. When electromagnetic radiation of energy hυ irradiates a molecule this energy can be:

- Transmitted
- Absorbed
- Scattered

From which Raman comes from scattering.

There are different types of scattering that can occur and these are shown in figure 2.4.1. Firstly there is Rayleigh scattering which can be looked at as an elastic collision between incident photons and the molecule.

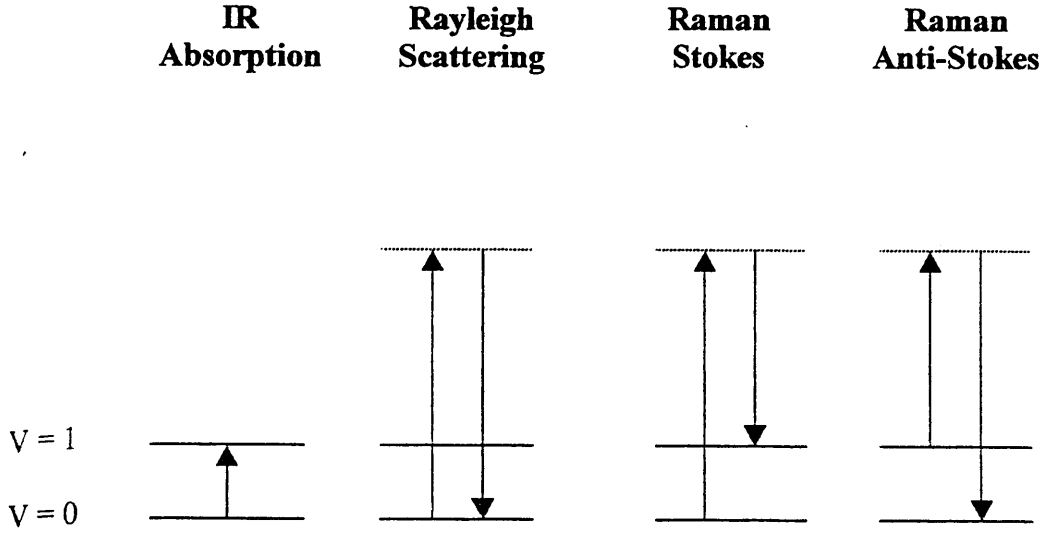

Figure 2.4.1: Diagram of the different types of scattering.

When the molecule interacts with an incident photon were the molecule is in ground vibrational state $\upsilon=0$, the molecule absorbs the photon and is raised momentarily to a high level $\upsilon=n$ which is not a stable energy level. Here the molecule loses the energy and normally returns to $\upsilon=0$ emitting a scattered photon with equal energy to the incident photon with the vibrational and electronic energy of the molecule remaining unchanged. A small proportion of molecules fall to the $\upsilon=1$ energy level this is

incident photon and the molecule. This means the scattered photon has less energy than the exciting photon. The difference is:

- $h\upsilon i - h\upsilon s = \Delta Em = h\upsilon m$

This means the vibrational energy or rotational energy is being changed by the amount ΔEm. So if a molecule gains energy from this meaning ΔEm is positive:

- $0r\ \upsilon s = \upsilon i - \upsilon m$

This gives rise to Stokes Lines.

Quantum mechanics allow another possibility that the molecule is initially in the excited state $\upsilon=1$ and then goes through the same process. The molecule is excited from $\upsilon=1$ and then falls to the ground level $\upsilon=0$ with the energy loss made up for by an emission of a photon whose energy is greater than that of the incident photon by $h\upsilon m$ giving AntiStokes lines. Boltzmann distribution of the ratio of the number of molecules in $\upsilon=1$ compared to $\upsilon=0$ at ordinary temperature will show that most of the molecules will exist in the ground state so therefore:

Stokes >> Antistokes

So this means the Stokes lines are much greater in intensity.

If a molecule is to be Raman active the molecular vibration must be accompanied by a change in the polarizability of the molecule. The polarizabilty is caused when a molecule is placed in an electric field where the protons and electrons experience oppositely directed forces causing an induced dipole moment.

2.4.2: Experimental.

Raman spectra were obtained using a Renishaw system 1000 Raman microscope. An argon ion laser (514.5nm) was used as the excitation source operated at a power of 20mW. Scans were obtained over a range of 150 to 4000 cm^{-1} with typically 10 to 20 accumulations of normally 10 seconds for each spectra. Samples were in powdered form and placed on a slide. These were firstly focused upon using a computer-controlled microscope and then focused with the laser. In certain experiments the laser power was varied using different filters to cut out laser power to the sample. Spectra were collected using a back-scattering geometry with a 180° angle between illuminating and the collected light. XY Raman spectra were also obtained. These were carried out over a straight line spanning around 4cm in length with 10 accumulations of 10 seconds each.

2.5: Powder X-ray Diffraction (XRD).

2.5.2: Theory.

A crystalline powder will consist of a large number of microcrystalline particles. This

will contain lattice planes present in every orientation.

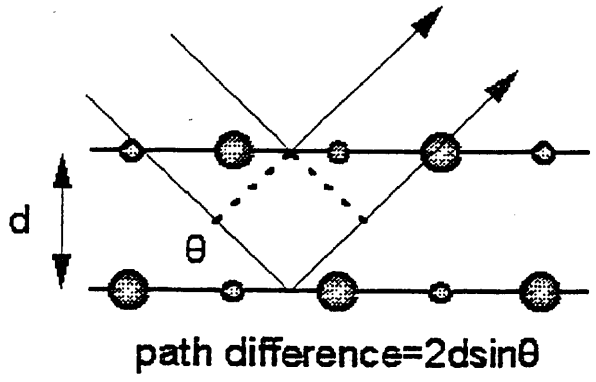

Figure 2.5.2: Diagram of X-ray scattering in a crystal.

The scattering of an impinging x-ray beam shown in figure 2.5.2 from A and D in neighbouring planes will produce IN PHASE diffracted x-ray beams of the additional distance travelled by the x-ray photon. This scattering from D is an integral number of wavelengths. The path difference BD + DC will depend on the lattice spacing or d_{hkl} which are known as the Miller indices for the planes. Additionally BD + DC will also be related to the angle of incidence of the x-ray beam θ. From this the following relationship between θ and d_{hkl} can be obtained.

- Path difference = BD + DC = $2d_{hkl} \sin\theta = n\lambda$
- = X-ray wavelength
- n = integer

$2d \sin\theta = n\lambda$ is the BRAGG EQUATION.

When a sample is moved through the angular range θ different sets of crystal planes present will satisfy the criteria in the Bragg equation producing a diffracted beam of

an angle 2θ. Hence the scattering of the x-ray beam by the planes gives a large number of diffraction maxima whose positions relate to the lattice parameters, Miller indices and the x-ray wavelength which gives structural information on the sample. The diffraction pattern is regarded as the fingerprint of the sample, which against a database phase identification is possible.

X-rays are used because distances between atoms or ions are typically a few Angstroms, which are comparable to the x-ray wavelength produced by the bombardment of metals by electrons. So both the distances and the wavelength of the beam are around 10^{-10}m. The technique is limited by particle size dimensions with particles that have diameters smaller than 30Å are not detectable.

2.5.2: Experimental.

X-ray diffraction patterns were recorded using a modified ENRAF NONIUS FR590 powder diffractometer. The diffractometer consists of three components; these are the x-ray source, sample mounting compartment and the X-ray detector. The x-ray source used was a Ge (III) monochromater producing Cu $K\alpha_1$ radiation with a wavelength of 1.54066 Å. The source was operated at 40 KV with a 30-mA current for the x-ray tube.

Samples were mounted into a cut-out in an aluminium holder. A flat surface relative to the holder was obtained to minimise errors in peak position and the x-rays were detected using a scintillation counter. . The sample was continuously rotated so that

an average picture of the sample is obtained by increasing the randomness of the orientation of the crystallites present. Diffractometer control and data acquisition was controlled by computer.

Diffractions were obtained with a PSD detector between 2 and 122°. Samples were ran from between 30 and 60 minutes each to obtained clear patterns. Data was analysed using Traces version 4, which obtained peak positions and their relative intensity. Phase identification was performed using Fein Marquart Associates Micro Powder Diffraction Search and Match, (μ-PDSM) software and patterns obtained compared to the entries in the database.

2.6: Temperature Programmed Reduction (TPR).

2.6.1: Theory.

Temperature programmed reduction (TPR) is a technique that can measure the reducibility of a metal oxide species in a supported or unsupported catalyst. The main information that TPR gives is the number of reducible species in the metal oxide and the ease in which these species can be reduced. This information is obtained by the number of defined peaks on the TPR profile and the temperature at which these peaks occur. By comparing different catalysts, in this study a range of loadings, it may be possible to compare their TPR profiles and try to explain differences in activity and selectivity.

TPR experiments are carried out upon the catalyst using a reductive gas usually hydrogen while the temperature is uniformly increased over a period of time.

$$MO + H_2 \rightarrow M + H_2O$$

Where MO is the metal oxide

During a TPR changes in the gas stream concentration from where the reduction is taking place are monitored using a thermal conductivity detector (TCD) and results are plotted against temperature.

2.6.2: Temperature Programmed Oxidation (TPO).

TPO is a technique that can indicate how easily and to what extent a catalyst can be reoxidised after it has been previously reduced. It is important to discover how easily catalysts are reoxidised as many catalytic oxidation systems undergo reduction and oxidation of the catalyst during reactions. If a catalyst was unable to be reoxidised then its lifetime could be quite short.

These experiments are done, as in this study in conjunction with TPR experiments. A first TPR experiment is performed followed by a TPO experiment. This is then repeated perhaps more than once to try to assess the redox behaviour of the catalyst. Performing these experiments can lead to information about the catalyst, for example if it undergoes any physical changes like particle distribution which would lead to temperature shifts and peak size differences in subsequent TPR experiments. These

might not be discovered performing just one TPR experiment as these changes could lead to lower activity and selectivity's over the catalysts lifetime.

2.6.3: Experimental.

TPR and TPR/TPO experiments were carried out on a Micromeritics AutoChem 2910. All samples used were pelleted to a uniform size of 300-600μm to ensure that the flow of gas was able to pass through the sample and not be blocked leading to a rise in pressure that would end the experiment. The samples were placed on a silica wool plug in a U-shaped quartz reactor tube. Enough sample was used in each experiment to give 0.025 to 0.03g of reducible material. At the start of each experiment a cold trap containing iso-propanol cooled to a thick paste with liquid nitrogen was prepared. This was prepared to trap water produced due to the reduction of the metal oxide with H_2 that would lead to a noisy spectrum. For TPR/TPO/TPR experiments this trap was prepared at the beginning of each individual cycle. The gas mixture used for TPR experiments was 10% hydrogen in argon and for the TPO experiments 10% oxygen in argon was used. These gases were fed into the reactor at a rate of 50ml min^{-1}. For all TPR and TPO experiments the temperature inside the reactor tube was ambient at the beginning and heated by the reactor oven at a rate of 10°C min^{-1} to a final temperature of 1000°C were the experiment ended and the oven returned to ambient.

2.7: Scanning Electron microscopy (SEM) and Energy Dispersive X-ray analysis (EDX).

Scanning Electron Microscopy (SEM) is a rapid and non-destructive technique used to investigate the microstructure and morphology of a wide range of sample materials. In catalysis it is a useful tool as the morphology and structure of the catalyst surface can play a significant role in its behaviour. This structure can effect the levels of conversion obtained and often plays an important role in the types of products formed and the selectivity at which they are made. The morphology of a catalyst structure can depend on the procedure from which it was made so a SEM image of a catalyst can be related to how the catalyst performed in both levels of conversion and/or selectivity. This could lead to the development of further catalysts with the same or improved morphology and microstructure. SEM can play an important role alongside other characterisation techniques that give evidence of surface and bulk species present within the catalyst. Some species detected may only occur depending upon the morphology of the catalyst and play a small or a greater role in the activity and selectivity of the catalyst.

The combination of scanning electron microscopy can be used in conjunction with the ability to perform elemental analysis (EDX) on very localised or larger areas of a sample makes it an invaluable technique for the investigation and characterisation of catalytic material. EDX analysis can be performed on most elements including O, N, F, and C up to larger elements and metal oxide determination.

Energy Dispersive X-ray microanalysis (EDX) achieves elemental analysis by collecting the X-rays generated when the incident electron beam interacts with the atoms of the sample. Each element in a sample produces X-rays with characteristic

energies whose peak intensities are related to the amount of the elements present. The energies of the X-ray photons are converted into electronic signals and are processed to produce an intensity spectrum in counts per second. The EDX technique can be used to display the compositional information in the form of X-ray distribution images or maps. These maps can be visually informative because they show the spatial distribution and relative concentration of the different elements within either a small section or all over the entire sample. They can give valuable information on concentration gradients and determining inter-elemental associations.

Chapter 3: Characterisation of catalysts.

3.1: Introduction.

All catalysts were characterised by the methods discussed in Chapter 2. The first methods to be discussed are BET, Raman spectroscopy, powder X-ray diffraction and TPR that were performed on all catalysts. This will lead to specific discussion on experiments performed on individual catalyst groups like *in situ* and XY Raman, TPR/TPO/TPR and SEM experiments.

3.2: B.E.T. adsorption

B.E.T surface area calculations are extremely useful since heterogeneous catalysis is the study of reactions at a catalyst surface. The measurement of this surface can be an indication of the activity of the catalyst although the technique does have a 10% error when a measurement is performed. Experimental conditions are described in section 2.3.

3.2.1: Molybdenum oxide supported on silica.

In Table 3.2.1 the results show that increasing the loading of the molybdenum supported on the silica decreases the surface area of the catalyst. The greatest drop was seen between the 5 Wt % loading and the 6 Wt %. This corresponds to between 0.17 and 0.204 monolayer coverage and thus an increase in the amounts of species being formed between the silica and the molybdenum oxides.

Table 3.2.1: BET surface areas for MoO_3/SiO_2 catalysts prepared.

MoO_3/SiO_2 Wt % loading	BET surface area/ m^2/g
SiO_2	194
2.5	168
3.5	161
5	109
6	56
6.9	49
10	45
15	35

The greater decrease around 0.17 and 0.204 monolayer coverage and above will be due to the formation of oxide species on top of previous layers decreasing the diameter of the pores and also the possible blocking of smaller pores at their entrance.

3.2.2: Vanadium oxide supported on silica.

Table 3.2.2: BET surface areas for V_2O_5/SiO_2 catalysts prepared.

V_2O_5/SiO_2 Wt % loading	BET surface area/ m^2/g
SiO_2	194
2.5	163
3.5	156
5	118
6	67
7	49
10	35
15	32

Table 3.2.2 shows that with increased loading of the catalysts the surface area decreases. This is gradual in the lower loadings but when you get to the loadings of 6 to 7 Wt % there is a drop of between 50 and 60 m^2/g when compared to the 5 Wt % loading. This is caused by the blocking of small pores in the silica and vanadium oxide layers forming on top of each other in larger pores. In comparison to the molybdenum oxide based catalysts the patterns are the same but the only difference is for each loading the vanadium oxide based catalysts have a slightly lower surface area.

3.2.3: Vanadium oxide supported on Boron nitride.

Table 3.2.3: BET surface areas for V_2O_5/BN catalysts prepared.

V_2O_5/BN Wt % loading	BET surface area /m^2/g
BN	7
7	6
21	6
35	5

The vanadium oxide supported on BN catalysts shown in Table 3.2.3 show much lower surface areas than their silica supported counterparts. Silica (BET 194 m^2/g) used in this study like other silicas available is a low density amorphous material that has been widely studied as a catalyst support. Boron nitride is a high density material and when tested here had a BET of only 7 m^2/g and this is an average of a small number of BET analyses performed due to the technique limitations especially at very

low surface areas. Catalysts containing vanadium oxide decreased in surface area the greater the loading prepared, but this drop was small at around 1-2 m^2/g but this does correspond to a drop in surface area of around 30 %.

3.3: Raman spectroscopy.

Raman is a technique that is used to investigate the surface of a catalyst. By assigning peaks obtained and comparing these to previous work it becomes possible to find out what species are present and whether the presence or absence of these species affects the selectivity and/or activity of the catalyst. This technique has many uses and in this study XY and *in situ* Raman experiments have been performed using catalyst performance conditions that are discussed in 3.6 and 3.7. The experimental conditions and theory are discussed in section 2.4.

3.3.1: Molybdenum oxide supported on silica.

Full Raman spectra can be found in Appendix Section A. The peaks obtained are summarised in Table 3.3.1.

In Table 3.3.1 these are the results when the varying loadings were analysed by Raman spectroscopy. Molybdenum oxide catalysts supported on silica gave good clear spectra. With increased loadings the spectra became more defined and the peaks were stronger and sharper with only the 2.5 Wt % loaded catalyst showing an amorphous spectrum.

Table 3.3.1: Raman peaks (cm^{-1}) obtained for various MoO_3/SiO_2 catalysts.

MoO_3/SiO_2 Wt % loading	Raman peaks cm^{-1}
SiO_2	N/a
2.5	N/a
3.5	994, 819, 672, 340
5	995, 819, 671, 291
6	995, 819, 671, 340, 293
6.9	989, 822, 671, 340, 293
10	995, 819, 737
15	995, 819, 737
Bulk MoO_3	986, 818, 657, 327, 277

Species present can be assigned to a dehydrated surface β-silicomolybdic acid species at 995cm^{-1}. An α-MoO_3 crystalline species corresponding to the stretching of a terminal Mo=O bond at 819cm^{-1}. Peaks at 737cm^{-1} and 291cm^{-1} are also indicative of crystalline MoO_3 [1]. The band at 986cm^{-1} which is present on the bulk MoO_3 sample is due to the vibration mode of a terminal Mo=O bond of isolated distorted octahedral mono-oxo-molybdenum oxide species [2]. Also on the bulk MoO_3 sample the bands at 657 and 277cm^{-1} can be assigned to orthorhombic molybdenum oxide [2].

3.3.2: Vanadium oxide supported on silica.

Full spectra can be found in Appendix A. The Raman peaks obtained are summarised in Table 3.3.2.

Table 3.3.2: Raman peaks (cm^{-1}) obtained for various V_2O_5/SiO_2 catalysts.

V_2O_5/SiO_2 Wt % loading	Raman peaks cm^{-1}
SiO_2	N/a
2.5	N/a
3.5	N/a
5	995, 764, 755, 698
6	995, 698
7	995, 698, 515
10	994, 698, 533, 406, 284
15	987, 698, 524, 404, 284
Bulk V_2O_5	985, 700, 526, 405, 303, 283

Table 3.3.2 shows results obtained analysing the varying loadings by Raman spectroscopy. Vanadium oxide catalysts supported on silica do not give good spectra due to fluorescence. All techniques were tried to limit this problem varying the power of the laser and the length of and the number of runs the sample was subjected to. On the higher loadings peaks at 994, 698, 406 and $284cm^{-1}$ corresponded to aggregated crystalline vanadium oxide with the medium loadings also showing the bands at 995 and 698 cm^{-1} [3]. The higher loadings of 10 and 15 Wt % V and bulk V_2O_5 bands at 404 and $284cm^{-1}$ are caused by a weak interaction between surface vanadium species [2]. Lower loadings displayed little or no peaks at all with the lowest giving amorphous silica spectra.

3.3.3: Vanadium oxide supported on Boron nitride.

Full Raman spectra can be found in Appendix A. The peaks obtained are summarised in Table 3.3.3.

Table 3.3.3: Raman peaks obtained (cm^{-1}) for various V_2O_5/BN catalysts.

V_2O_5/BN Wt % loadings	Raman peaks cm^{-1}
BN	N/a
7	N/a
21	995, 698
35	995, 697, 284

Table 3.3.3 shows the results of analysing the vanadium oxide on BN catalysts. The spectra like those obtained from the vanadium oxide supported on silica were not good due to fluorescence. The lowest loading gave no peaks at all and the 21 and 35 Wt % loading gave slight peaks at 995 and 698cm^{-1} that correspond to crystalline V_2O_5 [2].

3.4: Temperature Programmed Reduction.

TPR is a technique that measures the reducibility of an oxide species. The main piece of information that is obtained is the number of reducible species in a catalyst and this is shown by the number of defined peaks in a TPR profile. It has become an important characterisation technique and can be used to analyse the redox behaviour

of a metal oxide catalyst. The theory and experimental methods used can be found in section 2.6.

3.4.1: Molybdenum oxide supported on silica.

Full TPR profiles can be found in Appendix B. The peaks obtained are summarised in Table 3.4.1.

Table 3.4.1: TPR peaks for various MoO_3/SiO_2 catalysts.

MoO_3/SiO_2 Wt % loading	1st Reduction peak (C)	2nd Reduction peak (C)
2.5	480	660
3.5	485	670
5	490	700
6	490	705
6.9	495	715
10	600	750
15	600	780

Table 3.4.1 shows that when the loading of the catalyst is increased the position of both reduction peaks is shifted to a higher temperature. The reduction pattern for the molybdenum oxide catalysts supported on silica follows this reduction profile. [4]

- $MoO_3 \rightarrow MoO_2 \rightarrow Mo$ or $Mo^{+6} \rightarrow Mo^{+4} \rightarrow Mo^0$

The major shift in temperature is the first reduction peak from MoO_3 to MoO_2 between the medium loadings of 6 and 6.9 Wt % and the higher loadings of 10 and 15 Wt % is an increase of just over 100°C. This strongly suggests that there is a lot more MoO_3 crystallites in the higher loadings which require a higher temperature for the reduction from Mo^{+6} to Mo^{+4}, than are found in the lower loadings which contain more molybdenum-silica species in the catalyst. Another reason for the temperature shift could also be the case that particle size could be a contributing factor. The larger crystals of MoO_3 found on the higher loadings which are around 0.34 to 0.51 monolayer coverage could require a higher temperature for reduction due to H_2 diffusion limitations.

The second reduction peak has a more gradual temperature increase that is a result of the lower loaded catalysts containing more molybdenum oxide species in a lower oxidation state than the higher loaded catalysts that contain more MoO_3. Catalysts with a loading between 5 and 6.9 Wt % also have another small reduction peak on their profile between the two main reduction peaks. This indicates a small presence of a β-silicomolybdic acid species that can be detected on these loadings. The presence in higher loadings may be lost in the spectra due to the large second reduction peak or not present.

3.4.2: Vanadium oxide supported on silica.

Full TPR profiles can be found in Appendix B. The peaks obtained are summarised in Table 3.4.2.

Table 3.4.2: TPR peaks for various V_2O_5/SiO_2 catalysts.

V_2O_5/SiO_2 loading	1st Reduction peak (C)	2nd Reduction peak (C)	3rd Reduction peak (C)
2.5	500	N/a	N/a
3.5	250	525	N/a
5	500	N/a	N/a
6	510	N/a	N/a
7	510	570	N/a
10	515	580	650
15	520	590	660

Table 3.4.2 shows the interesting results gained by testing the various loadings with temperature programmed reduction. Even though there are up to three different peaks listed for one loading the profiles there is only one main peak with the exception of the 3.5 Wt % loading. The lower loaded catalysts yielded one sharp peak with a maxima between 500-510°C which corresponds to the reduction of V_2O_5 to V_2O_3, (V^{+5} to V^{+3}) which gets slightly broader with loading [5]. In the higher loadings the peak was much broader but not significantly higher in temperature indicating a much greater amount of reduction from V_2O_5 to V_2O_3 as well as bulk diffusion limitations due to particle size broadening the reduction peak. The highest loadings also have slight peaks at around 580 and 650°C that could be indicative of the way pure V_2O_5 reduces. This goes by the following scheme:

- $V_2O_5 \rightarrow V_6O_{13} \rightarrow V_2O_4 \rightarrow V_2O_3$ [5]

The 3.5 Wt % catalyst had an unusual narrow reduction peak at 250°C, which was reproducible. The rest of the reduction profile was the same after this peak corresponding to the other lower loaded catalyst TPR profiles. Other characterisation techniques performed on this catalyst like XRD and Raman failed to notice this as yet unidentified reduction peak. This peak is significant as the 3.5 Wt % catalyst displayed the greatest propane conversion over the lower temperatures investigated when compared to other catalysts studied.

3.4.3: Vanadium oxide supported on Boron nitride.

Full TPR profiles can be found in Appendix B. The peaks are summarised in Table 3.4.3.

Table 3.4.3: Various TPR peaks for V_2O_5/BN catalysts.

V_2O_5/BN Wt % loading	1st reduction peak (c)	2nd reduction peak (c)
7	600	N/a
21	575	N/a
35	620	700

The reduction peaks for the various V_2O_5/BN catalysts are displayed in table 3.4.3. The reduction behaviour of the 7 and 21 Wt. % loadings were similar with both exhibiting a broad reduction peak at 600 and 575°C respectively. The reduction profile of the 35 Wt % catalyst was different to the lower loadings. The reduction profile contained two peaks at 620 and 700°C. This indicates that the higher loaded

catalyst contains two reducible vanadium oxide species compared to the lower loadings one. The first peak could also correspond to the single peak seen on the lower loadings that has been shifted due to bulk diffusion limitations.

3.5: Powder X-ray Diffraction (XRD).

Powder X-ray diffraction is an important characterisation technique and investigates the bulk of a sample rather than the surface, which is what Raman spectroscopy investigates. The X-rays are scattered by the crystallites in the sample that leads to a characteristic pattern of intensities that can be matched to a database. The theory and experimental procedure are described in section 2.5. All powder XRD patterns for silica supported molybdenum and vanadium oxide catalysts can be found in Appendix Section C.

3.5.1: Molybdenum oxide supported on silica.

The patterns for the molybdenum oxide catalysts that were 6 Wt % and higher in loading displayed crystalline structures with the 15 Wt % being the most profound. These samples gave good diffraction patterns all displaying the formation of MoO_3 when compared to the μ-pdsm database. Lower loadings only gave amorphous patterns.

3.5.2: Vanadium oxide supported on silica.

The vanadium oxide based catalysts show much less crystalline structure in all loadings when compared to the molybdenum oxide based catalysts. The higher

loadings give the more crystalline diffraction patterns with the lower loadings giving amorphous patterns.

For both the silica supported molybdenum and vanadium catalysts the lower loadings gave amorphous powder XRD patterns. This indicates that there could be no vanadium or molybdenum species present in the sample as bare silica would give the same pattern. This though is not consistent with Raman and TPR analysis as both of these techniques indicate metal oxide species present in the lower loadings.

Reasons for this could be that in lower loadings amorphous molybdenum and vanadium phases have been produced when the catalysts were made. The lower loaded catalysts that are below the 5 Wt % loading with 0.17 monolayer coverage are much less likely to produce metal oxide crystallites that are often found in bulk. They are more likely to produce metal-silica phases like silicomolybdic acid which is a 2D layer and not detectable by XRD. Another reason could be that any crystallites that are produced in the lower loaded catalysts are smaller than the detectable limits of XRD of around 30Å so are not seen in a XRD pattern even though they are there.

3.5.3: Vanadium oxide supported on boron nitride.

Analysis by powder X-ray diffraction of these catalysts only indicated diffraction from the highly crystalline boron nitride phase. If any crystalline V_2O_5 was present its peaks were not visible due to the BN.

3.6: XY Raman spectroscopy.

XY Raman spectroscopy is a useful expansion upon regular Raman carried out. The previous Raman experiments mentioned before were a spectrum taken of a single point. XY Raman expands this, as a spectrum taken can be obtained using various single points on the sample or as in this case a series of Raman spectra along a 3 to 4cm line across the sample. This technique is a very good indication that the species present in the sample (in Raman the peaks produced) are present all over the catalyst. The only samples that this analysis was carried out upon were the MoO_3/SiO_2 catalysts due to their good spectra.

3.6.1: Molybdenum oxide supported on silica.

Table 3.6.1: Raman peaks (cm^{-1}) discovered for various MoO_3/SiO_2 when tested using XY Raman.

MoO_3/SiO_2 Wt % loading	Raman peaks cm^{-1}
SiO_2	N/a
2.5	N/a
3.5	994, 819, 672, 340
5	995, 819, 671, 291
6	995, 819, 671, 340, 293
6.9	990, 822, 671, 340, 293
10	995, 819, 737
15	995, 819, 737
Bulk MoO_3	986, 818, 657, 327, 277

Table 3.6.1 shows that when the MoO_3/SiO_2 catalysts were tested using this technique it showed that the catalysts produced have a uniform structure to them. The peaks that are obtained were also discovered when single Raman spectra were taken. These peaks are discovered all over the 3D map that is produced. Again with increased loadings the spectra became more defined and the peaks were stronger with only the 2.5 Wt % loaded catalyst showing an amorphous spectra. Species present can be assigned to a dehydrated surface β-silicomolybdic acid species at 995cm^{-1}. An α-MoO_3 crystalline species corresponding to the stretching of a terminal Mo=O bond at 819cm^{-1}. Peaks at 737cm^{-1} and 291cm^{-1} are also indicative of crystalline MoO_3 [1]. The band at 986cm^{-1} which is present on the bulk MoO_3 sample is due to the vibration mode of a terminal Mo=O bond of isolated distorted octahedral mono-oxo-molybdenum oxide species [2]. Also on the bulk MoO_3 sample the bands at 657 and 277cm^{-1} can be assigned to orthorhombic molybdenum oxide [2].

3.7: *In situ* Raman spectroscopy.

Another important Raman spectroscopy technique is *in situ* Raman. Using this technique gives information on whether the catalyst is changing structure during reaction conditions. The sample is mounted in a cell over which the gases used in microreactor studies are passed over the sample. The temperature is then increased to those used in the reaction conditions and Raman spectrums are taken so see if species present at ambient temperature change during the reaction conditions employed. These experiments also included Raman spectra taken with water being co-fed with the gas stream. In these studies MoO_3/SiO_2 catalysts were analysed due to their good

clear spectra. The theory and experimental conditions employed can be found in section 2.4.

3.7.1: Molybdenum oxide supported on silica.

A selection of *in situ* Raman spectra can be found in appendix A. Under reaction conditions no real changes were observed in the Raman spectra with analysis from room temperature up to the reaction conditions used for propane oxidation. The co-fed water experiments also showed that during this process no changes were occurring during reaction conditions. A list of peaks obtained can be found in section 3.6.

3.8: TPR/TPO experimental studies.

When TPR and TPO are used together they can help our understanding of the reduction and oxidation cycle of a catalyst. By performing these cycles of TPR and TPO experiments it is hoped that any irreversible changes to a catalyst can be detected. The theory and experimental conditions employed can be found in section 2.6. A selection of catalyst profiles can be found in appendix B.

3.8.1: Molybdenum oxide supported on silica.

A range of catalysts was tested to include a low, medium and high loaded catalyst. This was carried out to discover whether the amount of reducible metal oxide present in the catalyst effects the oxidation cycle of the catalyst. The catalysts tested peaks are summarised over the following three tables.

Table 3.8.1.1: Silica supported 2.5 Wt % Mo catalyst.

Experiment carried out	1st reduction / oxidation peak (C)	2nd reduction / oxidation peak (C)
1st TPR	480	660
2nd TPR	550	600

Table 3.8.1.2: Silica supported 6.9 Wt % Mo catalyst.

Experiment carried out	1st reduction / oxidation peak (C)	2nd reduction / oxidation peak (C)
1st TPR	500	730
2nd TPR	550	680

Table 3.8.1.3: Silica supported 15 Wt % catalyst

Experiment carried out	1st reduction / oxidation peak (C)	2nd reduction / oxidation peak (C)
1st TPR	600	780
2nd TPR	540	730

3.8.1.1: Discussion

When the second TPR experiment was conducted after the initial TPR and then a TPO, the profile always differed to the first with a shift in temperature downwards of the second reduction peak in the lower loaded catalysts but an increase in the temperature of the first reduction peak. For the higher 15 Wt % loading both its peaks increased for the second TPR. This ranged from 20 to 70°C for the first reduction

peak and 50 to 60°C for the second reduction peak. This shows that when the catalysts are reoxidised they do not produce an identical catalyst with the same structure. If similar species are present they are reduced easier on the second TPR indicating that some of the structure of catalyst is lost. This may affect selectivity and activity of the catalyst when it is undergoing reaction conditions.

3.8.2: Vanadium oxide supported on silica.

A range of catalysts was tested to include a low, medium and high loaded catalyst.

Table 3.8.2.1: Silica supported 2.5 Wt % V catalyst.

Experiment carried out	1st reduction / oxidation peak (C)	2nd reduction / oxidation peak (C)	3rd reduction / oxidation peak (C)
1st TPR	500	N/a	N/a
2nd TPR	495	N/a	N/a

Table 3.8.2.2: Silica supported 5 Wt % V catalyst.

Experiment carried out	1st reduction / oxidation peak (C)	2nd reduction / oxidation peak (C)	3rd reduction / oxidation peak (C)
1st TPR	520	N/a	N/a
2nd TPR	510	N/a	N/a

Table 3.8.2.3: Silica supported 10 Wt % V catalyst.

Experiment carried out	1st reduction / oxidation peak (C)	2nd reduction / oxidation peak (C)	3rd reduction / oxidation peak (C)
1st TPR	515	580	650
2nd TPR	500	570	630

3.8.2.1: Discussion

When the silica supported vanadium catalysts were tested they differed to the silica supported molybdenum with the second TPR reduction pattern being very similar to the initial TPR reduction pattern. The temperatures for the peaks in the second TPR are 5 to 15°C lower when compared to the initial temperatures. This shows that when the catalysts are fully reduced and then reoxidised they appear to form the same species in the catalyst. This could indicate why the silica supported vanadium catalysts show better selectivity towards oxygenated products when tested for alkane and alkene oxidation that is discussed later.

3.9: SEM and EDX microscopy.

As it was not possible to obtain any good powder XRD and laser Raman data on the boron nitride supported vanadium oxide catalysts these catalysts were analysed by SEM and EDX. Figure 3.9.1 shows the SEM image of the 35 Wt % V/BN catalyst.

The catalysts consisted of a single morphology that was angular and blocky in nature with a crystalline size of approximately 6μm. EDX studies scanning the V $K\alpha_1$ emission showed that the vanadium was well dispersed throughout the catalysts and was not present as large crystallites, this was also confirmed by the powder X–ray diffraction studies that showed a strong boron nitride diffraction pattern and not vanadium oxide.

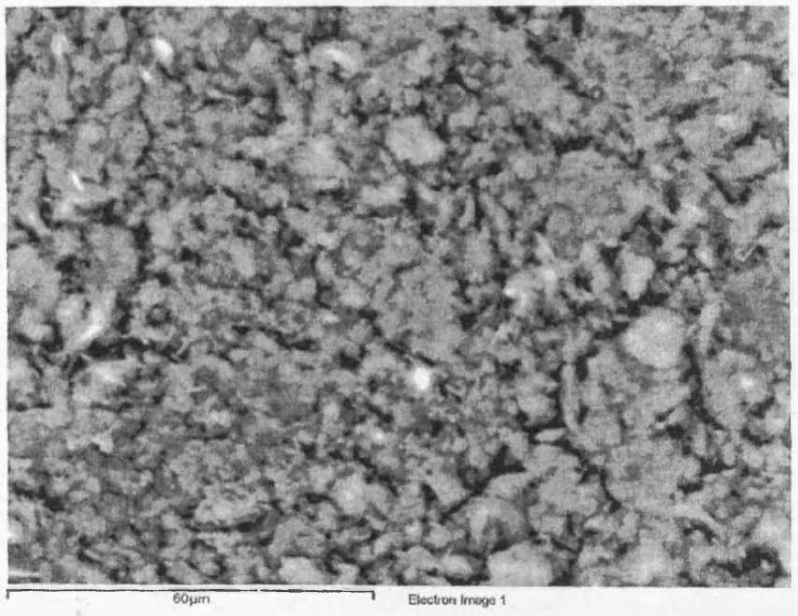

Figure 3.9.1. Scanning Electron microscope image of the 35 Wt % V/BN catalyst. (Scale bar=60μm)

3.10: Conclusions

From the characterisation studies used to analyse the catalysts prepared it is clear that differences occur when the loading of the metal oxide is changed. For the silica supported molybdenum and vanadium oxide catalysts the higher loaded catalysts all give evidence towards crystalline metal oxides on the surface. This is shown by decreased surface area measurements, highly crystalline powder XRD patterns,

Raman bands matching those on the bulk metal oxide and broader TPR profiles with an increase in reducible species. The lower loaded species generally gave amorphous non-crystalline patterns and smaller reduction profiles and greater surface areas when tested with the medium loaded catalysts displaying similarities to both high and low loaded catalysts when analysed.

The difficulty in analysing the boron nitride supported catalysts has led to less information about the species present but from the TPR profiles especially it is clear that there is a difference between the species produced on the boron nitride compared with those formed on the silica surface.

XY Raman experiments show that the surface of the silica supported molybdenum oxide catalysts is uniform in species present and *in situ* Raman shows that the species produced on the catalysts are not lost when they are exposed to the reactions conditions used in microreactor studies.

3.11: References.

[1] G. Mestl, T. Srinivasan, Catal. Rev.-Sci. Eng., **40** (4), 451-570 (1998).

[2] Faraldos, M., Banares, M.A., Anderson, J.A., Hu, H., Wachs, I.E., Fierro, J.L.G., J. of Catal. **160**, 214-221 (1996).

[3] M. Sharaml-Marth., J. Chem. Soc. Faraday Trans., **87** (16) 2635-2646 (1991)

[4] F. Arena, N. Giordano, A. Parmaliana, J. Catal., **167**, 66-76 (1997)

[5] M. Koranne, J. Goodwin, G. Marcelin, J. Catal., **148**, 369-377 (1994)

Chapter 4: Silica and boron nitride supported molybdenum and vanadium oxide catalysts for propane and propene oxidation.

4.1: Introduction

The selective oxidation of short chain alkanes by heterogeneous catalysis has been a major research aim for many years. In general the oxidation of these short chain alkanes requires relatively high temperatures in order to activate the alkane. At these temperatures unselective gas phase homogeneous chemistry can predominate and partial oxidation products can be destroyed. So studies aim to develop new catalysts and try to determine the influence of gas phase reactions and surface reactions in an attempt to promote more selective surface chemistry. Most of the recent studies have centred on the difficult transformation of methane into methanol and formaldehyde, using two of the most studied catalyst systems, which are silica supported molybdenum oxide and vanadium oxide [1]. The selective oxidation of propane by heterogeneous catalysis would be highly desired and could lead to a wide range of commercially required oxidation products including alkenes, aldehydes, alcohols and acids. Different research has been carried out on the selective oxidation of propane. Some work has centred on the oxidative dehydrogenation of propane [2] as the activation of the alkane suggests the first step is the production of propene [3] that leads to further selective oxidation of the alkene to products like acrolein. Research has also investigated the use of different supports including a potassium modified

silica supported iron catalyst [4] and a nickel, cobalt, molybdenum catalyst supported on silica [5]

This study centres on the use of silica supported molybdenum and vanadium oxide catalysts as these have been extensively studied for methane oxidation [1] with promising results obtained. The study has been extended for alkane oxidation by preparing a range of boron nitride supported vanadium oxide catalysts. Boron nitride has not been studied extensively as a support but there is a recent literature report supporting platinum on boron nitride [6]. Boron nitride is recognised as an inert material and it is also hydrophobic. This makes it the opposite of silica, which is regarded as an active material capable of selective oxidation [7] and also hydrophilic. The different properties of boron nitride when compared to silica maybe beneficial for potential alkane selective oxidation catalysts.

4.2: Propane oxidation

All the catalysts were tested for propane oxidation using the methods described in section 2.2.

4.2.1: Silica supported vanadium oxide catalysts.

The oxidation of propane over all tested V_2O_5/SiO_2 catalysts is shown in figure 4.2.1.1. A range of activity was exhibited and this was dependent on vanadium loading. These catalysts were also compared to a blank tube and just using bare but pelleted silica.

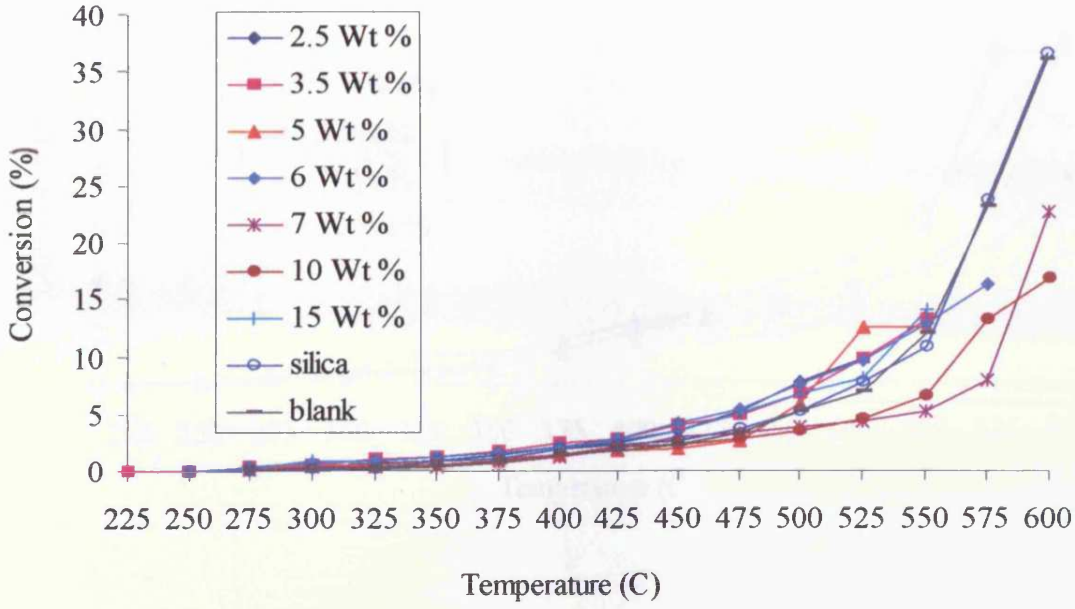

Figure 4.2.1.1: Conversion difference calculated for a range of V_2O_5 Silica supported catalysts.

When comparing the range of silica supported V_2O_5 catalysts they all behave in a very similar way. The light-off temperatures all range between 225°C and 275°C and all increase gradually up to approximately 475°C. After this temperature the medium to higher loadings of 7 Wt % and 10 Wt %, conversion does not increase at the same rate as the other catalysts. These continue at a lower rate of conversion but are still active at higher temperatures than the other loadings except when compared to the blank tube and silica. The light-off temperatures of the blank and silica are also higher at around 300-325°C.

To look closer at the catalysts tested a selected range of low, medium and high loaded catalysts are presented in figure 4.2.1.2.

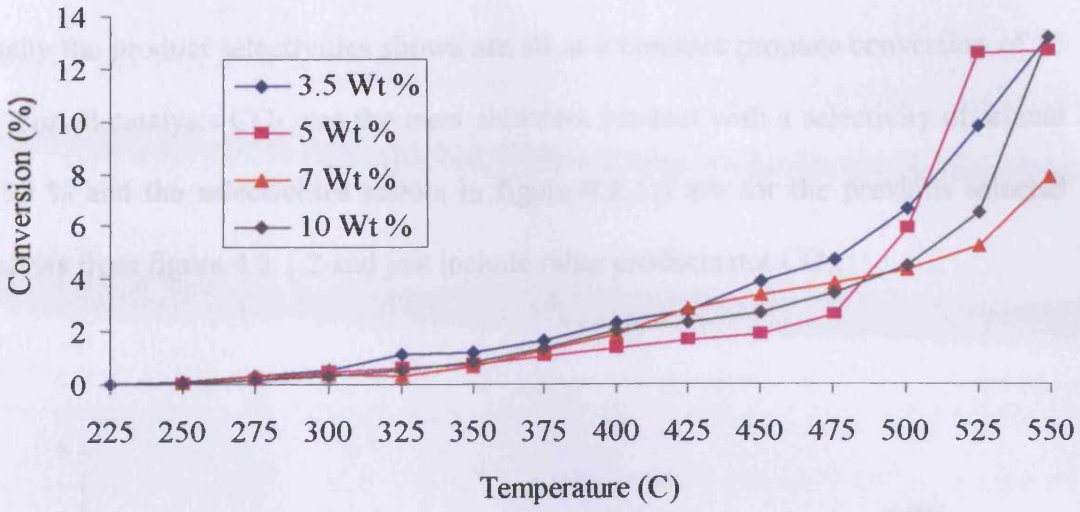

Figure 4.2.1.2: Conversion difference calculated for a select number of V_2O_5 silica supported catalysts.

Figure 4.2.1.2 shows the conversion of a selection of catalysts over a range of loadings. Conversion for all increases gradually with the 3.5 Wt % having both the lowest light-off temperature of 225°C and having the best rate of conversion up to 500°C. At 525°C the 5 Wt % loading has the best rate of conversion. Between 500°C and 525°C figure 4.2.1.2 shows that the activity of the higher loadings of 7 and 10 Wt % is decreased when compared to the lower loadings but these catalysts are active still at higher temperatures unlike the lower loadings. This suggests that having a highly dispersed vanadium oxide species on the silica in the lower loadings is beneficial to the activity of the catalysts at lower temperatures. At 550°C the 3.5, 5 and 10 Wt % catalysts all show very similar activity and are much more active when compared to the 7 Wt % loading.

The selectivity to products are shown in figure 4.2.1.3 and to compare the catalysts equally the product selectivities shown are all at a constant propane conversion of 10 %. For all catalysts CO_2 was the most abundant product with a selectivity of around 90-95 % and the selectivities shown in figure 4.2.1.3 are for the previous selected catalysts from figure 4.2.1.2 and just include other products not CO_2.

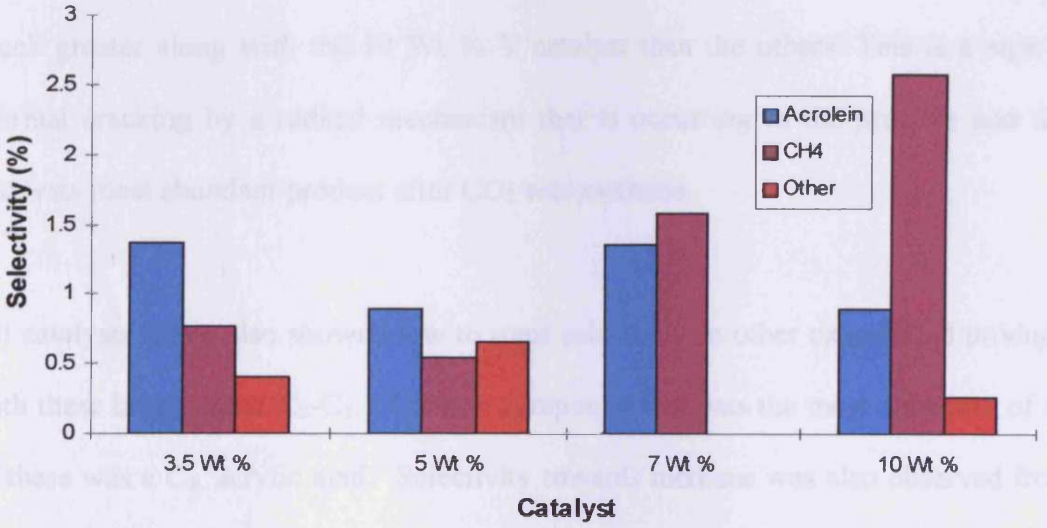

Figure 4.2.1.3: Product selectivity for V_2O_5 silica supported catalysts at a constant conversion of 10%.

The selectivity to other products at 10 % conversion is shown in figure 4.2.1.3. CO_2 was by far the most abundant product produced and comes from the complete oxidation of propane. The most abundant selectively oxidised product in all catalysts was acrolein. The 3.5 Wt % catalyst had the best selectivity to acrolein when compared to all the V_2O_5/SiO_2 catalysts tested rising up to just under 2 % at a slightly higher rate of conversion. This is significant as this catalyst also had overall the best activity of all those tested.

3.5 Wt % and the other catalysts that it is compared to. This higher temperature co be the reason that at 10 % conversion the 7 Wt % catalyst selectivity to methan much greater along with the 10 Wt % V catalyst than the others. This is a sign thermal cracking by a radical mechanism that is occurring to the propane and catalysts most abundant product after CO_2 was methane.

All catalysts tested also showed low to trace selectivity to other oxygenated produ with these being either C_2-C_3. The one compound that was the most abundant of of these was a C_3, acrylic acid. Selectivity towards methane was also observed fr the process of thermal cracking via a radical mechanism in all catalysts with selectivity towards it increasing when the temperatures tested for these reactions w at their highest. As mentioned before the 7 Wt % activity was lower than the ot catalysts tested at higher temperatures. This may suggest that when this catalyst tested more propane was converted to methane by a radical mechanism wi compared to the other catalysts rather than converting the propane to selectiv oxidised products. The 7 Wt % catalyst did show selectivity to acrolein at mu higher temperatures possibly meaning the acrolein was made in the gas phase, wh this catalyst was tested only trace amounts of other C_3 oxygenated products w observed.

All other Wt % loaded catalysts tested in this study gave similar results showing selectivity to acrolein as the most abundant selectively oxidised product, some other C_3 oxygenates in trace amounts and methane. For all catalysts CO_2 was the main product and this was in the region of 90-95 %.

4.2.2: Silica supported molybdenum oxide catalysts.

The oxidation of propane over a range of MoO_3/SiO_2 catalysts is shown in figure 4.2.2.1. A range of activity was exhibited which was dependent on molybdenum loading. These catalysts are presented here with comparison to pelleted silica and just a blank tube.

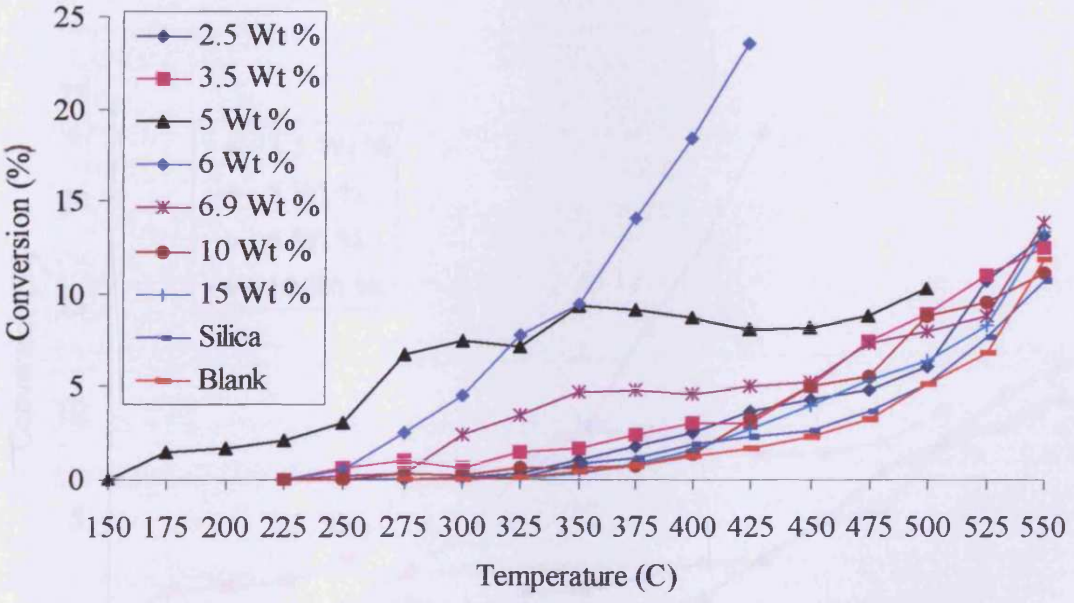

Figure 4.2.2.1: Conversion difference calculated for a range of MoO_3 silica supported catalysts.

The results shown in figure 4.2.2.1 show that a range wide of activity is exhibited and this was dependent on the loading of molybdenum. The 5 Wt % loading was active with a much lower light-off temperature of 150°C compared to around 225 to 250°C for the other loadings. The 6 Wt % catalyst was by far the most active having the greatest activity around 400-425°C. All other loadings except the 6.9 Wt % had a very similar activity with this catalyst showing increased activity between 300 and 425°C. When compared to the blank and silica the activity of the supported catalysts is greater up to 525°C. At much greater temperatures the silica and blank tube show much increased activity but this can be put down to gas phase chemistry.

Figure 4.2.2.2 compares a smaller range of catalysts covering low, medium and high loadings and there are some noticeable differences.

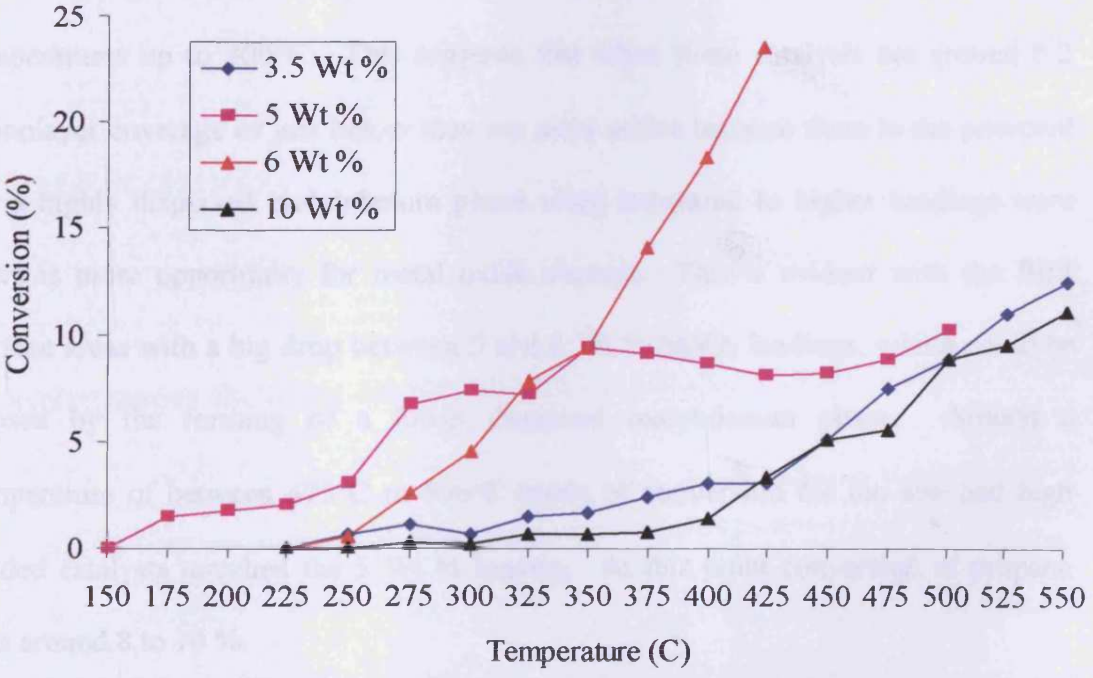

Figure 4.2.2.2: Comparison of various catalysts MoO_3 on silica.

Figure 4.2.2.2 shows that the lower 3.5 Wt % and the higher 10 Wt % catalysts are much less active at lower temperatures than the medium loadings. The 5 Wt % catalyst has a light-off temperature that is around 75°C lower than other silica supported molybdenum oxide catalysts and this was reproducible. The 6 Wt % catalyst was by far the most active and by 425°C it was converting propane at around 23 % consuming nearly all of the molecular oxygen in the reaction feed. This compares to under 5 % activity for the 3.5 and 10 Wt % catalysts at the same temperature and approximately 10 % conversion for the 5 Wt %. The 6 Wt % catalyst had 0.204 monolayer coverage of the silica by MoO_3 which was calculated to be a loading of 29.5 Wt %.

The 5 Wt % conversion was steadier than the 6 Wt % but much more increased than the other catalyst loadings. When comparing the 3.5 and 10 Wt % loadings the 3.5 Wt % catalyst had the higher rate of conversion overall, especially at lower temperatures up to 400°C. This suggests that when these catalysts are around 0.2 monolayer coverage or just below they are more active because there is the potential for a highly dispersed molybdenum phase when compared to higher loadings were there is more opportunity for metal oxide clusters. This is evident with the BET surface areas with a big drop between 5 and 6 Wt % MoO_3 loadings, which could be caused by the forming of a lower dispersed molybdenum phase. Around a temperature of between 475°C to 500°C levels of conversion for the low and high loaded catalysts matched the 5 Wt % loading. At this point conversion of propane was around 8 to 10 %.

Figure 4.2.2.3 shows product selectivities excluding CO_2, which was the most abundant product and is approximately 95 % for all temperatures and conversion analysed. These are presented at a propane conversion of 10 % and include the previously selected range of catalysts from figure 4.2.2.2 and are just for the partial products detected.

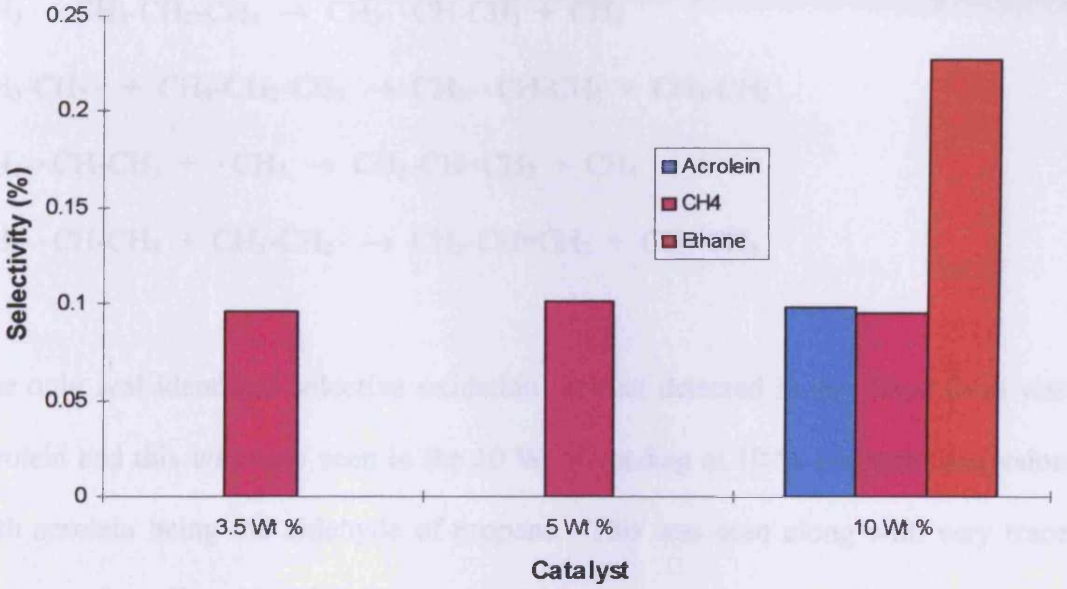

Figure 4.2.2.3: Product selectivities for various MoO_3 silica supported catalysts at a constant conversion of 10%.

Figure 4.2.2.3 shows that when testing the catalysts for the reaction of propane with molecular oxygen the major product of any presented catalyst was always carbon dioxide in the range of around 98 %. This was true for any temperature tested from initial light-off to the highest temperatures tested. The 6 Wt % loading only product at any point was CO_2. The 3.5, 5 and 10 Wt % molybdenum oxide on silica catalysts produced trace amounts of other substances. The bulk of these came via the radicalic mechanism of propane to its components with methane being the most predominant,

ethane and trace amounts of propene with more propane possibly being reduced by oxidative dehydrogenation to propene. This mechanism can be shown to produce these products by the following way:

$CH_3\text{-}CH_2\text{-}CH_3 \rightarrow CH_3\cdot + \cdot CH_2\text{-}CH_3$

$CH_3\cdot + CH_3\text{-}CH_2\text{-}CH_3 \rightarrow CH_3\text{-}\cdot CH\text{-}CH_3 + CH_4$

$CH_3\text{-}CH_2\cdot + CH_3\text{-}CH_2\text{-}CH_3 \rightarrow CH_3\text{-}\cdot CH\text{-}CH_3 + CH_3\text{-}CH_3$

$CH_3\text{-}\cdot CH\text{-}CH_3 + \cdot CH_3 \rightarrow CH_3\text{-}CH{=}CH_2 + CH_4$

$CH_3\text{-}\cdot CH\text{-}CH_3 + CH_3\text{-}CH_2\cdot \rightarrow CH_3\text{-}CH{=}CH_2 + CH_3\text{-}CH_3$

The only real identified selective oxidation product detected in any trace form was acrolein and this was only seen in the 10 Wt % loading at 10 % propane conversion with acrolein being the aldehyde of propene. This was seen along with very trace amounts of acrylic acid which is the acid of propene

The other catalysts tested in this series again showed the greatest selectivity to CO_2 at approximately 98 %. They all showed trace selectivity to acrolein and to a lesser extent acrylic acid and also to methane. The levels of C_3 oxygenates other than acrolein over all silica supported molybdenum catalysts was only trace amounts.

Figure 4.2.2.4 shows a comparison of activities for medium loaded molybdenum oxide silica supported catalysts and just silica for the oxidation of propane.

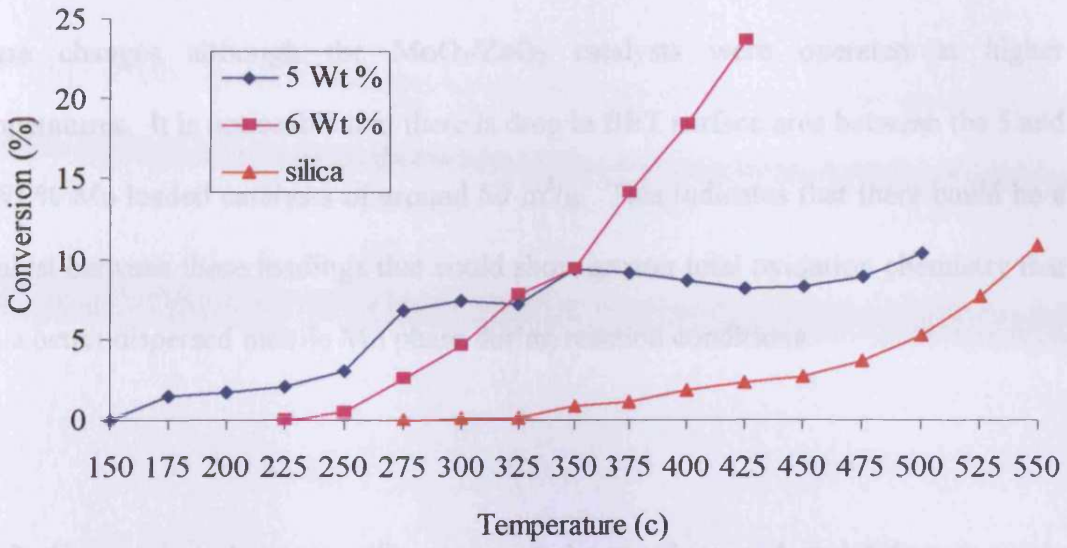

Figure 4.2.2.4: Comparison of conversions of medium loaded MoO_3/SiO_2 catalysts and silica blank.

As described earlier the medium loaded catalysts showed greater activity at lower temperatures than the other catalysts tested. Figure 4.2.2.4 illustrates this activity by comparing the medium loaded catalysts to a silica blank tested under the same conditions. This shows that firstly the activity of the catalysts is dependent on the molybdenum loading being much more active throughout the temperature range studied than silica alone. These medium loaded catalysts show selectivity for CO_2 much greater than the other loadings tested and it's the 6 Wt % loadings only product at any temperature tested and this catalyst is 0.204 of the calculated theoretical monolayer coverage. Similar high total oxidation activity was observed when ZrO_2 catalysts containing Mo that were much closer to monolayer coverage [8]. It was noted from *in situ* Raman studies that when the catalyst was running at reaction conditions the Mo spreads over the support and maximum Mo dispersion is achieved at theoretical monolayer coverage. A similar highly dispersed Mo phase on the silica support could be formed on the 6 Wt % Mo catalyst that may account for the high

oxidation activity although *in situ* Raman studies carried out did not indicate any phase changes although the MoO_3/ZnO_2 catalysts were operated at higher temperatures. It is noticeable that there is drop in BET surface area between the 5 and 6 Wt % Mo loaded catalysts of around 50 m^2/g. This indicates that there could be a catalyst between these loadings that could show greater total oxidation chemistry that has a better dispersed mobile Mo phase during reaction conditions.

4.2.3: Comparison between silica supported vanadium and molybdenum oxide catalysts.

Comparing the two different oxide systems both reacted in a very similar fashion to each other excluding the high total oxidation activity of the 5 and 6 Wt % medium loaded Mo catalysts. Figure 4.2.3.1 shows a comparison of conversion for a low and high (3.5 and 10 Wt %) loaded catalysts.

The lower loaded catalysts for both systems are more active at lower temperatures than their higher loaded counterparts. Only at 425°C was the 10 Wt % Mo catalyst displaying better activity than a lower loaded catalyst. The 3.5 Wt % Mo catalyst also displays greater activity than the 3.5 Wt % V catalyst at all temperatures. The one major difference is the selectivity to products other than CO_2.

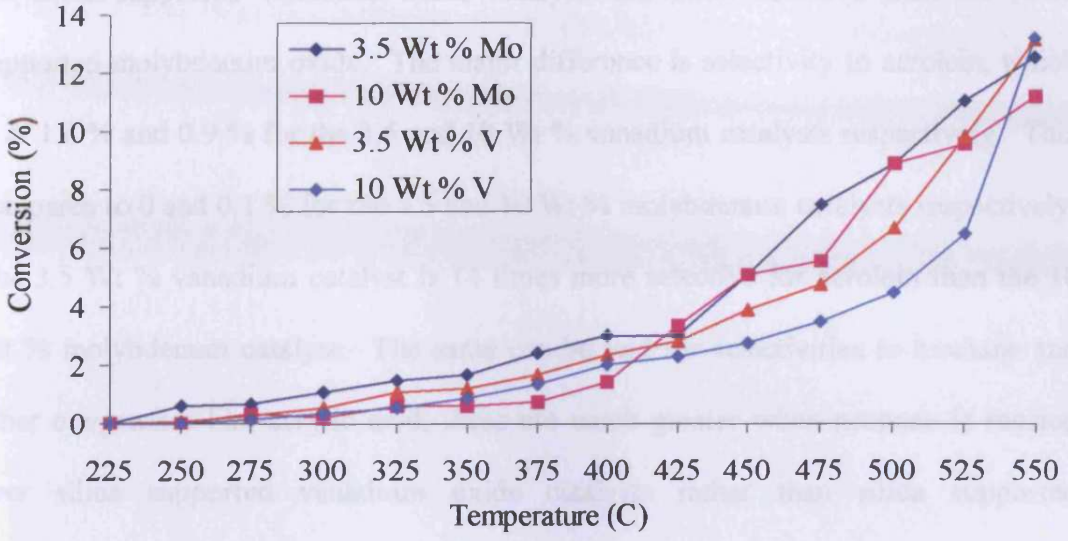

Figure 4.2.3.1: Comparison of conversion for propane oxidation for high and low loaded silica supported Mo and V oxide catalysts.

Figure 4.2.3.2 shows the selectivity to products excluding CO_2, which is always the major product obtained.

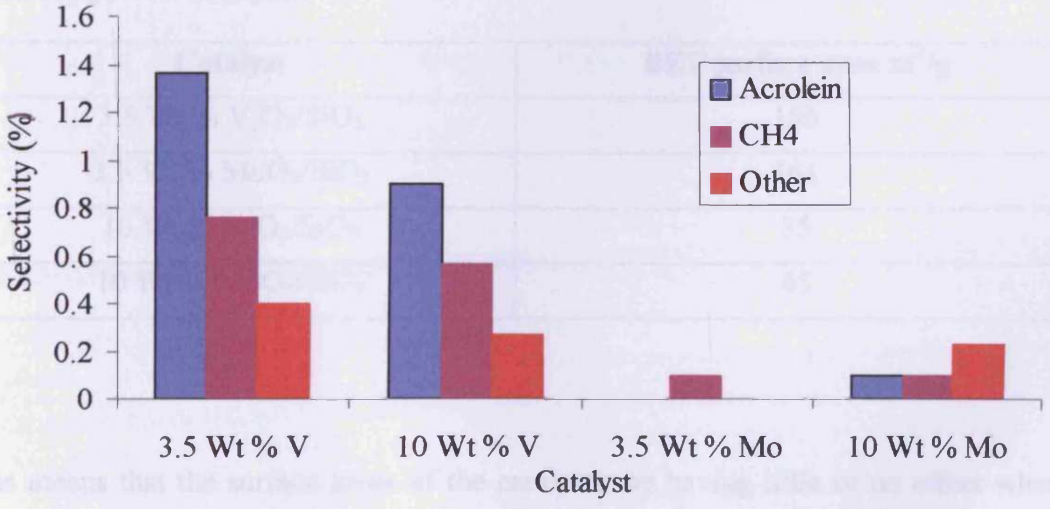

Figure 4.2.3.2: Selectivity to products over high and low loaded Mo and V oxide catalysts other than CO_2 at constant conversion of 10%.

These figures are calculated at a constant conversion of 10 %. This figure shows that the silica supported vanadium oxide catalysts are more selective than the silica supported molybdenum oxide. The major difference is selectivity to acrolein, which is at 1.4 % and 0.9 % for the 3.5 and 10 Wt % vanadium catalysts respectively. This compares to 0 and 0.1 % for the 3.5 and 10 Wt % molybdenum catalysts respectively. The 3.5 Wt % vanadium catalyst is 14 times more selective for acrolein than the 10 Wt % molybdenum catalyst. The same can be said for selectivities to methane and other oxygenates like acrylic acid, these are much greater when propane is reacted over silica supported vanadium oxide catalysts rather than silica supported molybdenum.

The surface areas are also comparable as shown in table 4.2.3.1.

Table 4.2.3.1: Comparison of BET surface areas for 3.5 and 10 Wt % Mo and V silica supported catalysts.

Catalyst	BET surface area m^2/g
3.5 Wt % V_2O_5/SiO_2	156
3.5 Wt % MoO_3/SiO_2	161
10 Wt % V_2O_5/SiO_2	35
10 Wt % MoO_3/SiO_2	45

This means that the surface areas of the catalysts are having little or no effect when the two different oxide systems are compared. The increased selectivity to partial oxidation products in the vanadium oxide system may suggest that on the surface of

the silica supported vanadium catalysts there are more active sites present for this. The surface of the silica supported molybdenum oxide catalysts might contain species or active sites for combustion.

4.2.4: Boron nitride supported vanadium oxide catalysts.

These results show that when silica supported molybdenum and vanadium oxides are compared their activity is pretty equal but selectivity to partially oxidised products is much greater in the vanadium system. A different support was used to see if any improvements to selectivity occurred or improved activity. Boron nitride has not been studied extensively as a support but some recent literature using platinum supported boron nitride catalysts have been reported. [6]. Boron nitride differs greatly to silica when the two are compared. Firstly silica generally has a high surface area (BET surface area of 194 m^2/g in this study) compared to boron nitrides low surface area (BET surface area of 7 m^2/g here). Secondly both react differently in the presence of water as silica is hydrophilic and boron nitride is hydrophobic. These factors could lead to interesting differences in the way the two supports react when activity and selectivities are compared.

Figure 4.2.4.1 shows the activity of a series of vanadium catalysts supported on boron nitride and tested for propane oxidation.

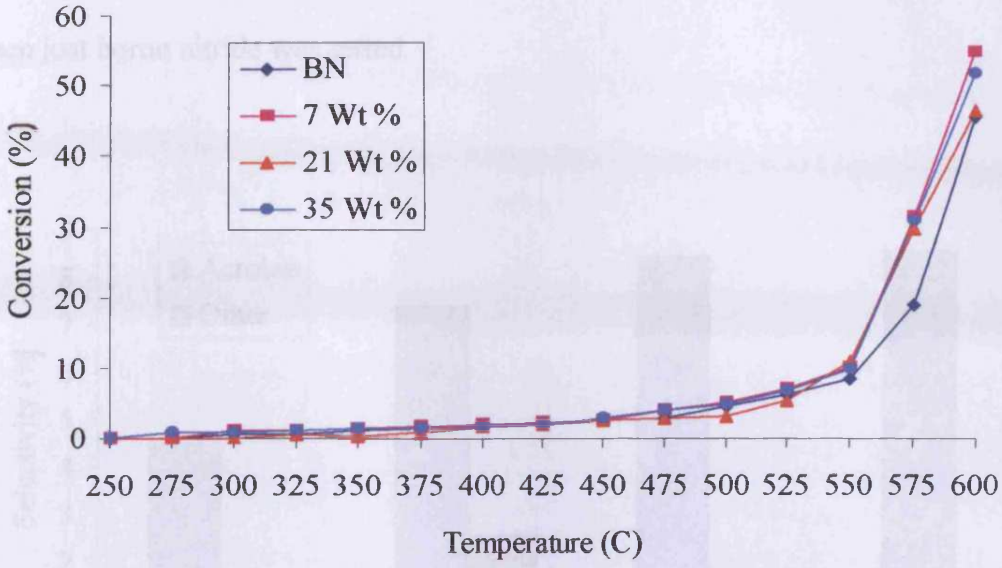

Figure 4.2.4.1. Activity for propane oxidation over Boron nitride supported vanadium oxide catalysts.

Figure 4.2.4.1 shows that for the boron nitride supported vanadium oxide catalysts and the boron nitride there is little difference between activity when comparing them at any temperature with all showing broadly similar activity. Only at higher temperatures when comparing the supported catalyst's activity against just the boron nitride the activity of the supported catalysts is slightly higher between 550-600°C.

Figure 4.2.4.2 shows the selectivity to partially oxidised products at 10 % conversion. Acrolein is the most abundant selectively oxidised product in all the boron nitride catalysts tested. These range from approximately 7.5 to 8.5 % in the boron nitride supported vanadium oxide catalysts to around 4 % selectivity when the boron nitride blank was tested. This shows that although boron nitride itself shows selectivity to acrolein the addition of vanadium oxide to the surface doubles this selectivity. This is also true for other partially oxidised species produced like acrylic acid which have a

selectivity of around 1.5 to 2 % on the supported catalysts compared to around 0.5 % when just boron nitride was tested.

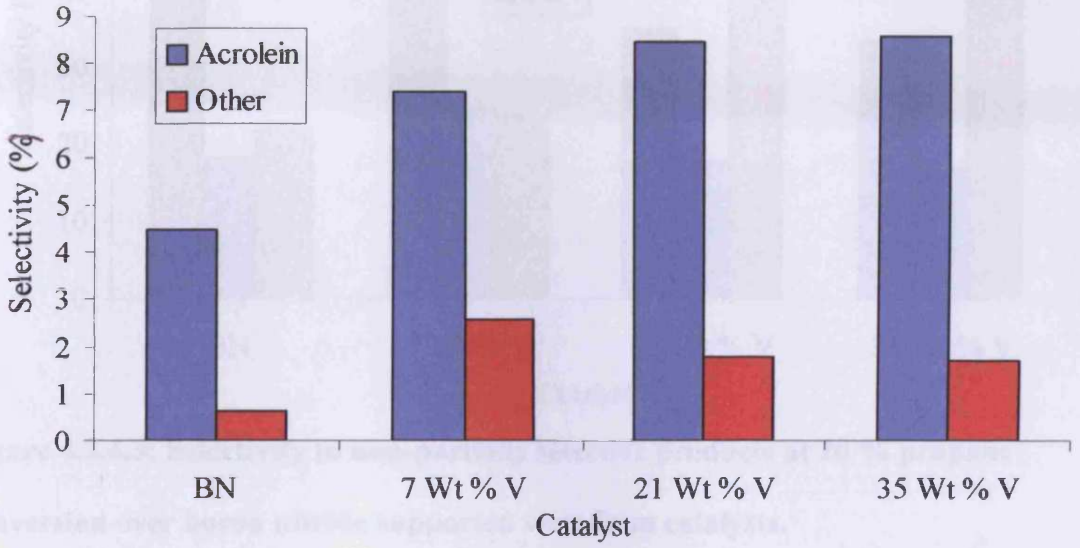

Figure 4.2.4.2: Selectivity to partially oxidised products at 10 % propane conversion on boron nitride supported vanadium oxide catalysts.

Figure 4.2.4.3 shows the selectivities to other products made at a constant propane conversion of 20 %. Acrolein at this rate of conversion is still made at around the same selectivity as well as other products like acrylic acid but the selectivity to other products change. CO_2 is the dominant non-selective product that was seen over the lower temperature range tested. At higher temperatures tested methane and carbon monoxide are both abundant. Over all the catalysts tested including the boron nitride blank methane selectivity is almost the same. The major difference between the catalysts is that the higher loading of 21 and 35 Wt % vanadium show a greater selectivity towards carbon monoxide around double that of the blank and 7 Wt % catalyst. These catalysts show selectivity for carbon dioxide.

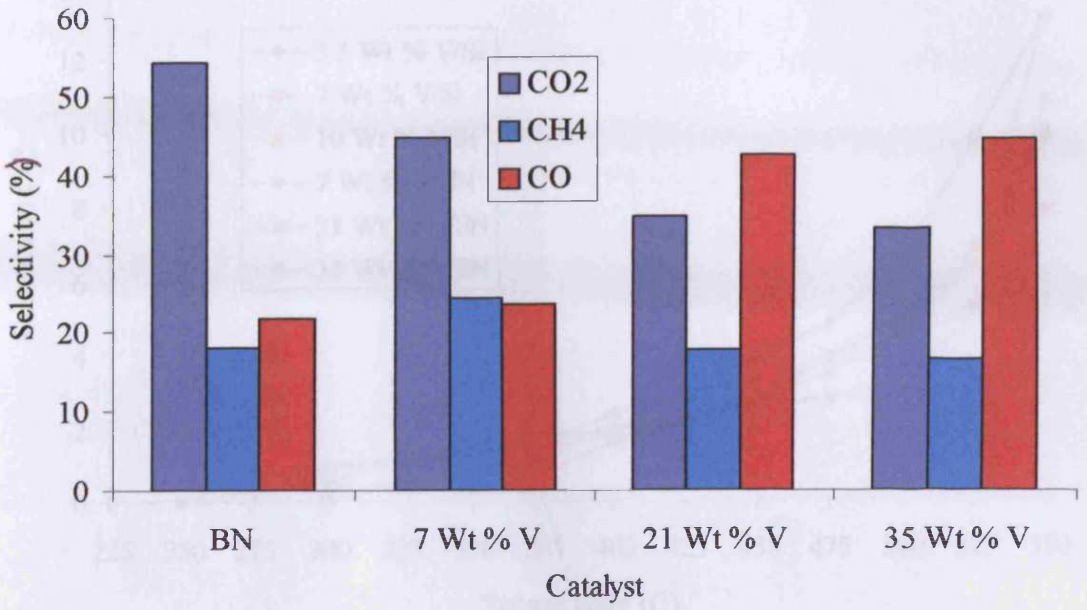

Figure 4.2.4.3: Selectivity to non-partially selective products at 20 % propane conversion over boron nitride supported vanadium catalysts.

4.2.5 Comparison of boron nitride and silica supported vanadium oxide catalysts.

Figure 4.2.5.1 shows a comparison of the activity for propane oxidation over boron nitride and silica supported vanadium oxide catalysts. The catalysts all show similar activity in the lower temperature range tested. After 425°C the 3.5 Wt % V_2O_5/SiO_2 shows an increased activity compared to the other catalysts tested. Also at 425°C the 21 Wt % V_2O_5/BN catalyst shows the worst activity of those tested although this activity recovers at 550°C. The activity presented shows that whether using high surface area silica or low surface area boron nitride the activities are pretty similar for the oxidation of propane. This suggests that gas phase oxidation is predominant due to boron nitride being an inert material.

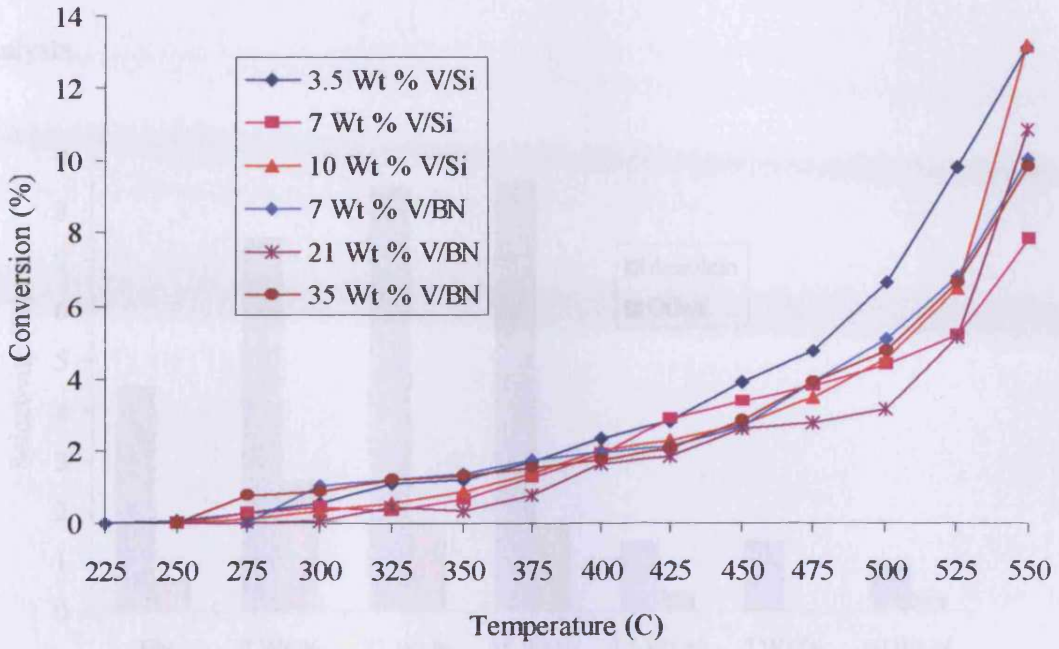

Figure 4.2.5.1: Activity for propane oxidation over boron nitride and silica supported vanadium oxide catalysts.

When the selectivity of the two supports are compared there are much improved results. Figure 4.2.5.2 shows the selectivity to acrolein and other selectivity oxidised products like acrylic acid at a constant propane conversion of 10 %.

Although similar activities in both systems are seen, the boron nitride supported vanadium oxide catalysts display much increased selectivity to acrolein and other C_3's like acrylic acid. The selectivity to acrolein in the 21 and 35 Wt % V/BN is around 8 times greater than in the silica supported catalysts at the same rate of conversion. The bare boron nitride also shows increased selectivity being around 4 times greater than the silica supported catalysts for acrolein. For other products like acrylic acid the

boron nitride supported catalysts are about 5 times more selective than the silica based catalysts.

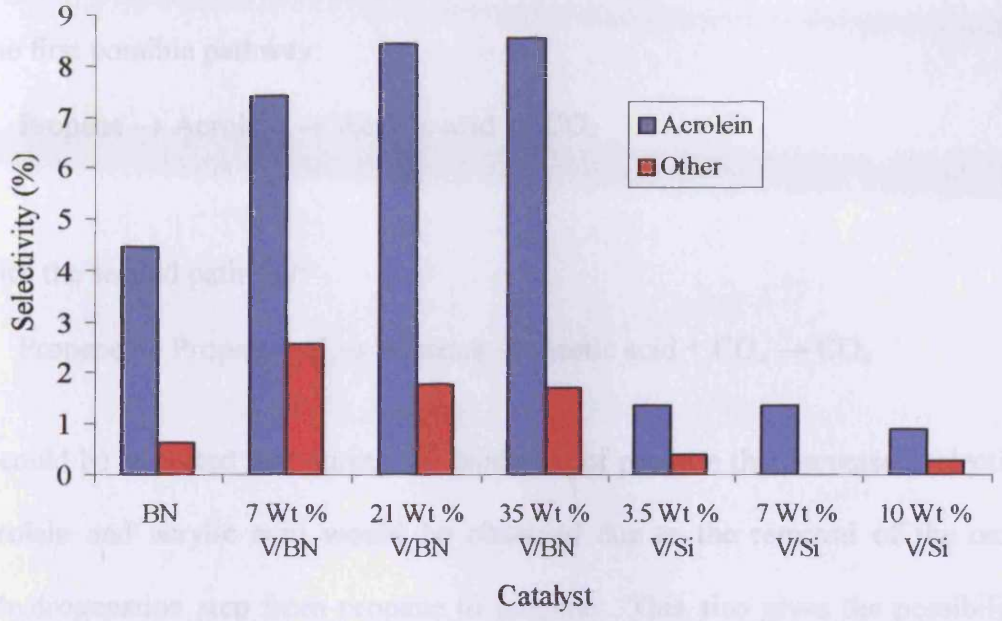

Figure 4.2.5.2: Selectivity for acrolein at constant propane conversion of 10 % for various silica and boron nitride supported vanadium oxide catalysts.

4.3: Propene oxidation.

All the catalysts were tested for propene oxidation using the methods described in section 2.2. From the results obtained for propane oxidation which included the production of the alkene aldehyde, acrolein as the major partial oxidation product the oxidation of propene was tested to observe whether there was similarities between the oxidation of both gases in both conversion and selectivity. The partial oxidation of propane to acrolein suggests that the initial reaction of the propane is to undergo oxidative dehydrogenation to propene. The propene then is partially oxidised to acrolein, which can be further oxidised to acrylic acid and combustion products. M.

Ai [3] proposed that the oxidation of propane goes via either two routes with the first step the oxidative dehydrogenation to propene. This is followed by

The first possible pathway:

- Propene → Acrolein → Acrylic acid → CO_x

With the second pathway:

- Propene → Propan-2-ol → Acetone → Acetic acid + CO_x → CO_x

It could be expected that during the oxidation of propene that increased selectivity to acrolein and acrylic acid would be observed due to the removal of the oxidative dehydrogenation step from propane to propene. This also gives the possibility that selectivity towards acrolein may be seen at lower temperatures, as less energy would be needed to initially turn propane to propene.

4.3.1: Silica supported vanadium oxide catalysts.

The oxidation of propene over a range of silica supported vanadium oxide catalysts is shown in figure 4.3.1.1. A range of activity was exhibited and this was dependent on vanadium loading. These catalysts were also compared to a blank tube and bare pelleted silica.

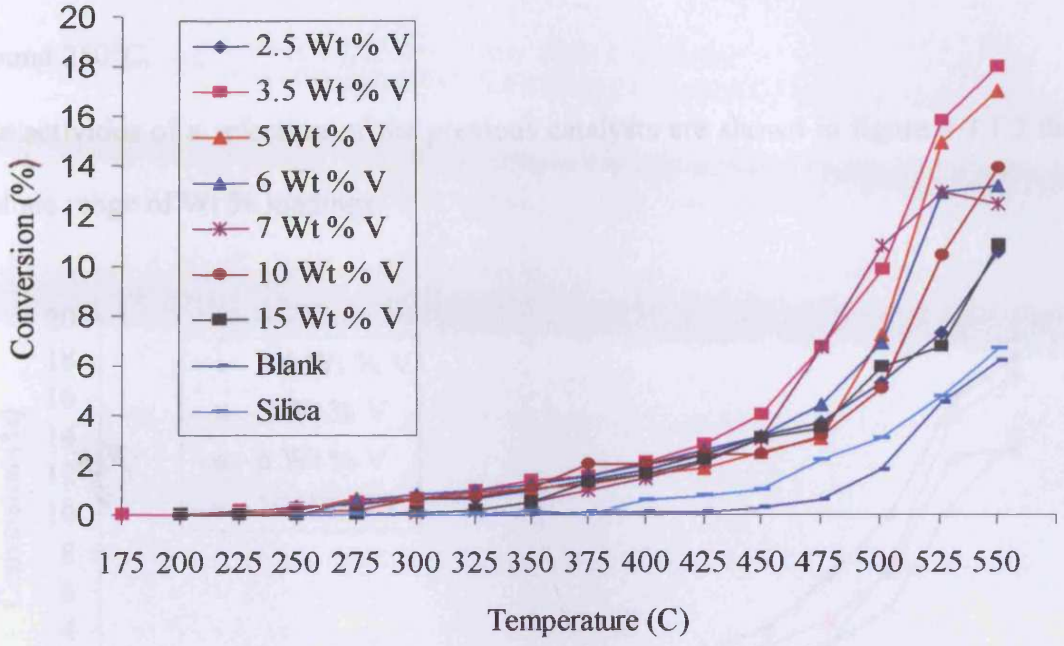

Figure 4.3.1.1: Activity for propene oxidation calculated over a range of silica supported vanadium oxide catalysts.

The vanadium supported catalysts all showed broadly similar activity up to 425°C. They all displayed similar light-off temperatures of between 175 and 200°C. Between 450 and 500°C the 3.5 and 7 Wt % loaded catalysts showed an increased activity compared to the other loadings. After 500°C a wider range of activities were demonstrated by the various loadings with the 3.5 and 5 Wt % catalysts the most active between 525 and 550°C with activities of around 17-18 % conversion of propene. The medium loadings of 6, 7 and 10 Wt % all demonstrated a similar activity at 550°C of around 12 to 14 % conversion. The lowest and highest loadings tested (2.5 and 15 Wt %) were the least active at higher temperatures with conversion levels of around 10 %. All loadings tested at these temperatures were more active

than the silica and blank reactor tube whose light-off temperatures were also higher at around 250°C.

The activities of a selection of the previous catalysts are shown in figure 4.3.1.2 that include range of Wt % loadings.

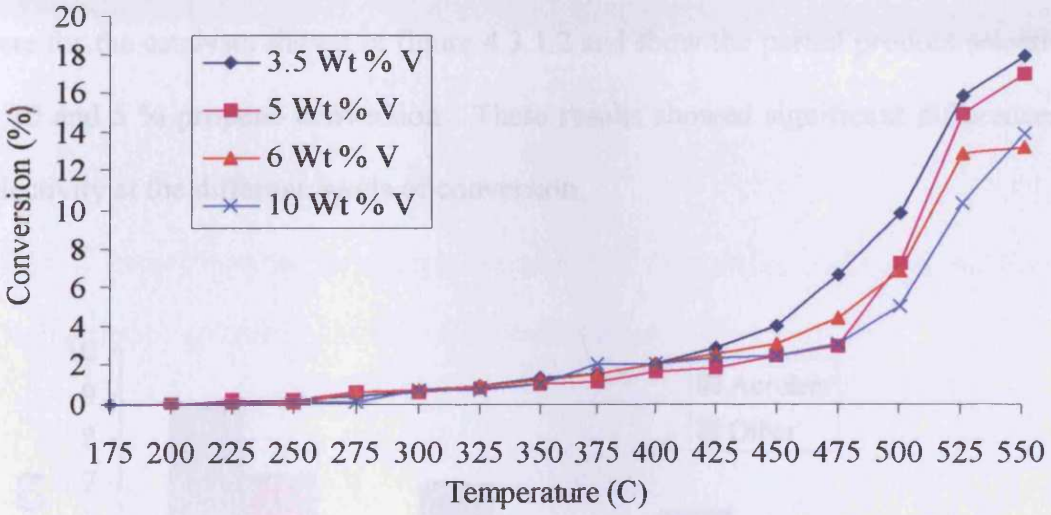

Figure 4.3.1.2: A selection of silica supported vanadium catalysts for the oxidation of propene.

In figure 4.3.1.2 the 3.5 Wt % catalyst showed much greater activity after 425°C than the other medium loaded catalysts and was around 2-3 % more active. After 500°C the 5 Wt % catalyst showed similar activity to the 3.5 Wt % and they were about 4 % higher in conversion than the 6 and 10 Wt % loadings. This higher activity in low to medium loaded catalysts was seen in the propane studies using silica supported vanadium catalysts in section 4.2.1 where the 3.5 Wt % catalyst was also the most active. This activity could be due to a much more dispersed active phase present in the low to medium silica supported vanadium catalysts. Having very low levels of vanadium present on the surface (~2.5 Wt %) seems to have an activating effect on

conversion when compared to bare silica but better activation was found in the higher loadings of 3.5 and 5 Wt % as well as other higher loadings.

The selectivities of products other than CO_2, which was the most abundant at higher levels of conversion analysed, are shown in figure 4.3.1.3 and figure 4.3.1.4. These were for the catalysts shown in figure 4.3.1.2 and show the partial product selectivity at 10 and 5 % propene conversion. These results showed significant differences in selectivity at the different levels of conversion.

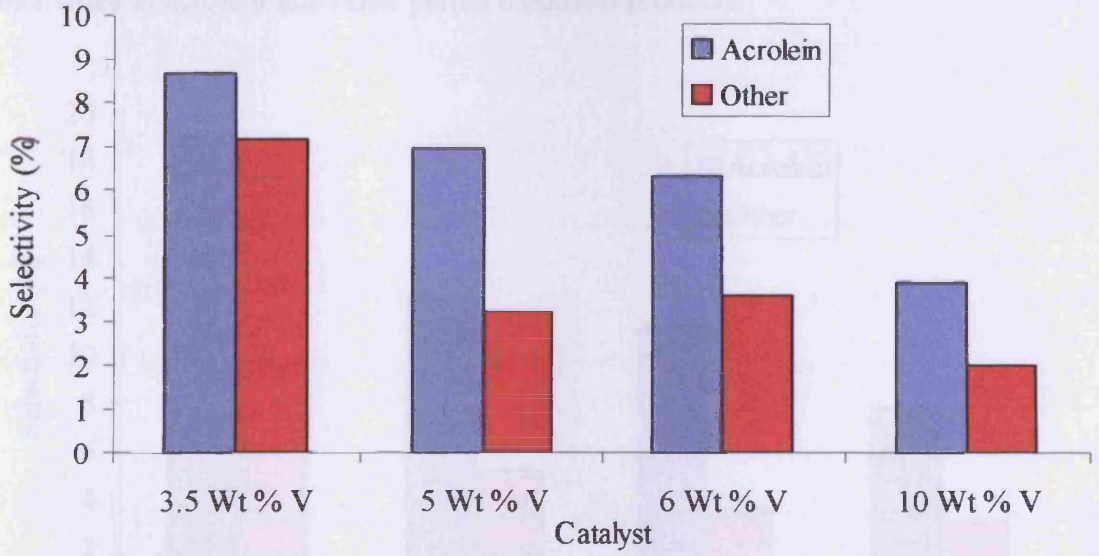

Figure 4.3.1.3: Selectivity to products other than CO_2 at 10 % propene conversion over silica supported vanadium oxide catalysts.

At the higher level of 10 % propene conversion shown in figure 4.3.1.3 the selectivity to acrolein was highest in the lower loaded vanadium catalysts. The selectivity to acrolein falls the higher the loading tested. The selectivities range from approximately 9 % for the 3.5 Wt % loading down to around 5 and 7 % selectivity for the 6 and 5 Wt % catalysts respectively, with the 10 % Wt loading having a selectivity

of around 4 %. This was also true when comparing the other products made like acrylic acid. The 3.5 Wt % had the highest selectivity at around 7 % compared to the 10 Wt % loading which had a selectivity of approximately 2 % with the medium loadings displaying selectivity at around 3 to 4 %. At this level of conversion the only other product seen was CO_2 which was the most abundant product made at around 85-95 % selectivity with trace amounts of other C_2 and C_3 oxygenates also present.

When a lower level of conversion is analysed the results are improved for the selectivities to acrolein and other partial oxidation products.

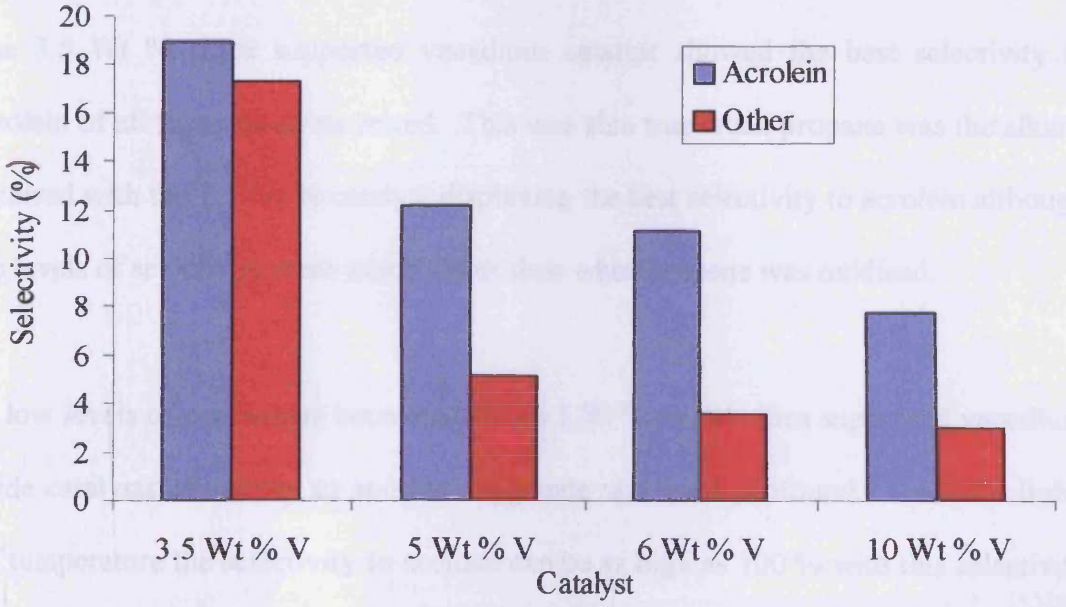

Figure 4.3.1.4: Selectivity to products other than CO_2 at 5 % propene conversion over silica supported vanadium oxide catalysts.

The 3.5 Wt % selectivity, shown in figure 4.3.1.4 to acrolein increases from 9 % at 10 % propene conversion to approximately 19 % at 5 % propene conversion. This was also true of the other partial oxidation products made which increased from 7 to 17 %

selectivity at the lower 5 % propene conversion level. The other loadings follow the same pattern with levels of selectivity to acrolein increasing by 4 to 5 % at a lower level of 5 % propene conversion. The selectivities to other products like acrylic acid increased by 2 to 3 %, with the trend that selectivity to acrolein and other partial oxidation products decreased with loading was followed at the lower 5 % propene conversion level.

At these levels of conversion the major product was CO_2 with selectivities between 80 and 90 % for the 5, 6 and 10 Wt % loadings down to approximately 65 % for the lower 3.5 Wt % catalyst.

The 3.5 Wt % silica supported vanadium catalyst showed the best selectivity to acrolein of all these catalysts tested. This was also true when propane was the alkane oxidised with the 3.5 Wt % catalyst displaying the best selectivity to acrolein although the levels of selectivity were much lower then when propene was oxidised.

At low levels of conversion between 0.01 to 1.50 % on the silica supported vanadium oxide catalysts selectivity to another oxygenate was quite profound. From the light-off temperature the selectivity to acetone can be as high as 100 % with this selectivity dropping as the temperature increases with the selectivity to CO_2 increasing in its place. This product generally disappears at around 375-400°C before the production of acrolein and acrylic acid begins. This product was not observed when the silica supported molybdenum oxide catalysts were tested using the same conditions and when the boron nitride supported vanadium catalysts were also tested. This suggests that the silica supported vanadium oxide catalysts are capable of inserting an oxygen

atom to the secondary carbon of the alkene with a rearrangement of the hydrogen present upon the alkene to produce the ketone.

4.3.2: Silica supported molybdenum oxide catalysts.

A range of silica supported molybdenum oxide catalysts were tested for propene oxidation. The methods used are described in section 2.2. The results of the activity of the catalysts are shown in figure 4.3.2.1 and are compared to silica and a blank tube.

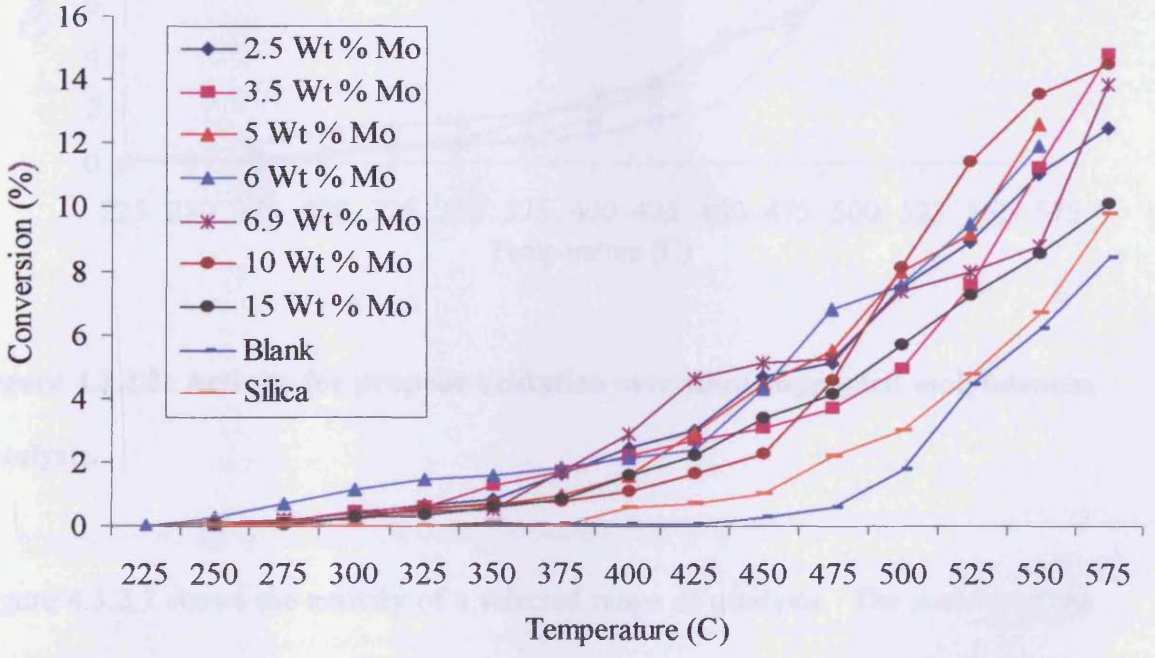

Figure 4.3.2.1: Activity for propene oxidation over silica supported molybdenum oxide catalysts.

Figure 4.3.2.1 showed that when studying the silica supported molybdenum oxide catalysts, activity was dependent on molybdenum loading as a range of activities are obtained. All catalysts have light-off temperature of between 225 and 250°C. At lower temperatures between 250 and 375°C the 6 Wt % catalyst was the most active which was consistent from propane oxidation although this activation was much lower in the propene oxidation. Between 375 and 450°C the 6.9 Wt % catalyst was the most active and the 10 Wt % catalyst was the least active.

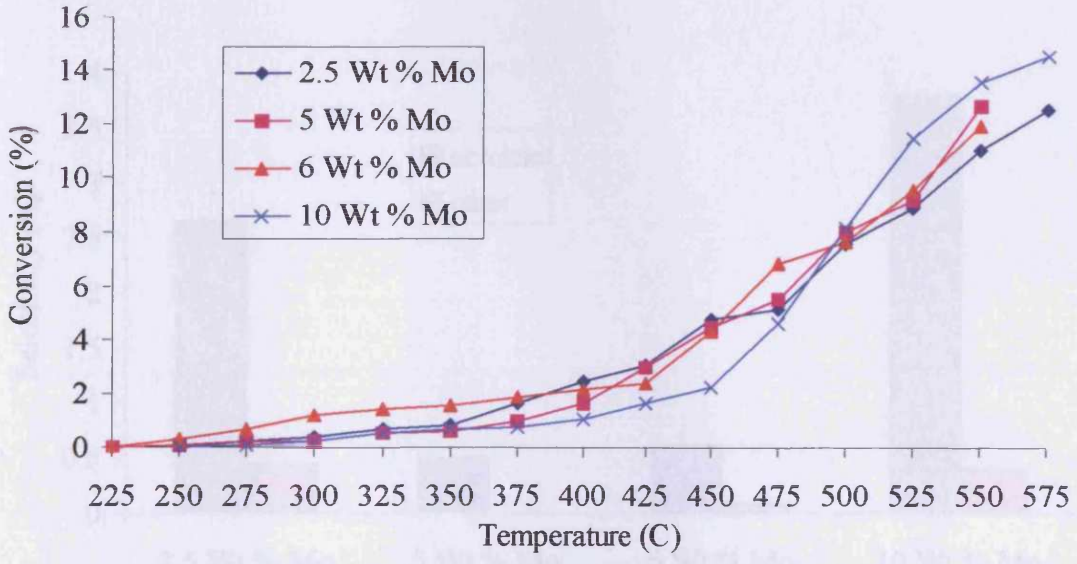

Figure 4.3.2.2: Activity for propene oxidation over silica supported molybdenum catalysts.

Figure 4.3.2.2 shows the activity of a selected range of catalysts. The activity of the 10 Wt % catalyst changes after 475°C. Before this temperature its activity is much lower than the other loadings from 375°C but by 500°C it was the most active catalyst for the rest of the temperatures analysed. The activity of the blank and silica compared to the supported catalysts are considerably lower between 250 and 450°C.

When the selectivities of the silica supported molybdenum oxide catalysts were compared the same results occur that were evident when the selectivities of the vanadium catalysts were compared. They show that the selectivity to partial oxidation products depends on the level of conversion.

Figure 4.3.2.3 shows the selectivity to products other than CO_2 at 10 % propene conversion. For all of these catalysts including those not shown, the selectivity to CO_2 was always the greatest at around 90-95 %.

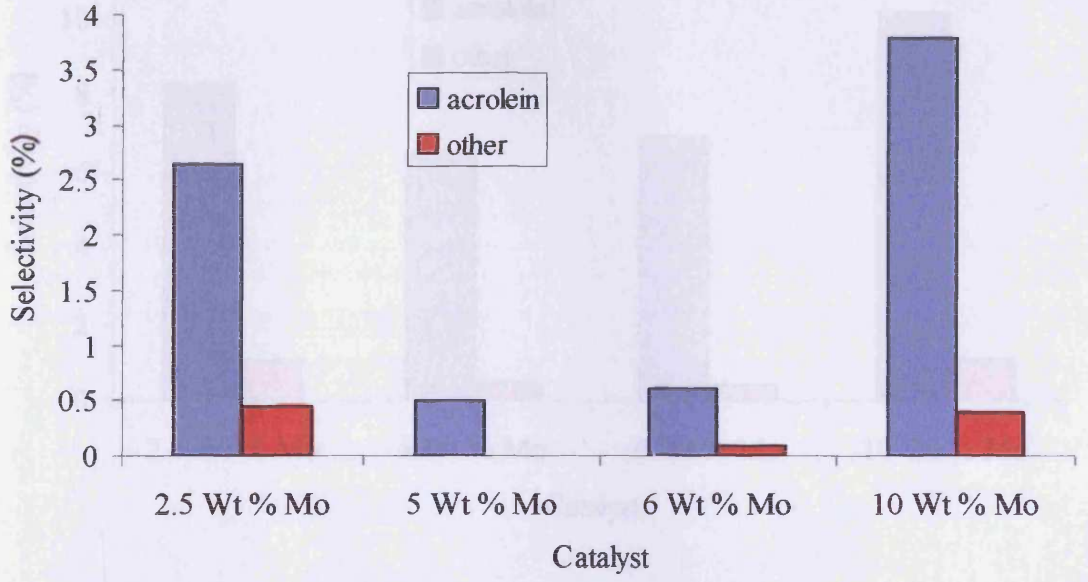

Figure 4.3.2.3: Selectivity to products other than CO_2 at 10 % propene conversion over silica supported molybdenum catalysts.

A wide range of selectivities for acrolein was shown, dependent on the loading of the catalyst. For the lower 2.5 and higher 10 Wt % catalysts this selectivity was approximately 2-3 %. The medium 5 and 6 Wt % loaded catalysts the selectivity to acrolein was decreased to around 0.5 % and these catalysts also have little or no

selectivity to other partial oxidation products like acrylic acid. The lower and higher loaded catalysts had a selectivity to other partial products at approximately 0.5 %.

Figure 4.3.2.4 shows the selectivity to products other than CO_2 at 5 % propene conversion over silica supported molybdenum catalysts. CO_2 was the most abundant product made at this level of conversion at around 85 to 90 %.

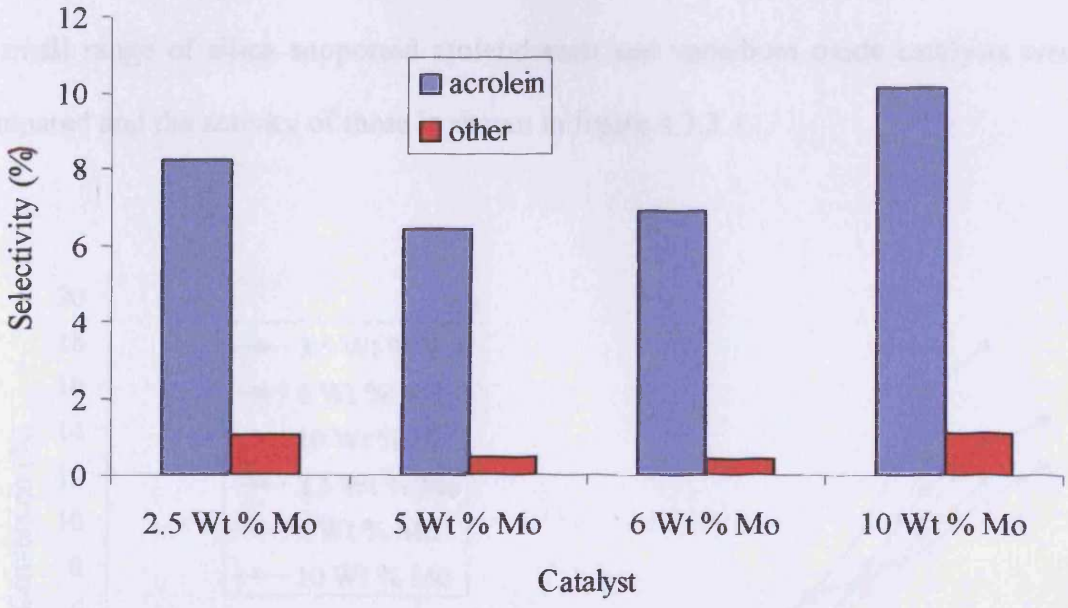

Figure 4.3.2.4: Selectivity to products other than CO_2 at 5 % propene conversion over silica supported molybdenum oxide catalysts.

At the lower level of 5 % propene conversion all catalysts showed increased selectivity to acrolein. The 2.5 and 10 Wt % catalysts showed selectivity to acrolein which was approximately 3 times greater than at 10 % propene conversion at between 8 and 10 % respectively. The biggest increase in selectivity to acrolein was in the medium loaded 5 and 6 Wt % catalysts. At 5 % propene conversion they displayed

selectivity towards acrolein of approximately 6 %, and this was around 12 times greater than at 10 % propene conversion. The selectivity to other partial oxidation products like acrylic acid was also increased at 5 % propene conversion to around 0.75 to 1 %.

4.3.3: Comparison between silica supported molybdenum and vanadium oxide catalysts.

A small range of silica supported molybdenum and vanadium oxide catalysts were compared and the activity of these is shown in figure 4.3.3.1.

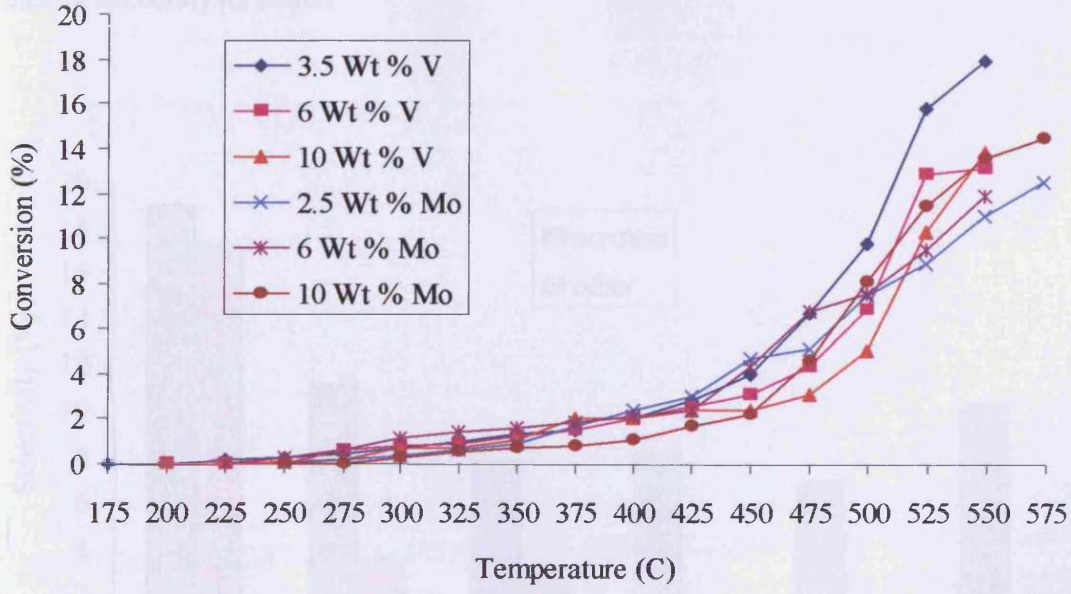

Figure 4.3.3.1: Activity for propene oxidation over silica supported molybdenum and vanadium catalysts.

The activities for the range of different silica supported molybdenum and vanadium oxide catalysts showed that they have similar activity up to 450°C. After 475°C the 3.5 Wt % catalyst showed the best activity of all the catalysts, which was also the most selective when it came to partial oxidation products with the rest having similar activity up to 575°C.

The range of silica supported molybdenum and vanadium oxide catalysts showed similar activity when they are compared together but the selectivities to partial oxidation products differ between the two ranges of catalysts. Figure 4.3.3.2 shows the selectivity to acrolein and other partial oxidation products at 5 % propene conversion over the two ranges of catalysts. CO_2 is the most abundant product formed in all catalysts tested.

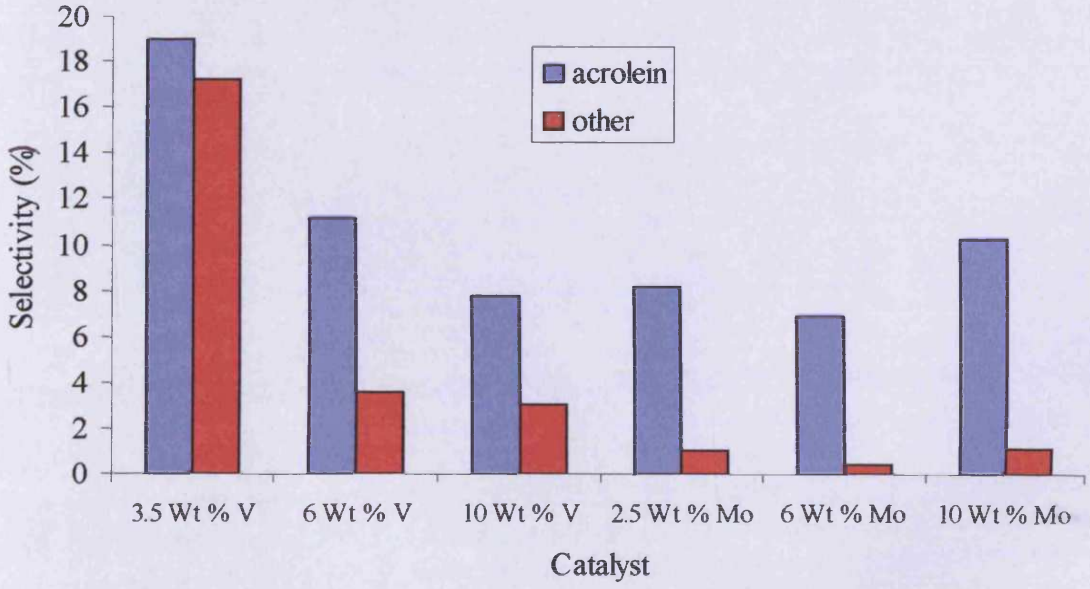

Figure 4.3.3.2: Selectivity to products other than CO_2 at 5 % propene conversion over silica supported molybdenum and vanadium oxide catalysts.

At the lower level of 5 % propene conversion the selectivities to acrolein are similar in all catalysts but the 3.5 Wt % vanadium catalyst and these range from about 7 to 10 %. The 3.5 Wt % vanadium catalyst showed much greater selectivity to acrolein (19 %) and other products like acrylic acid (17 %). A major difference between the silica supported molybdenum and vanadium oxide catalysts was the selectivity to other products like acrylic acid which are approximately 3 times higher in the vanadium based catalysts than molybdenum.

At higher levels of propene conversion a difference emerges between the two systems. Figure 4.3.3.3 shows the selectivity of acrolein and other partial oxidation products at 10 % propene conversion. This does not include CO_2, which is the most abundant product in all catalysts at levels of approximately 85-95 %.

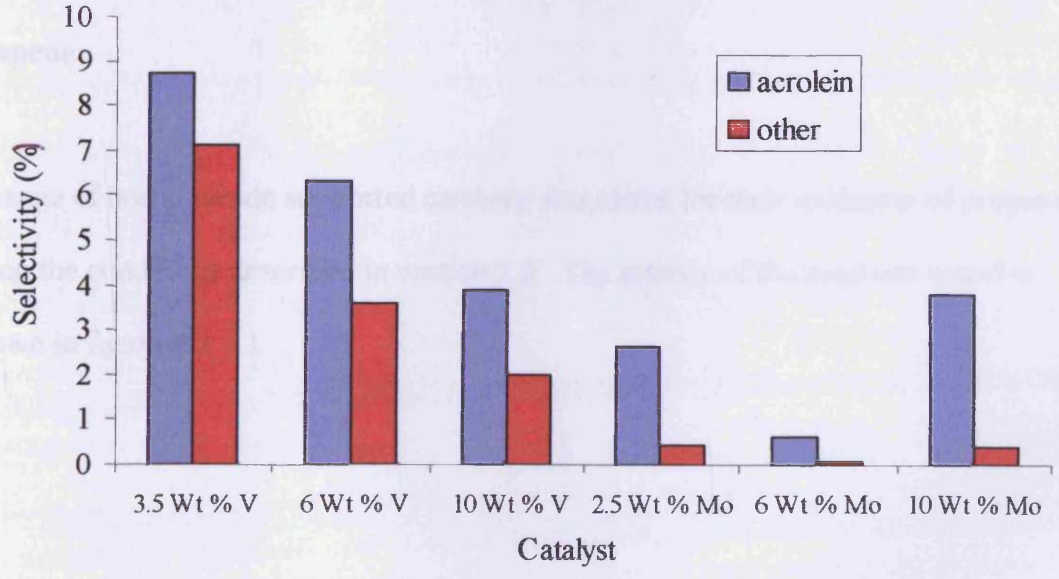

Figure 4.3.3.3: Selectivity to products other than CO_2 at 10 % propene conversion over silica supported molybdenum and vanadium catalysts.

The lower loaded 3.5 and 6 Wt % vanadium catalysts showed selectivity to acrolein that was 2-3 times greater than the best molybdenum based catalysts with selectivities up to 9 %. The other major difference was the selectivity to other partial oxidation products like acrylic acid. For the vanadium based catalysts the selectivities range from 2 to 7 % compared to around 0.5 % for the molybdenum based catalysts meaning the vanadium based catalysts are up to 14 times more selective than their molybdenum counterparts. The same was true when the catalysts were tested for propane oxidation which the silica supported vanadium based catalysts displaying better selectivity towards acrolein and other partial oxidation products like acrylic acid.

4.3.4: Boron nitride supported vanadium oxide catalysts for the oxidation of propene.

A range of boron nitride supported catalysts was tested for their oxidation of propene using the conditions described in section 2.2. The activity of the catalysts tested is shown in figure 4.3.4.1.

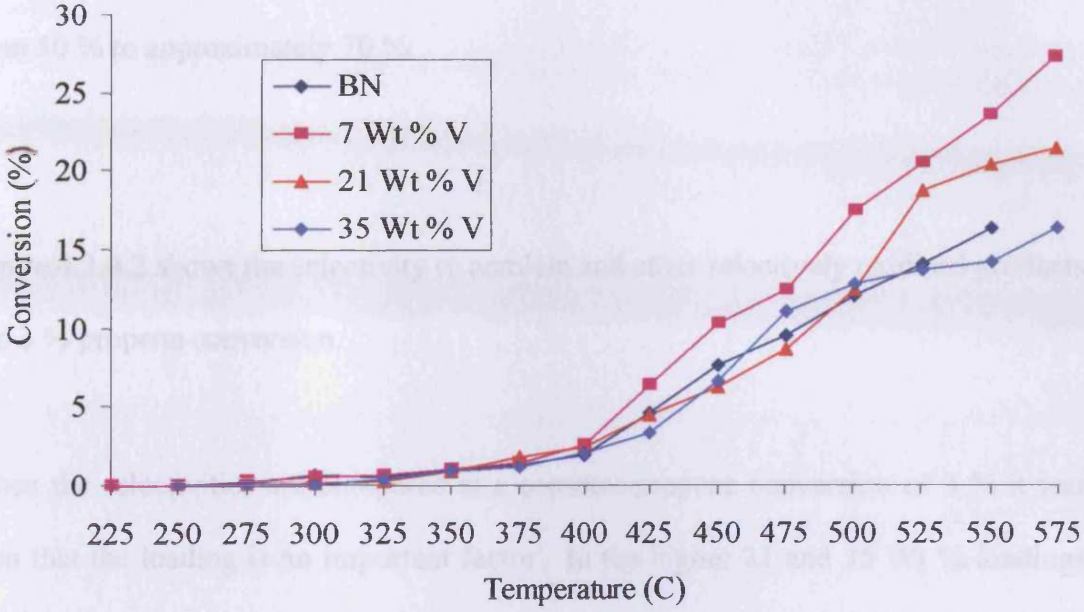

Figure 4.3.4.1: Activity for propene oxidation over boron nitride supported vanadium oxide catalysts.

All catalysts tested displayed very similar activity up to 400°C with all catalysts having a light-off temperature between 225 and 250°C. After 400°C the 7 Wt % catalyst showed the best activity at all temperatures tested with the boron nitride blank and the 21 and 35 Wt % catalysts showing similar activity up to 500°C. After 500°C the 21 Wt % catalyst showed more improved activity than the boron nitride and 35 Wt % catalyst although its activity was not as good as the 7 Wt %. For propene oxidation it seems that low to medium loaded catalysts show the better activity than the high loadings and boron nitride blank. The presence of vanadium oxide promoted the activity of oxidation of propene but at higher loadings this promotion decreases.

When comparing the catalysts for the selectivity to partial oxidation products like acrolein a difference was seen depending on the level of propene conversion. The

product with the highest selectivity at these conversions was CO_2 and this ranged from 50 % to approximately 70 %.

Figure 4.3.4.2 shows the selectivity to acrolein and other selectively oxidised products and 3 % propene conversion.

When the selectivities are compared at a constant propene conversion of 3 % it was seen that the loading is an important factor. In the higher 21 and 35 Wt % loadings there was much increased levels of selectivity to acrolein and other selective products like acrylic acid. Selectivity to acrolein was around 40 % in both catalysts compared to between 20-25 % selectivity in the 7 Wt % and the boron nitride.

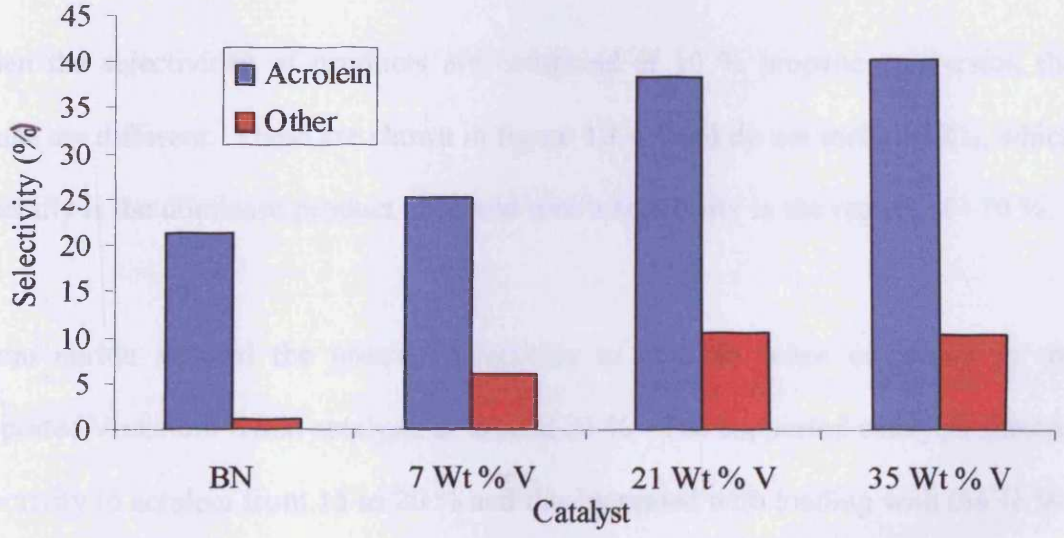

Figure 4.3.4.2: Selectivity for partial oxidation products over boron nitride supported vanadium oxide catalysts at 3 % propene conversion.

This increase was less pronounced when comparing the selectivity of other products like acrylic acid, with the three supported catalysts showing greater selectivity towards these products than when just boron nitride is tested.

This suggests that at lower levels of conversion, which are found at lower temperatures typically ~400°C, the vanadium species present on the catalyst surface help stabilise selectively oxidised products produced like acrolein. This might lead to the supported catalyst selectively oxidising acrolein to acrylic acid rather than to result in deeper oxidation to CO_2, which was more in evidence on the bare boron nitride. The other major product found at these levels of conversion during testing was CO_2, but when the selectivity to partially oxidised products were added together and compared to CO_2, in the higher loaded catalysts at 3 % propane conversion the selectivities are approximately 50/50.

When the selectivities of products are compared at 10 % propene conversion the results are different. These are shown in figure 4.3.4.3 and do not include CO_2, which generally is the dominant product observed with a selectivity in the region of ~70 %.

Boron nitride showed the greatest selectivity to acrolein when compared to the supported vanadium oxide catalysts at around 25 %. The supported catalysts showed selectivity to acrolein from 15 to 20 % and this increased with loading with the 35 Wt % having the highest selectivity. The selectivity to other partially oxidised products follows the same trend when compared to the results at a lower propene conversion of 3 %. Boron nitride showed the lowest selectivity to other products like acrylic acid at

around 1 %. This selectivity increased from 3.5 to 8 % when the boron nitride supported vanadium oxide catalysts increased in loading.

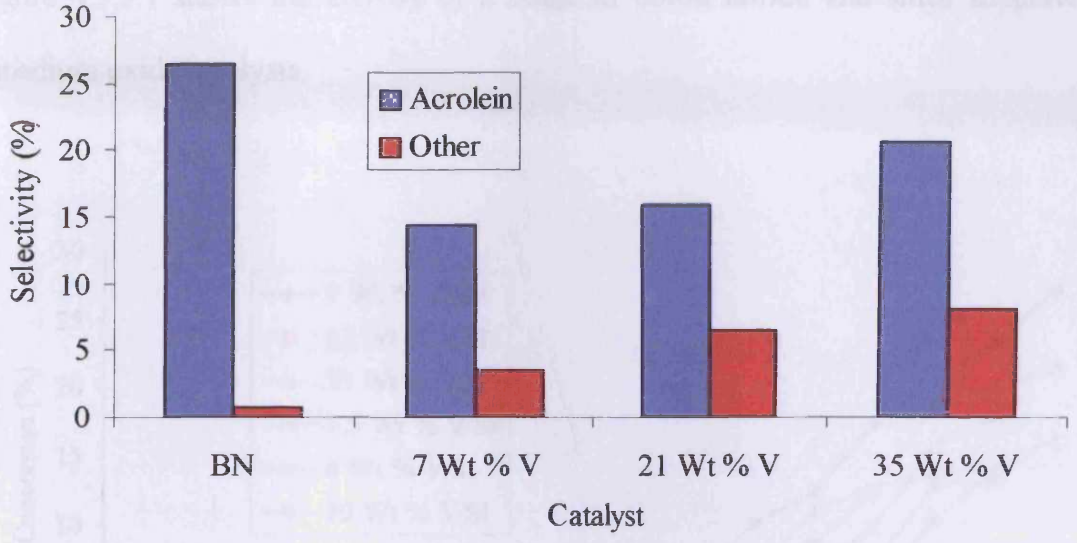

Figure 4.3.4.3: Selectivity for partial oxidation products over boron nitride supported vanadium oxide catalysts at 10 % propene conversion.

This supports the suggestion that the supported vanadium catalysts for the oxidation of propene are better at stabilising the selective products like acrolein that are produced and further partially oxidising them to acrylic acid. This ability to do this increased when the loading of vanadium on the catalyst was higher. The other product produced in this study at 10 % propene conversion was CO_2 for the boron nitride supported vanadium catalysts with some carbon monoxide seen when testing the boron nitride at the highest temperatures.

4.3.5: Comparison between boron nitride and silica supported vanadium oxide catalysts.

Figure 4.3.5.1 shows the activity of a range of boron nitride and silica supported vanadium oxide catalysts.

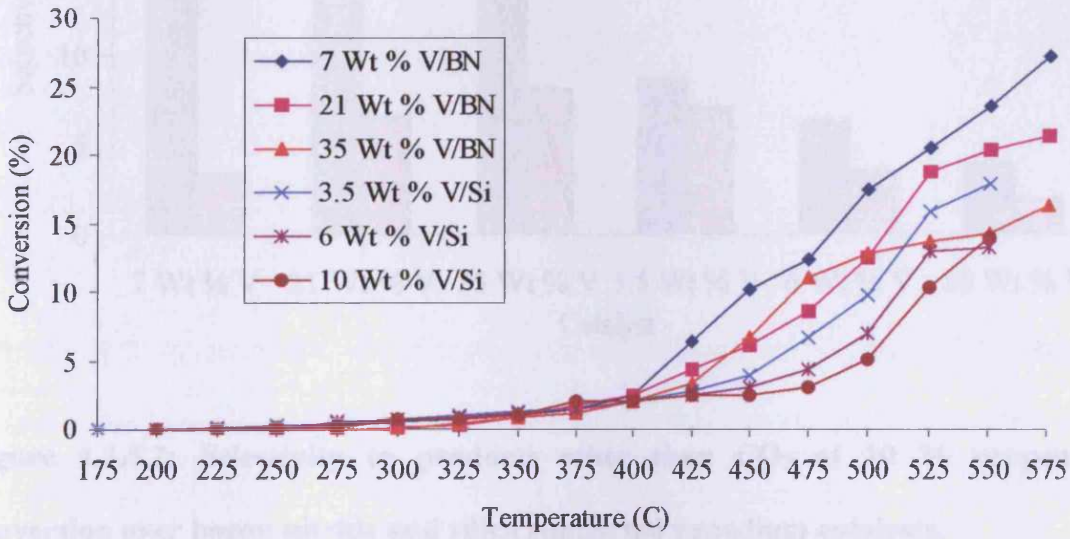

Figure 4.3.5.1: Activity for propene conversion over boron nitride and silica supported vanadium catalysts.

Comparing the activity of the different catalysts there was little difference in activity up to 400°C. The silica supported catalysts have a lower light-off temperature which is around 175 to 200°C compared to 225°C for the boron nitride supported catalysts. Above 400°C the boron nitride catalysts showed increased activity compared to the silica supported catalysts with the 7 Wt % V/BN catalyst having the best activity of all the catalysts above this temperature. Above 525°C the 3.5 Wt % V/Si showed better activity than the least active boron nitride catalyst, the 35 Wt % V/BN. This increased activity for the boron nitride supported vanadium catalysts at higher

temperatures suggests that the activity could be down to some gas phase chemistry due to the inactive nature of the support.

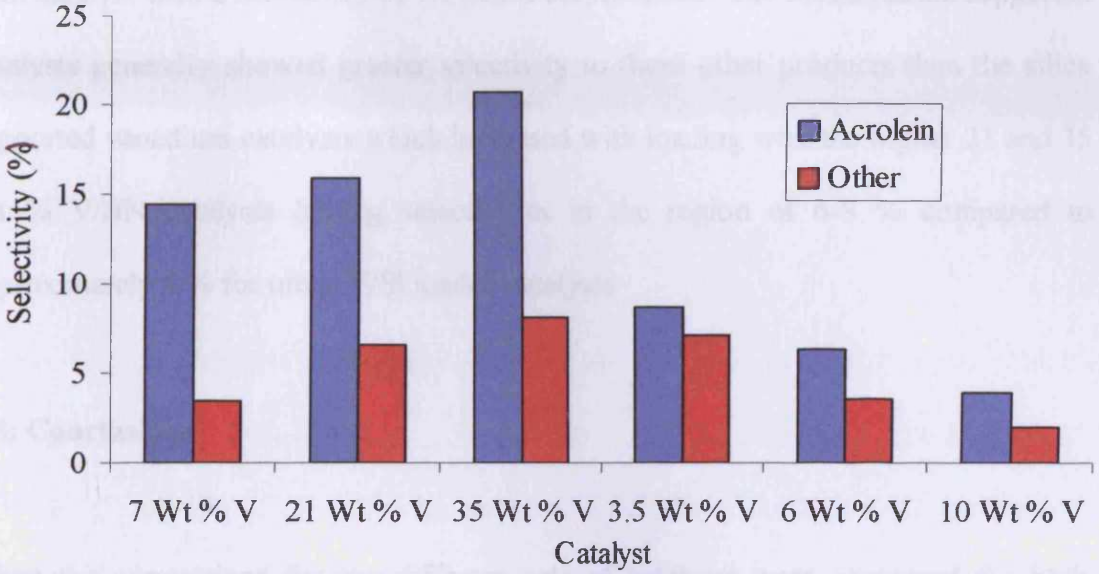

Figure 4.3.5.2: Selectivity to products other than CO_2 at 10 % propene conversion over boron nitride and silica supported vanadium catalysts.

The selectivity of the boron nitride and silica supported vanadium catalysts to products other than CO_2 are shown in figure 4.3.5.2. CO_2 was the most abundant product made over all catalysts. The selectivities are calculated at a propene conversion of 10 %.

Comparing the two different supported sets of catalysts showed that overall the boron nitride supported catalysts displayed greater selectivity to acrolein at 10 % propene conversion with all three catalysts displaying selectivity at approximately 15 to 20 %. The most selective silica supported vanadium catalyst towards acrolein was the 3.5 Wt % V/Si catalyst with levels of selectivity at approximately 8.7 %. The other silica

supported vanadium catalysts showed selectivity between 4 to 6.5 % for acrolein. The selectivity to other products like acrylic acid was greatest for the 35 Wt % V/BN catalyst at around 8.1 %. For this product the next best catalyst was the 3.5 Wt % V/Si catalyst with a selectivity of 7.1 % for acrylic acid. The boron nitride supported catalysts generally showed greater selectivity to these other products than the silica supported vanadium catalysts which increased with loading with the higher 21 and 35 Wt % V/BN catalysts having selectivities in the region of 6-8 % compared to approximately 4 % for other V/Si loaded catalysts.

4.5: Conclusions

When the conversions for the different sets of catalysts were compared for both propane and propene oxidation there is little difference in the levels and light-off temperatures. When the selectivity for partial oxidation products are compared for the two different gases the propene results showed a considerable increase in selectivity for acrolein and acrylic acid. This is a result of the easier conversion to acrolein from propene that occurs when compared to propane, which goes through an initial oxidative dehydrogenation step to produce the alkene. Selectivities increased up to 10 times higher when propene was used instead of propane with selectivity to these partial oxidation products being observed at earlier temperatures.

4.5.1: Propane

For propane oxidation on a range of silica supported vanadium and molybdenum oxide catalysts, activity was dependent upon loading with all catalysts being more

active than bare silica and a blank tube. The catalysts tested all showed similar activity except the medium loaded 5 and 6 Wt % Mo catalysts which were much more active at lower temperatures and over the whole range tested. An increase in activity was seen on the medium loaded vanadium catalysts which suggests that with these catalysts and the medium loaded molybdenum catalysts which are about 0.2 of the calculated monolayer, that a highly dispersed metal oxide on the silica support increases activity for propane oxidation.

Selectivities to products over all catalysts at the temperature ranges tested always gave CO_2 as the major product. Silica supported vanadium catalysts tested had selectivities between 0.5 to 1.4 % for acrolein and almost all catalysts had lower level selectivities for other partial oxidation products like acrylic acid at around ~0.5 %. The silica supported molybdenum catalysts were much less selective towards acrolein (~ 0.1-0.2 %) and other partial oxidation products with the active medium loaded 5 and 6 Wt % Mo loadings producing only CO_2.

For the boron nitride supported catalysts activity was similar when compared to the silica supported vanadium catalysts but the selectivity towards acrolein was greatly increased. Boron nitride supported vanadium catalysts displayed selectivity of between 7 and 8.5 % for acrolein and this was much greater than the silica supported vanadium catalysts with the best being 1.4 % selectivity to acrolein. The boron nitride based catalysts also showed greater selectivity to other partial oxidation products like acrylic acid than the silica based catalysts.

4.5.2: Propene

The range of silica supported vanadium and molybdenum catalysts tested showed similar activity and were dependent upon loading. The loadings that are about 0.2 of the calculated monolayer were the most active for both sets of catalysts but the great increase in activity for propene oxidation was not seen on the medium loaded 5 and 6 Wt % molybdenum catalyst that was seen for propane oxidation. Both sets of catalysts showed greater selectivity towards acrolein and other partial oxidation products than for propane oxidation with the 3.5 Wt % V catalyst the most selective of all silica supported tested. At lower levels of propene conversion (5 %) the selectivity towards acrolein was similar in both sets of catalysts tested with the silica supported vanadium catalysts having greater selectivity towards other partial oxidation products. At a higher level of 10 % propene conversion the vanadium based catalysts were the most selective for all partial oxidation products with the molybdenum based catalysts showing greater selectivity towards combustion.

When the boron nitride supported vanadium catalysts are tested for propene oxidation they showed greater activity at higher temperatures than the silica supported vanadium catalysts. Selectivities for acrolein at 3 % propene conversion are approximately 40 % on the higher loaded V/BN catalysts compared to 20-25 % on the lower loaded catalyst and the boron nitride. When comparing vanadium based boron nitride to the silica based catalysts, selectivities towards acrolein were greater overall for the boron nitride supported vanadium catalysts. The selectivity towards acrolein was approximately 15-20 % compared to between approximately 8-12 % at a propene conversion of 10 % for the silica supported V catalysts, only with the 3.5 Wt % silica supported V catalyst having the second highest selectivity overall at ~17 % for

acrolein. At these levels of conversion the boron nitride based catalysts were the most selective towards other products like acrylic acid.

4.6: References.

[1] Hall, T.J., Hargreaves, J.S.J., Hutchings, G.J., Joyner, R.W. and Taylor S.H., Fuel Process. Technol., 42 (1995) 151-178.

[2] Parmaliana, A., Sokolovskii, V., Miceli, D. and Giordano, N., Appl. Catal. A, 135 (1996) L1-L5.

[3] Ai, M., Catal. Today., 13 (1992) 679-684.

[4] Teng, Y. and Kobayashi, T., Catal. Lett., 55 (1998) 33-38.

[5] Stern, D.L. and Grasselli, R.K., 3rd World Congress on Oxidation Catalysis, (1997) 357-365

[6] Wu, J.C.S., Lin, Z.A., Pan, J.W. and Rei, M.H., Appl. Catal. A, 219 (2001) 8.

[7] Sun, Q., Herman, R.G. and Klier, K., Catal. Lett., 16 (1992) 251-261.

[8] Brown, A.S.C., Hargreaves, J.S.J., Palacios, M-L., Taylor, S.H., Supported Catalysts and Their Applications, Ed. D.C. Sherrington and A.P. Kybett, Royal Society of Chemistry, Cambridge June 2001, pp152-165.

Chapter 5 - Silica and Boron Nitride Supported Molybdenum and Vanadium Oxide Catalysts for Propane Oxidation with and without the Presence of Water.

5.1: Introduction

The presence of water in the gas stream has been shown to have differing effects upon the activity of catalysts for a variety of oxidation reactions. It has been shown to inhibit the activity of supported palladium catalysts [1] and the total oxidation of propane over a manganese oxide catalyst [2]. The same group [2] also showed that the addition of water (2.6 %) to the gas stream had a promoting effect on the activity of a uranium oxide catalyst in the complete oxidation of benzene and propane. The level of water present in the gas stream does appear to have an effect [2] with a higher concentration of water (12.1 %) inhibiting the activity of the uranium oxide catalyst for complete oxidation. The level of activity achieved for this amount of co-fed water was lower than the activity seen in the absence of any co-fed water. For this study selective oxidation is the desired result with an inhibited activity possibly promoting the partial oxidation of propane. A study by M. Ai [3] suggested that higher concentrations of oxygen and co-fed water were favourable for obtaining high yields of acrylic acid from the oxidation of propane and that the addition of water might effect the partial oxidation products made.

A selected range of catalysts that were tested for propane oxidation in Chapter 4 have been tested for propane oxidation. The catalysts were tested by having water co-fed via the alkane as described in section 2.2 with reaction conditions kept the same for

the non co-fed water propane oxidation. These are presented by comparing both the co-fed and non co-fed water results for a particular catalyst.

5.2 Silica supported molybdenum oxide catalysts.

The range of catalysts tested was picked to include a low, medium and high loading. The effect of the water upon the activity and selectivity of the catalysts was dependent on loading with differences observed over the ranges tested.

5.2.1: Silica supported 2.5 Wt % Mo catalyst.

The activity of the 2.5 Wt % Mo catalyst is shown in figure 5.2.1.1 for the oxidation of propane both in the presence of co-fed water and without.

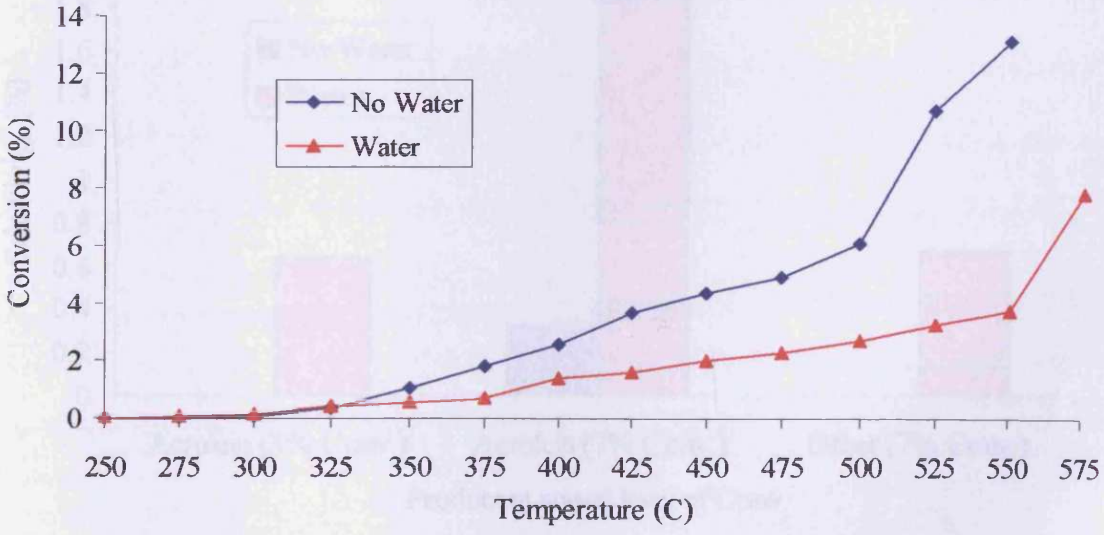

Figure 5.2.1.1: Activity for propane oxidation over 2.5 Wt % Mo catalyst in the presence and without co-fed water.

The presence of water when testing the 2.5 Wt % Mo catalyst overall lowers the activity of propane oxidation. Both reaction conditions had similar light-off temperatures of around 250 to 275°C and showed the same activity up to 325°C. After this temperature in the absence of water there was increased activity for propane oxidation and it was approximately twice as active up to 500°C. After 500°C the activity for propane oxidation for the 2.5 Wt % Mo catalyst in the absence of water was greatly increased with a similar increase in activity not seen until after 550°C in the presence of water. At 550°C the activity in the absence of water was around 13 % compared to around 3.5 % in the presence of water.

This decrease in activity had a large influence on the selectivity of the products formed with increased levels of selectivity to acrolein and these selectivities are shown at a constant propane conversion of both 3 and 7 %.

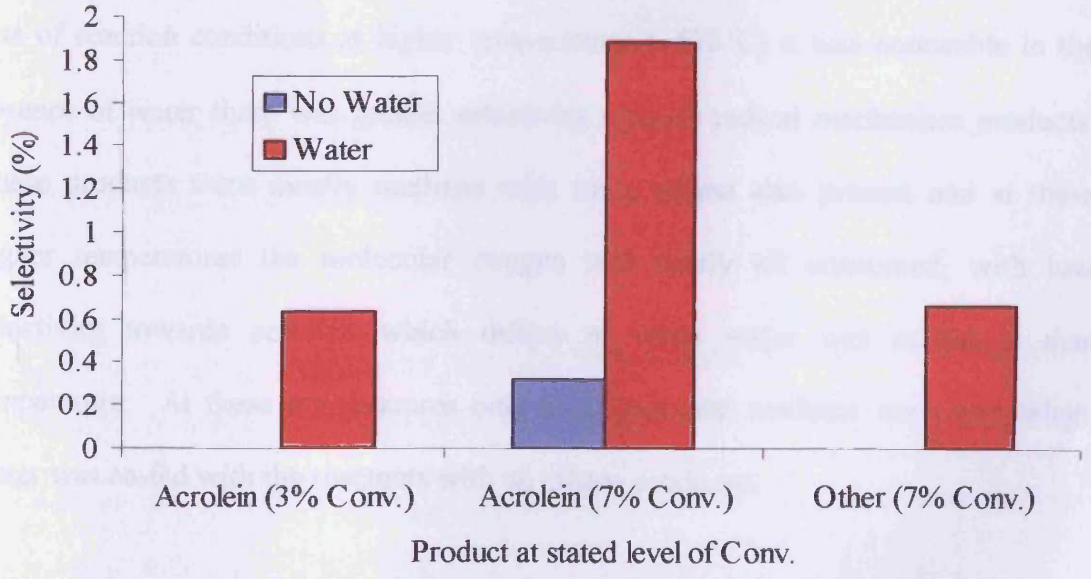

Figure 5.2.1.2: Selectivity to products other than CO_2 at 3 and 7 % propane conversion over a silica supported 2.5 Wt % Mo catalyst with and without co-fed water.

Figure 5.2.1.2 shows the selectivities at different rates of conversion for partial oxidation products. At these conversions CO_2 was the most abundant product formed at around 95 % selectivity. At 3 % propane conversion no acrolein or other products like acrylic acid were observed in the absence of co-fed water. When water was co-fed with the gas stream a selectivity of 0.6 % for acrolein was observed at 3 % propane conversion although no other partial oxidation products were seen. This increase in selectivity for partial oxidation products was greater at a propane conversion of 7 % with a selectivity of 1.8 % for acrolein in the presence of co-fed water compared to 0.3 % selectivity without water. The selectivity to other products like acrylic acid increased in the presence of water to around 0.6 % compared to zero when there was no water present. With the suppressed activity these comparisons are around 50-75°C different, so the increased selectivities when water was co-fed with the gas stream are at higher temperatures meaning some or more gas phase chemistry could be influencing the selectivities. When the selectivities are compared for the two sets of reaction conditions at higher temperatures (~575°C) it was noticeable in the absence of water there was greater selectivity towards radical mechanism products. These products were mostly methane with some ethane also present and at these higher temperatures the molecular oxygen was nearly all consumed, with low selectivity towards acrolein which differs to when water was co-fed at that temperature. At these temperatures only small amounts methane were seen when water was co-fed with the reactants with no ethane produced.

5.2.2: Silica supported 5 Wt % Mo catalyst.

The medium loaded 5 Wt % catalyst was tested for the oxidation of propane in both the presence and absence of co-fed water. The activities of these two different conditions are shown in figure 5.2.2.1.

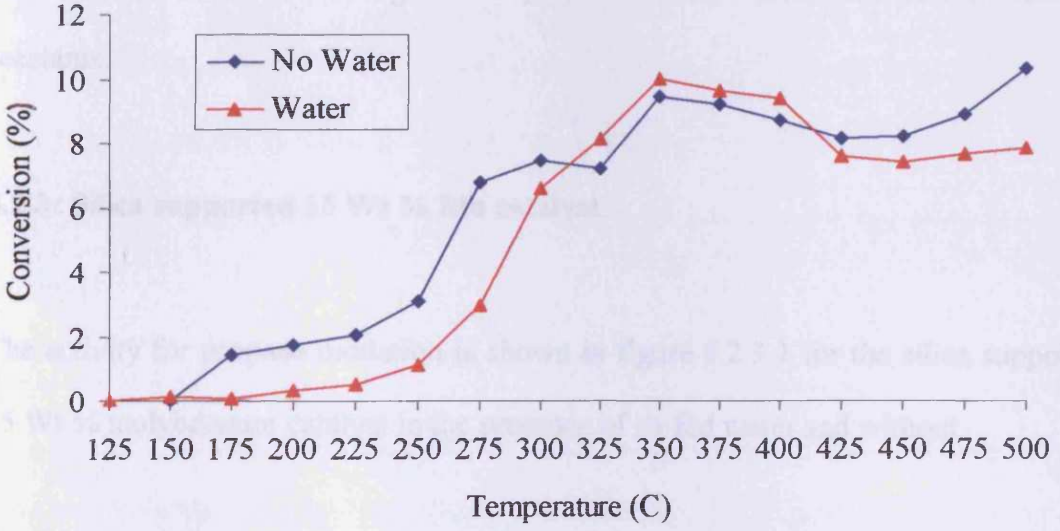

Figure 5.2.2.1: Activity for propane conversion over 5 Wt % Mo catalyst with and without the presence of co-fed water.

The presence of water up to 300°C lowers the activity of the 5 Wt % Mo catalyst. The light-off temperature was lower in the presence of water by 25°C at 125°C but the initial activity increased steadily over the next 100°C. Between 150-300°C the activity started to increase for the co-fed water experiment at the same rate as when water was absent from the reaction conditions. Between 300-325°C the activity of the silica supported 5 Wt % Mo catalyst was greater in the presence of water. The increased activity in the presence of water for propane oxidation continues for another

100°C and then between 400-425°C the activity of the 5 Wt % catalyst became greater in the absence of water and this increased activity continued over the rest of the temperature range tested.

When the catalysts were compared for their selectivities to products both catalysts showed ~99.8-100 % selectivity to CO_2 at all temperatures and conversions tested with trace methane at the highest temperatures when water was co-fed with the reactants.

5.2.3: Silica supported 15 Wt % Mo catalyst

The activity for propane oxidation is shown in figure 5.2.3.1 for the silica supported 15 Wt % molybdenum catalyst in the presence of co-fed water and without.

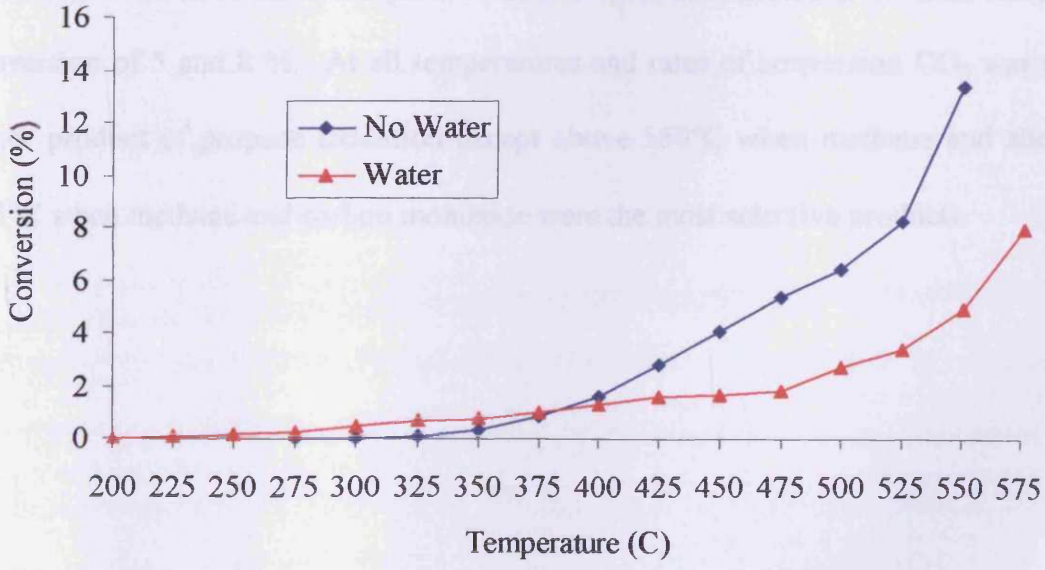

Figure 5.2.3.1: Activity for propane oxidation over silica supported 15 Wt % Mo catalyst in the presence of co-fed water and without.

The activity of the silica supported 15 Wt % Mo catalyst showed two distinctive differences in the presence and absence of co-fed water. At low temperatures the presence of water promotes the activity for propane oxidation and this continues up to 375°C. The activity when water was co-fed was only slightly higher than when no water was present and all of this activity was below 1 % conversion. The light-off temperature was also 25°C lower when water was co-fed with the reaction gas stream. After 375°C the activity becomes much greater when water was not present while the co-fed water activity steadily increased. The difference in activity at 550°C was 14 % conversion in the absence of water compared to 4 % conversion in the presence of co-fed water.

This difference in activity had a major influence on the selectivity to products when the two different reaction conditions were compared. Figure 5.2.3.2 shows the selectivity to acrolein and other partial oxidation products formed at constant rates of conversion of 5 and 8 %. At all temperatures and rates of conversion CO_2 was the major product of propane oxidation except above 550°C when methane and above 575°C when methane and carbon monoxide were the most selective products.

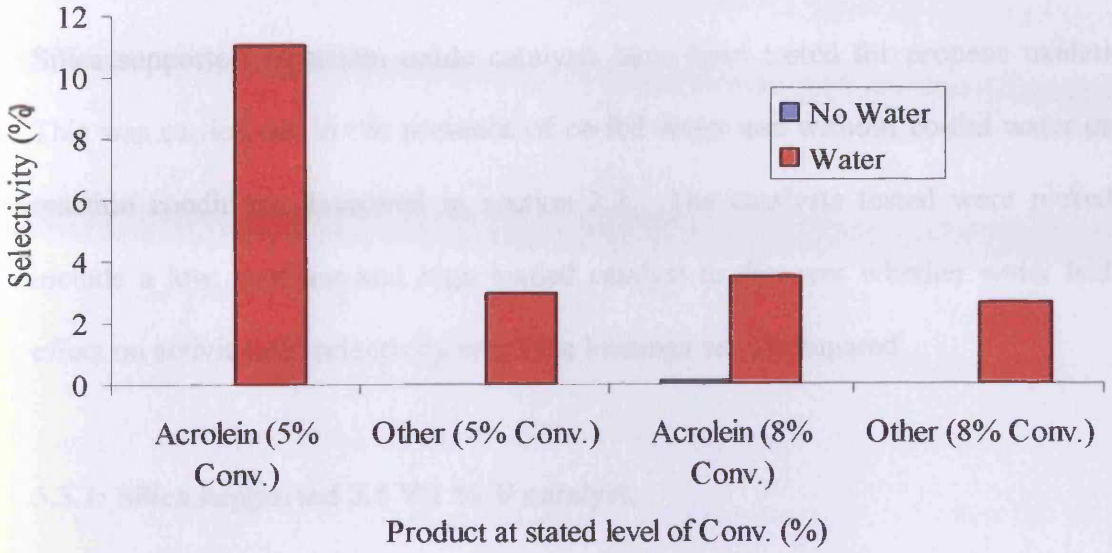

Figure 5.2.3.2: Selectivity to products other than CO_2 at 5 and 8 % propane conversion over silica supported 15 Wt % Mo catalyst in the presence of co-fed water and without.

Figure 5.2.3.2 showed that selectivity to partial oxidation products was greatly increased in the presence of co-fed water. At a propane conversion of 5 % the selectivity to acrolein was approximately 11 % compared to none in the absence of water. The levels of other partial oxidation products like acrylic acid was also evident at around 3 % compared to zero again when water was not co-fed with the reactants. At a higher level of 8 % propane conversion the difference between the two reactions conditions was lower but the presence of water again promoted selectivity to partial oxidation products. The selectivity in the presence of water for acrolein was ~3.5 % compared to 0.15 % when water was absent. The selectivity to acrylic acid and others in the presence of water was 2.5 % compared to zero when water was not present.

5.3: Silica supported vanadium oxide catalysts.

Silica supported vanadium oxide catalysts have been tested for propane oxidation. This was carried out in the presence of co-fed water and without co-fed water using reaction conditions described in section 2.2. The catalysts tested were picked to include a low, medium and high loaded catalyst to discover whether water had an effect on activity and selectivity when the loadings were compared.

5.3.1: Silica supported 3.5 Wt % V catalyst.

The activity of the silica supported 3.5 Wt % V catalyst is shown in figure 5.3.1.1 for propane oxidation in the presence and absence of co-fed water.

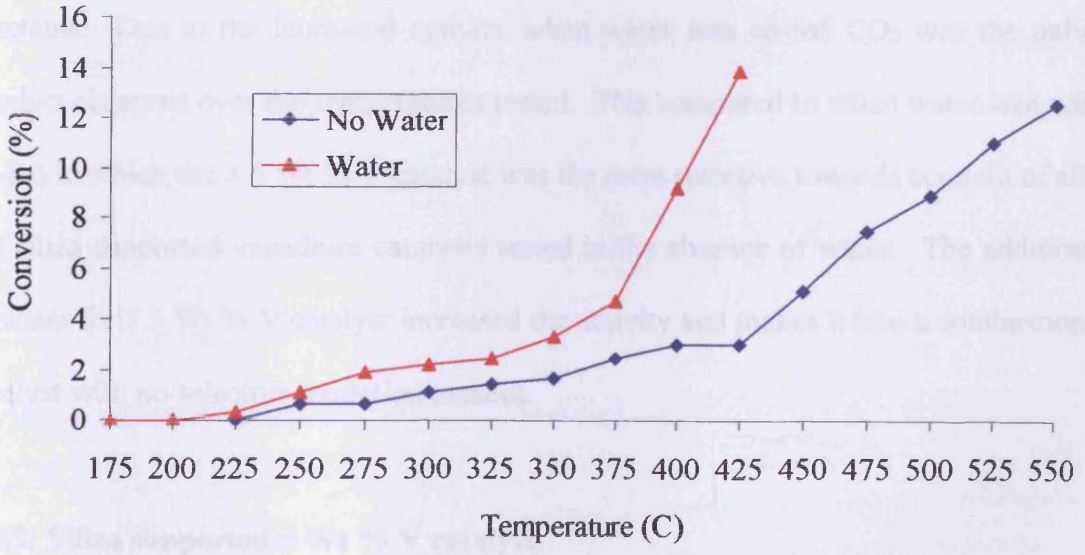

Figure 5.3.1.1: Activity for propane oxidation over silica supported 3.5 Wt % catalyst in the presence and absence of co-fed water.

Figure 5.3.1.1 showed that the presence of water upon the activity of the silica supported 3.5 Wt % V catalyst was to promote the activity for propane oxidation. At all temperatures tested the activity of the reaction with co-fed water was greater than in the absence of water. Between 250 and 375°C the activity when water was co-fed is approximately twice that when water was absent. Above 375°C the activity when water was present is greatly increased. At 400°C the activity was around 3 times greater and at 425°C it was around 5 times greater than when water was not present. Beyond these temperatures the catalyst in the presence of water used up all the molecular oxygen in the reaction stream. In the absence of co-fed water the catalyst was still active for over 100°C more but was not as active as the catalyst when water was co-fed at 425°C which had approximately 14 % conversion.

The selectivity of the products formed was affected by the addition of water to the reactants. Due to the increased activity when water was co-fed CO_2 was the only product observed over the temperatures tested. This compared to when water was not co-fed in which the 3.5 Wt % V catalyst was the most selective towards acrolein of all the silica supported vanadium catalysts tested in the absence of water. The addition of water for 3.5 Wt % V catalyst increased the activity and makes it into a combustion catalyst with no selective oxidation present.

5.3.2: Silica supported 5 Wt % V catalyst.

The activity for propane oxidation for the 5 Wt % V catalyst is shown in figure 5.3.2.1 in the presence and absence of co-fed water.

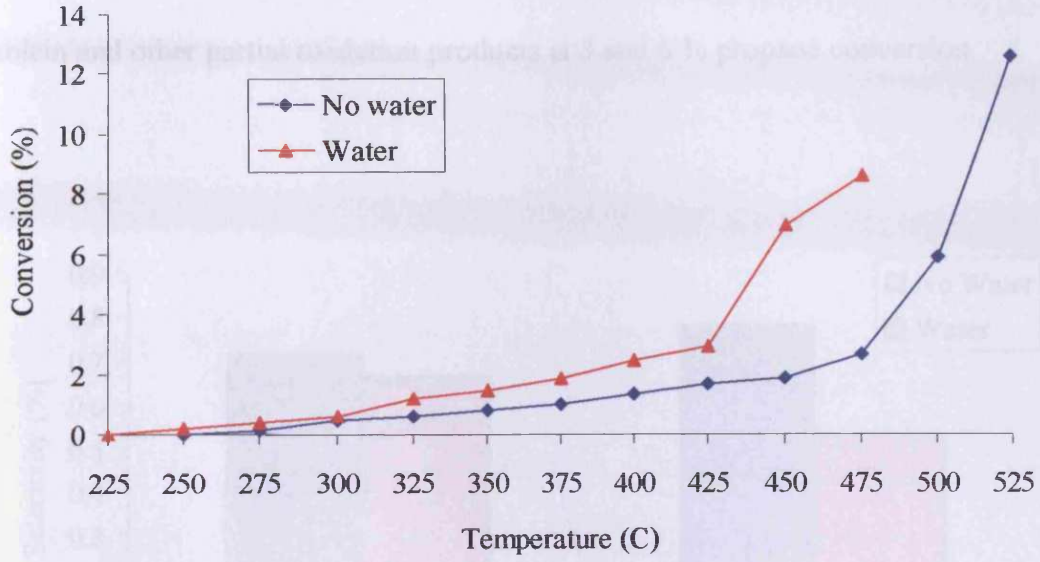

Figure 5.3.2.1: Activity for propane oxidation over silica supported 5 Wt % V catalyst in the presence and absence of co-fed water.

The activity for the 5 Wt % V catalyst when water was co-fed for propane oxidation was increased compared to when no water was present. This increased activity was gradual from 225 to 425°C with the activity when co-fed water was present approximately twice the activity when no water is present. After 425°C the activity of the co-fed water reaction was greatly increased compared to when no water is present. At 475°C activity was at 8.5 % propane conversion when water was co-fed compared to 2.5 % conversion when water was absent and only after 475°C does the activity significantly increase when water was not co-fed with the reactants.

The difference in selectivity for partial oxidation products like acrolein was little affected by the two different reaction conditions with CO_2 always the major product

up to 475°C. At this temperature when water was co-fed with the reactants carbon monoxide was the most selective product. Figure 5.3.2.2 shows the selectivity for acrolein and other partial oxidation products at 3 and 6 % propane conversion.

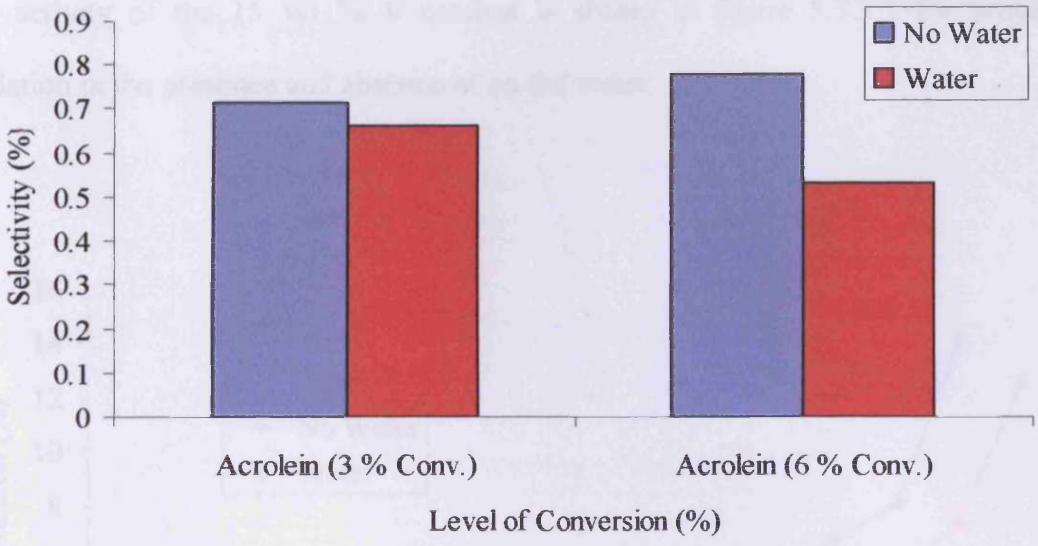

Figure 5.3.2.2: Selectivity to products other than CO_2 at 3 and 6 % propane conversion for silica supported 5 Wt % V catalyst in the presence and absence of co-fed water.

The selectivity for acrolein and other partial oxidation products like acrylic acid were similar in the presence and absence of water. The levels of selectivity were lower when water was co-fed, more so at the higher rate of 6 % propane conversion. This was evident in the lower silica supported 3.5 Wt % V catalyst in section 5.3.1 which only gave CO_2 as a product when water was co-fed with the reactants compared to being the most selective silica supported vanadium catalyst for partial oxidation when

water was absent. Water co-feeding led to increased combustion in the lower loaded silica supported vanadium oxide catalysts at the expense of partial oxidation products.

5.3.3: Silica supported 15 Wt % V catalyst.

The activity of the 15 Wt % V catalyst is shown in figure 5.3.3.1 for propane oxidation in the presence and absence of co-fed water.

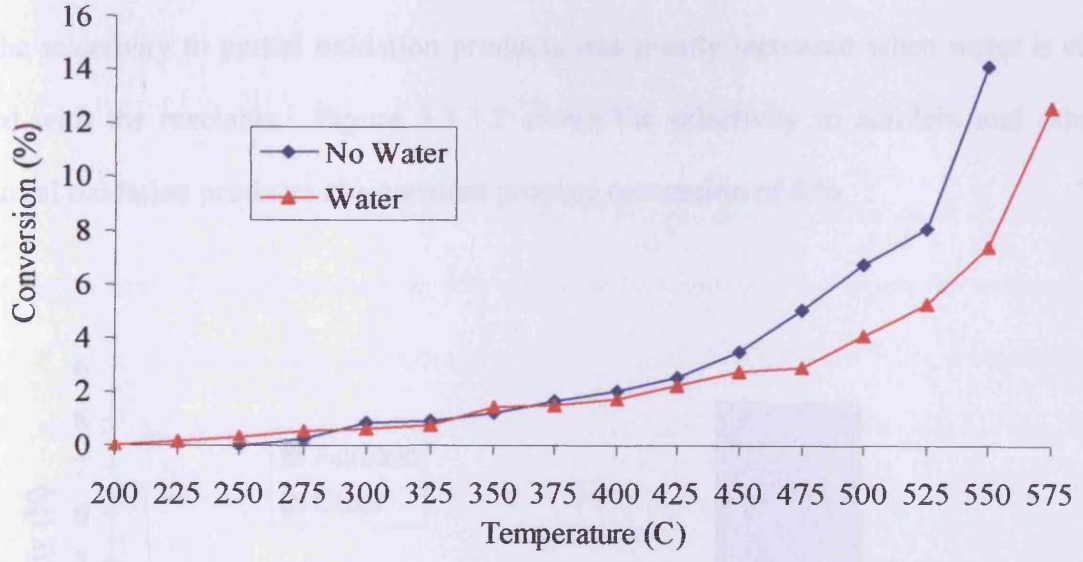

Figure 5.3.3.1: Activity for propane oxidation over silica supported 15 Wt % V catalyst in the presence and absence of co-fed water.

Figure 5.3.3.1 shows that the activity for the silica supported 15 Wt % V catalyst when water was present and was absent for propane oxidation. This shows that the activity for the two different reaction conditions were very similar from 200 to 425°C. After this temperature range when water was not co-fed with the reactants the activity

was greater than when compared to water was co-fed with the reactants. Between 425 and 525°C the activity when water was not co-fed is approximately 1-2 times greater than when water was co-fed. The levels of conversion after 425°C between the two different reaction conditions increased at a similar rate but the co-fed water reaction level of conversion was shifted approximately around 25°C higher in temperature when compared to the same level of conversion when water was not co-fed. This meant a propane conversion of approximately 8 % in the absence of water that was achieved at 525°C would be seen at approximately 550°C in the presence of water.

The selectivity to partial oxidation products was greatly increased when water is co-fed with the reactants. Figure 5.3.3.2 shows the selectivity to acrolein and other partial oxidation products at a constant propane conversion of 8 %.

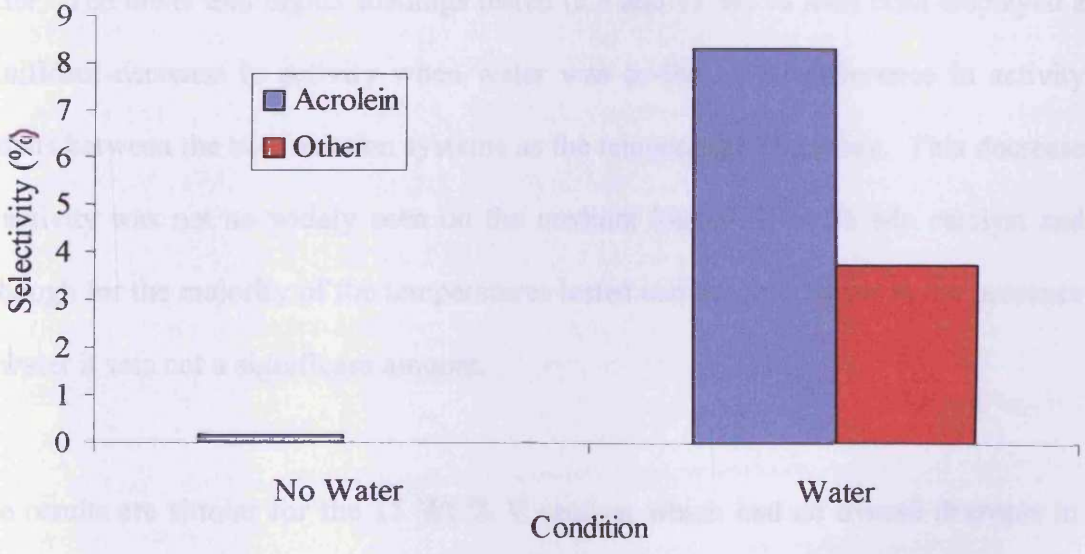

Figure 5.3.3.2: Selectivity to products other than CO_2 at 8 % propane conversion over silica supported 15 Wt % V catalyst with and without co-fed water.

At all temperatures analysed CO_2 was the major product formed. The selectivity to acrolein increases from 0.15 % to 8.5 % when water was co-fed with the reactants at a constant propane conversion of 8 % which was approximately 56 times greater. When water was co-fed the selectivity to other partial oxidation products also increased from zero to 3.8 %. The only other products seen were at the higher temperatures analysed in which both systems produced methane with the higher selectivity when water was co-fed between 1-5 % compared to approximately 0.5 % when water was absent.

5.4: Discussion of silica supported molybdenum and vanadium catalysts.

The presence of water during propane oxidation over silica supported molybdenum catalysts generally inhibited activity when compared to their activity in the absence of water. The lower and higher loadings tested (2.5 and 15 Wt % Mo) both displayed a significant decrease in activity when water was co-fed. The difference in activity widens between the two reaction systems as the temperature increases. This decrease in activity was not so widely seen on the medium loaded 5 Wt % Mo catalyst and although for the majority of the temperatures tested activity was lower in the presence of water it was not a significant amount.

The results are similar for the 15 Wt % V catalyst which had an overall decrease in activity when tested for propane oxidation in the presence of water although at lower temperatures (<375°C) there was a marginal increase in activity when water was co-fed. The presence of co-fed water on the lower loaded 3.5 and 5 Wt % V catalysts had a promoting effect on their activity with both catalysts having significantly

improved activity when compared to the activity when the catalysts were tested in the absence of water. The presence of the water has differing effects depending on the catalyst tested. Taylor et al. [2] proposed that the increase in activity for the complete oxidation of propane over uranium oxide was due to the modification of the uranium oxides surface by hydroxylation which aids hydrocarbon activation. This could be what's happening on the lower loaded silica supported vanadium catalysts and on the 15 Wt % V catalyst at lower temperatures with a modification of the surface due to hydroxyl groups, which promote activity. This modification could also have the opposite effect upon activity with the presence of water on the surface blocking active sites and lowering activity by restricting the sites for both propane and oxygen activation.

These changes in activity are backed up by the selectivity to partial oxidation products when water is co-fed compared to when water is absent from the effluent stream. The 3.5 Wt % V catalysts activity was promoted in the presence of water but its selectivity to products was changed to 100 % complete combustion compared to this catalyst being the most selective to acrolein of all the silica supported catalysts in the absence of water. The 5 Wt % V catalyst also displayed increased activity in the presence of water but its selectivity for combustion reactions also increased. The other catalysts excluding the 5 Wt % Mo catalyst, which in both the presence and absence of co-fed water displayed similar activity and 100 % selectivity to CO_2, showed both inhibited activity and increased selectivity to partial oxidation products. This suggests that the water is blocking active sites on the catalyst surface that lead in the end to complete combustion to CO_2. This would work by firstly the water blocking the surface and

lowering the number of active sites available for propane activation. As it is believed [3] that the oxidation of propane is sequential going via:

$$\text{Propane} \rightarrow \text{Propene} \rightarrow \text{Acrolein} \rightarrow \text{Acrylic acid} \rightarrow CO_x$$

The lower number of active sites available because they are being blocked by water on the surface means a lower number of the partial oxidation products are able to go through the sequential route and be converted into carbon oxides. This would lead to increased selectivity towards the likes of acrolein and acrylic acid whilst lowering the activity compared to when water is absent.

5.5: Boron nitride supported vanadium catalysts.

A range of boron nitride supported vanadium catalysts has been tested for propane oxidation with and without co-fed water in reaction conditions described in section 2.2. The activity of these catalysts when water is co-fed is shown in figure 5.5.1.

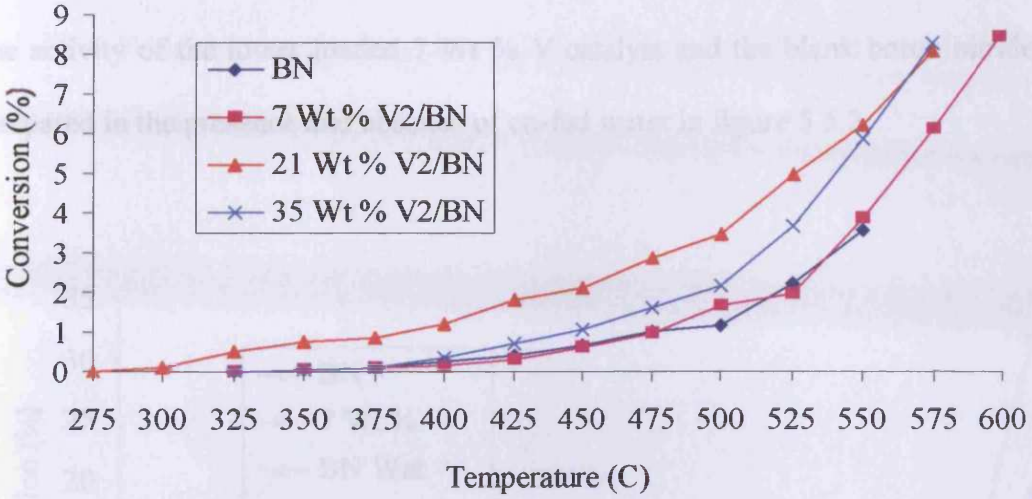

Figure 5.5.1: Activity for propane oxidation over boron nitride supported vanadium catalysts in the presence of co-fed water.

Figure 5.5.1. shows that the activity of the higher loaded 21 and 35 Wt % catalysts was greater than the lower loaded 7 Wt % V catalyst and the boron nitride blank. This was especially increased in the 21 Wt % catalyst, which was the most active catalyst in the presence of water over all temperatures tested. The catalyst was 2 to 3 times more active than the next best 35 Wt % V catalyst between 400 and 500°C. The lower loaded 7 Wt % catalyst and the blank boron nitride activity was much lower and levels of conversion that compare to the higher loadings were shifted 25 to 50°C higher in temperature. Boron nitride is hydrophobic which suggests that any interaction of the water with the surface requires a higher temperature, something that also occurs on the lowest loading of 7 Wt % V which will have more boron nitride exposed on the surface than the higher loadings. The co-fed water on the higher loadings will have more surface vanadium oxide to interact with and gives increased activity at lower temperatures.

The activity of the lower loaded 7 Wt % V catalyst and the blank boron nitride are compared in the presence and absence of co-fed water in figure 5.5.2.

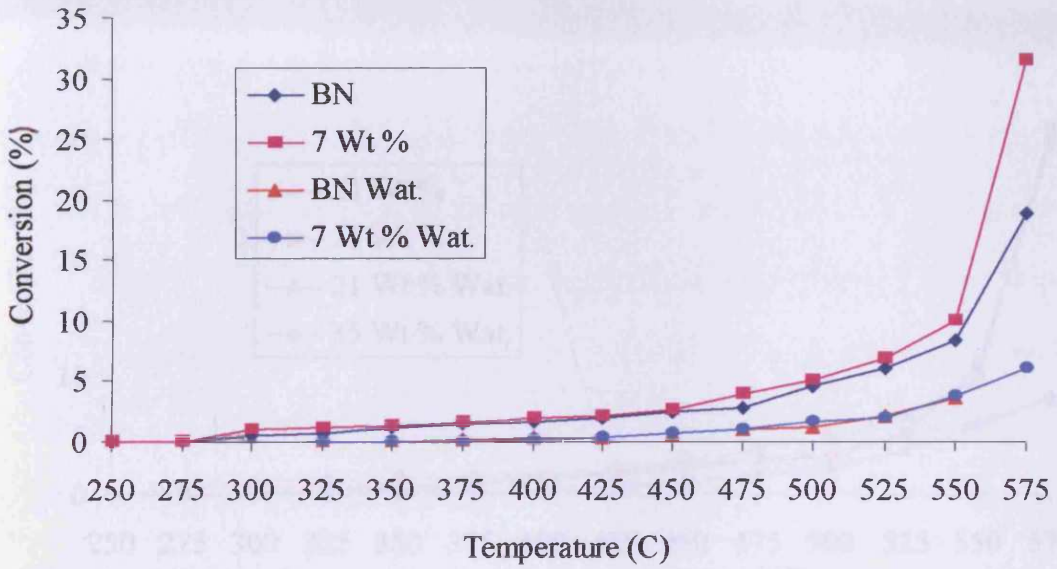

Figure 5.5.2: Activity for propane oxidation over boron nitride and 7 Wt % V/BN catalyst in the presence and absence of co-fed water.

Comparing the two different reaction conditions shows that when water was co-fed in the gas stream the boron nitride and 7 Wt % V catalyst were less active than when water was not present. This trend was over all temperatures analysed with the co-fed water experiments having light-off temperatures 75°C higher than when water was not co-fed with the reactants. This shows that the water was suppressing the activity of the hydrophobic boron nitride and the lowest loaded catalyst. This continued up to the highest temperatures analysed with the catalysts that are without co-fed water showing much increased activity above 550°C compared to when co-fed water was present.

When comparing the higher loadings there was a smaller difference in the activity between the catalysts in the presence and absence of water. The activity of the 21 and 35 Wt % V/BN catalysts in the presence and absence of water is shown in figure 5.5.3.

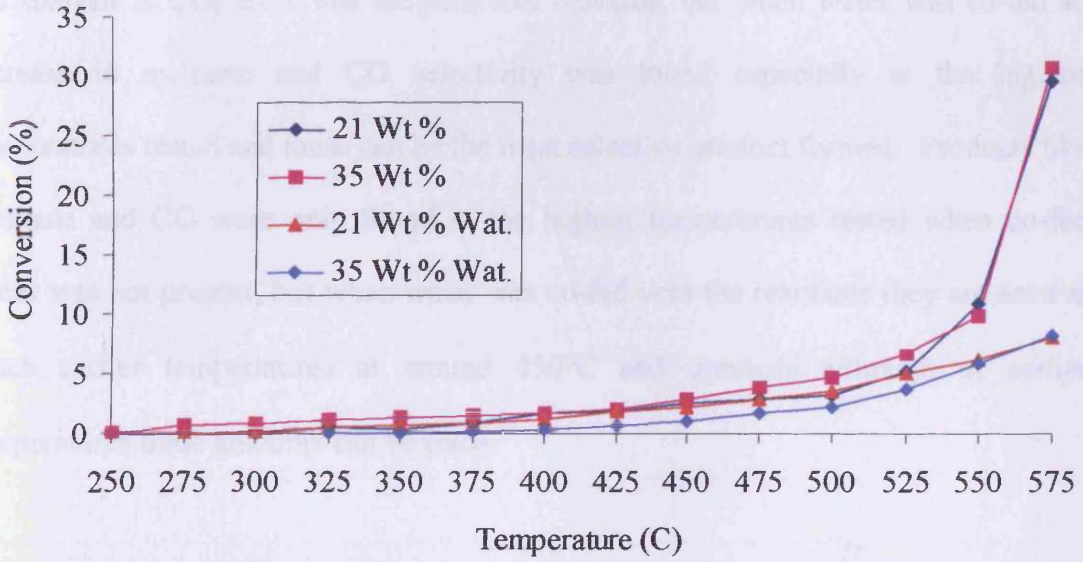

Figure 5.5.3: Activity for propane oxidation over 21 and 35 Wt % boron nitride supported catalysts in the presence and absence of co-fed water.

Comparing the two different reaction conditions shows that up to 500°C they were similar in activity. Over all temperatures the 35 Wt % V catalyst absent of co-fed water was the most active whilst the same catalyst in the presence of water was the least active. The effect of co-feeding water had little effect on the 21 Wt % V catalyst, as its activity was very similar to the same catalyst when water was absent up to 525°C. The light-off temperatures are 25-50°C higher when water was co-fed but the activity of the two different reaction conditions was comparable up to 525°C. Above this temperature the catalysts without the presence of water are much more

active, with the water present suppressing the activity of the catalysts at these temperatures.

The boron nitride supported vanadium catalysts selectivities are very different when comparing results in the presence and absence of water. The main product throughout the analysis is CO_2 from low temperatures onwards, but when water was co-fed an increase in methane and CO selectivity was found especially at the highest temperatures tested and these can be the most selective product formed. Products like methane and CO were only found in the highest temperatures tested when co-fed water was not present, but when water was co-fed with the reactants they are seen at much earlier temperatures at around 450°C and upwards although at earlier temperatures these amounts can be trace.

When the catalysts have water co-fed in the gas stream the selectivity to acrolein and other partial oxidation products were found at much lower rates of conversion and thus at much lower temperatures. Acrolein was formed around 75°C lower in the presence of water and it occurs at the same time products like methane are starting to be formed aswell as other partial oxidation products. Figure 5.5.4 compares the selectivity to acrolein and other partial oxidation products at a constant rate of propane conversion of 3.5 % in the presence of co-fed water. At this rate of conversion CO_2 was the major product formed with some methane and trace CO for all catalysts when water was present. At the same level of conversion shown in figure 5.5.4 in the absence of water CO_2 was the only product formed for the boron nitride supported vanadium oxide catalysts and blank boron nitride with no selectivity towards acrolein seen until about 4.5-5 % propane conversion.

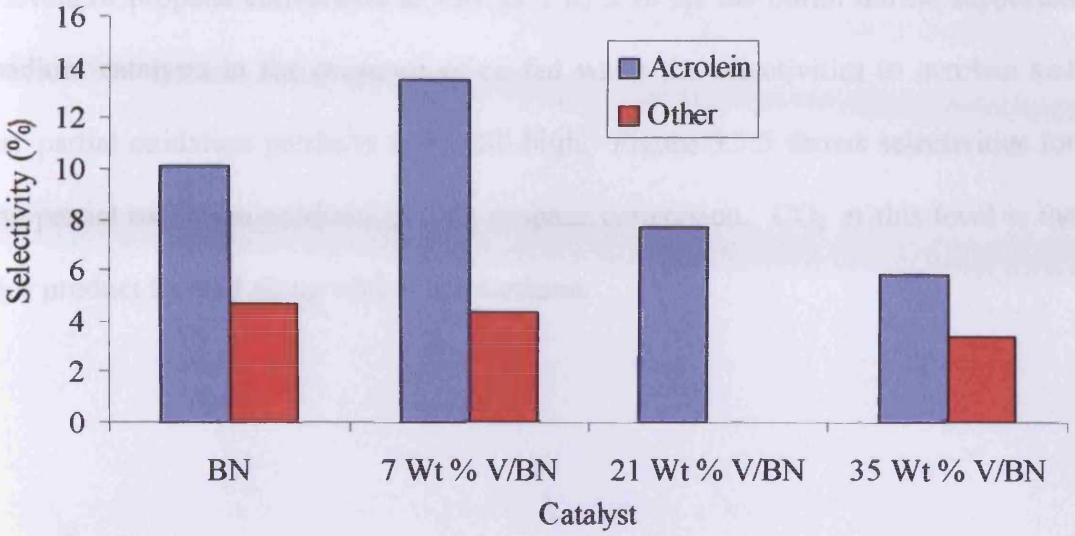

Figure 5.5.4: Selectivity to partial oxidation products at 3.5 % propane conversion over boron nitride supported vanadium catalysts in the presence of water.

Figure 5.5.4 shows that the lower loaded 7 Wt % V catalyst and the blank boron nitride had the better selectivity to acrolein (13.5 and 10 % selectivity respectively) and to other partial oxidation products like acrylic acid than the higher loaded boron nitride supported 21 and 35 Wt % V catalysts. These lower loaded catalysts displayed less activity when they are compared with the 21 Wt % V/BN catalyst, which has the greatest activity. This lower activity suggests that even though the water is suppressing the activity of the catalysts it was improving the selectivity towards selective oxidation products especially acrolein. The higher loaded catalysts with their greater activity are displaying more combustion chemistry in the presence of co-fed water than the lower loaded counterparts. But these catalysts are selectively oxidising propane to products like acrolein at a level of conversion of 3.5 % compared to when water is not co-fed when only combustion occurs.

At levels of propane conversion as low as 1 to 2 % for the boron nitride supported vanadium catalysts in the presence of co-fed water the selectivities to acrolein and other partial oxidation products were still high. Figure 5.5.5 shows selectivities for these partial oxidation products at 2 % propane conversion. CO_2 at this level is the major product formed along with some methane.

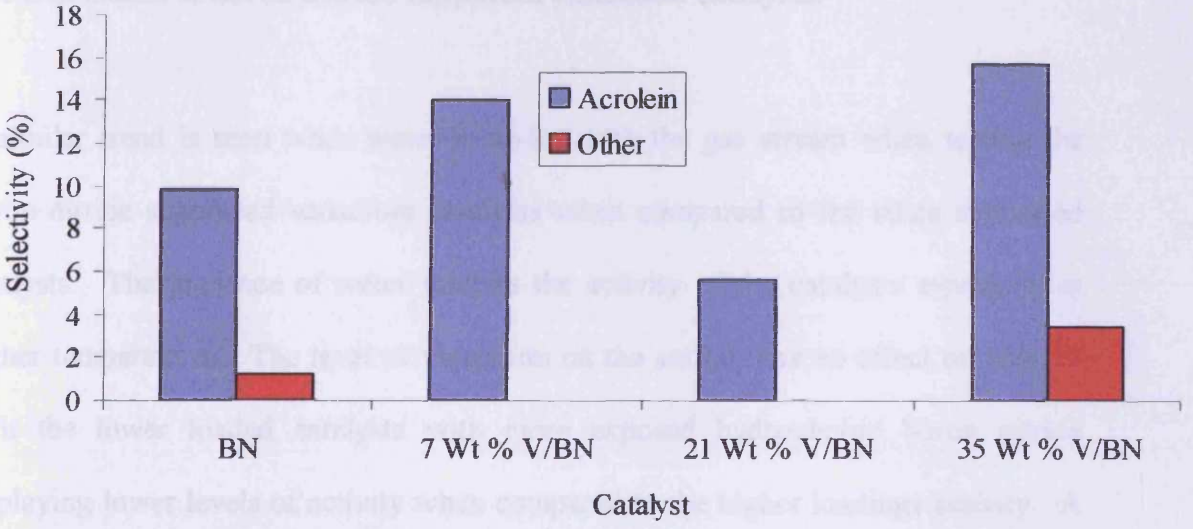

Figure 5.5.5: Selectivity to partial oxidation products at 2 % propane conversion over boron nitride supported vanadium catalysts in the presence of water.

Figure 5.5.5 shows that selectivity towards acrolein was greatest in the 7 and 35 Wt % V/BN catalysts, which was 14 and 15.5 % respectively. These levels of acrolein selectivity and those at 3.5 % propane conversion shown in figure 5.5.4 are higher than at any point when the catalysts were tested for propane oxidation in the absence of water. At the level of 2 % propane conversion the 21 Wt % V/BN catalyst showed the lowest selectivity towards acrolein and other partial oxidation products and

showed more combustion chemistry. At 2 % propane conversion the selectivities towards other partial oxidation products like acrylic acid were lower than at 3.5 % propane conversion. These ranged from 3 to 4 % selectivity at 3.5 % propane conversion excluding the 21 Wt % V/BN catalyst compared to 1 to 2 % selectivity at a propane conversion of 2 % again excluding to 21 Wt % and 7 Wt % V/BN catalysts which show no selectivity.

5.6: Discussion of boron nitride supported vanadium catalysts.

A similar trend is seen when water is co-fed with the gas stream when testing the boron nitride supported vanadium catalysts when compared to the silica supported catalysts. The presence of water inhibits the activity of the catalysts especially at higher temperatures. The level of vanadium on the surface has an effect on activity with the lower loaded catalysts with more exposed hydrophobic boron nitride displaying lower levels of activity when compared to the higher loadings activity. A reason for this could be that the greater levels of vanadium available on the surface leads to an increased level of active sites for propane activation, with a greater chance that no water is blocking them. This compares to the surface of the lower loadings, which will have smaller levels of vanadium resulting in fewer active sites with a greater chance that a water molecule could block these sites.

The selectivities shown by the catalysts seem to support this view. Although all the catalysts are selective to acrolein and other partial oxidation products at much lower temperatures and conversions in the presence of water than in the absence, the lower

loaded catalysts are more selective towards partial oxidation. The 7 Wt % V/BN catalyst activates lower levels of propane in the presence of water due to the lower number of active sites available when compared to higher loadings. This leads to the catalyst also being able to activate lower levels of any partial oxidation product like acrolein further to carbon oxides due to decreased levels of active sites which increases these selectivities.

5.7: Conclusions.

The results show that when water was co-fed with the reactants when testing silica supported molybdenum oxide catalysts for propane oxidation the activity was generally suppressed. This was seen especially in the low loaded 2.5 Wt % Mo catalyst and above 400°C for the 15 Wt % Mo catalyst. The medium 5 Wt % catalyst in the presence of water displayed similar activity and selectivity to CO_2 to when water was not present. Selectivity towards partial oxidation products like acrolein was greatly increased when water is present especially when the water was suppressing activity. Selectivities compared at constant conversions between the two reaction conditions had levels of selectivity towards acrolein up to 56 times greater at 8 % propane conversion using the 15 Wt % Mo catalyst.

For the silica supported vanadium catalysts water promoted the activity of the catalysts with lower loadings over all temperatures. For the higher 15 Wt % loading the activity was greater when co-feeding water at lower temperatures but above

425°C the catalyst tested without water was the most active. Product selectivities change depending on the loading tested and depends on what effect the water had upon activity. In the lower loaded 3.5 Wt % V catalyst which saw higher activity, combustion products were seen with just CO_2 observed when water was co-fed. This catalyst was the most selective towards partial oxidation when water was not present. On the higher 15 Wt % V loading which had a general decrease in activity, a large increase in selectivity towards acrolein and other partial oxidation products was seen in the presence of water.

For the boron nitride supported vanadium catalysts activity was generally suppressed in the presence of water and this was especially so in the boron nitride blank and the lowest loaded 7 Wt % V/ BN catalyst compared to when water was absent. The activity of the higher loadings was greater for propane oxidation than in the lower loadings with the 21 Wt % V/BN catalyst being the most active. This activity in the 21 Wt % catalyst lowered its selective partial oxidation chemistry and produced much lower levels of acrolein and more CO_2 when compared to the lower 7 Wt % loading and the boron nitride. These displayed the best selectivity towards acrolein and other partial oxidation products at a propane conversion level of 3.5 % with selectivities of between 10 and 13.5 % for acrolein. This selectivity was not seen at these low levels of propane conversion in the absence of water when the catalysts were tested, with the only product seen being CO_2.

5.8: References

[1] Chiuparu, D. and Pfefferle, L., Catal. Today 209 (2000) 415.

[2] Harris, R.H., Boyd, V.J., Hutchings, G.J. and Taylor, S.H., Catal. Lett. 78 (2002) 369-372.

[3] Ai, M., Catal. Today., 13 (1992) 679-684.

Chapter 6: Silica and boron nitride supported molybdenum and vanadium oxide catalysts for methane and ethane oxidation.

6.1: Introduction

The direct conversion of alkanes by heterogeneous catalytic selective oxidation to more commercially viable products like alcohols, aldehydes and acids as been a major research aim for many years. The selective oxidation of methane to methanol and formaldehyde is regarded as a difficult transformation and has been researched extensively over the previous years [1]. Many of the catalysts studied show similar performance, with product selectivities limited by gas phase chemistry [2]. The conversion of methane and ethane by partial oxidation could be a more viable process, resulting in the lowering of the reaction temperature and reducing the influence of unselective gas phase chemistry. Heterogeneous catalysis would enhance the more selective surface catalysed reactions.

Most of the previous work has centred on the oxidation of methane using silica supported molybdenum and vanadium catalysts [1]. The selective oxidation of ethane to ethanal and acetic acid is thermodynamically feasible and the suitability of these silica supported catalysts for methane oxidation suggests that selective ethane oxidation using these catalytic systems should also be possible [3].

A selection of silica supported molybdenum and vanadium catalysts along with boron nitride supported vanadium catalysts have been tested for methane and ethane oxidation.

6.2: Methane oxidation.

All the catalysts were tested for methane oxidation using the methods described in section 2.2.

6.2.1: Silica supported vanadium oxide catalysts.

A range of catalysts was selected to include low, medium and high loadings of silica supported vanadium oxide to test whether the amount of vanadium of the surface effects conversion and selectivity. Figure 6.2.1.1 shows a range of catalysts and these are compared to bare silica and the analysis tested without a catalyst present in a blank reactor tube.

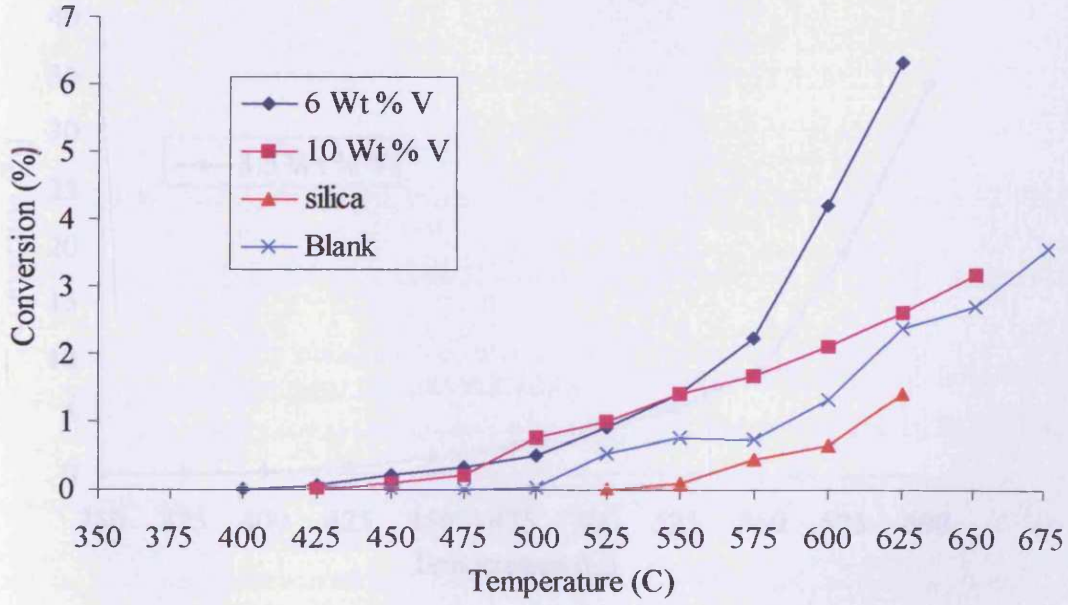

Figure 6.2.1.1: Activity for methane oxidation over silica supported vanadium catalysts.

When analysing the silica supported 6 and 10 Wt % V catalysts their activity was greater than when compared to the blank reaction tube and silica and this trend was found over the entire temperature range tested. The blank reactor tube was also more active than bare silica with approximately twice the activity. The silica supported 6 and 10 Wt % catalysts had lower light-off temperatures by 25-50°C than the blank reactions and showed similar activity up to 550°C. After this temperature the 6 Wt % V catalyst had the greater activity with a methane conversion of 6.3 % compared to 2.6 % for the 10 Wt % V catalyst at 625°C.

A 3.5 Wt % V catalyst was also tested and displayed much greater activity than the silica supported catalysts in figure 6.2.1.1. The activity of the 3.5 Wt % V catalyst is shown in figure 6.2.1.2 separately due to the high levels of conversion attained.

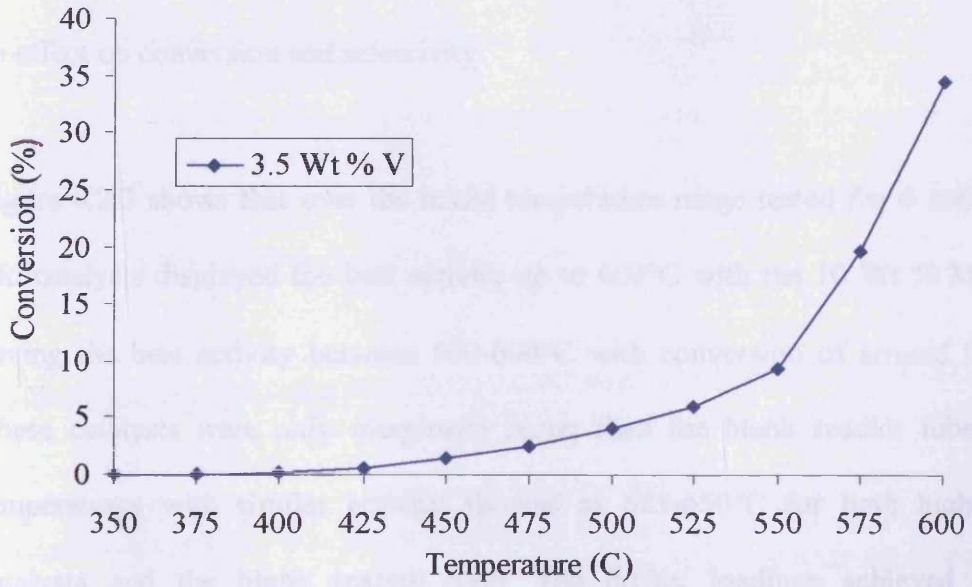

Figure 6.2.1.2: Activity for methane oxidation over 3.5 Wt % Vanadium catalyst.

This catalyst showed greater activity over all the temperatures analysed with a conversion of 34.4 % at 600°C compared to 4.1 % for the 6 Wt % V catalyst which was the second most active of the silica supported vanadium catalysts tested. This catalysts light-off temperature was also 50°C lower than the supported silica vanadium catalysts shown in figure 6.2.1.1 at 350°C. When the selectivities for products were compared for the silica supported vanadium catalysts as well as the silica and blank reactor tube they all produced CO_2 at 100 % selectivity over the whole temperature range tested.

6.2.2: Silica supported molybdenum oxide catalysts.

A selected range of catalyst to include a low, medium and high molybdenum loading was tested for methane oxidation with the results shown in figure 6.2.2. These are compared to bare silica and a blank reactor tube to discover whether the loading has an effect on conversion and selectivity.

Figure 6.2.2 shows that over the initial temperature range tested the 6 and 10 Wt % Mo catalysts displayed the best activity up to 600°C with the 10 Wt % Mo catalyst having the best activity between 500-600°C with conversion of around 0.5-1.5 %. These catalysts were only marginally better than the blank reactor tube at lower temperatures with similar activity showed at 625-650°C for both higher loaded catalysts and the blank reactor tube. The higher loadings achieved levels of conversion of between 4-5 % at the highest temperatures tested.

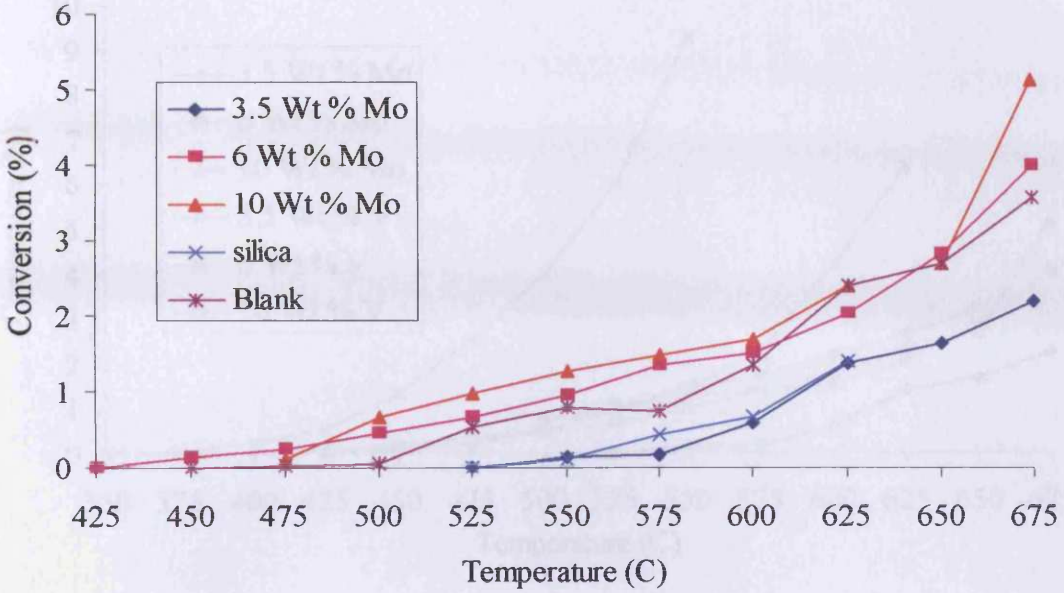

Figure 6.2.2: Activity for methane conversion over silica supported molybdenum oxide catalysts.

The 3.5 Wt % Mo catalysts activity was much lower than both the higher loadings and the blank reactor tube and was similar to when bare silica was tested with conversion of approximately 2 % at the highest temperature analysed. When the silica supported molybdenum catalysts were analysed for products they all produced CO_2 at 100 % selectivity over all the temperatures analysed.

6.2.3: Comparison of silica supported molybdenum and vanadium catalysts.

The two sets of silica supported metal oxide catalysts are compared in figure 6.2.3. This includes the highly active 3.5 Wt % V catalyst but the higher levels of methane conversion have been omitted for the figure.

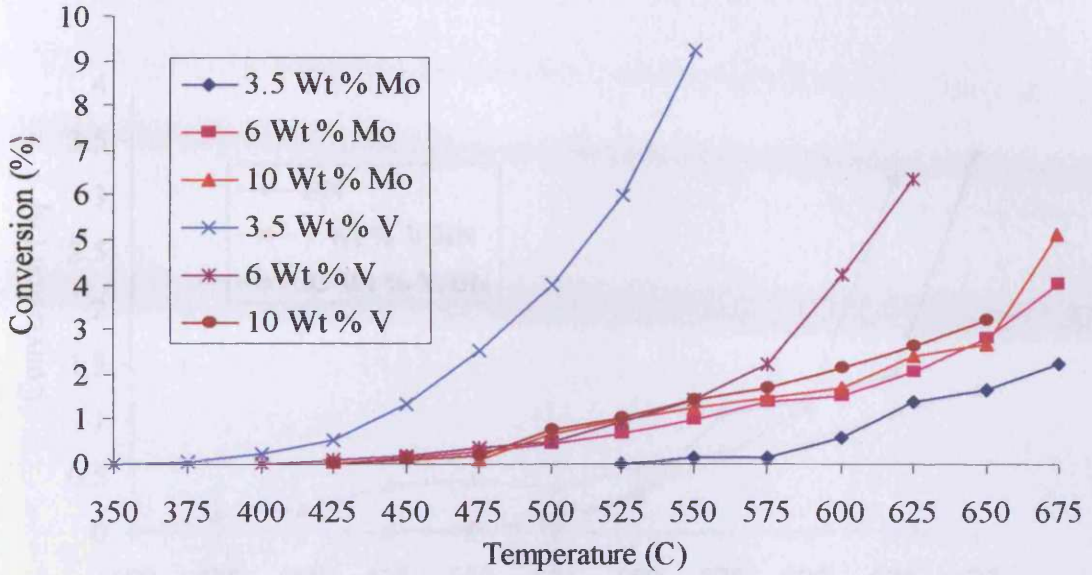

Figure 6.2.3: Activity for methane oxidation over a range of silica supported vanadium and molybdenum catalysts.

Figure 6.2.3 shows the silica supported vanadium catalysts were more active for methane oxidation than their molybdenum oxide counterparts. The 3.5 Wt % V catalyst had a greater activity over all the temperatures tested with a lower light-off of 350°C. The 6 and 10 Wt % catalysts for both metal oxide systems were very similar in activity up to 550°C, after which the activity increased greatly for the 6 Wt % V catalyst. The silica supported 10 Wt % V catalyst was marginally more active than the silica supported molybdenum oxide catalysts at the higher temperatures tested.

6.2.4: Boron nitride supported vanadium oxide catalysts.

The range of boron nitride supported vanadium oxide catalysts was tested for methane oxidation with selected catalyst results shown in figure 6.2.4.1.

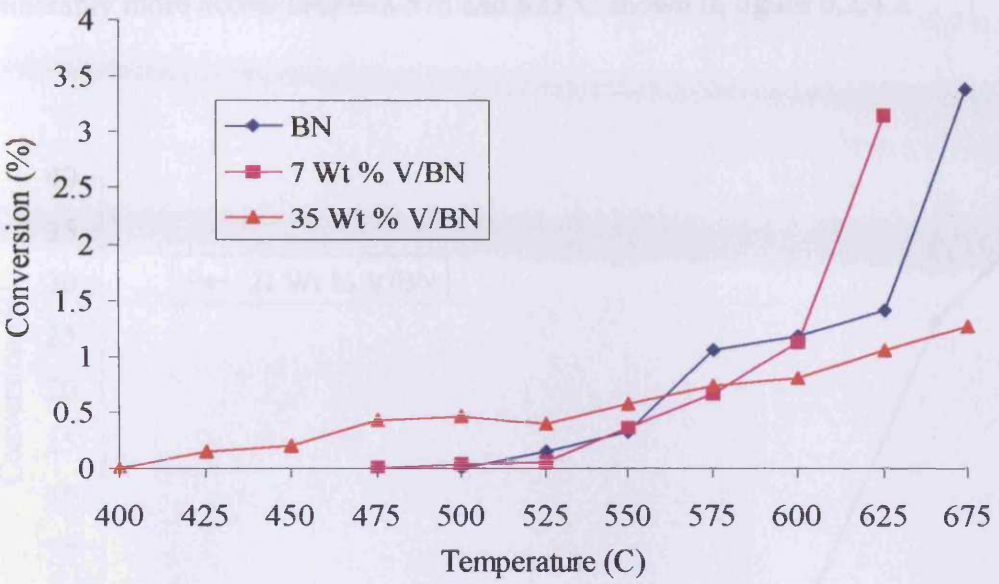

Figure 6.2.4.1: Activity for methane oxidation of a range of boron nitride supported vanadium catalysts.

For methane oxidation the loadings play an important factor when comparing the boron nitride supported vanadium catalysts. The higher loading of 35 Wt % V/BN had a much lower light-off temperature than the lower loaded 7 Wt % V/BN and the blank boron nitride of 400°C compared to 475-500°C. The activity of the 35 Wt % V/BN catalyst increased steadily over the temperature range tested. At lower temperatures the 35 Wt % V catalyst was more active up to 550°C than the lower loaded 7 Wt % V and the boron nitride and reached a maximum level of methane conversion of approximately 1 % at 675°C. Above 600°C the lower loadings were more active reaching methane conversion levels of around 3.5 % with the 7 Wt % V/BN catalyst achieving this conversion 25°C lower than the blank boron nitride.

The 21 Wt % V/BN catalyst was also tested for methane oxidation and was considerably more active between 575 and 625°C shown in figure 6.2.4.2.

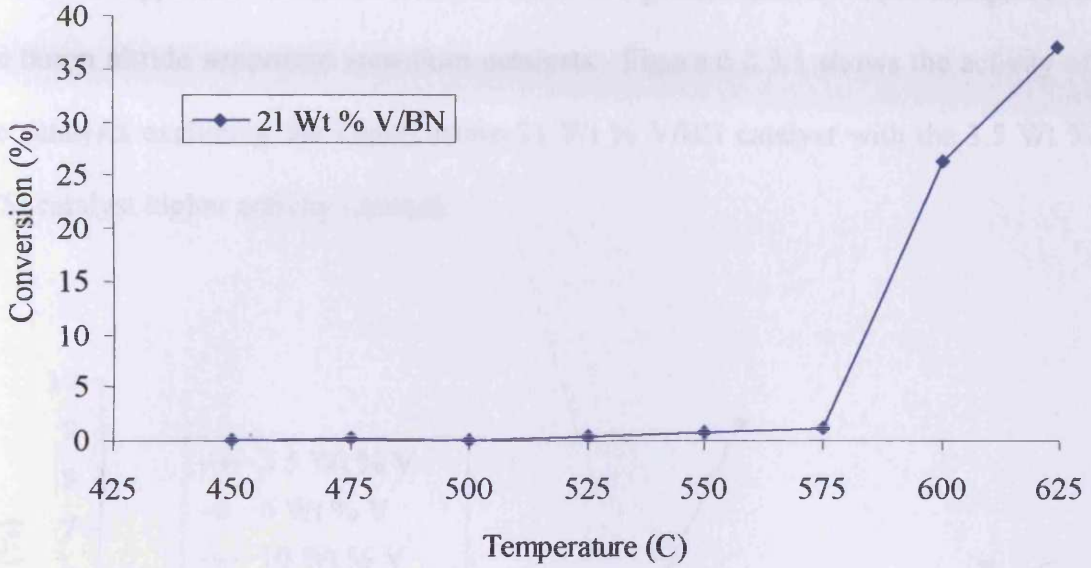

Figure 6.2.4.2: activity for methane oxidation for the boron nitride supported 21 Wt % vanadium catalyst.

The 21 Wt % V/BN catalyst achieved levels of conversion of between 26-36 % between 575 and 625°C although its activity was similar to the other boron nitride supported catalysts at the lower temperatures of 425-575°C.

When the boron nitride supported catalysts were analysed for selectivities to products all but the 21 Wt % V/BN catalysts tested gave 100 % selectivity to CO_2 at all temperatures analysed. This catalyst between 600-625°C when tested showed selectivity for carbon monoxide at around 50 % with small amounts of ethane also present and was the only catalyst of all those tested for methane oxidation that had selectivity to a product other than CO_2.

6.2.5: Comparison of silica and boron nitride supported vanadium oxide catalysts.

The silica supported vanadium catalysts show the greater activity when compared to the boron nitride supported vanadium catalysts. Figure 6.2.5.1 shows the activity of the catalysts excluding the highly active 21 Wt % V/BN catalyst with the 3.5 Wt % V/Si catalyst higher activity omitted.

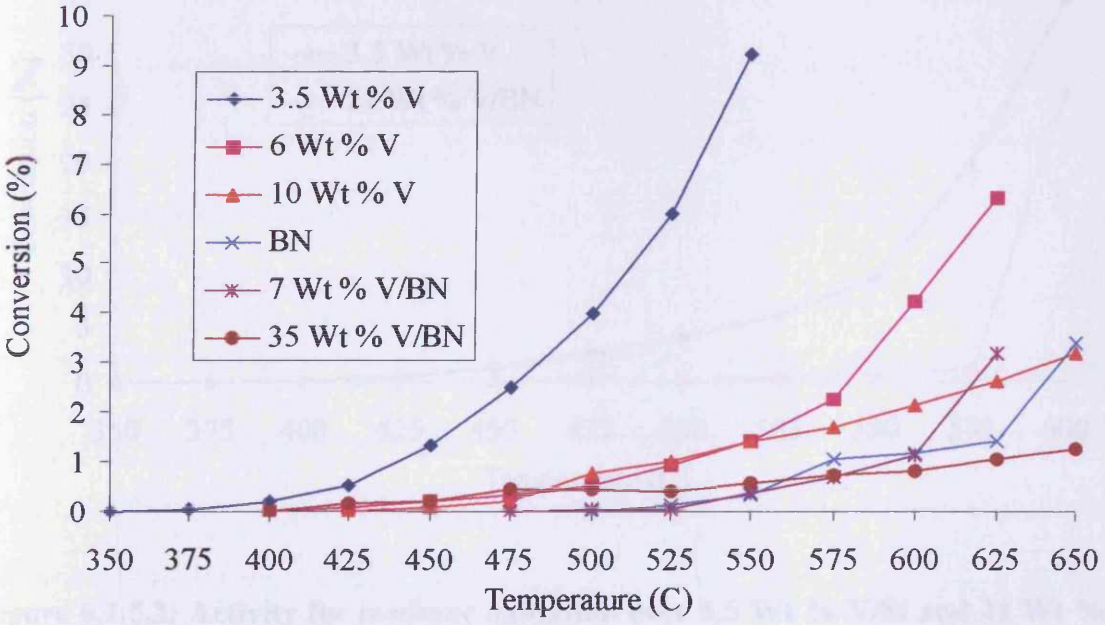

Figure 6.2.5.1: Activity for methane oxidation over silica and boron nitride supported vanadium catalysts.

The 3.5 Wt % catalyst showed the greater activity over all the temperatures tested. The activities of the 6 and 10 Wt % V/Si catalysts were equal to the 35 Wt % V/BN catalyst up to 500°C before becoming the more active catalysts up to 550°C. After this temperature the 6 Wt % V/Si loadings activity increased further than the 10 Wt %

catalyst. Only at the highest temperatures tested do the lower loaded boron nitride supported catalysts become more active than the 10 Wt % V/Si.

When the two catalysts with the highest activity were compared the silica supported 3.5 Wt % catalyst is the most active over the entire temperature range tested and is shown in figure 6.2.5.2.

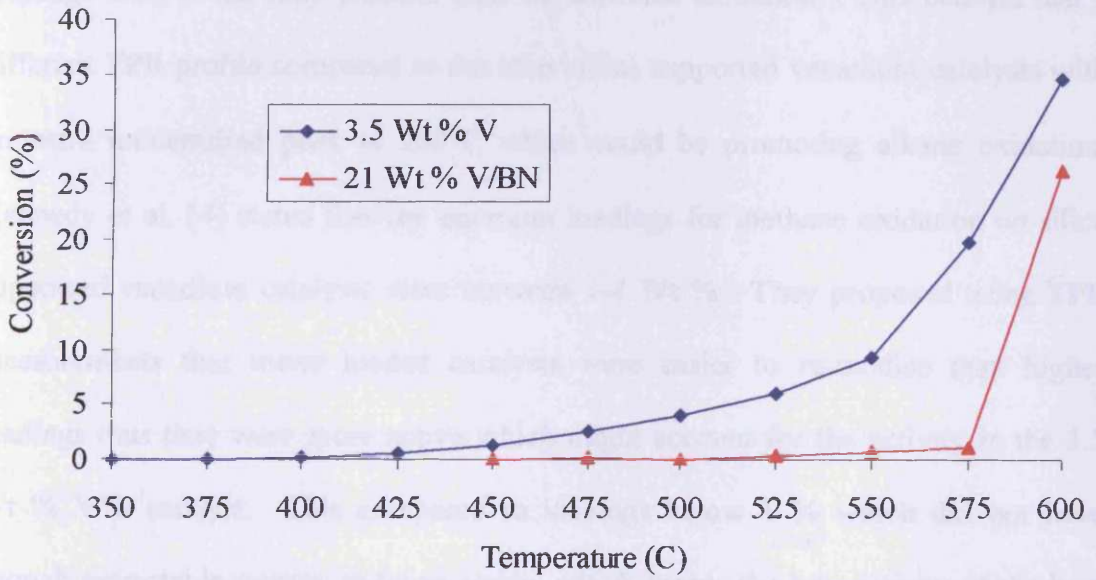

Figure 6.2.5.2: Activity for methane oxidation over 3.5 Wt % V/Si and 21 Wt % V/BN catalysts.

The 3.5 Wt % V/Si catalyst showed a much steadier increase in activity with a level of conversion of 34.4 % at 600°C compared to 26.1 % for the 21 Wt % V/BN catalyst. Excluding the 21 Wt % V/BN loading all silica and boron nitride supported catalysts showed 100 % selectivity towards CO_2 with the 21 Wt % V/BN catalyst showing selectivity to ethane and carbon monoxide at the highest temperatures tested.

6.2.6: Methane discussion.

When the silica supported vanadium oxide catalysts were tested for methane oxidation the 3.5 Wt % V catalyst was found to be much more active than the higher loadings and the blank reactions that were also tested for methane oxidation. This same catalyst also showed one of the best activities for propane oxidation displaying the best selectivity towards acrolein for the silica supported vanadium catalysts although CO_2 is the only product seen for methane oxidation. This catalyst had a different TPR profile compared to the other silica supported vanadium catalysts with an extra unidentified peak at 250°C which could be promoting alkane oxidation. Kennedy et al. [4] stated that the optimum loadings for methane oxidation on silica supported vanadium catalysts were between 1-4 Wt %. They proposed using TPR measurements that lower loaded catalysts were easier to re-oxidise than higher loadings thus they were more active which might account for the activity in the 3.5 Wt % V/Si catalyst. This compared to loadings below 1 % which did not have enough extractable oxygen to be as active, which means the low activity of the bare silica when tested could be due to this result.

The activity of the silica supported molybdenum catalysts was only slightly improved than when compared to a blank reactor tube for the higher loadings with the lowest 2.5 Wt % Mo catalyst showing a lower level of activity similar to bare silica. This shows that the conversion of methane over the higher loaded catalysts is promoted by molybdenum at lower temperatures when compared to the blank reactor tube. There is also a much greater increase in activity when the higher loadings are compared to low loaded catalysts and bare silica. At higher temperatures gas phase chemistry

becomes a factor resulting in equal levels of conversion between the higher loaded catalysts and the blank reactor tube whilst exposed silica upon low loadings has a negative effect upon methane conversion. Parmaliana et al. [5] stated that the addition of molybdenum upon silica generally had a promoting effect upon fumed silica, which is used as a support in this study. It appears that in general an increase in the amount of molybdenum (> 2.5 Wt % Mo) promotes the activity of the catalyst for methane oxidation although this activity is dependent upon the loading of the catalyst. The 6 Wt % Mo loading was the most active silica supported molybdenum catalyst when tested for methane oxidation which was also true when the oxidation of propane was studied in Chapter 4.

When the two silica supported metal oxide catalysts are compared the vanadium based catalysts are the most active for methane oxidation. Miceli et al [6] studied the oxidation of methane over a range of silica supported molybdenum and vanadium catalysts and they found that the vanadium based catalysts were more active than the molybdenum based. They proposed a model of the silica surface that included an active site for the activation of O_2. The addition of MoO_3 partially masks these active sites whilst the V_2O_5 also partially masks the same active sites but consequently produces new sites which are also active for O_2 activation promoting the activity of the silica supported vanadium catalysts compared to silica supported molybdenum based.

The activity of the boron nitride based catalysts could be related to the silica supported vanadium catalysts proposed by Kennedy et al. [4]. The blank boron nitride and the 7 Wt % V/BN catalyst are lower in activity than the higher loaded 21

and 35 Wt % V/BN at lower temperatures. This may be due to these catalyst having not enough extractable oxygen like those proposed below 1 Wt % V/Si although the oxygen can only come from the vanadium oxide present in the catalyst and not the support. If the vanadium also provides active sites there will be more present on the higher loadings resulting in an increase in activity for methane oxidation. This is especially observed on the 21 Wt % V/BN catalyst although this seems to have a negative effect at higher temperatures on the 35 Wt % V/BN catalyst, which becomes the least active at higher temperatures.

The only product produced by all catalysts was CO_2 and two main reaction pathways have been proposed for methane oxidation over silica supported molybdenum and vanadium catalysts. Spencer and Pereira [7] proposed that methane oxidation takes place on silica supported vanadium catalysts using molecular oxygen in a sequential manner making primarily formaldehyde which is further oxidised to carbon monoxide and finally further oxidised to CO_2. Spencer [8] also proposed that when silica supported molybdenum catalysts were used for methane oxidation using molecular oxygen it can go via parallel reaction pathways. The first is the same sequential route described by Spencer [7] with an additional second route oxidising methane direct to carbon dioxide. The results show that in the conditions employed that any intermediate products that may have been made using the catalyst systems were further oxidised to form the most stable product CO_2.

6.3: Ethane oxidation.

All the catalysts were tested for ethane oxidation using the methods described in section 2.2. The GC analysis differed slightly for ethane oxidation analysis by having a later valve change to bring the Poropak Q column back in series after 10.0 minutes. This is to analyse clearly the amount of ethane injected with the analysis time extended to 15 minutes to allow all possible partial oxygenated products to come through the Poropak Q column.

6.3.1: Silica supported molybdenum oxide catalysts.

A selected range of silica supported molybdenum oxide catalysts were tested for ethane oxidation and are shown in figure 6.3.1.

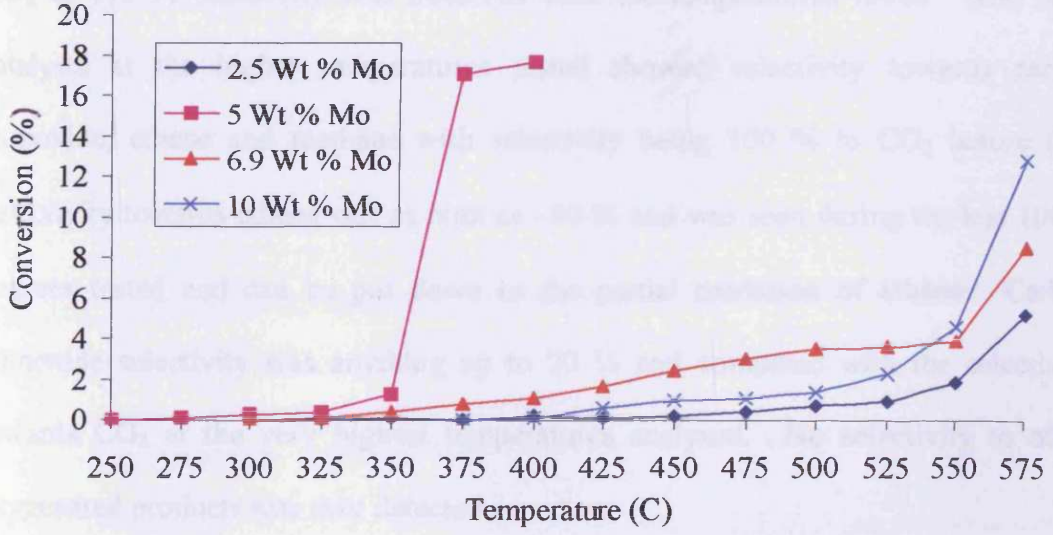

Figure 6.3.1: Activity for ethane oxidation over silica supported molybdenum catalysts.

A range of activity was exhibited that was dependent upon Mo loading. The 5 Wt % catalyst was the most active showing appreciable ethane conversion above 250°C but above 350°C a massive increase in conversion was seen from 1.3 to 17.1 %. After this temperature there was not a significant increase in conversion before the molecular oxygen was all consumed from the reaction feed. The 6.9 Wt % Mo catalyst was the most active of the others tested between 350-525°C displaying an increased level of conversion compared to the 10 Wt % catalyst which was the next which displayed the lowest activity of all the temperatures analysed. At 575°C the 2.5 Wt % Mo catalyst had an ethane conversion of 5 % compared to the 6.9 and 10 Wt % Mo catalysts which displayed activity of approximately 8.5 and 12.5 % respectively.

When the products were analysed a similar trend was seen over all the silica supported molybdenum catalysts except the 5 Wt % Mo/Si. For this catalyst only CO_2 at 100 % selectivity was observed over the temperatures tested. The other catalysts at the higher temperatures tested showed selectivity towards carbon monoxide, ethene and methane with selectivity being 100 % to CO_2 before this. Selectivity towards ethene was as high as ~80 % and was seen during the last 100°C degrees tested and can be put down to the partial oxidation of ethane. Carbon monoxide selectivity was anything up to 20 % and competed with the selectivity towards CO_2 at the very highest temperatures analysed. No selectivity to other oxygenated products was ever detected.

6.3.2: Boron nitride supported vanadium catalysts.

A range of boron nitride supported vanadium catalysts was tested for ethane oxidation with the results shown in figure 6.3.2.

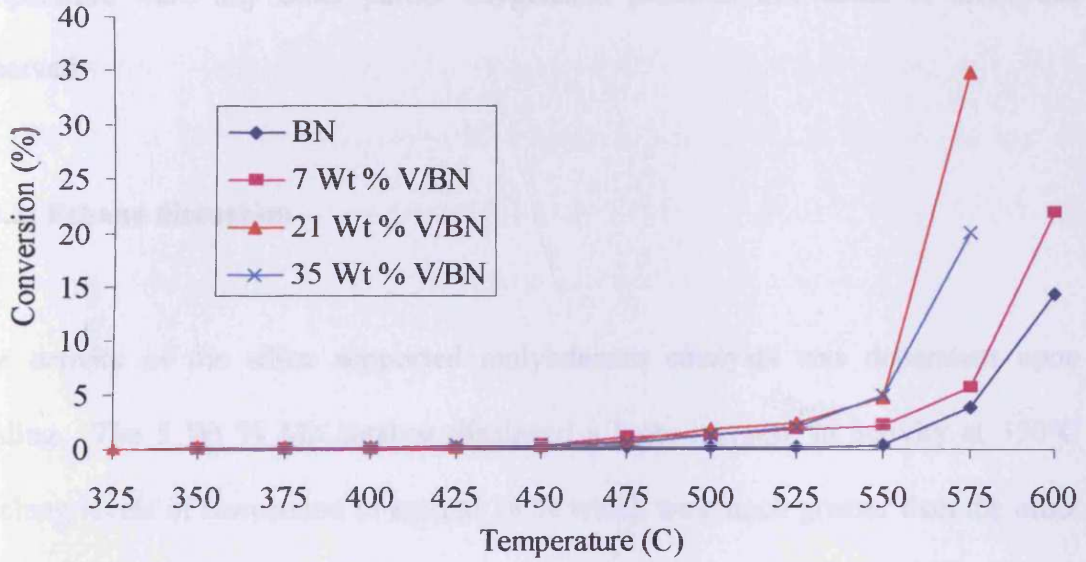

Figure 6.3.2: Activity for ethane conversion over a range of boron nitride supported vanadium catalysts.

The activity displayed was similar over the boron nitride supported catalysts up to 525°C with light-off temperatures of around 325-350°C and activity in the region of 2 %. The blank boron nitride catalyst had a lower activity in this region up to 0.25 %. After 550°C the higher loaded 21 and 35 Wt % V/BN catalysts showed the greater activity which was 34.7 and 19.9 % respectively at 575°C compared to the lower loaded 7 Wt % V/BN catalyst and the boron nitride whose activity was 22 and 14.5 % respectively at 600°C.

Selectivity to products was similar over all the catalysts tested with CO_2 the predominant product up to the later temperatures tested. After 525°C, selectivity towards ethene was dominant with up to 80-90 % selectivity. At these higher temperatures selectivity towards methane and carbon monoxide was seen with 1-5 % selectivity to methane and 5-20 % selectivity to carbon monoxide normal. At no temperature were any other partial oxygenated products like acids or aldehydes observed.

6.3.3: Ethane discussion

The activity of the silica supported molybdenum catalysts was dependent upon loading. The 5 Wt % Mo catalyst displayed a large increase in activity at 350°C reaching levels of conversion of around 18 % which was much greater than the other catalysts tested. This was similar to when propane was oxidised in Chapter 4 where this catalyst and the 6 Wt % Mo showed much greater activity than the other molybdenum catalysts tested. The 6.9 Wt % Mo catalyst was also displayed higher ethane oxidation than the other catalysts tested which is something that was also observed for propane oxidation. Lower levels of conversion when ethane is compared to propane are to be expected as ethane contains stronger C-H bond energies than are found in propane.

Boron nitride supported vanadium oxide catalysts showed two distinct levels of conversion. All loadings were similar at lower temperatures tested but at higher temperatures the higher loaded 21 and 35 Wt % catalysts were more active than the lower loaded and the blank boron nitride. This suggests that the higher loadings have

more oxygen available to take part in ethane oxidation making them more active especially at higher temperatures were oxygen exchange will be greater [4].

Product selectivities at lower temperatures over the catalysts tested gave CO_2 at 100 %. At higher temperatures other products were made with methane and carbon monoxide but the most selective product was ethene which had selectivities up to 80-90 %. Batiot and Hodnett [9] reported that the conversion of ethane to ethene was expected to be highly selective and predicted yields close to 50 %. This is because the first step in the transformation of hydrocarbons is expected to be the cleavage of C-H bonds because they are more exposed than C-C bonds present. The production of ethene can be called a partial oxidation product if it is formed by O_2.

$$C_2H_6 + \tfrac{1}{2} O_2 \rightarrow C_2H_4 + H_2O$$

At no point were other partial oxidation products observed.

6.4: Conclusions

For methane oxidation the silica supported vanadium catalysts were in general the most active of those tested with the 3.5 Wt % V/Si catalyst showing the greatest activity of all. The 21 Wt % V/BN catalyst also showed much increased activity at higher temperatures than all the other catalysts tested. The catalysts were more active than their bare support alone but some catalysts activity was equal to just a blank reactor tube suggesting that gas phase chemistry is predominant in the oxidation of methane. The only product that was observed during methane oxidation was CO_2 for any of the catalysts tested regardless of the temperature or the level of conversion.

For ethane oxidation the 5 Wt % V/Si catalyst was the most active but produced only CO_2. For the other silica supported catalysts the 6.9 Wt % catalyst was the second most active with the 2.5 Wt % V/Si the least active over all temperatures tested. The boron nitride supported catalysts were similar in activity up to the highest temperatures tested when the higher loaded 21 and 35 Wt % catalysts were more active than the lower loaded 7 Wt % V/BN catalyst and the boron nitride blank.

Product selectivity was similar over the two different ranges tested with CO_2 predominant at lower temperatures with 100 % selectivity. At higher temperatures other products were formed with ethene the most dominant from the partial oxidation of ethane with molecular oxygen. Carbon monoxide and methane were also produced at these higher temperatures but no other partial oxidation products like acetic acid were seen.

6.5: References

[1] Hall, T.J., Hargreaves, J.S.J., Hutchings, G.J., Joyner, R.W. and Taylor S.H., Fuel Process. Technol., **42** (1995) 151-178.

[2] Hutchings, G.J., Scurrell, M.S. and Woodhouse, J.R., Chem. Soc. Rev., **18** (1989) 251.

[3] Taylor, S.H., Fast Stream Application EPSRC, (1999)

[4] Kennedy, M., Sexton, A., Kartheuser, B., MacGiolla Coda, E., MacMonagle, J.B. and Hodnett, B.K., Catal. Today, **13** (1992) 447-454.

[5] Parmaliana, A., Frusteri, F., Miscelli, D., Mezzapica, A. and Scurrell, M.S., Appl. Catal. **78**. (1991) L7-L12.

[6] Miceli, D., Arena, F., Parmaliana, A., Scurrell, M.S. and Sokolovskii, V., Catal. Lett., **18** (1993) 283-288.

[7] Spencer N.D., Pereira C.J., J. Catal., **116** (1989) 339-406

[8] Spencer N.D., J Catal., **109** (1988) 187-195

[9] Batiot, C. and Hodnett, B.K., Appl. Catal. A. **137** (1996) 179

7.1 Conclusions.

From the oxidation of propane and propene it is clear that catalysts containing vanadium are more selective than those based around molybdenum. This is the case when the two silica systems are compared although the medium loaded molybdenum catalysts are very active for combustion. When the two different supports are compared the results suggest that the boron nitride supported vanadium catalysts are the more selective and active than the silica supported vanadium catalysts.

For propane oxidation on silica supported vanadium oxide catalysts, activity was dependent upon loading with all catalysts being more active than bare silica and a blank tube. Selectivities to products over all catalysts at the temperature ranges tested always gave CO_2 as the major product. Selectivities towards acrolein were approximately 1.4 % in the most selective silica supported catalyst, the 3.5 Wt % V at a propane conversion of 10 %. Other catalysts tested had selectivities between 0.5 to 1.2 % for acrolein and all catalysts had lower selectivities for other partial oxidation products like acrylic acid at around ~0.5 %.

Silica supported molybdenum oxide catalysts were also dependent on Mo loading for propane oxidation. The low and high loadings displayed similar activity when compared but the medium 5 and 6 Wt % Mo catalysts show much greater activity and at a lower light-off temperature. The selectivity to acrolein and other products was affected with the medium loadings producing only CO_2. The other low and high loaded catalysts displayed some trace selectivity towards acrolein and other partial oxidation products but these were much lower than the vanadium counterparts with the main product being CO_2.

For the boron nitride supported catalysts activity was similar when compared to the silica supported vanadium catalysts but the selectivity towards acrolein was greatly increased. At 10 % propane conversion the boron nitride catalysts displayed selectivity of between 7 and 8.5 % for acrolein with the blank boron nitride having a selectivity of approximately 4 %. These levels are much greater than the silica supported vanadium catalysts with the best being 1.4 % selectivity to acrolein. The boron nitride based catalysts also show greater selectivity to other partial oxidation products like acrylic acid than the silica based catalysts.

The same trends were seen when the catalysts were tested for propene oxidation. The loadings with around 0.17 to 0.23 theoretical monolayer coverage were the most active for both sets of catalysts although no great increase in activity was seen for the medium loaded 5 and 6 Wt % molybdenum catalyst that was seen for propane oxidation. Both sets of catalysts showed greater selectivity towards acrolein and other partial oxidation products than for propane oxidation with the 3.5 Wt % V catalyst the most selective of all silica supported tested. At lower levels of propene conversion (5 %) the selectivity towards acrolein was similar in both sets of catalysts tested with the silica supported vanadium catalysts having better selectivity towards other partial oxidation products. At a higher level of 10 % propene conversion the vanadium based catalysts were the most selective for all partial oxidation products.

When the boron nitride supported vanadium catalysts are tested for propene oxidation they showed greater activity than the silica supported vanadium catalysts. Selectivities for acrolein at 3 % propene conversion are approximately 40 % on the higher loaded V/BN catalysts compared to 20-25 % on the lower loaded catalyst and the boron nitride. Selectivities towards acrolein were greatest of all catalysts tested for the boron nitride supported vanadium catalysts. Selectivity towards acrolein was

approximately 15-20 % for V/BN catalysts compared to between approximately 8-12 % at a propene conversion of 10 % for the silica supported V catalysts, except the 3.5 Wt % silica supported V catalyst which had the second highest selectivity overall at ~17 % for acrolein. At these levels of conversion the boron nitride based catalysts were the most selective towards other products like acrylic acid.

The effect of co-feeding water with the reactants can have different results on activity and selectivities even for catalysts tested that are the same group. If the water promotes activity as in the 3.5 Wt % V/Si catalyst selectivity towards partial oxidation is lost and this catalyst produced only CO_2. The presence of co-fed water inhibited the activity of the 15 Wt % V/Si catalyst but selectivity to products like acrolein was greatly improved. The same results were found for the silica supported molybdenum catalysts where in general the co-fed water suppressed activity but improved selectivity compared to when water was absent from the reactants. The water could be having two effects with a change of the surface structure in some catalysts improving activity and another effect where the water is bonding to active sites which is lowering propane conversion. The presence of the water blocking active sites may be occurring where partial oxidation products like acrolein are being oxidised further to CO_2. The boron nitride supported vanadium catalysts activity was inhibited in the presence of water, which might be expected for a hydrophobic inert support. But selectivities towards partial oxidation products were seen at much lower levels of conversion and temperature compared to the absence of water.

For methane oxidation the vanadium supported catalysts were in general more active than the supported molybdenum catalysts but this activity produced selectivity for CO_2 only. Ethane oxidation showed that the 5 Wt % Mo/Si catalyst was the most active silica supported catalyst which followed from propane oxidation where is was

active again but for both reactions CO_2 was the only product. The other catalysts tested were less active but at higher temperatures had selectivities for other products. Ethene was the major product seen and was produced from the partial oxidation of ethane but no other selectively oxidised products were seen.

Characterisation data obtained for the catalysts showed that in general on the silica supported catalysts that increasing the loading increased the level of metal oxide present in the catalyst. Some the results obtained can be compared with activity with the silica supported 3.5 Wt % vanadium catalyst having the best selectivity to acrolein for propane oxidation in the absence of water when compared to the range silica supported catalysts tested. This catalyst had a TPR profile showing a peak at 250°C that was reproducible that could be responsible for this increased acrolein selectivity. *In situ* Raman analysis showed that the surface does not change during reaction conditions either in the presence or absence of water.

In summary the results show that vanadium oxide is more selective for partial oxidation than molybdenum for alkane oxidation. In general vanadium is also more active apart from the medium loaded silica supported molybdenum catalysts which showed high activity at low temperatures for propane combustion. The development of new catalysts is possible with the boron nitride supported vanadium catalysts showing better selectivity and activity than the silica supported catalysts. Silica has been widely researched over the previous years with many of the possible variables tested to improve catalyst design and optimise catalyst testing. Boron nitride has been rarely studied as a support and the results presented were performed using general catalyst conditions used to test the silica supported catalysts. Different catalyst preparation methods, the use of different boron nitrides and the changing of the way

the catalysts are tested could all be done to improve selectivity and activity of these catalysts. The use of co-fed water is also another important factor with improved selectivities for partial oxidation seen on many of the catalysts tested at lower levels of conversion.

7.2: Future work.

The development and optimisation of the boron nitride supported vanadium catalysts in their design and testing.

The use of co-fed water in the catalytic testing of other gases like propene, ethane and methane to compare with the reactions carried out on propane.

The optimisation of the co-fed water testing varying the amounts of water to try and improve selectivity and activty.

Appendix A: Raman spectra.

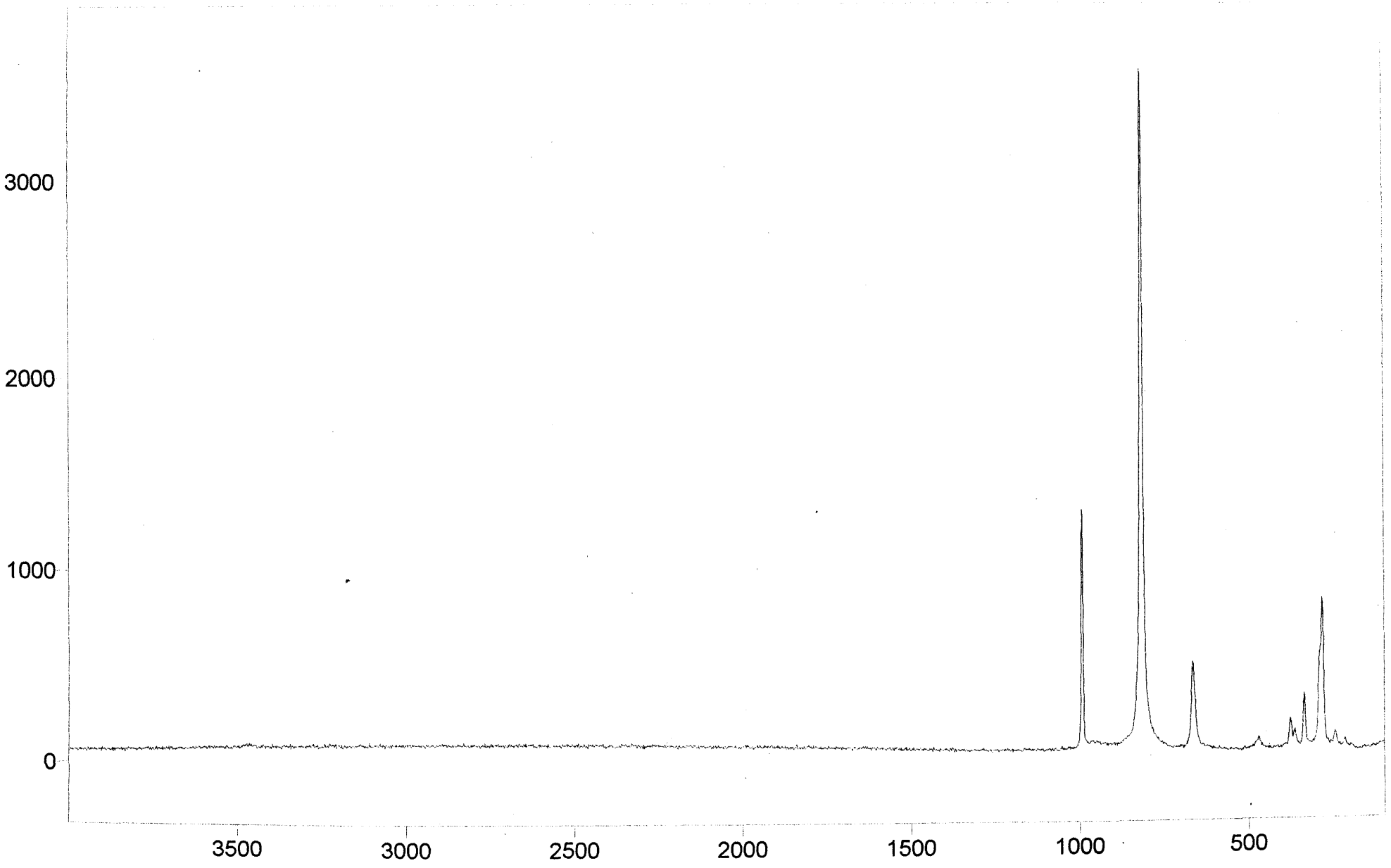

Counts / Raman Shift (cm-1)

Silica supported 10 Wt % Mo Catalyst

Appendix A: Raman spectra.

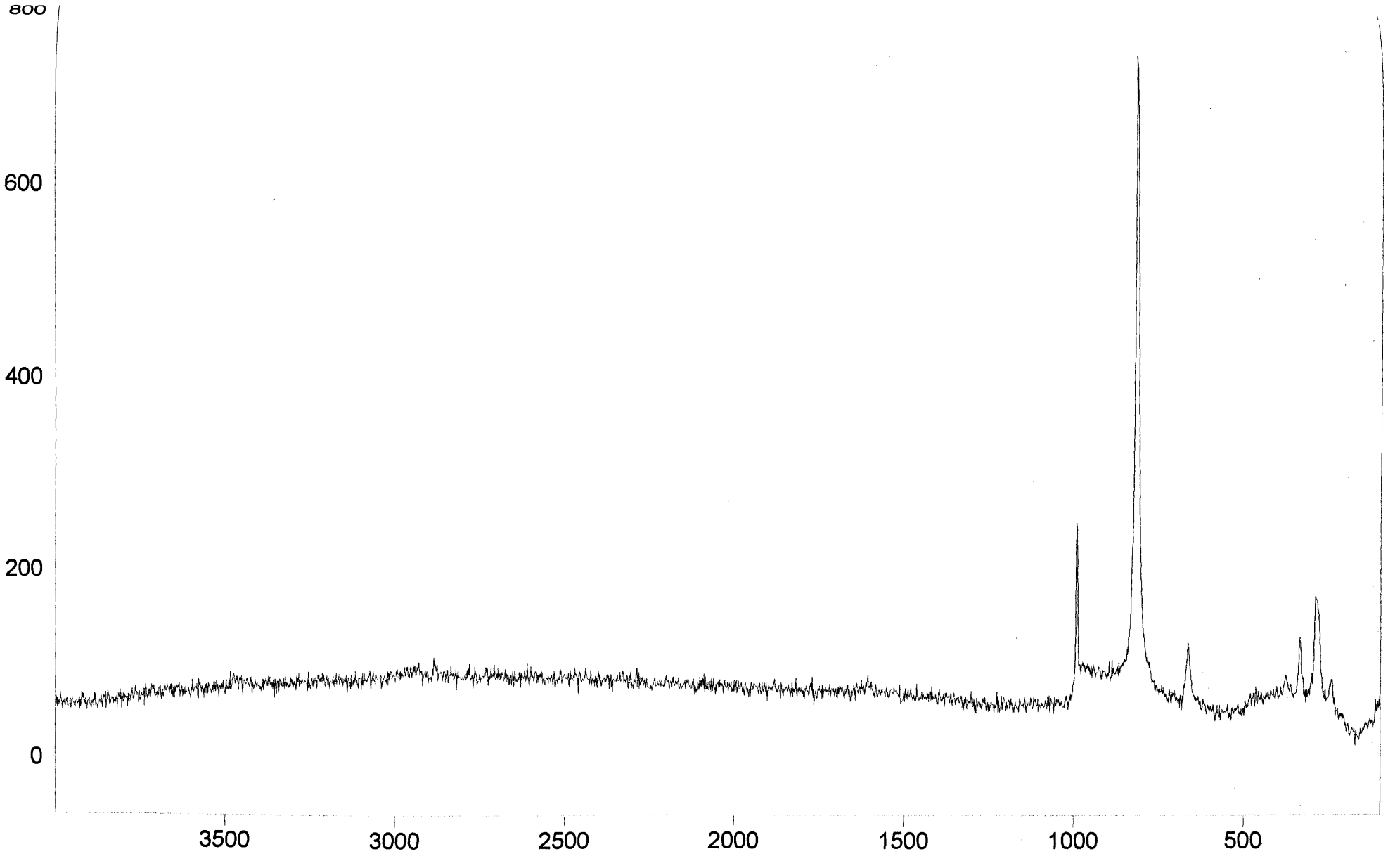

Silica supported 10 Wt % Mo Catalyst. In situ Raman 100°C

Appendix A: Raman spectra.

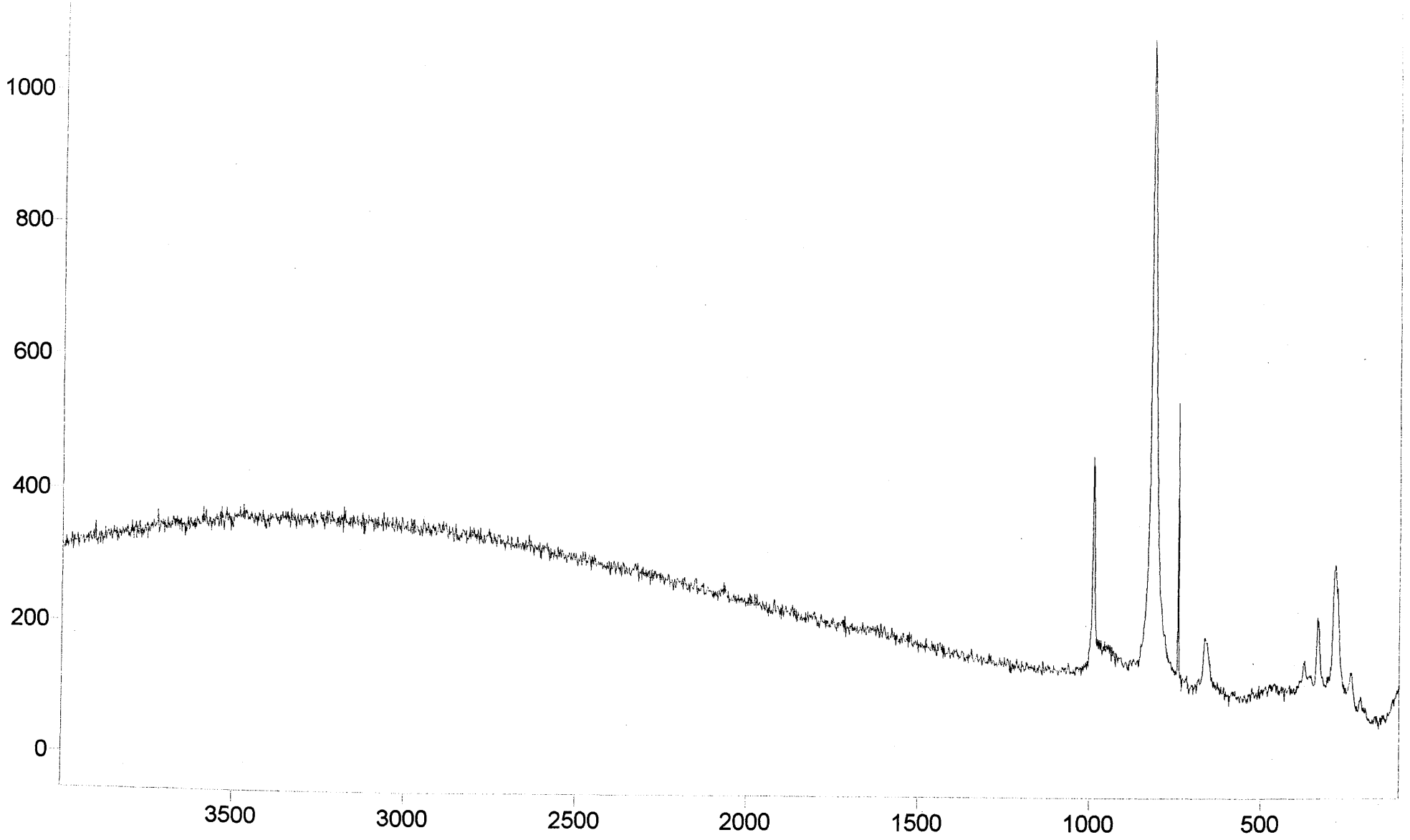

Silica supported 10 Wt % Mo Catalyst. In situ Raman 300°C

Appendix A: Raman spectra.

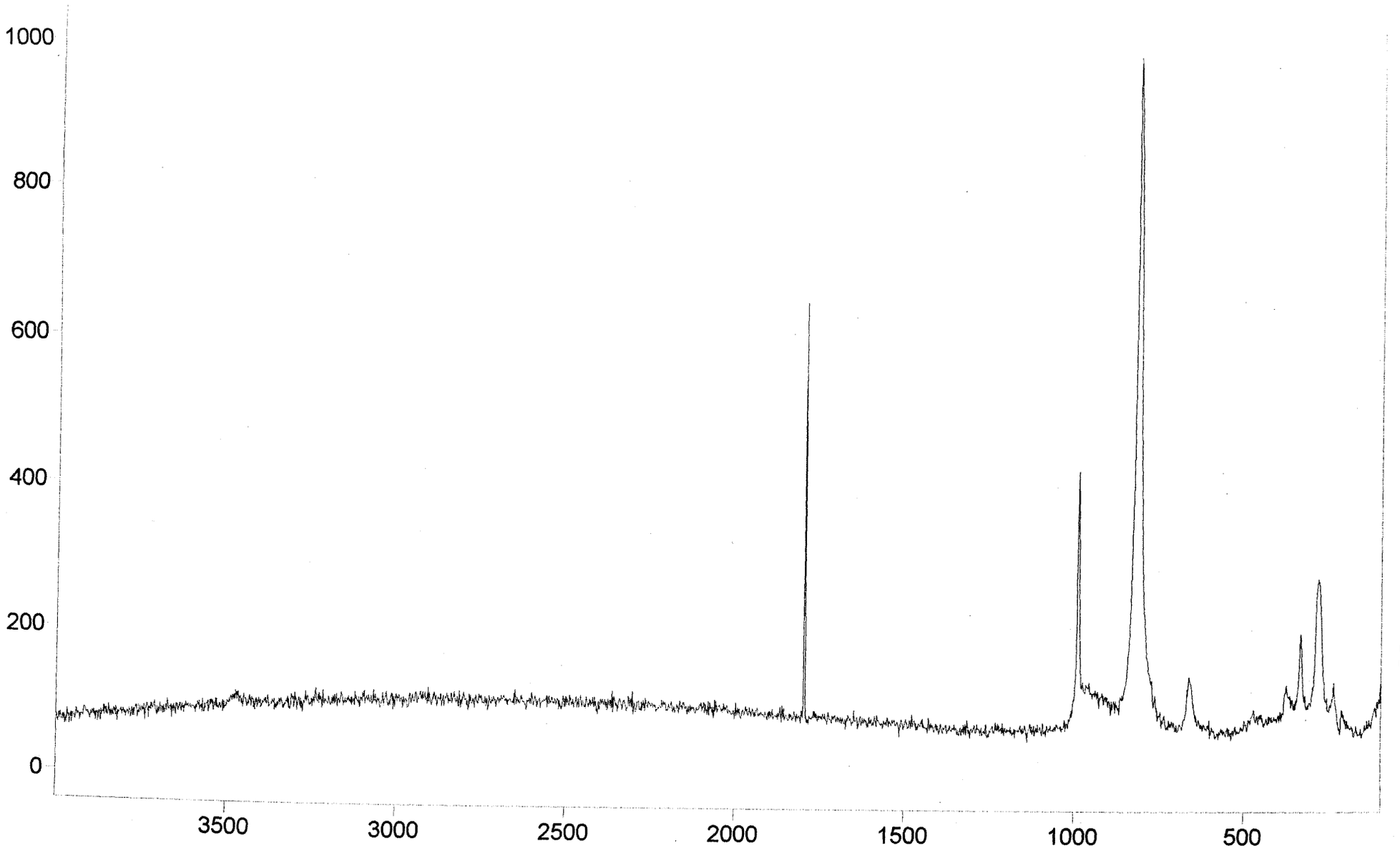

Silica supported 10 Wt % Mo Catalyst. In situ Raman 400°C

Appendix A: Raman spectra.

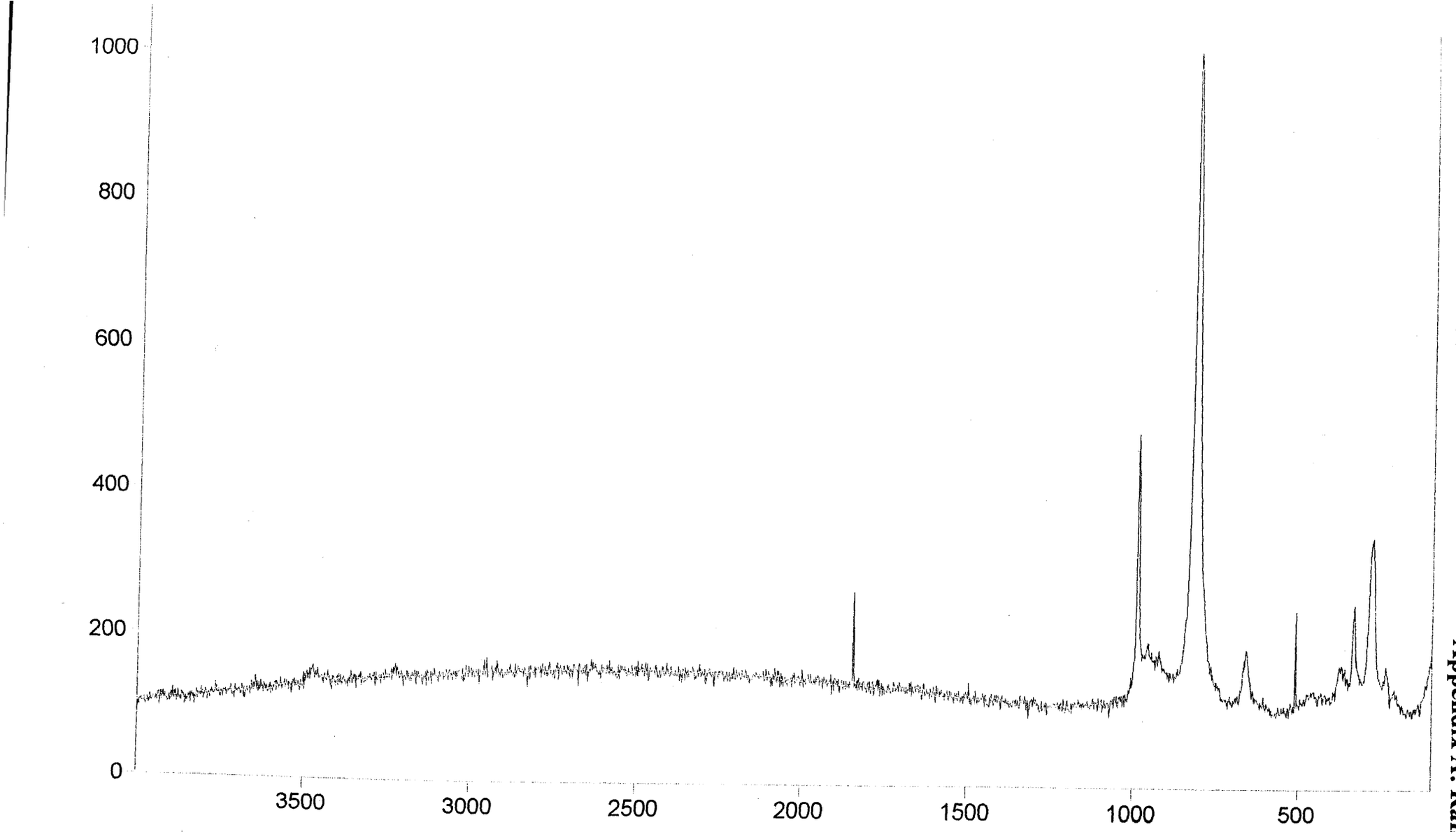

Silica supported 10 Wt % Mo Catalyst. In situ Raman 500°C

Appendix A: Raman spectra.

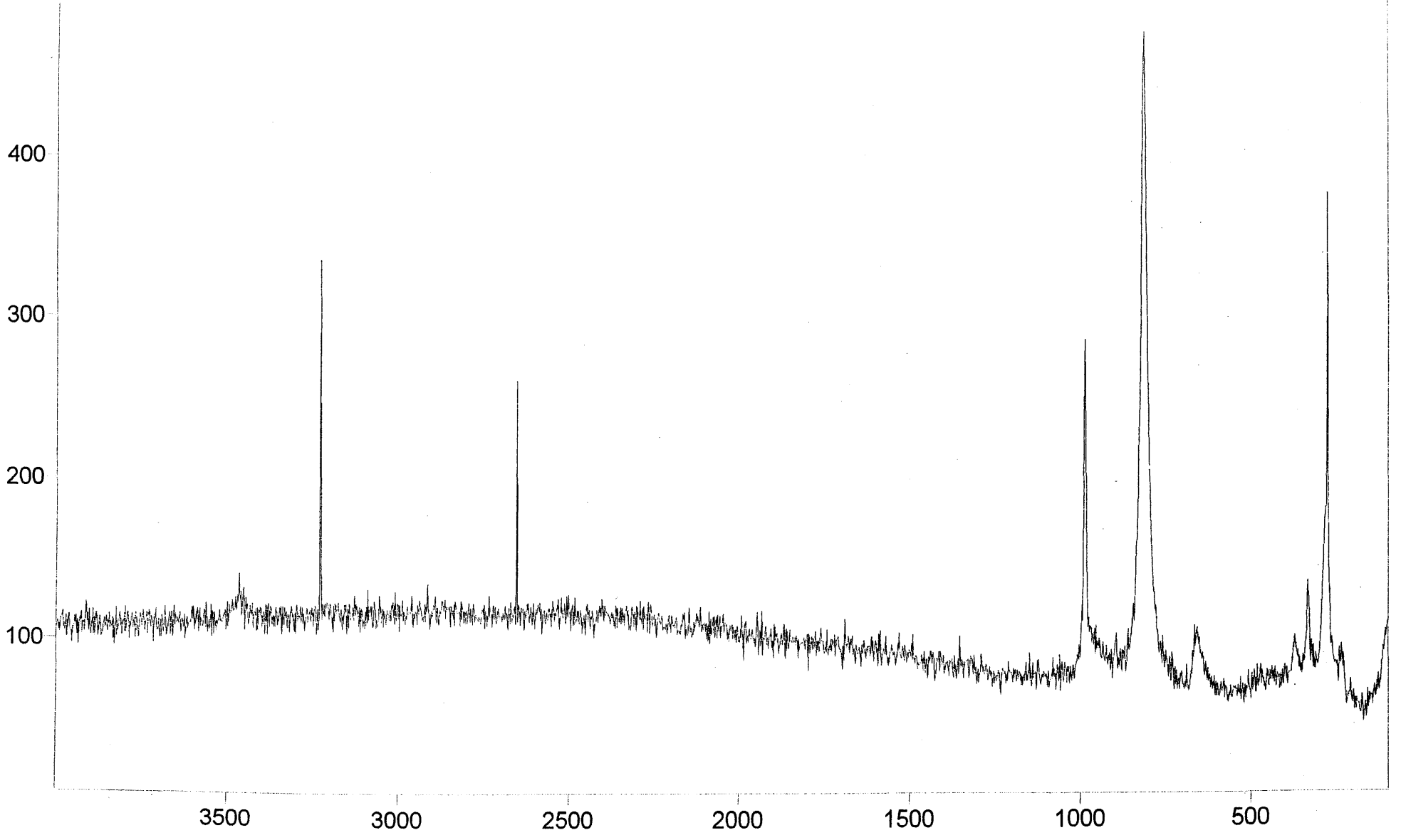

Silica supported 10 Wt % Mo Catalyst. In situ Raman 600°C

Appendix A: Raman spectra.

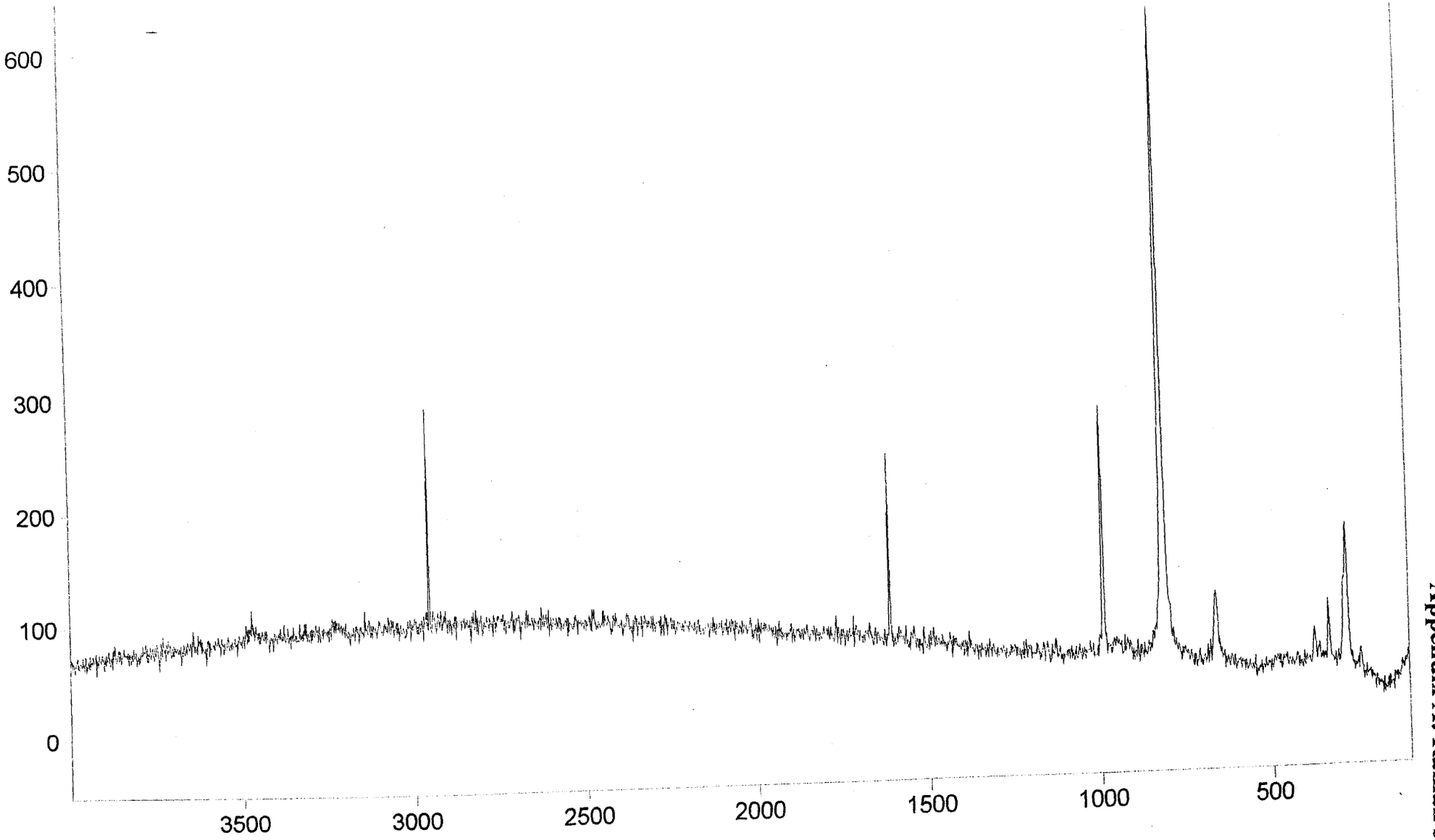

Silica supported 15 Wt % Mo Catalyst

Appendix A: Raman spectra.

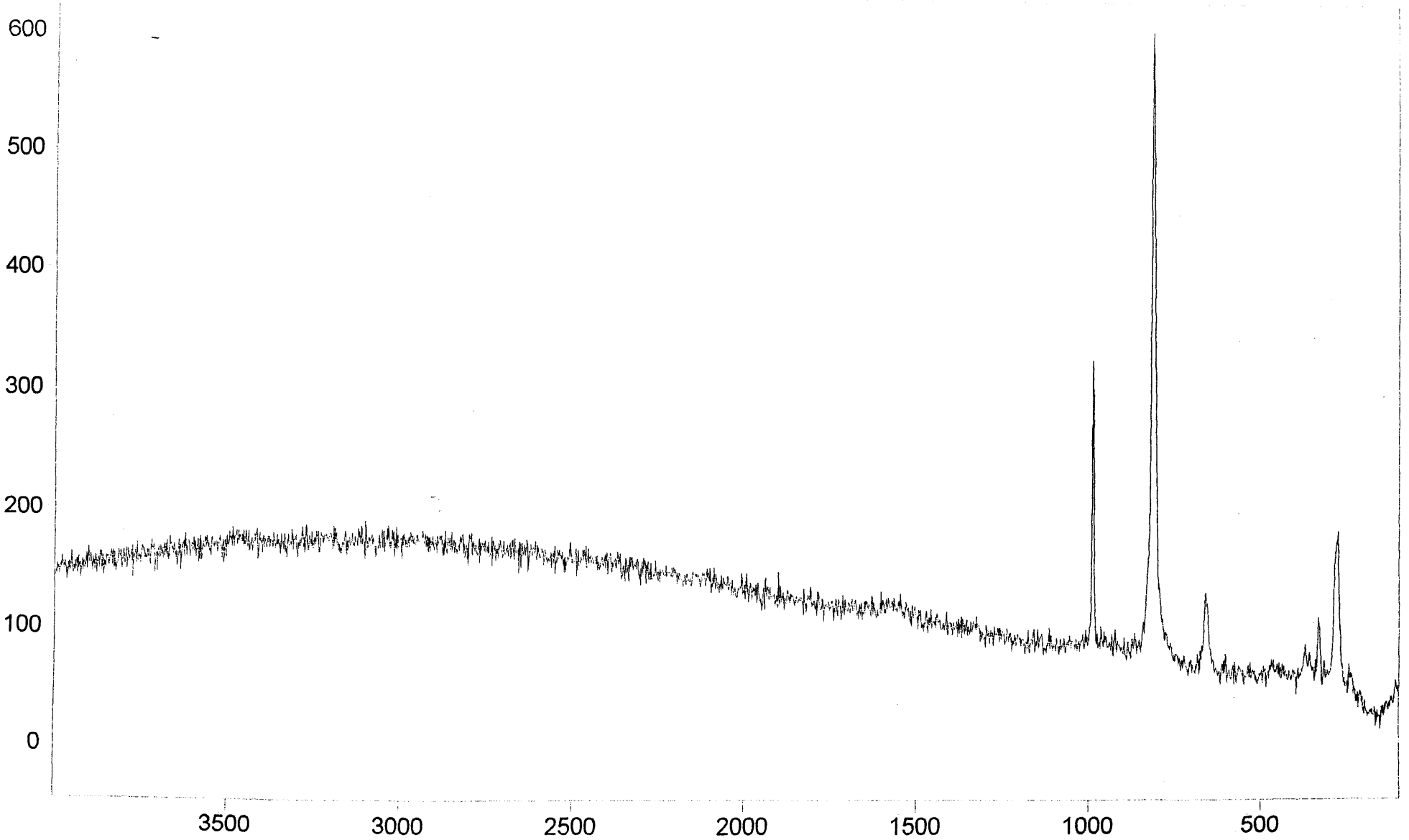

Silica supported 15 Wt % Mo Catalyst. In situ Raman 200°C

Appendix A: Raman spectra.

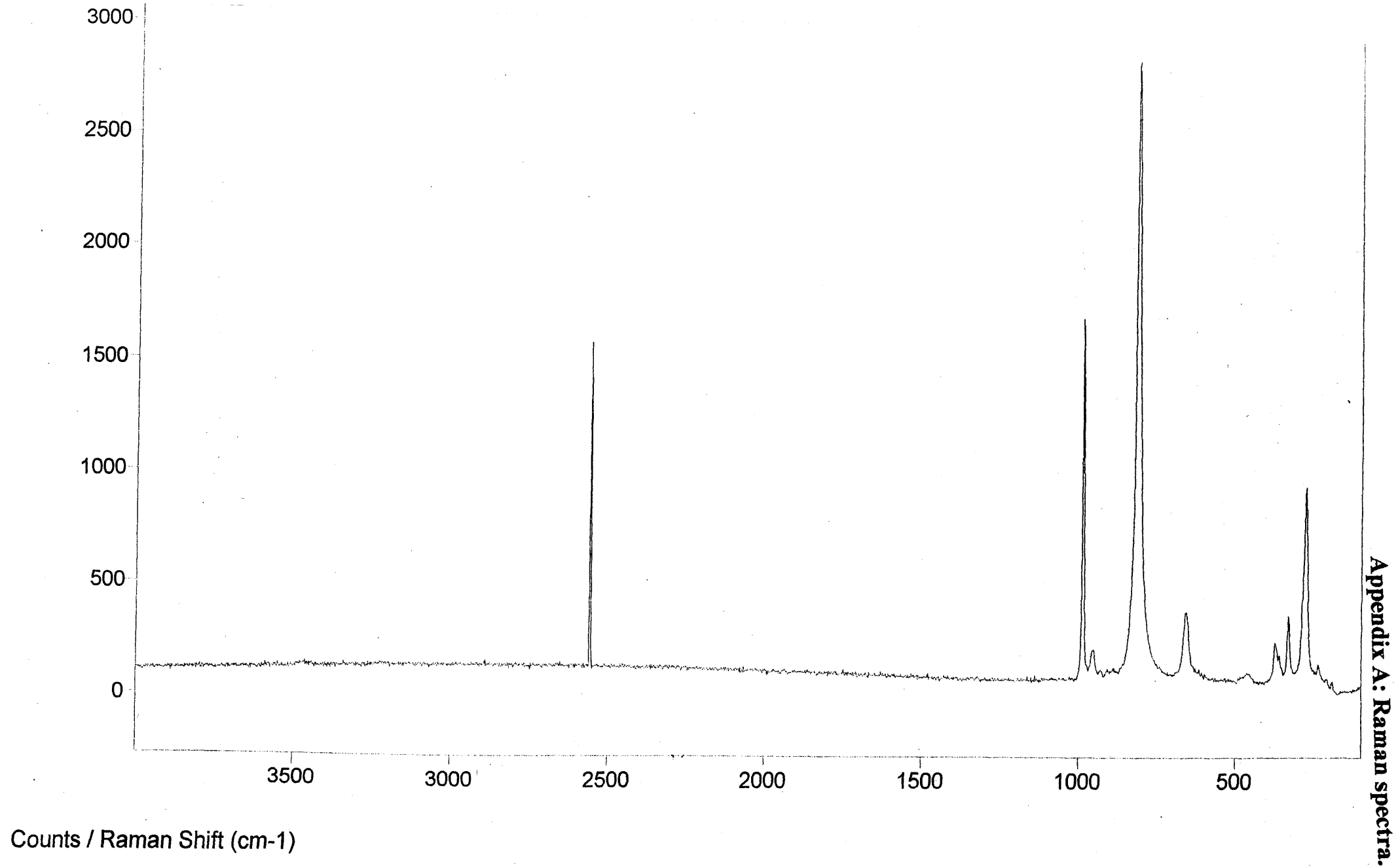

Appendix A: Raman spectra.

Silica supported 15 Wt % Mo Catalyst. In situ Raman 400°C

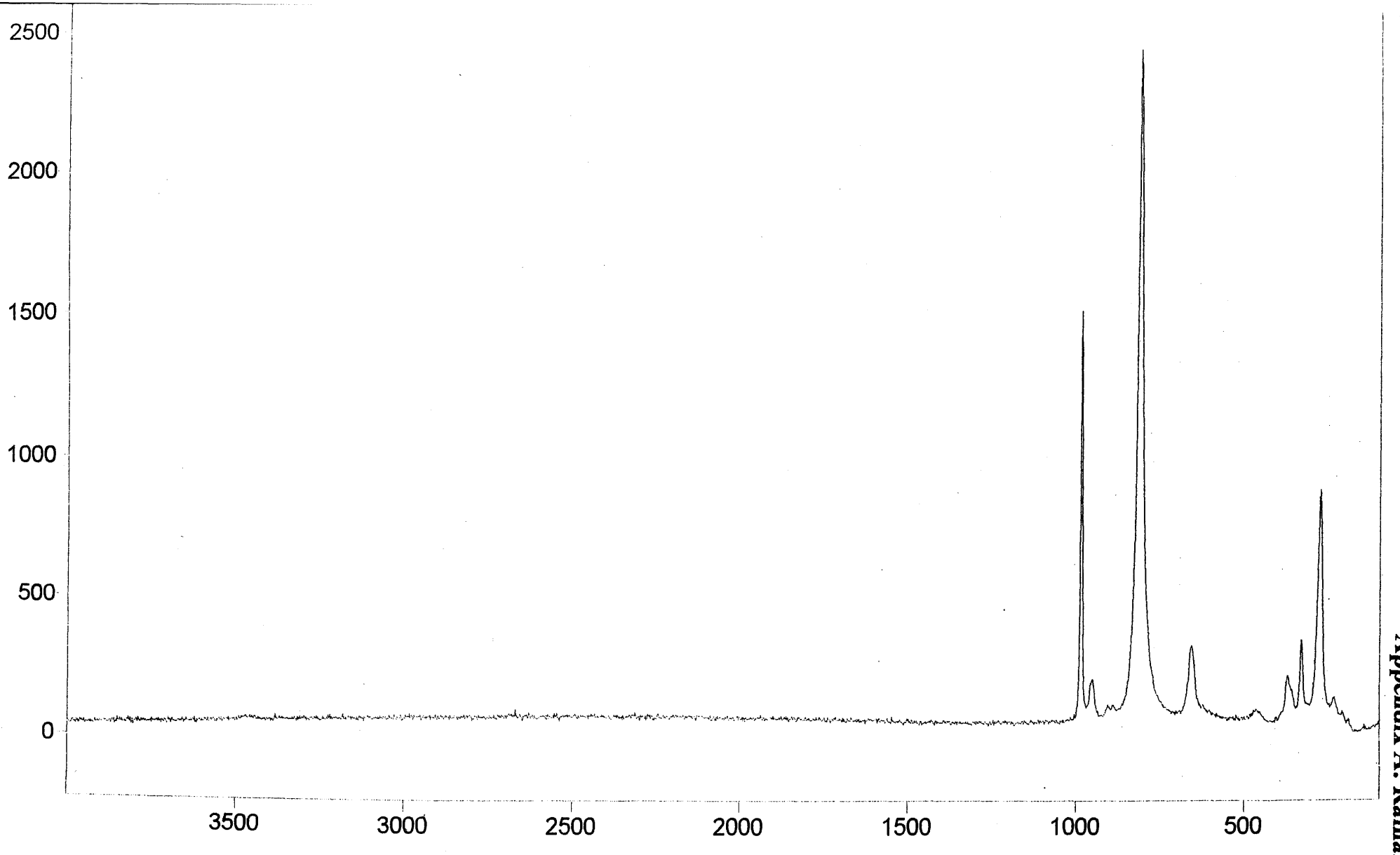

Silica supported 15 Wt % Mo Catalyst. In situ Raman 500°C

Appendix A: Raman spectra.

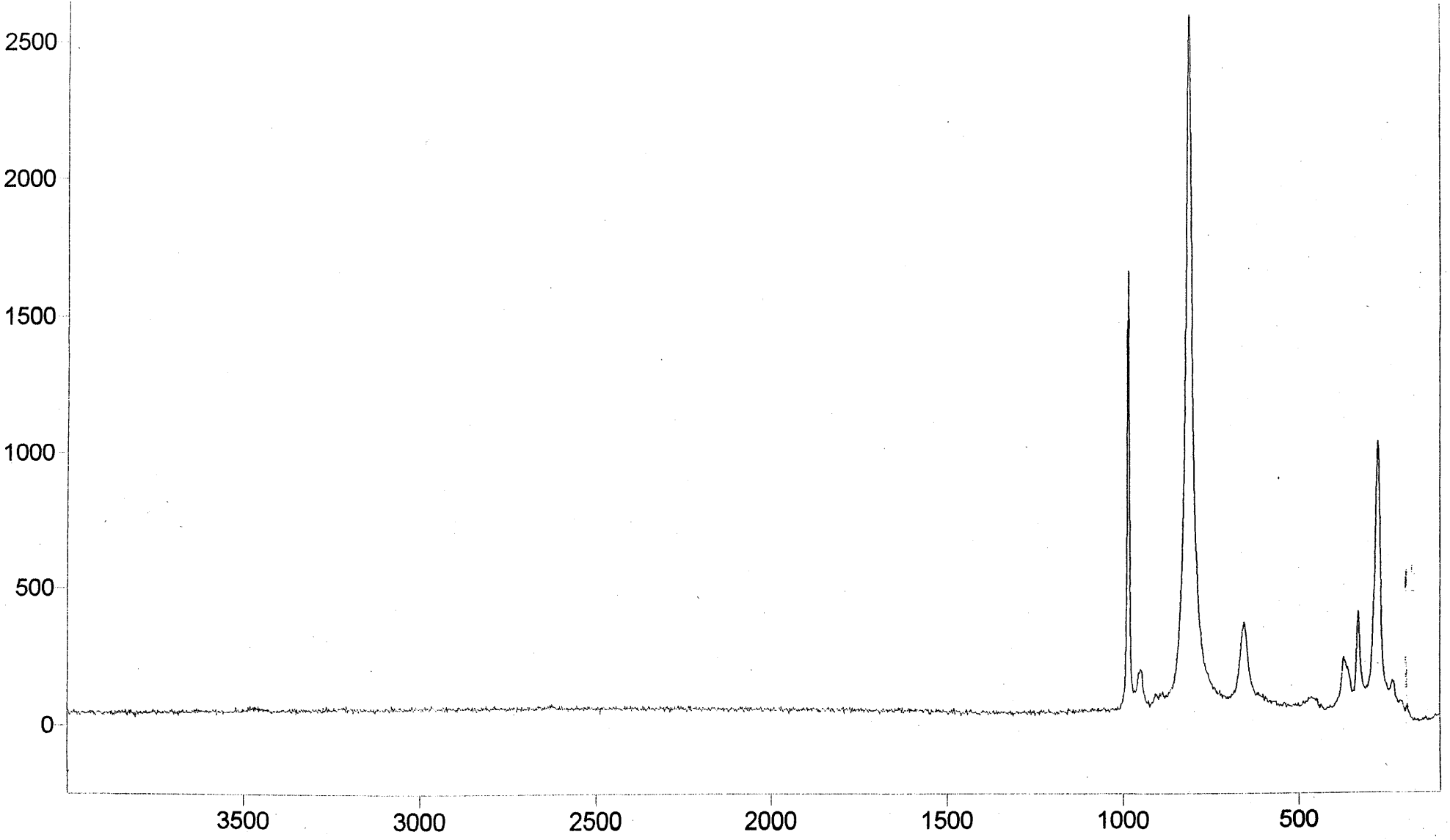

Silica supported 15 Wt % Mo Catalyst. In situ Raman 600°C

Appendix A: Raman spectra.

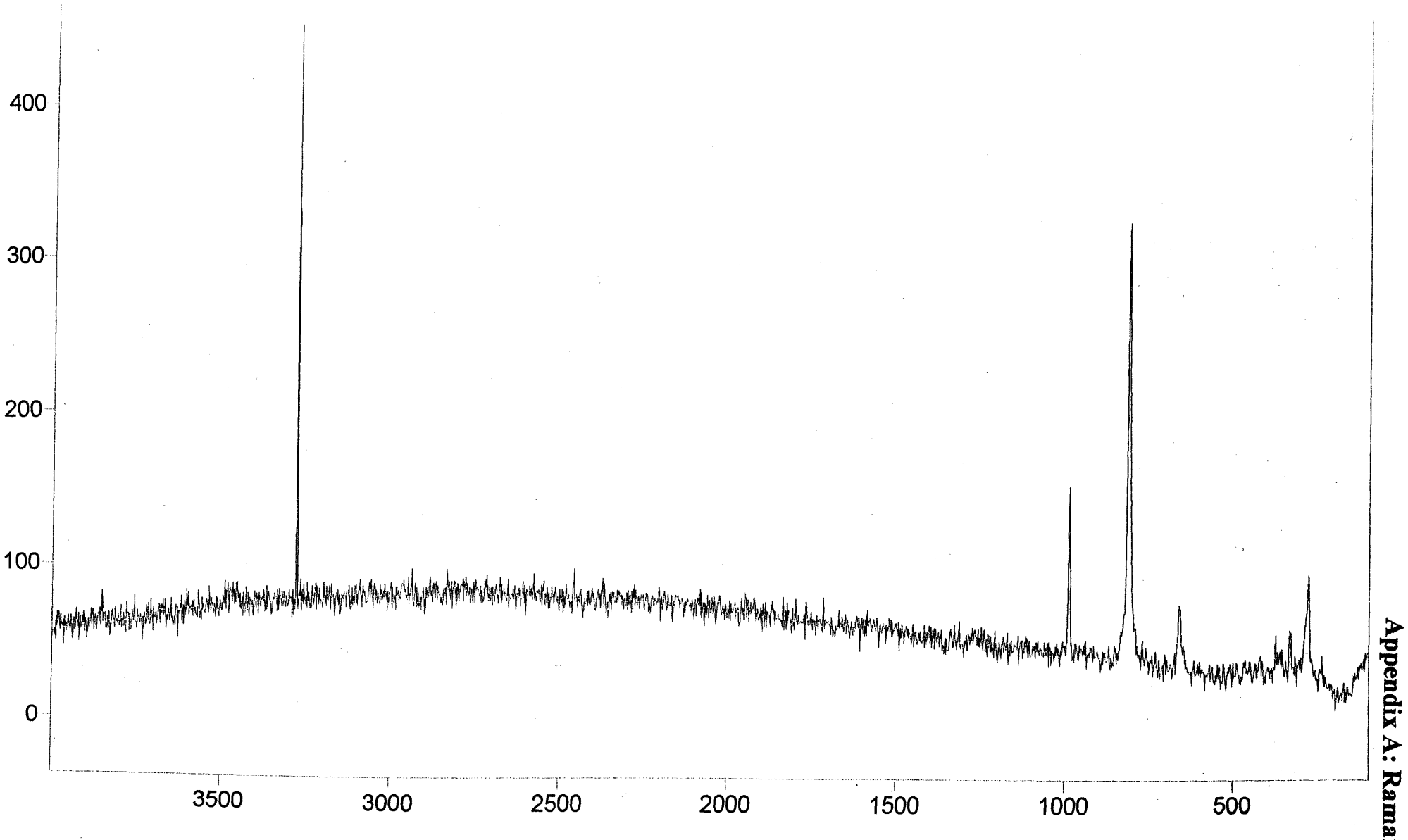

Silica supported 15 Wt % Mo Catalyst. In situ Raman 25°C with co-fed water

Appendix A: Raman spectra.

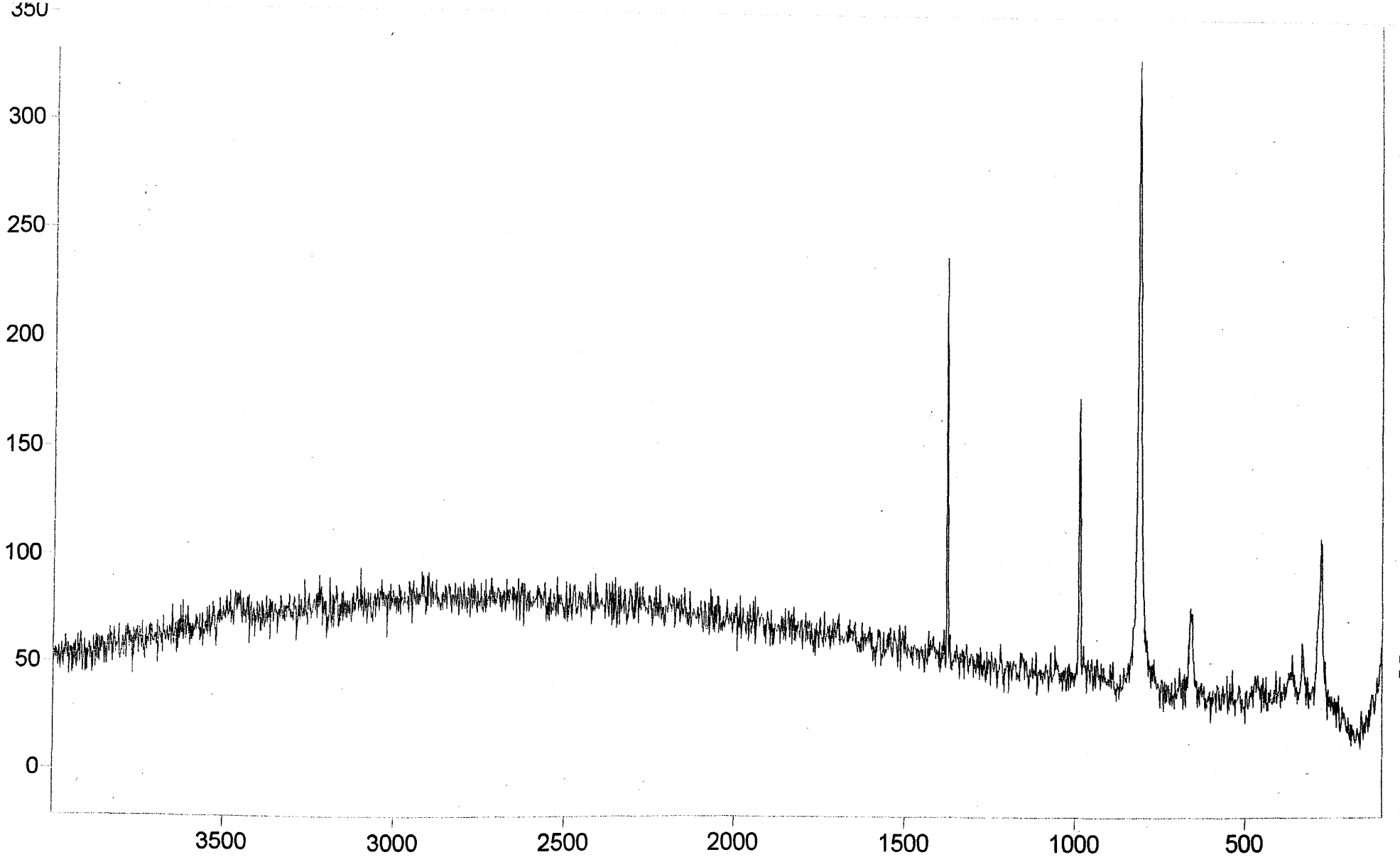

Silica supported 15 Wt % Mo Catalyst. In situ Raman 100°C with co-fed water

Appendix A: Raman spectra.

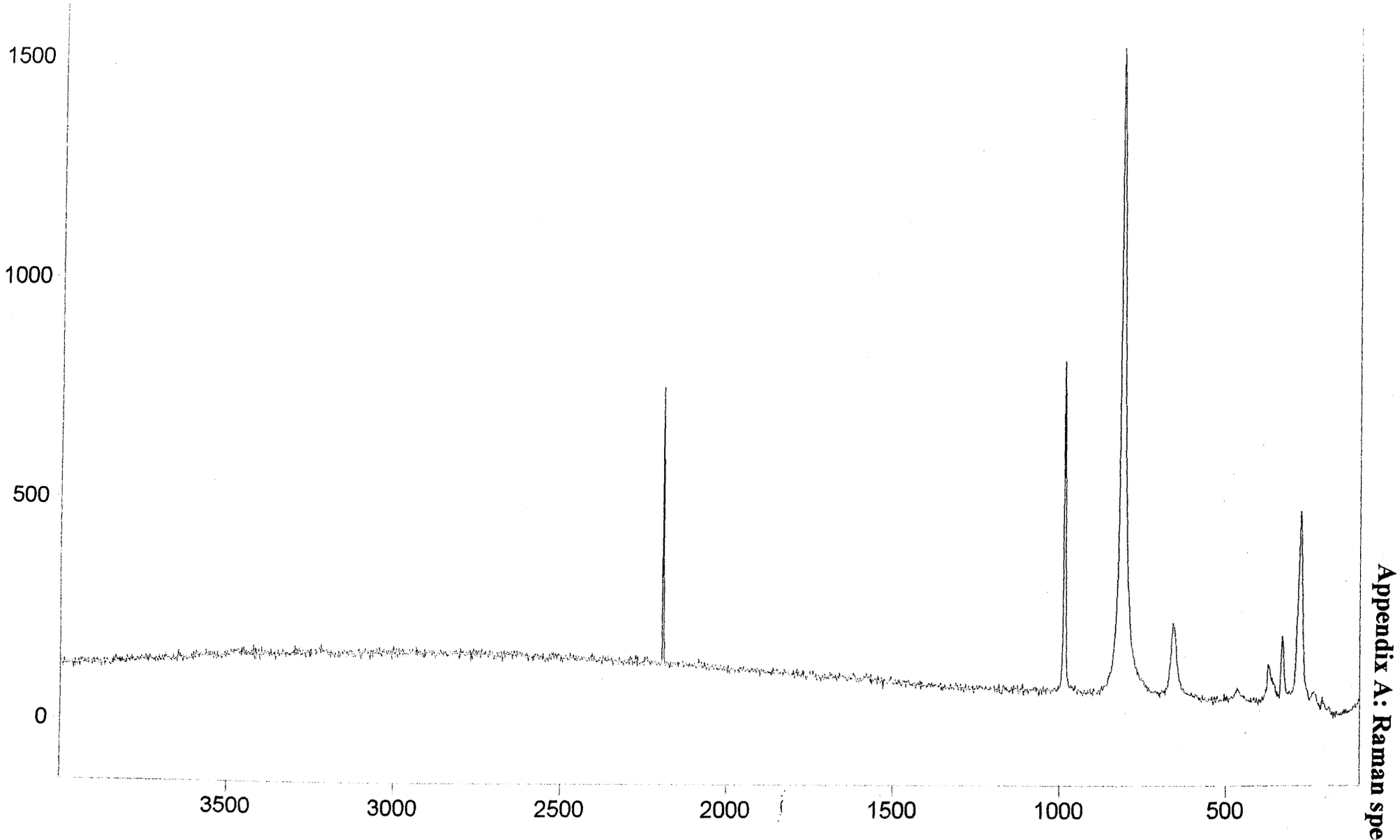

Appendix A: Raman spectra.

Silica supported 15 Wt % Mo Catalyst. In situ Raman 300°C with co-fed water

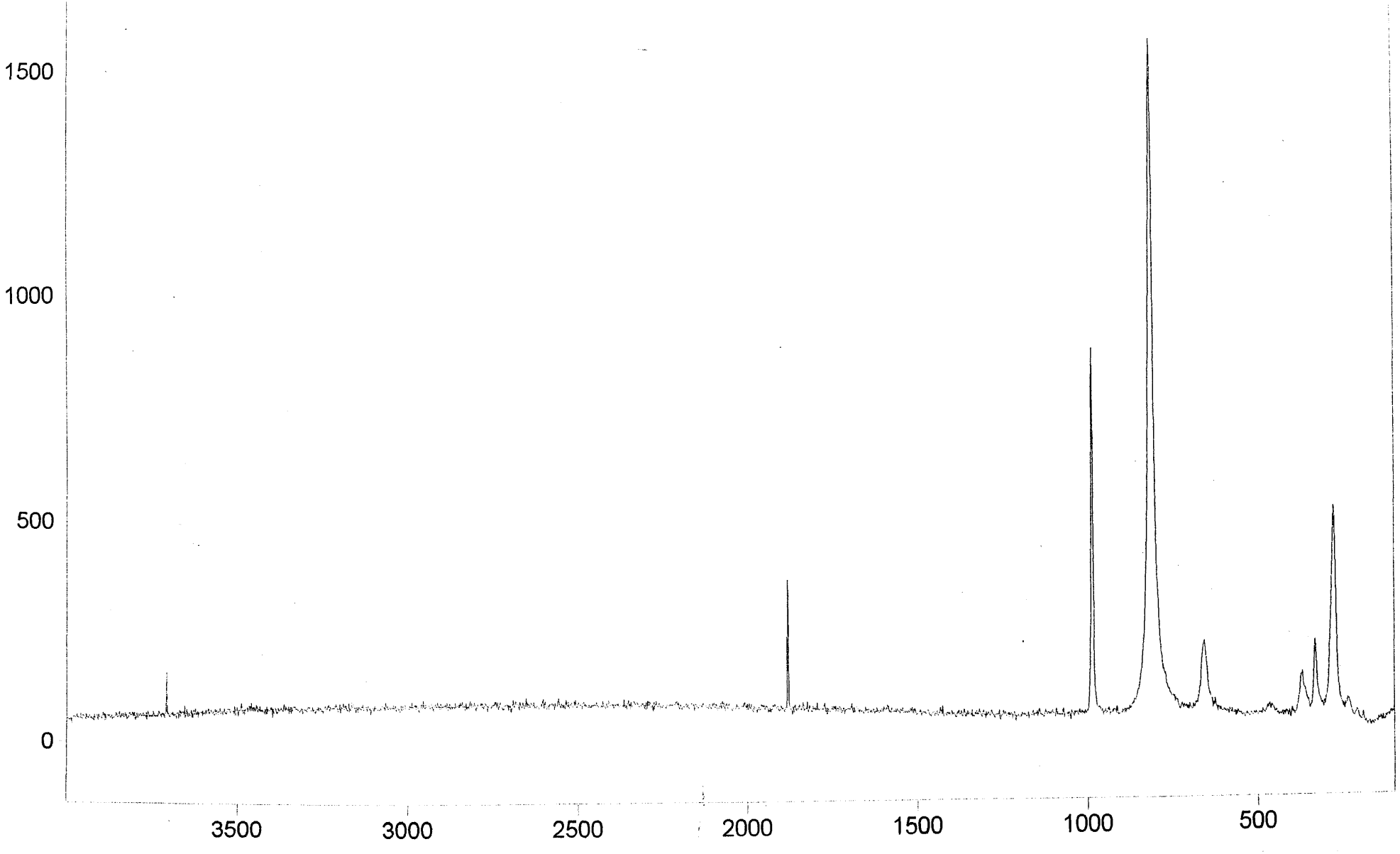

Appendix A: Raman spectra.

Silica supported 15 Wt % Mo Catalyst. In situ Raman 400°C with co-fed water

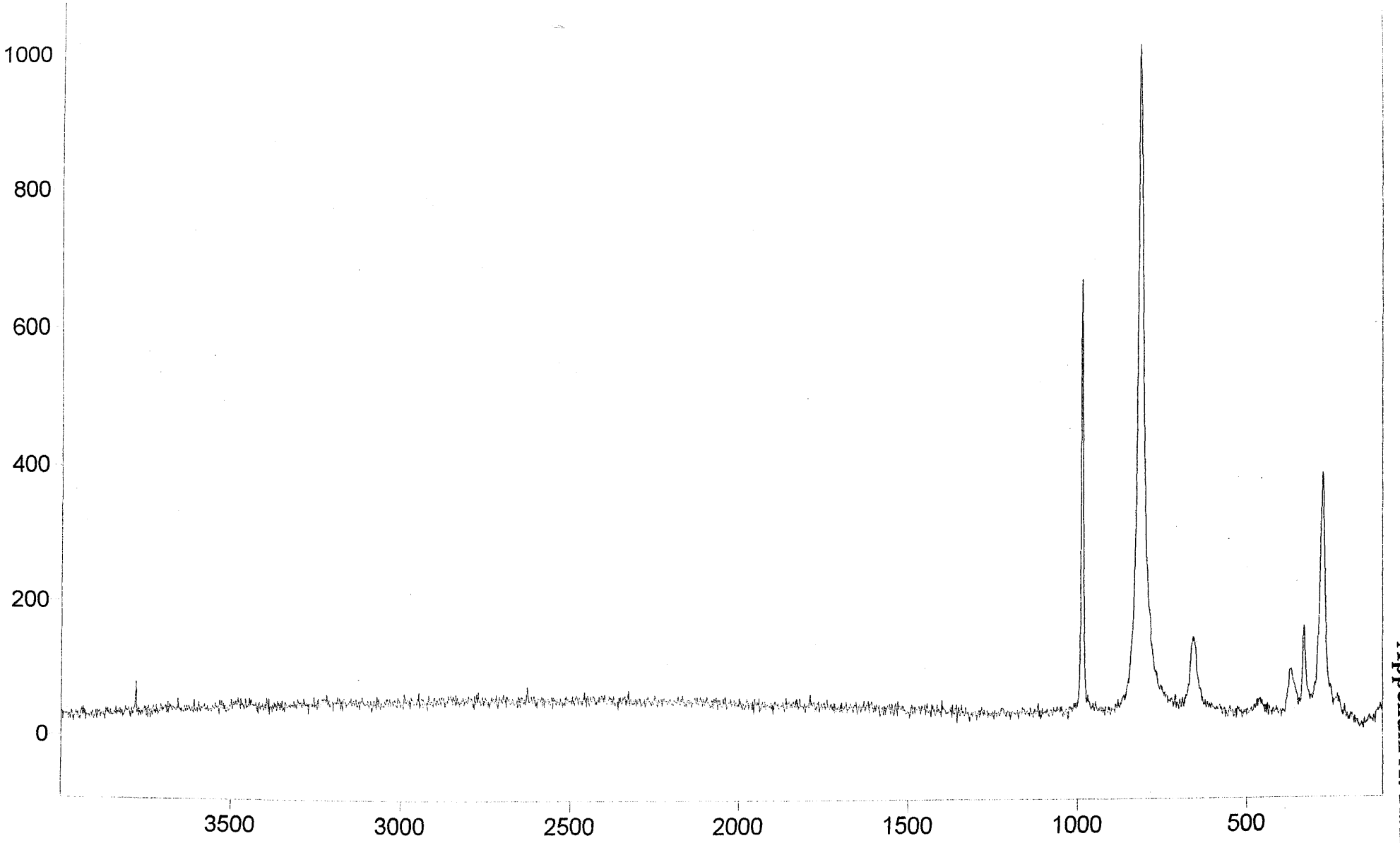

Silica supported 15 Wt % Mo Catalyst. In situ Raman 500°C with co-fed water

Appendix A: Raman spectra.

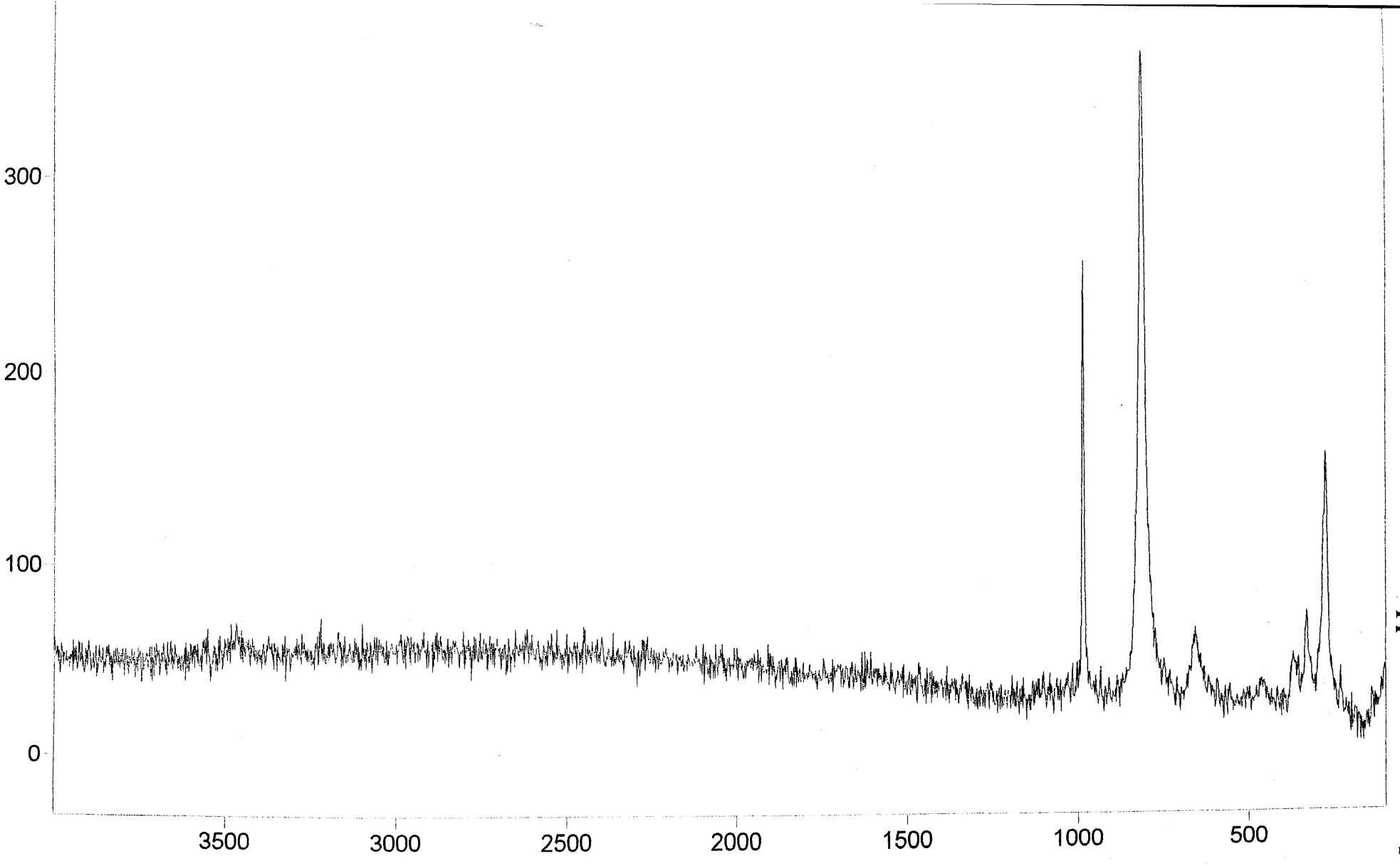

Appendix A: Raman spectra.

Silica supported 15 Wt % Mo Catalyst. In situ Raman 600°C with co-fed water

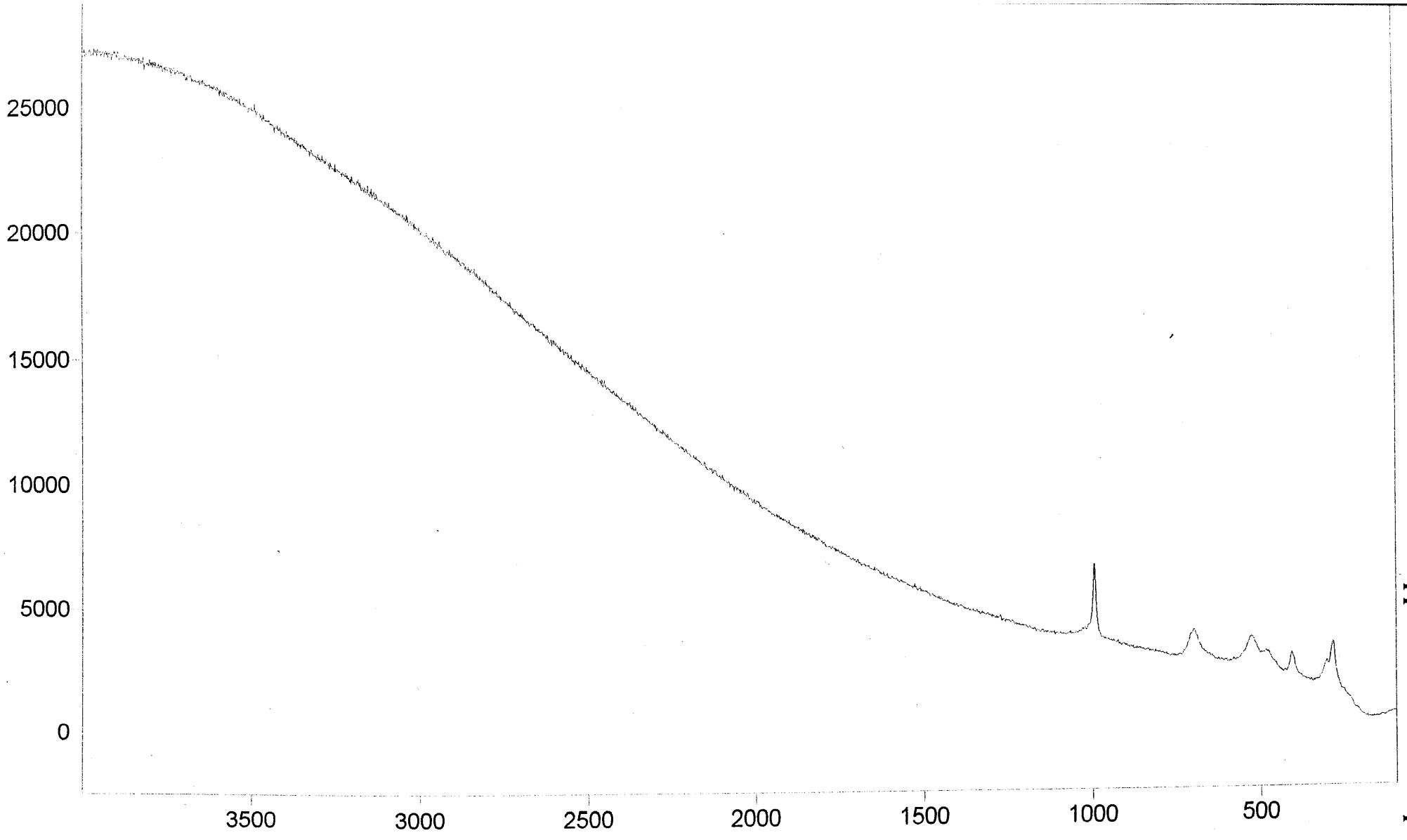

Silica supported 10 Wt % V Catalyst

Appendix A: Raman spectra.

Appendix B: TPR and TPO profiles.

Appendix B: TPR and TPO profiles

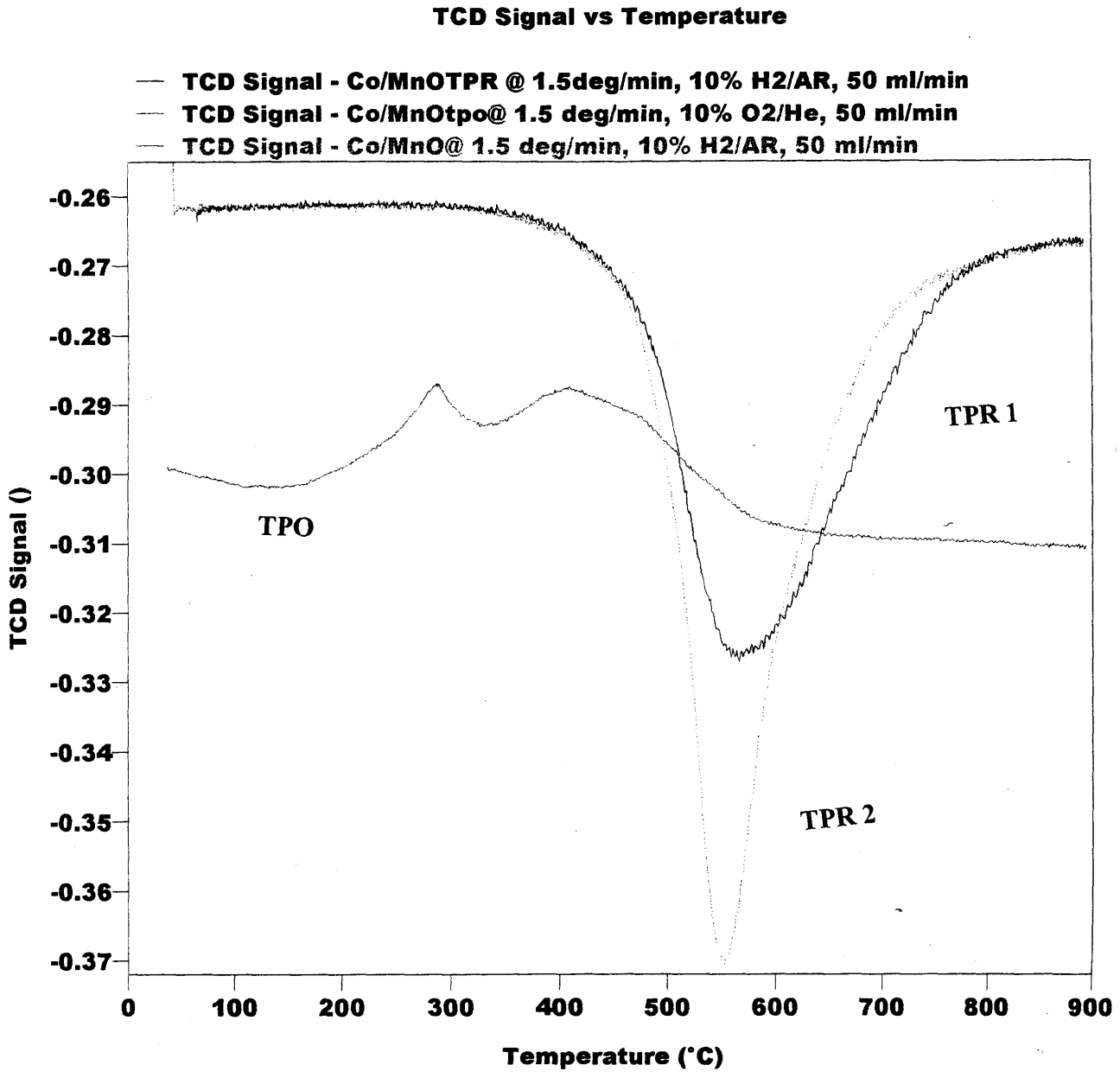

Appendix B: TPR and TPO profiles

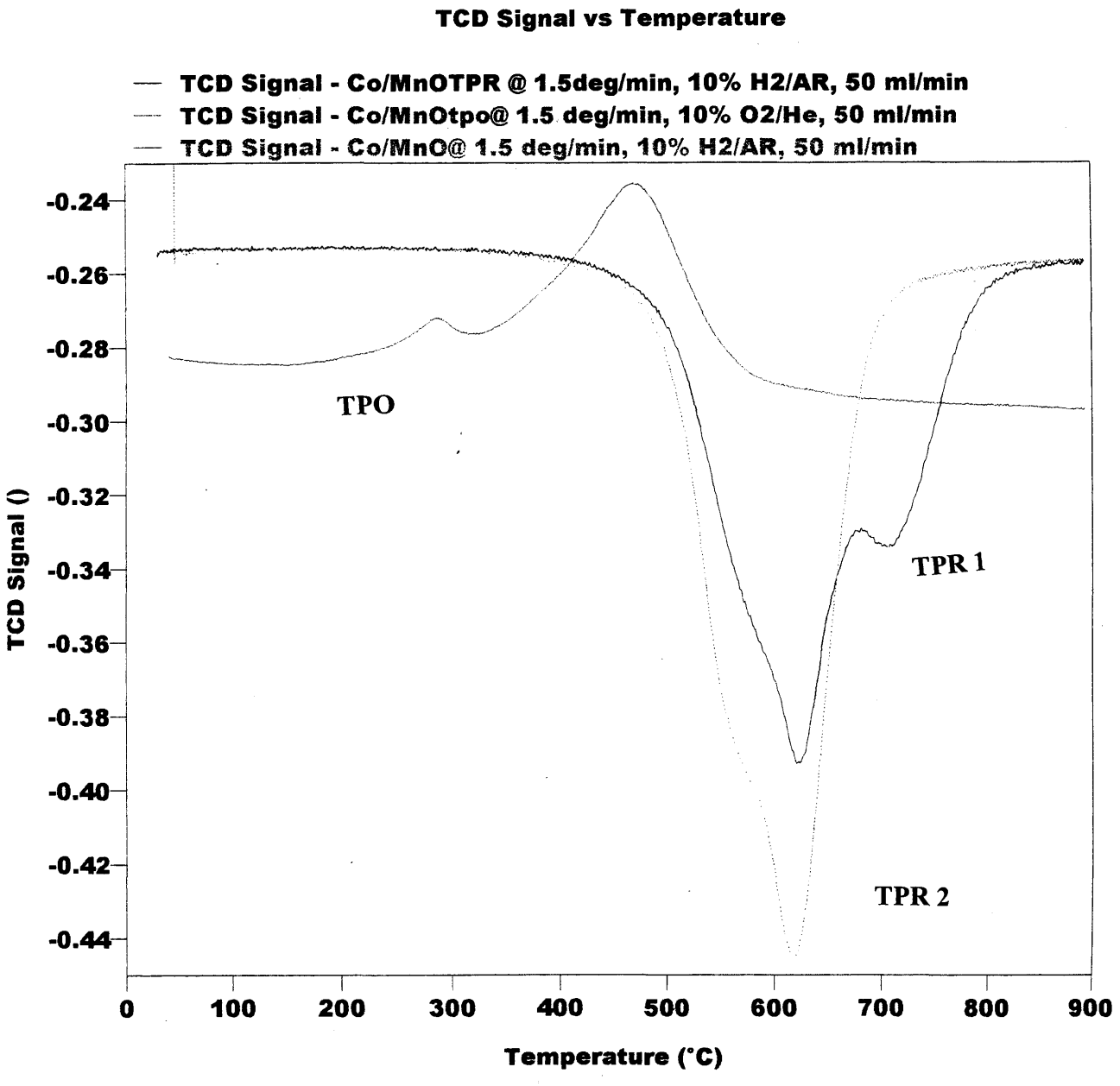

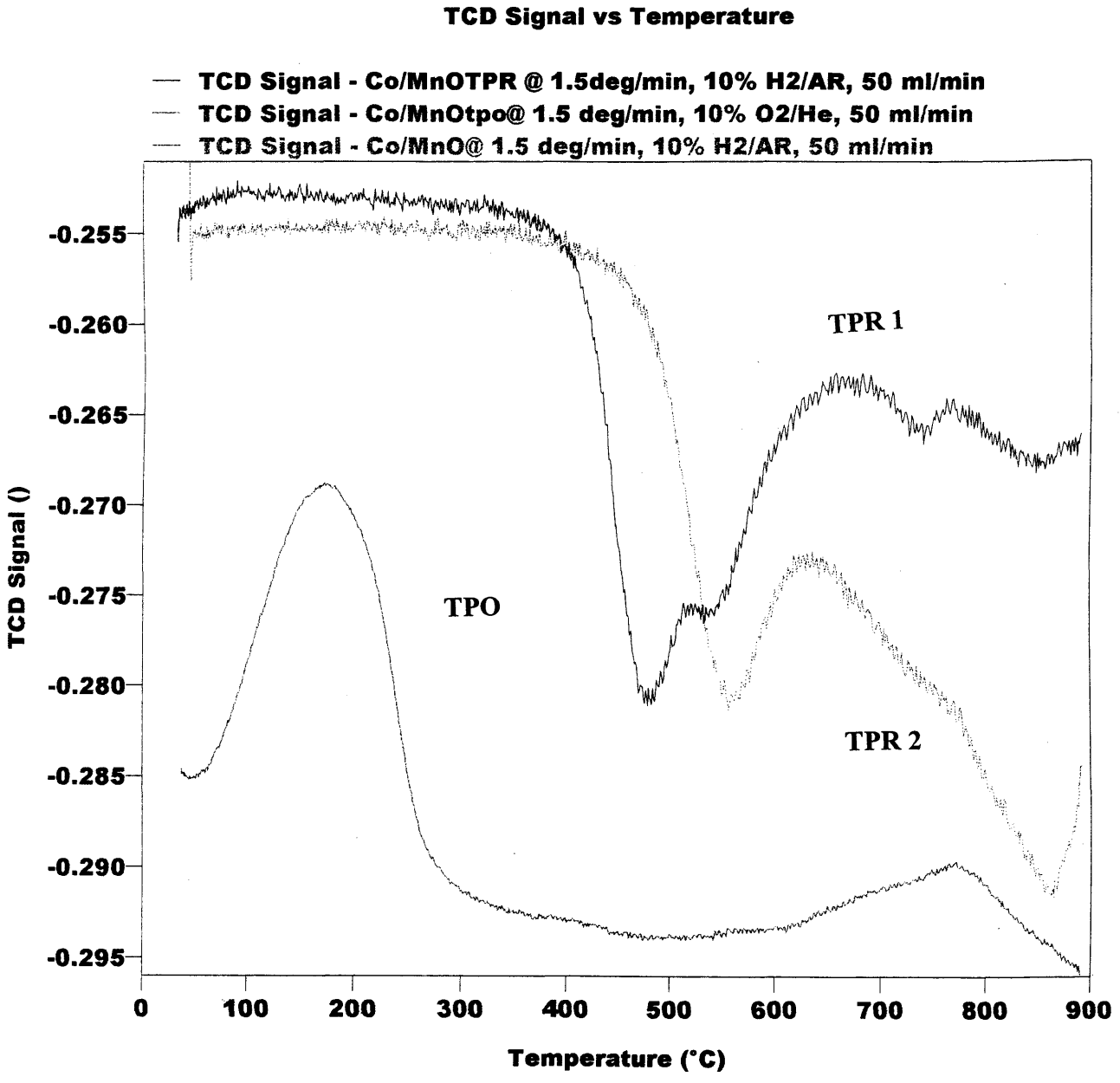
TCD Signal vs Temperature
TCD Signal - Co/MnOTPR @ 1.5deg/min, 10% H2/AR, 50 ml/min
TCD Signal - Co/MnOtpo@ 1.5 deg/min, 10% O2/He, 50 ml/min
TCD Signal - Co/MnO@ 1.5 deg/min, 10% H2/AR, 50 ml/min
TCD Signal ()
-0.255
-0.260
-0.265
-0.270
-0.275
-0.280
-0.285
-0.290
-0.295
TPR 1
TPO
TPR 2
0
100
200
300
400
500
600
700
800
900
Temperature (°C)

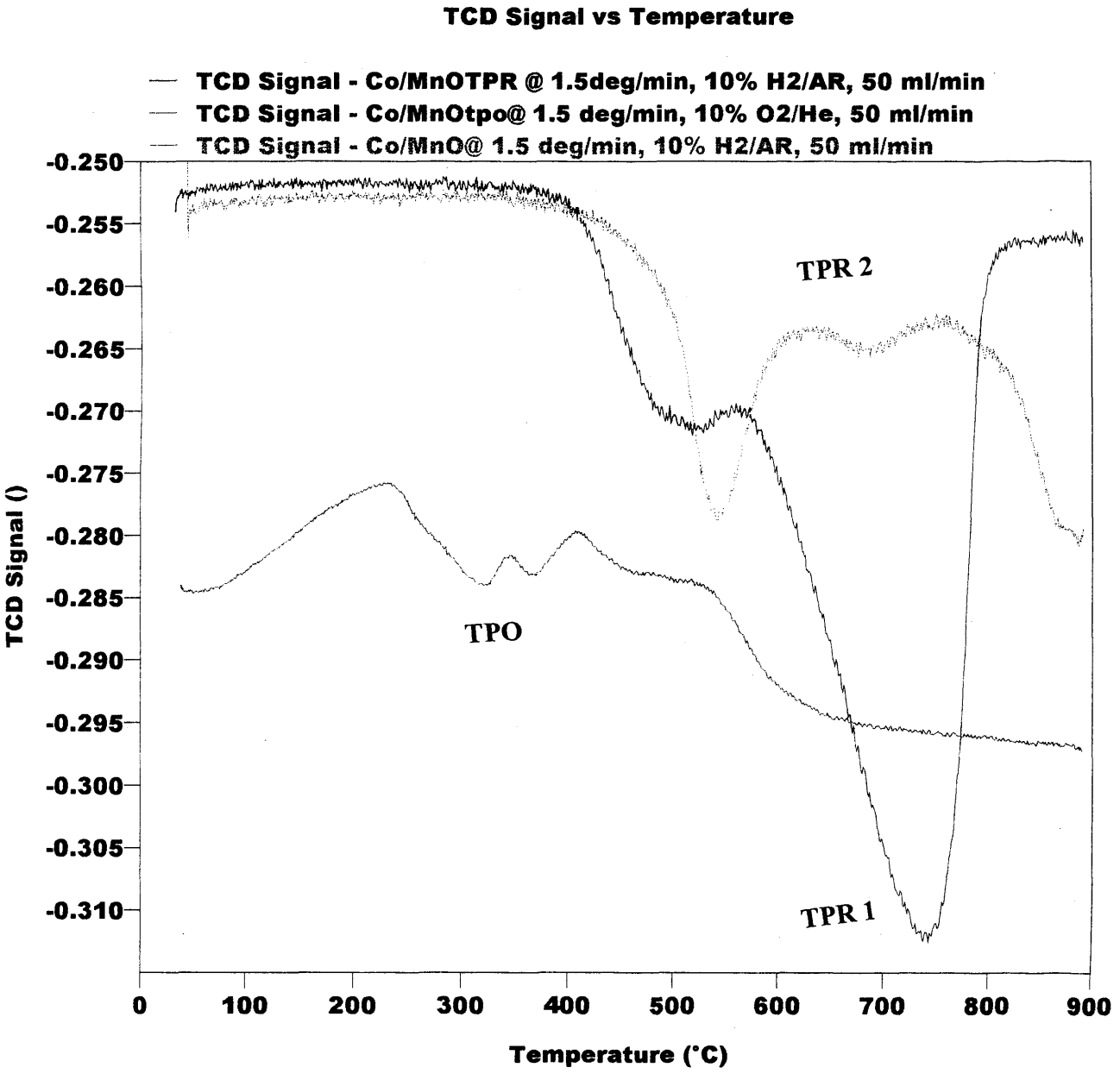
TCD Signal vs Temperature
TCD Signal - Co/MnOTPR @ 1.5deg/min, 10% H2/AR, 50 ml/min
TCD Signal - Co/MnOtpo@ 1.5 deg/min, 10% O2/He, 50 ml/min
TCD Signal - Co/MnO@ 1.5 deg/min, 10% H2/AR, 50 ml/min
TCD Signal ()
-0.250
-0.255
-0.260
-0.265
-0.270
-0.275
-0.280
-0.285
-0.290
-0.295
-0.300
-0.305
-0.310
TPR 2
TPO
TPR 1
0
100
200
300
400
500
600
700
800
900
Temperature (°C)

Appendix C: Powder X-ray Diffraction Patterns

Appendix C: Powder X-Ray diffraction patterns

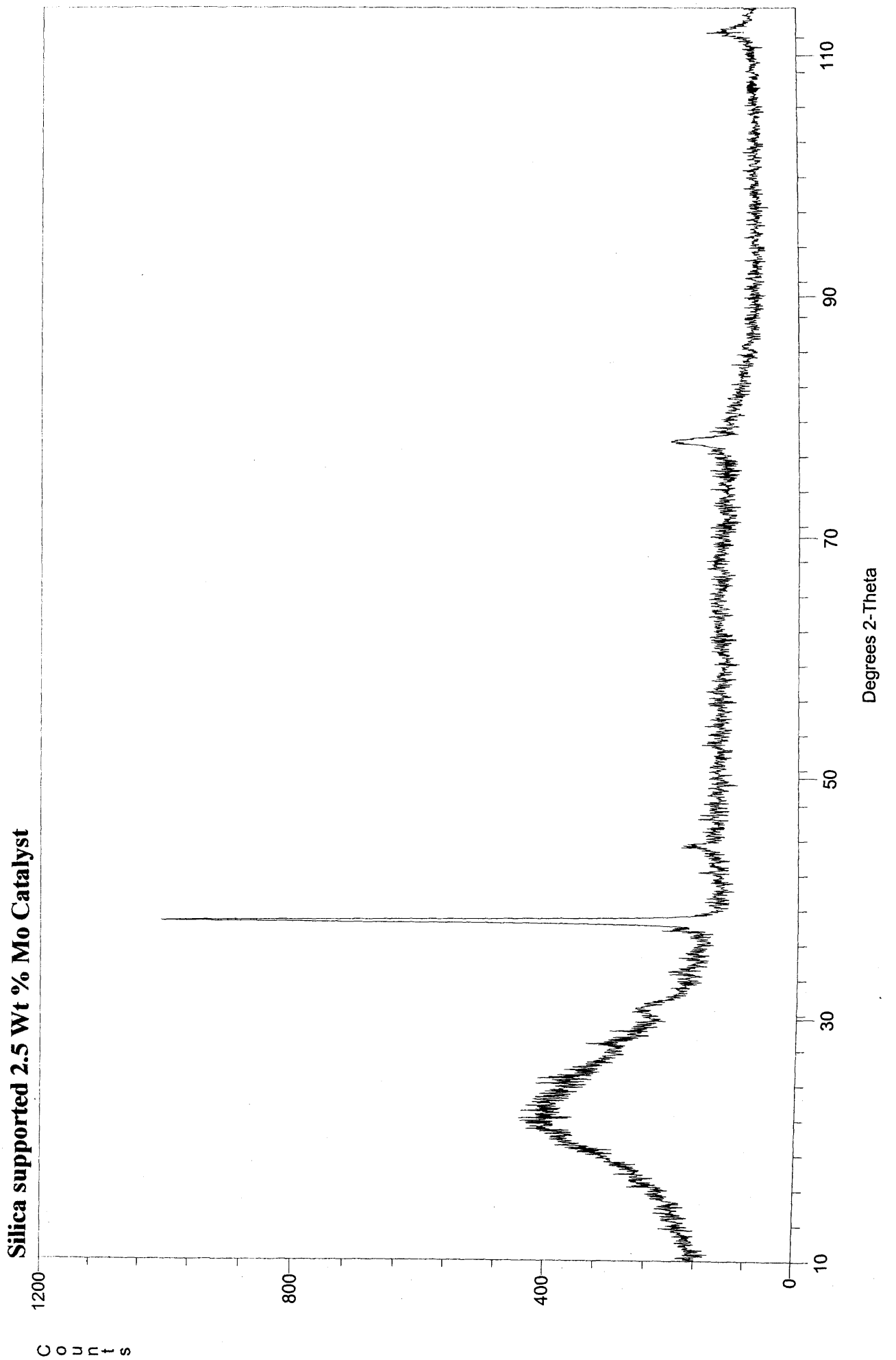

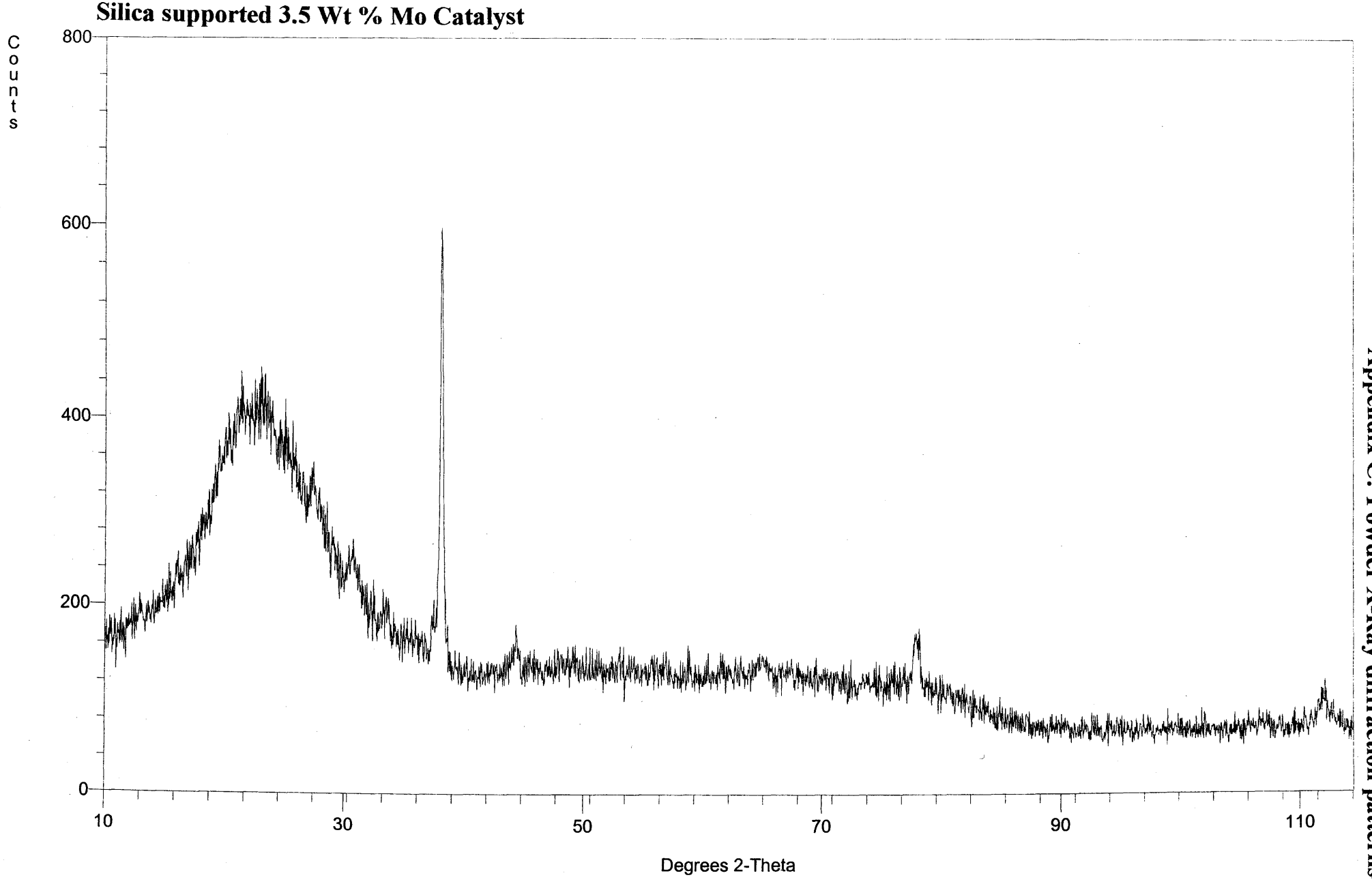

Appendix C: Powder X-Ray diffraction patterns

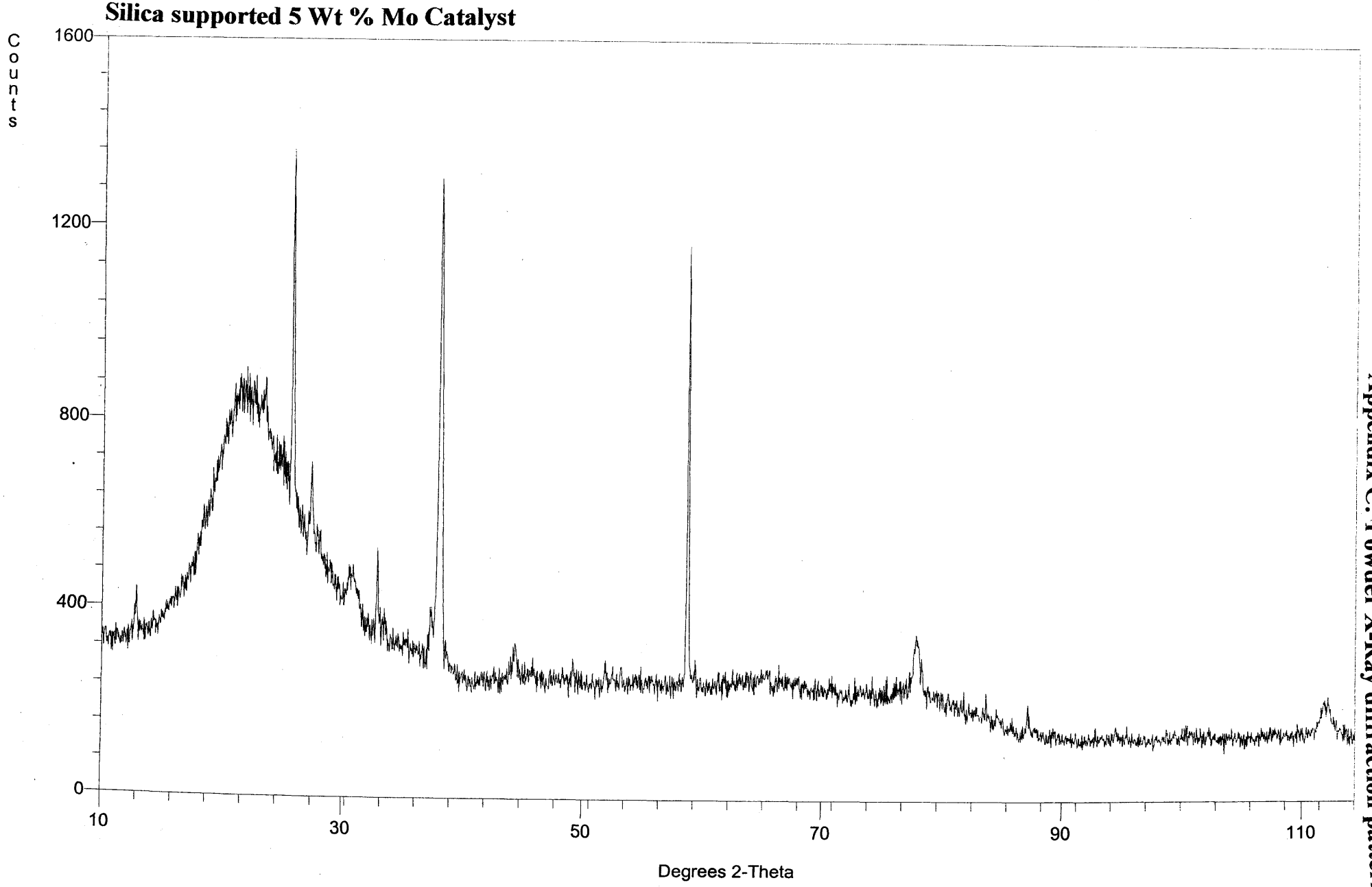

Appendix C: Powder X-Ray diffraction patterns

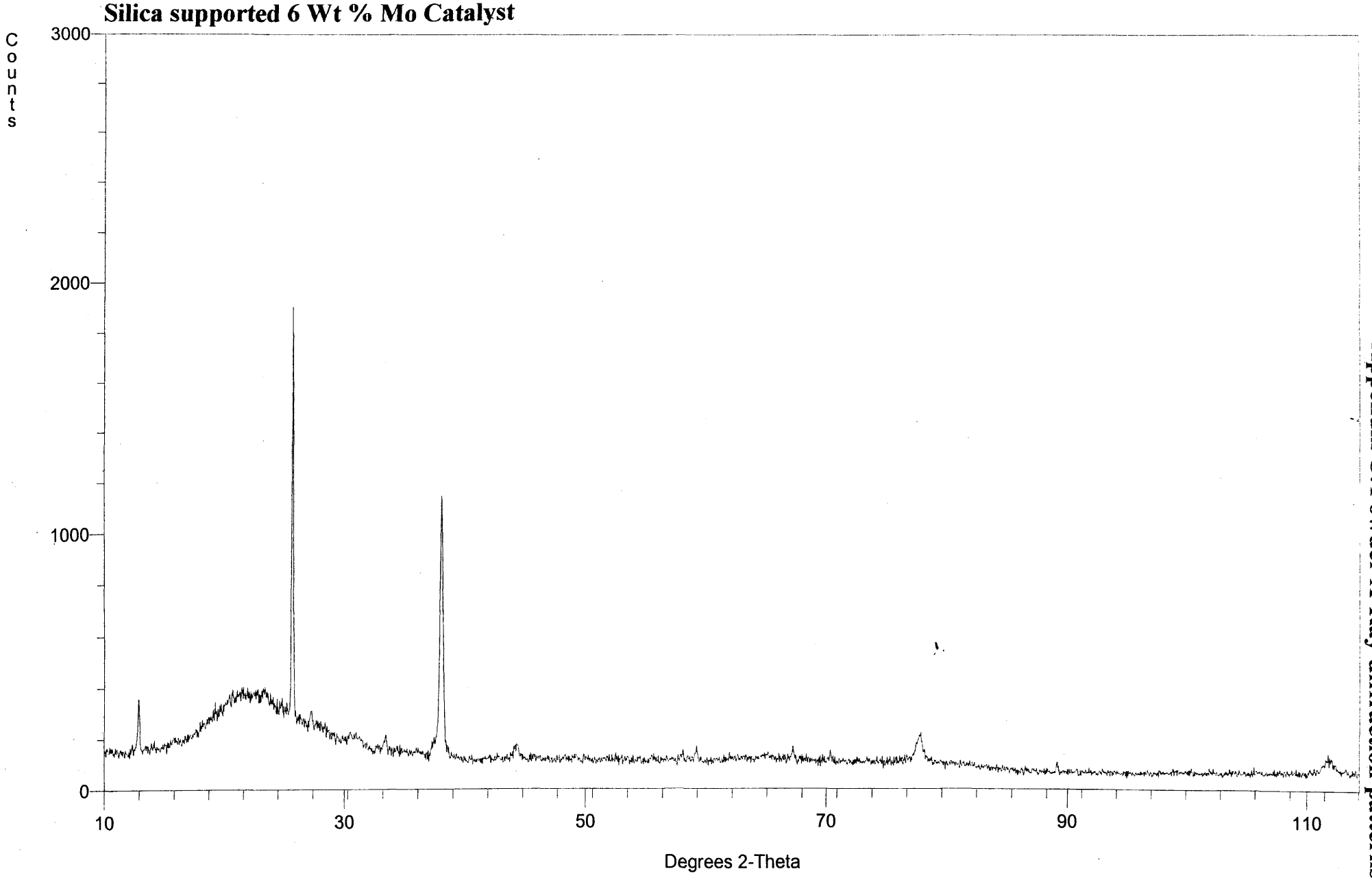

Appendix C: Powder X-Ray diffraction patterns

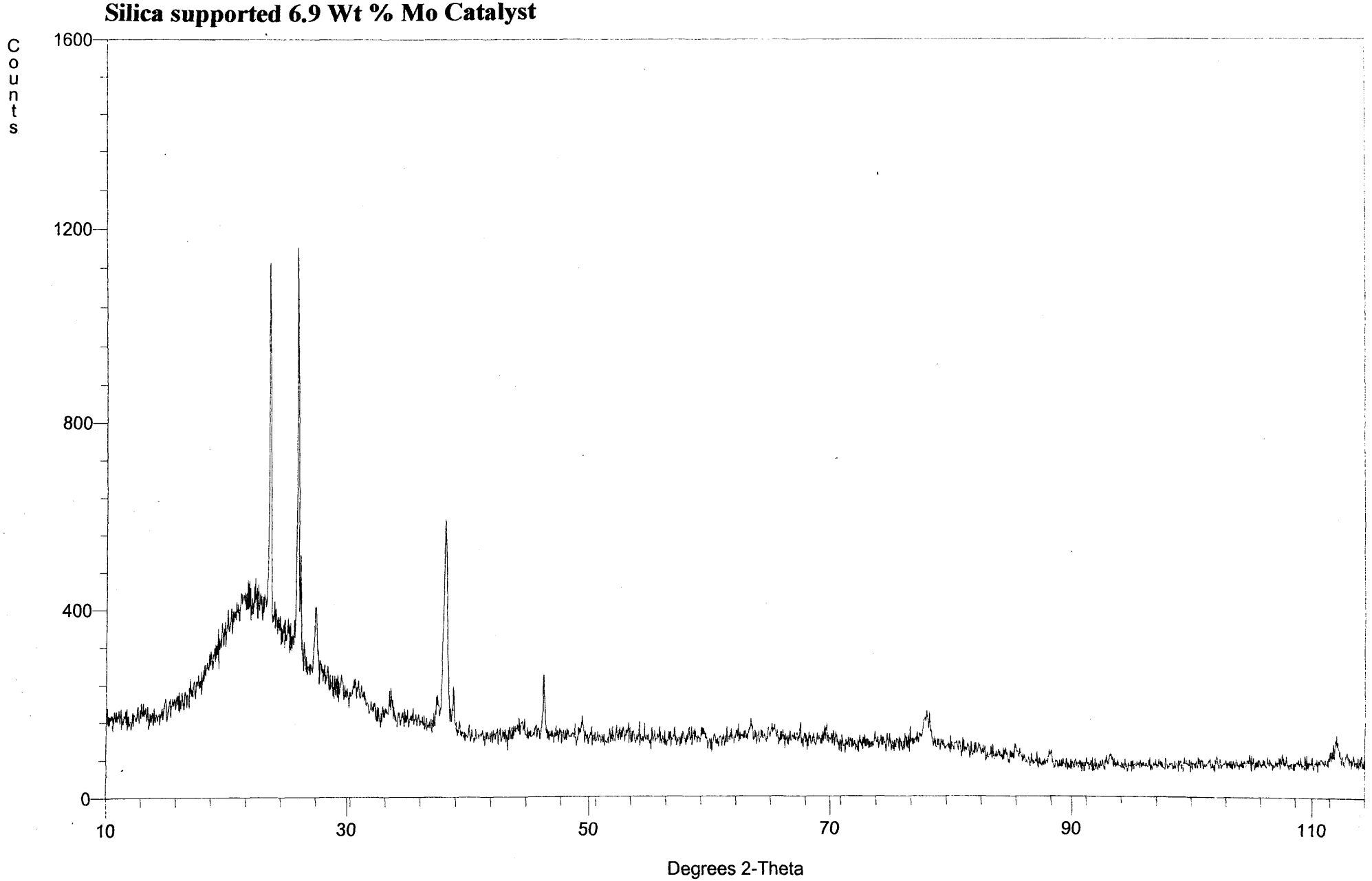

Appendix C: Powder X-Ray diffraction patterns

Appendix C: Powder X-Ray diffraction patterns

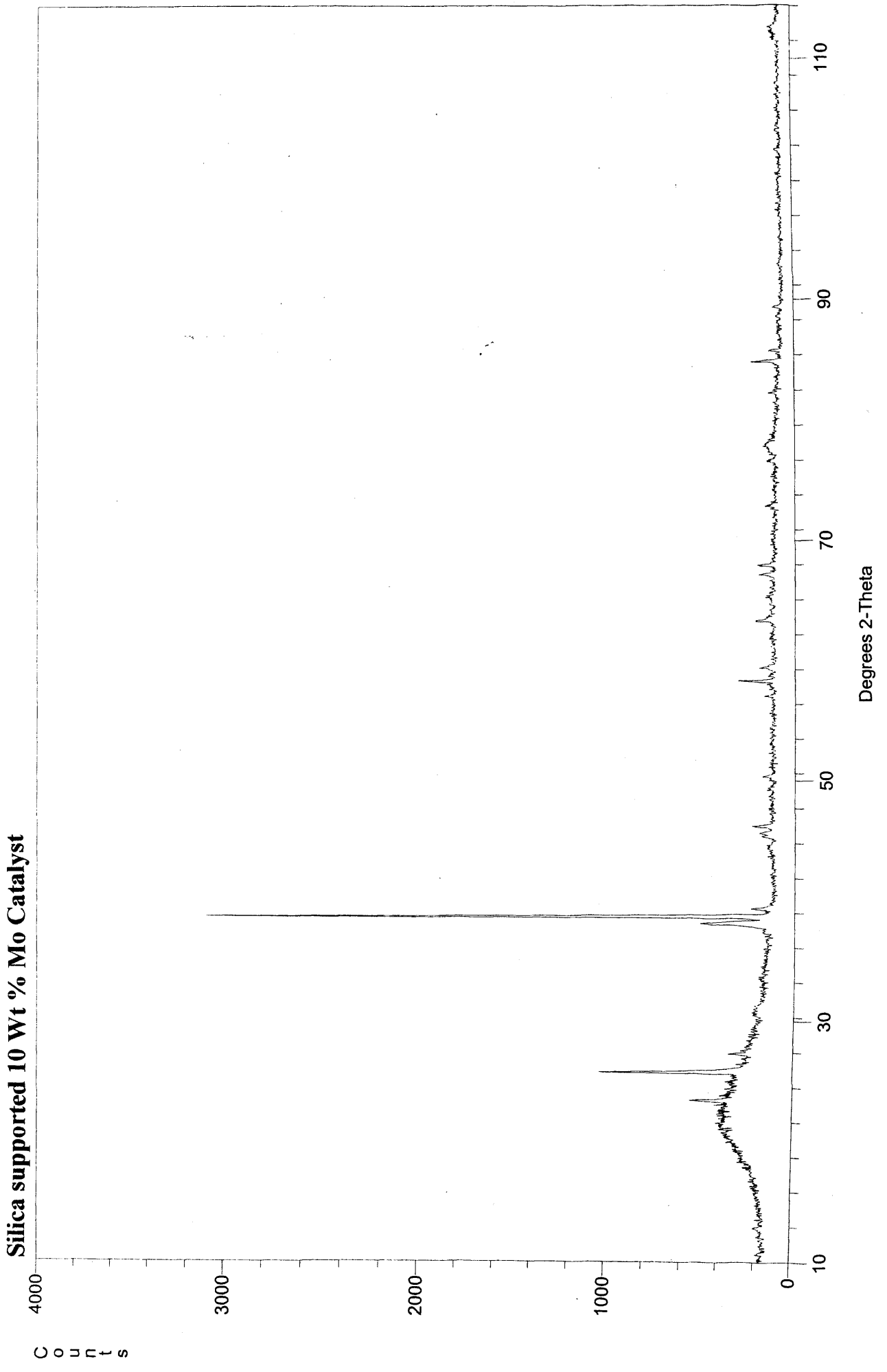

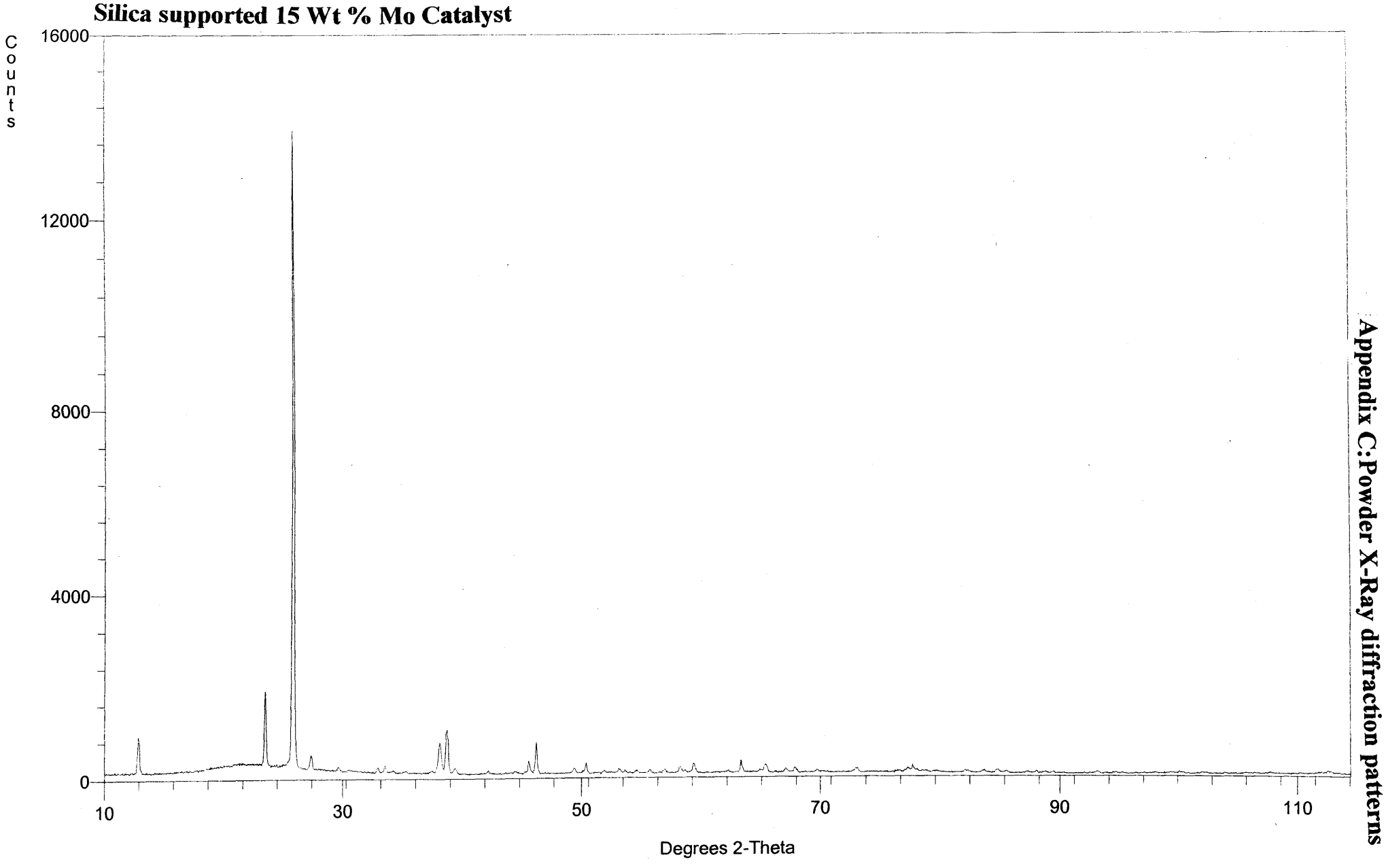

Appendix C:Powder X-Ray diffraction patterns

Appendix C: Powder X-Ray diffraction patterns

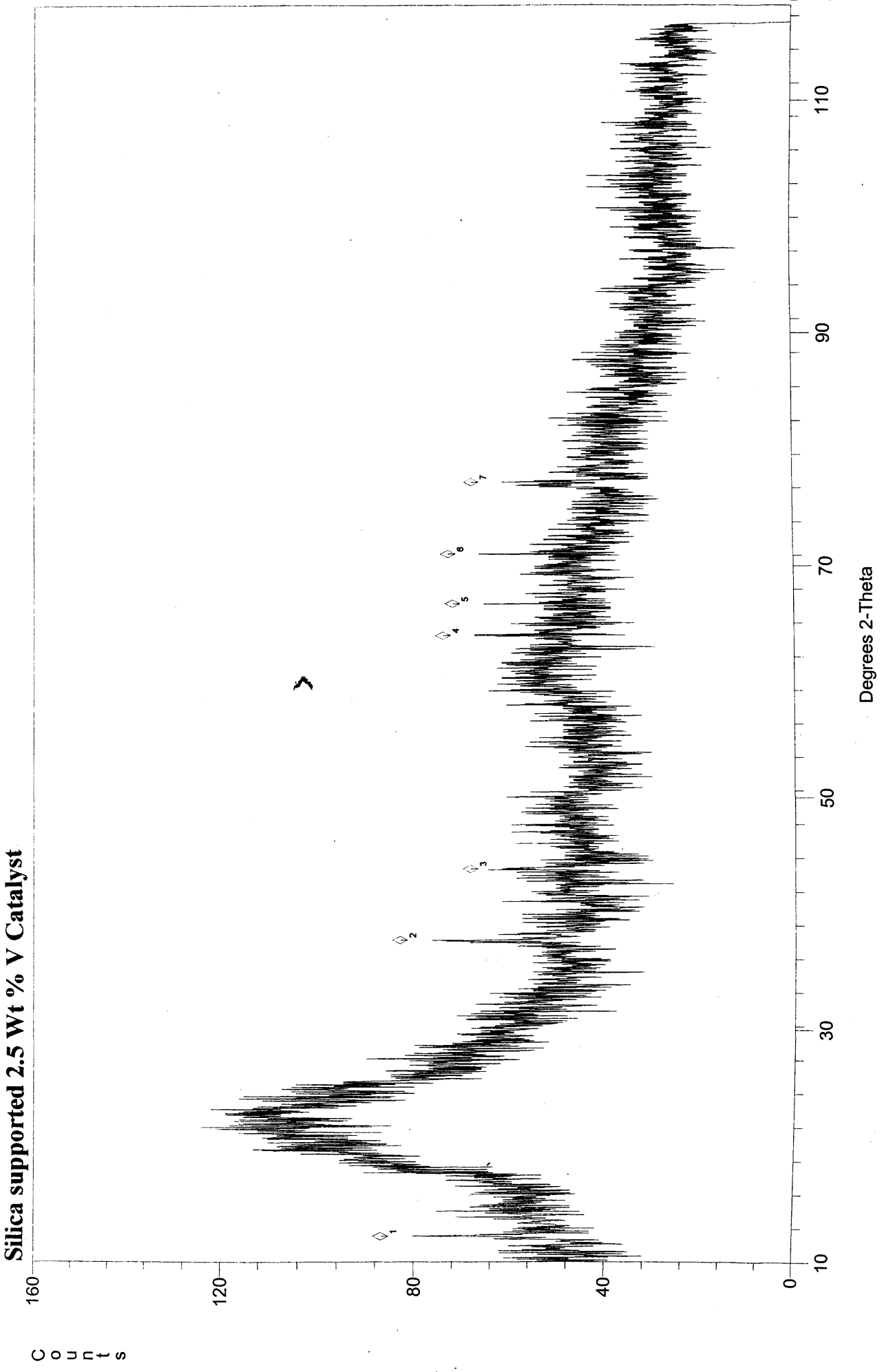

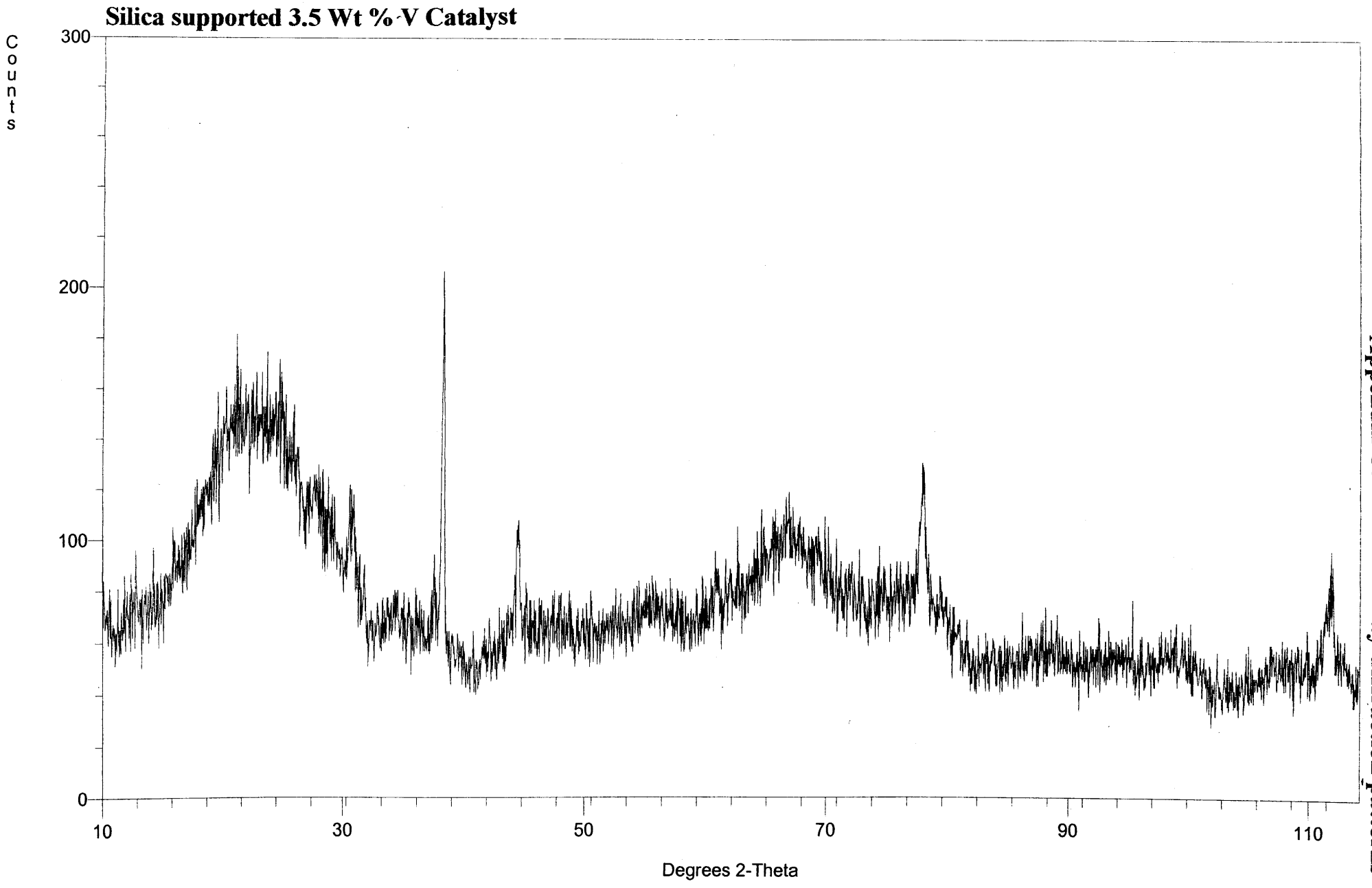

Appendix C: Powder X-Ray diffraction patterns

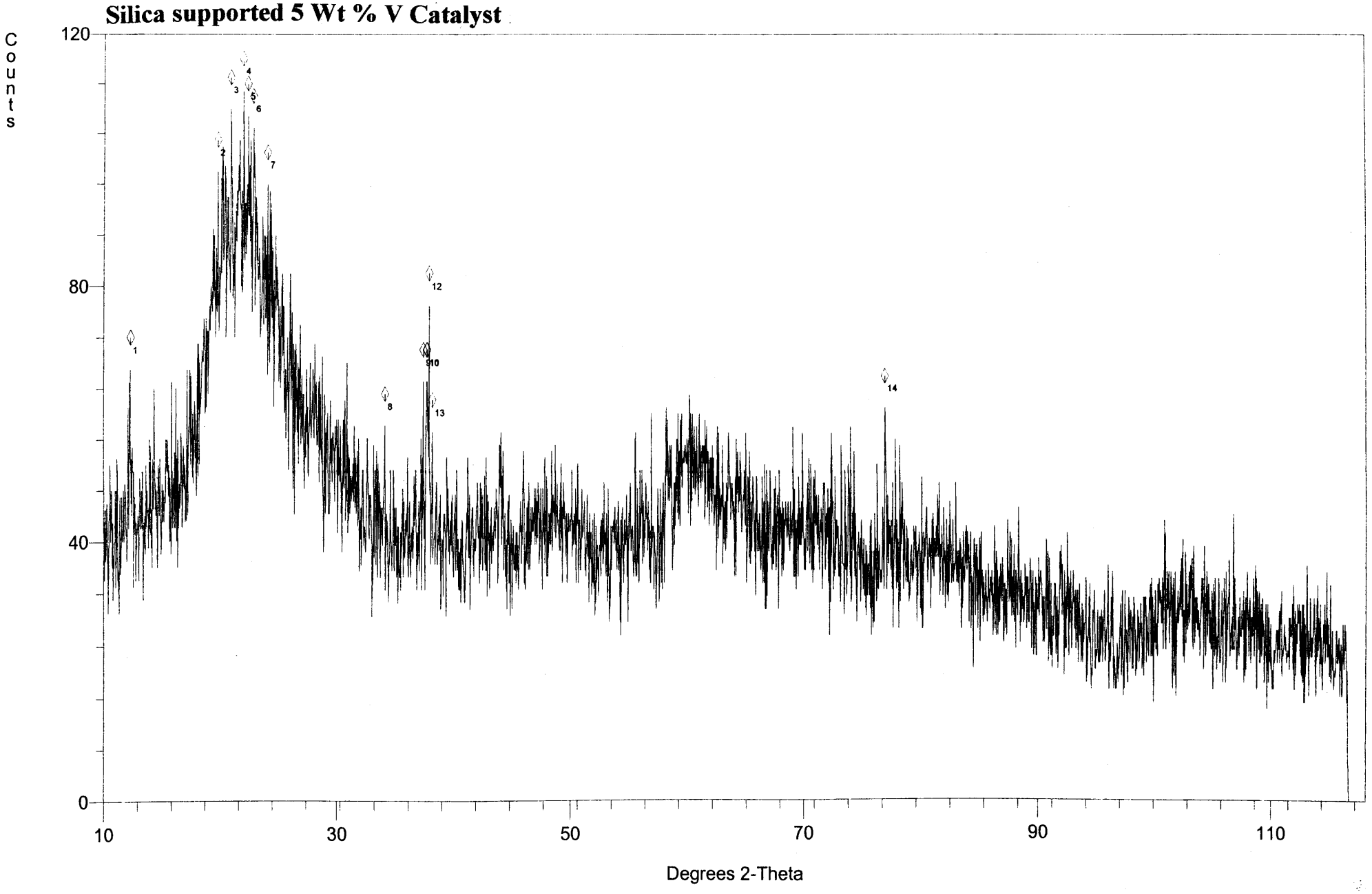

Appendix C: Powder X-Ray diffraction patterns

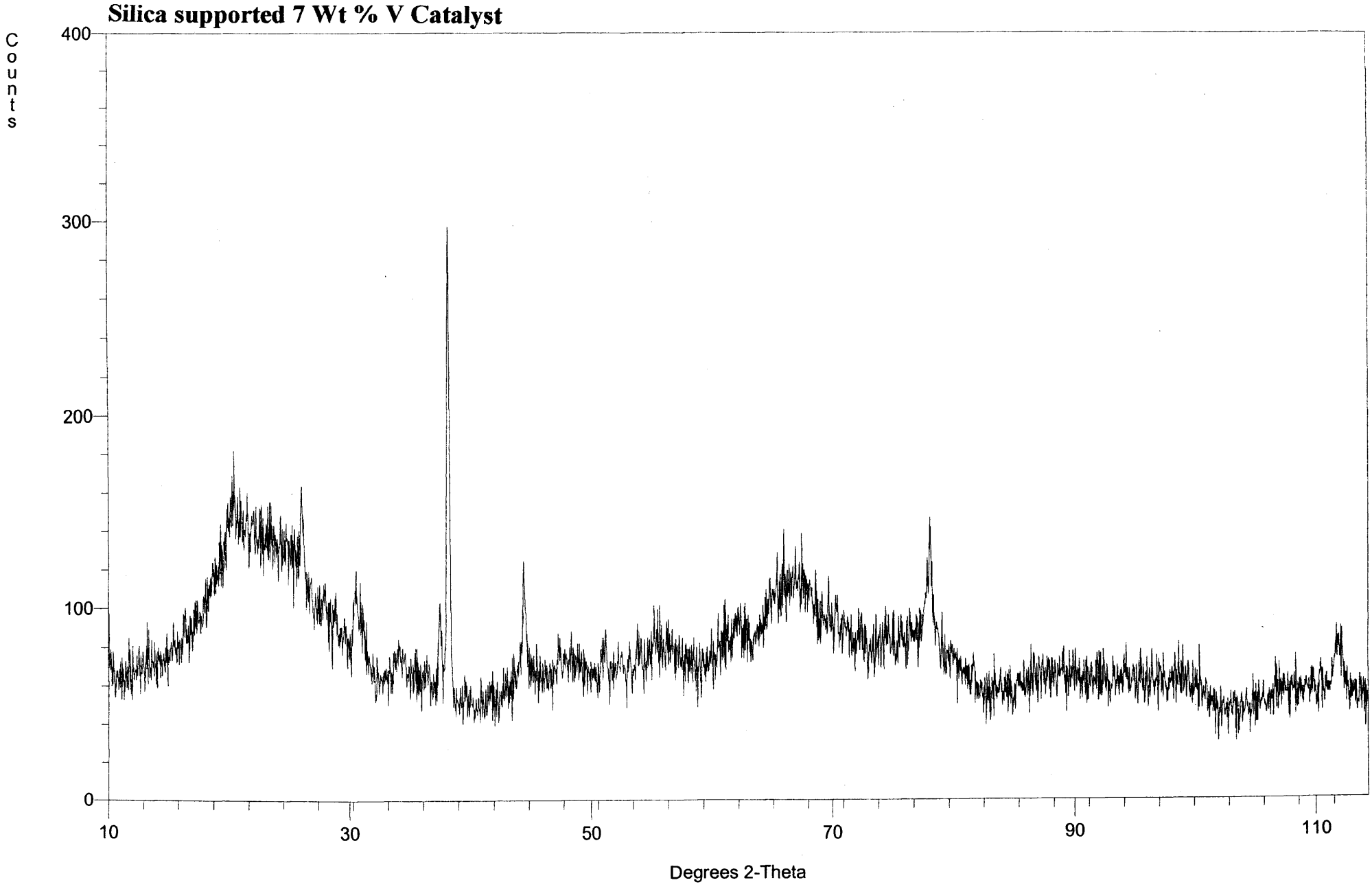

Appendix C: Powder X-Ray diffraction patterns

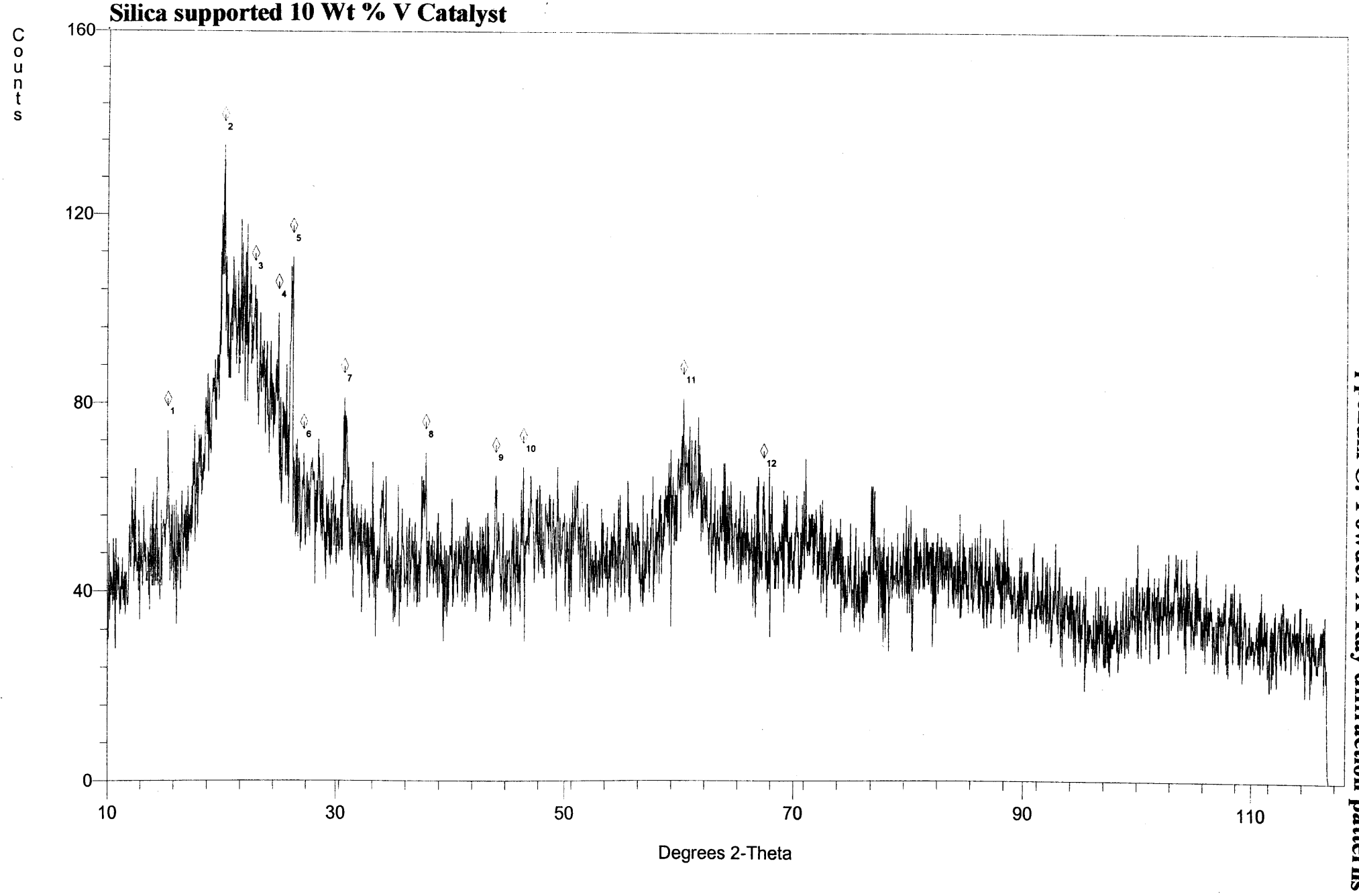

Appendix C: Powder X-Ray diffraction patterns

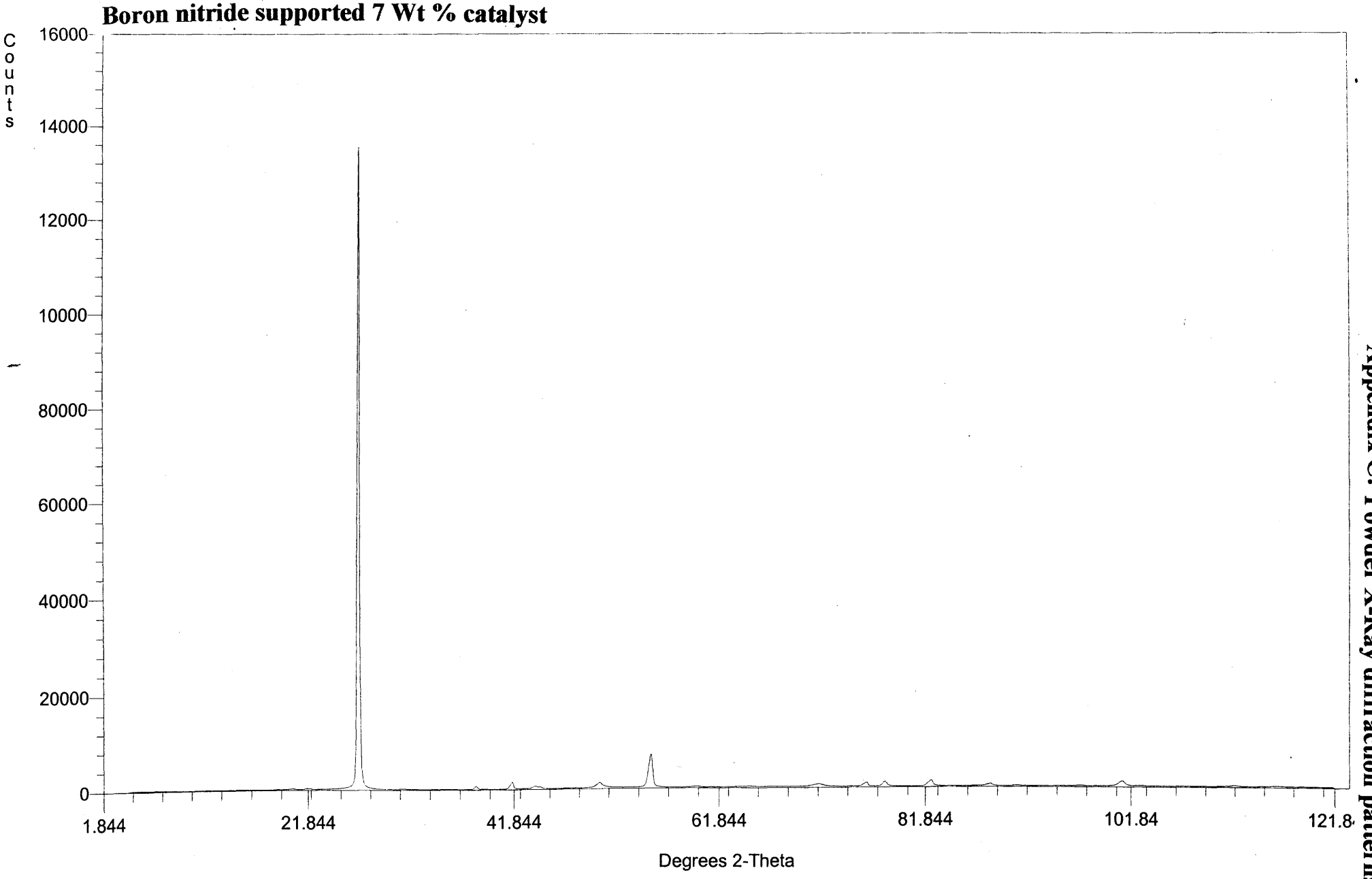

Appendix C: Powder X-Ray diffraction patterns

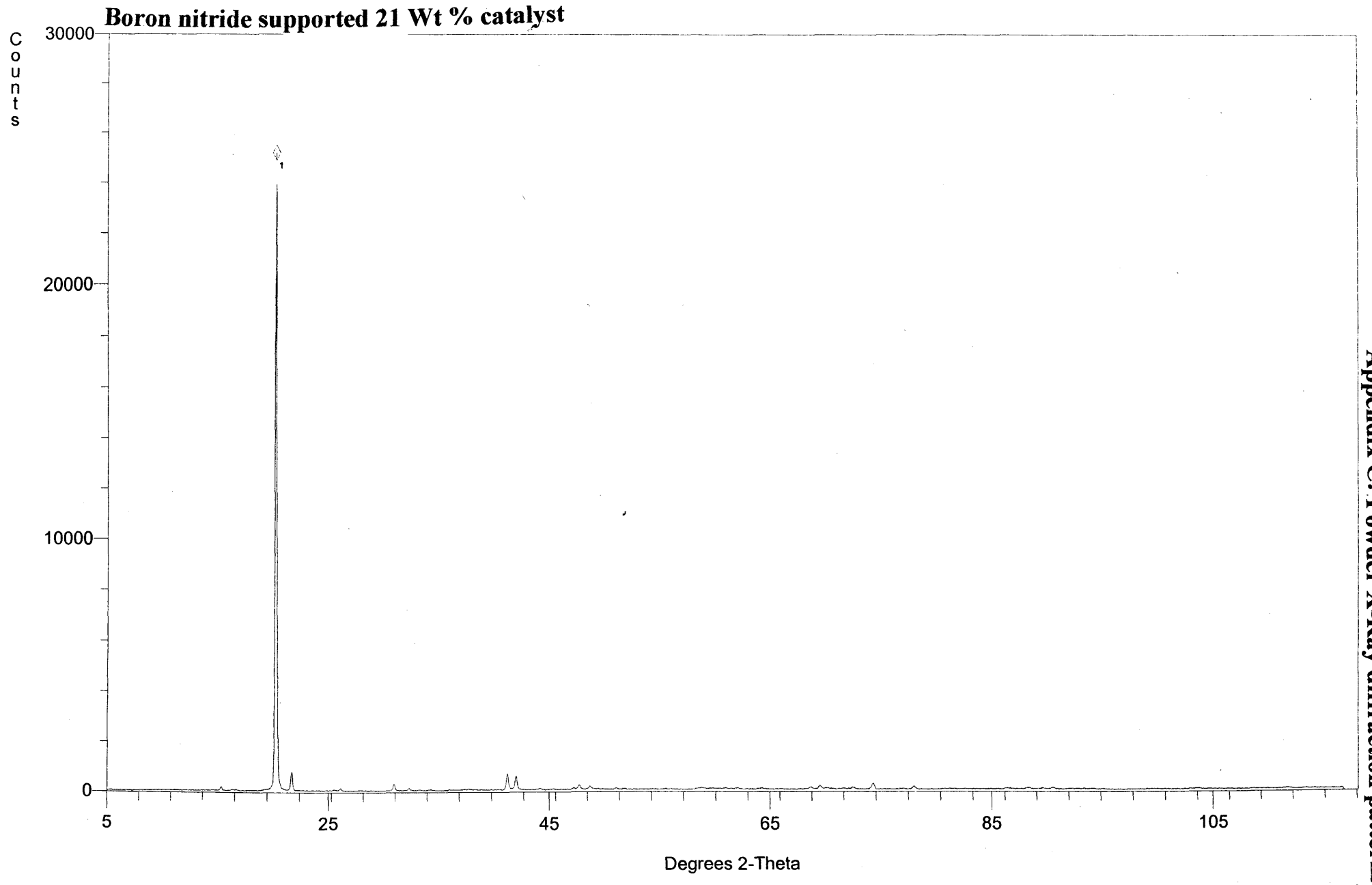

Appendix C: Powder X-Ray diffraction patterns

Appendix D: Catalyst data.

Appendix D:

1: Propane oxidation

1.1: Silica supported Vanadium catalysts.

Table 1.1.1: Silica supported 2.5 Wt % Vanadium oxide catalyst.

			Selectivities (%)					
Temp (C)	**Conver. (%)**	**Carbon balance**	**CO_2**	**Meth.**	**Acrol.**	**Acrylic acid**	**CO**	**Eth.**
250	0	99.9						
275	0.02	99.9	100					
300	0.26	99.7	100					
325	0.65	99.4	100					
350	0.88	99.3	100					
375	1.45	98.8	100					
400	2.04	98.4	100					
425	2.47	98.5	100					
450	3.44	98.7	100					
475	5.11	98.9	100					
500	7.68	100.1	100					
525	9.70	103.6	99.8	0.16	0.09			

Appendix D:

1: Propane oxidation

Table 1.1.2: Silica supported 3.5 Wt % Vanadium oxide catalyst.

			Selectivities (%)					
Temp (C)	**Conver. (%)**	**Carbon balance**	**CO_2**	**Meth.**	**Acrol.**	**Acrylic acid**	**CO**	**Eth.**
225	0	100						
250	0.07	99.9	100					
275	0.28	99.7	100					
300	0.55	99.5	100					
325	1.09	9.0	100					
350	1.17	99.0	100					
375	1.66	98.6	100					
400	2.31	98.2	100					
425	2.77	98.3	100					
450	3.85	98.1	100					
475	4.72	98.8	100					
500	6.64	99.8	99.8		0.15			
525	9.78	102.0	97.6	0.76	1.21	0.40		
550	13.10	96.2	96.6	1.25	1.87	0.31		

Appendix D:

1: Propane oxidation.

Table 1.1.3: Silica supported 5 Wt % Vanadium oxide catalyst.

			Selectivities (%)					
Temp (C)	**Conver. (%)**	**Carbon balance**	**CO_2**	**Meth.**	**Acrol.**	**Acrylic acid**	**CO**	**Eth.**
250	0	100.0						
275	0.15	99.9	100					
300	0.43	99.6	100					
325	0.58	99.4	100					
350	0.77	99.3	100					
375	1.02	99.2	100					
400	1.32	99.1	100					
425	1.63	98.9	100					
450	1.83	99.2	100					
475	2.60	99.4	99.4		0.62			
500	5.87	98.5	99.2	0.31	0.78	0.17		
525	12.49	94.8	81.5	0.64	1.02	0.75	16.12	
550	12.56	94.4	70.1	0.98	0.84	0.65	27.38	

Appendix D:

1: Propane oxidation

Table 1.1.4: Silica supported 6 Wt % Vanadium oxide catalyst.

			Selectivities (%)					
Temp (C)	**Conver. (%)**	**Carbon balance**	**CO_2**	**Meth.**	**Acrol.**	**Acrylic acid**	**CO**	**Eth.**
250	0	100.0						
275	0.26	99.8	100					
300	0.64	99.4	100					
325	0.92	99.1	100					
350	1.27	98.9	100					
375	1.55	98.7	100					
400	2.01	98.4	100					
425	2.68	98.2	100					
450	4.17	98.7	100					
475	5.34	97.5	100					
500	7.51	97.2	100					
525	9.51	97.9	99.6	0.44				
550	12.81	99.6	97.8	2.04	0.17			
575	16.24	99.0	96.7	3.21	0.13			

Appendix D:

1: Propane oxidation

Table 1.1.5: Silica supported 7 Wt % Vanadium oxide catalyst.

			Selectivities (%)					
Temp (C)	**Conver. (%)**	**Carbon balance**	**CO_2**	**Meth.**	**Acrol.**	**Acrylic acid**	**CO**	**Eth.**
250	0	100.0	100					
275	0.28	99.7	100					
300	0.41	99.6	100					
325	0.32	99.7	100					
350	0.63	99.4	100					
375	1.25	98.9	100					
400	1.89	98.3	100					
425	2.85	97.3	100					
450	3.33	98.0	100					
475	3.76	97.8	100					
500	4.35	97.7	100					
525	5.18	97.7	98.9	0.47	0.56			
550	7.83	96.2	95.5	1.28	1.26	0.86		1.12
575	21.78	94.1	92.4	7.60	2.21			0.81

Appendix D:

1: Propane oxidation

Table 1.1.6: Silica supported 10 Wt % Vanadium oxide catalyst.

			Selectivities (%)					
Temp (C)	**Conver. (%)**	**Carbon balance**	**CO_2**	**Meth.**	**Acrol.**	**Acrylic acid**	**CO**	**Eth.**
275	0	100.0						
300	0.12	99.9	100					
325	0.31	99.7	100					
350	0.51	99.6	100					
375	0.85	99.3	100					
400	1.36	98.9	100					
425	2.01	98.6	100					
450	2.27	98.6	100					
475	2.71	99.1	100					
500	3.45	99.4	100					
525	4.49	100.2	99.2	0.52	0.26			
550	6.44	100.0	97.6	2.03	0.36	0.21		
575	13.12	100.1	93.3	5.17	1.30	0.34		
600	16.82	94.4	81.6	9.35	2.67	0.9	5.34	

Appendix D:

1: Propane oxidation

Table 1.1.7: Silica supported 15 Wt % Vanadium oxide catalyst.

			Selectivities (%)				
Temp (C)	**Conver. (%)**	**Carbon balance**	**CO_2**	**Meth.**	**Acrol.**	**Acrylic acid**	**CO**	**Eth.**
250	0	100					
275	0.19	99.8	100				
300	0.80	99.2	100				
325	0.90	99.2	100				
350	1.20	99.0	100				
375	1.62	98.7	100				
400	1.98	98.6	100				
425	2.49	98.7	00				
450	3.43	98.7	100				
475	4.99	106.3	100				
500	6.70	99.8	100				
525	8.04	98.6	99.6	0.23	0.16		
550	14.10	94.0	99.3	0.54	0.21		

Appendix D:

1: Propane oxidation

1.2: Silica supported Molybdenum catalysts.

Table 1.2.1: Silica supported 2.5 Wt % molybdenum oxide catalyst.

			Selectivities (%)					
Temp (C)	**Conver. (%)**	**Carbon balance**	**CO_2**	**Meth.**	**Acrol.**	**Acrylic acid**	**CO**	**Eth.**
250	0	99.6						
275	0.02	99.9	100					
300	0.09	99.7	100					
325	0.33	99.8	100					
350	1.03	99.7	100					
375	1.81	99.4	100					
400	2.57	99.4	100					
425	3.68	99.8	100					
450	4.34	98.2	100					
475	4.88	98.2	100					
500	6.09	98.9	99.0	0.78	0.32			
525	10.67	99.0	96.3	3.38	0.36			
550	13.13	88.1	82.4	14.36	2.28			0.94

Appendix D:

1: Propane oxidation

Table 1.2.2: Silica supported 3.5 Wt % molybdenum oxide catalyst.

			Selectivities (%)					
Temp (C)	**Conver. (%)**	**Carbon balance**	**CO_2**	**Meth.**	**Acrol.**	**Acrylic acid**	**CO**	**Eth.**
225	0	100.0						
250	0.62	99.4	100					
275	1.09	98.9	100					
300	0.65	99.4	100					
325	1.44	98.6	100					
350	0.64	98.6	100					
375	2.41	98.1	100					
400	3.00	98.2	100					
425	3.00	99.4	100					
450	5.08	99.3	100					
475	7.49	99.3	100					
500	8.88	101.8	100					
525	11.00	103.0	99.9	0.10				
550	12.48	102.3	98.8	0.99	0.11			0.15

Appendix D

1. Propane oxidation

Table 1.2.3: Silica supported 5 Wt % molybdenum oxide catalyst.

			Selectivities (%)					
Temp (C)	**Conver. (%)**	**Carbon balance**	**CO_2**	**Meth.**	**Acrol.**	**Acrylic acid**	**CO**	**Eth.**
150	0	100						
175	1.44	99.6	100					
200	1.73	98.1	100					
225	2.05	97.5	100					
250	3.06	98.1	100					
275	6.75	99.6	100					
300	7.42	100.1	100					
325	7.19	99.5	100					
350	9.39	99.5	100					
375	9.15	99.0	100					
400	8.67	99.1	100					
425	8.11	98.8	100					
450	8.19	101.0	100					
475	8.86	99.8	99.9	0.06				
500	10.27	99.7	99.9	0.10				

Appendix D

1: Propane oxidation

Table 1.2.4: Silica supported 6 Wt % molybdenum oxide catalyst.

			Selectivities (%)					
Temp (C)	**Conver. (%)**	**Carbon balance**	**CO_2**	**Meth.**	**Acrol.**	**Acrylic acid**	**CO**	**Eth.**
225	0	101.9						
250	0.54	100.0	100					
275	2.55	99.7	100					
300	4.66	98.3	100					
325	7.81	98.4	100					
350	9.40	99.9	100					
375	14.08	99.7	100					
400	18.34	98.3	100					
425	23.49	97.4	99.8		0.2			

Appendix D

1: Propane oxidation

Table 1.2.5: Silica supported 6.9 Wt % molybdenum oxide catalyst.

			Selectivities (%)					
Temp (C)	**Conver. (%)**	**Carbon balance**	**CO_2**	**Meth.**	**Acrol.**	**Acrylic acid**	**CO**	**Eth.**
225	0	100.0						
250	0.21	99.8	100					
275	0.35	99.7	100					
300	2.46	97.7	100					
325	3.52	99.5	100					
350	4.70	99.6	100					
375	4.87	100.0	100					
400	4.61	97.8	100					
425	5.08	97.7	100					
450	5.21	98.4	100					
475	7.35	96.6	100					
500	7.96	98.6	100					
525	8.79	96.5	99.9	0.12				
550	13.84	99.3	98.4	1.0	0.27			0.33

Appendix D

1: Propane oxidation

Table 1.2.6: Silica supported 10 Wt % molybdenum oxide catalyst.

			Selectivities (%)					
Temp (C)	**Conver. (%)**	**Carbon balance**	**CO_2**	**Meth.**	**Acrol.**	**Acrylic acid**	**CO**	**Eth.**
250	0	100.0						
275	0.02	99.2	100					
300	0.32	99.3	100					
325	0.22	99.9	100					
350	0.19	100.8	100					
375	0.60	100.6	100					
400	0.63	99.5	100					
425	1.42	98.6	100					
450	3.30	98.1	100					
475	5.04	100.5	100					
500	5.57	99.4	9.9		0.11			
525	8.87	99.3	99.6	0.10	0.10			0.23
550	9.52	99.2	98.6	0.53	0.08			0.82

Appendix D

1: Propane oxidation.

Table 1.2.7: Silica supported 15 Wt % molybdenum oxide catalyst.

			Selectivities (%)					
Temp (C)	**Conver. (%)**	**Carbon balance**	**CO_2**	**Meth.**	**Acrol.**	**Acrylic acid**	**CO**	**Eth.**
275	0	99.0						
300	0.02	99.2	100					
325	0.06	98.2	100					
350	0.28	98.5	100					
375	0.80	98.8	100					
400	1.55	99.3	100					
425	276	99.2	100					
450	4.04	99.6	100					
475	5.37	99.5	100					
500	6.41	99.2	100					
525	8.25	99.5	99.5	0.35	0.13			
550	13.39	97.2	97.0	2.94	0.14			

Appendix D

1: Propane oxidation.

1.3: Silica and blank empty reaction tube.

Table 1.3.1: Silica blank

			Selectivities (%)					
Temp (C)	**Conver. (%)**	**Carbon balance**	**CO_2**	**Meth.**	**Acrol.**	**Acrylic acid**	**CO**	**Eth.**
275	0	100.0						
300	0.10	100.1	100					
325	0.15	99.9	100					
350	0.84	99.9	100					
375	1.11	99.2	100					
400	1.86	99.0	100					
425	2.27	98.4	100					
450	2.62	98.2	100					
475	3.67	98.5	100					
500	5.16	98.2	99.6		0.38			
525	7.64	97.5	98.3	1.00	0.72			
550	10.76	98.2	93.5	5.94	0.55			

Appendix D

Propane oxidation

Table 1.3.2: Blank empty reaction tube

			Selectivities (%)					
Temp (C)	**Conver. (%)**	**Carbon balance**	**CO_2**	**Meth.**	**Acrol.**	**Acrylic acid**	**CO**	**Eth.**
275	0							
300	0.05	100.0						
325	0.11	99.2	100					
350	0.37	98.9	100					
375	0.71	98.6	100					
400	1.31	98.8	100					
425	1.69	99.0	100					
450	2.27	99.1	100					
475	3.22	99.5	100					
500	5.18	99.2	100					
525	6.79	99.6	99.2	0.55	0.30			
550	11.92	99.5	94.0	3.81	0.26			1.98

Appendix D

1: Propane oxidation.

1.4: Boron nitride supported vanadium oxide catalysts.

Table 1.4.1: Boron nitride blank.

			Selectivities (%)					
Temp (C)	**Conver. (%)**	**Carbon balance**	**CO_2**	**Meth.**	**Acrol.**	**Acrylic acid**	**CO**	**Acet.**
250	0	100.0						
275	0.01	99.6	100					
300	0.43	99.4	100					
325	0.61	98.9	100					
350	1.13	98.6	100					
375	1.44	98.5	100					
400	1.60	98.2	100					
425	2.04	97.9	100					
450	2.49	97.9	100					
475	2.78	98.3	97.3		2.70			
500	4.55	98.3	96.8		3.17			
525	6.08	97.8	94.7	1.56	3.72			
550	8.31	96.4	89.1	6.29	4.46	0.10		
575	18.80	95.3	73.7	18.03	5.19	0.64	1.99	0.47
600	45.44	93.6	60.7	25.54	3.14	1.14	9.09	0.43

Appendix D

1: Propane oxidation

Table 1.4.2: Boron nitride supported 7 Wt % Vanadium catalyst.

			Selectivities (%)					
Temp (C)	**Conver. (%)**	**Carbon balance**	**CO_2**	**Meth.**	**Acrol.**	**Acrylic acid**	**CO**	**Acet.**
250	0	100.0						
275	0.01	99.0	100					
300	1.05	98.9	100					
325	1.19	98.8	100					
350	1.33	98.4	100					
375	1.72	98.1	100					
400	1.94	98.1	100					
425	2.12	97.7	100					
450	2.62	97.3	100					
475	3.87	97.0	100					
500	5.06	96.5	97.6		2.45			
525	6.80	95.9	90.1	5.06	4.85			
550	10.01	94.6	73.7	16.27	7.40	1.49		1.08
575	31.32	75.6	45.0	24.32	5.03	1.19	23.5	1.01
600	54.58	74.8	35.5	31.57	2.18	1.88	27.7	1.15

Appendix D

1: Propane oxidation

Table 1.4.3: Boron nitride supported 21 Wt % Vanadium catalyst.

			Selectivities (%)					
Temp (C)	**Conver. (%)**	**Carbon balance**	**CO_2**	**Meth.**	**Acrol.**	**Acrylic acid**	**CO**	**Acet.**
250	0	100.0						
275	0.01	100.0	100					
300	0.06	100.1	100					
325	0.45	99.6	100					
350	0.34	99.7	100					
375	0.76	99.3	100					
400	1.60	98.5	100					
425	1.86	98.3	100					
450	2.58	97.6	100					
475	2.76	97.6	100					
500	3.12	97.3	100					
525	5.14	96.5	93.1	4.53	2.39			
550	10.81	92.0	66.6	23.15	8.42	1.09		0.71
575	29.57	76.1	34.7	17.76	3.17	1.52	42.0	0.83
600	46.17	62.4	29.1	23.83	1.75	1.40	42.9	1.06

Appendix D

1: Propane oxidation

Table 1.4.4: Boron nitride supported 35 Wt % Vanadium catalyst.

			Selectivities (%)					
Temp (C)	**Conver. (%)**	**Carbon balance**	**CO_2**	**Meth.**	**Acrol.**	**Acrylic acid**	**CO**	**Acet.**
250	0	100.0						
275	0.73	100.1	100					
300	0.88	99.9	100					
325	1.16	100.1	100					
350	1.31	99.5	100					
375	1.50	99.1	100					
400	1.74	97.7	100					
425	2.05	97.6	100					
450	2.77	97.2	100					
475	3.85	97.2	100					
500	4.72	99.2	97.9		2.11			
525	6.64	94.7	91.7	4.21	4.13			
550	9.78	92.0	79.6	10.19	8.54	1.21		0.48
575	30.60	76.8	57.7	17.31	3.54	1.32	19.1	1.01
600	51.45	61.7	43.1	20.54	2.87	1.87	31.2	0.42

Appendix D:

2: Propene oxidation

2.1: Silica supported Vanadium catalysts.

Table 2.1.1: Silica supported 2.5 Wt % Vanadium oxide catalyst.

			Selectivities (%)					
Temp (C)	**Conver. (%)**	**Carbon balance**	**CO_2**	**Meth.**	**Acrol.**	**Acrylic acid**	**CO**	**Acet.**
200	0							
225	0.08	100.0						100
250	0.34	99.8						90.42
275	0.39	99.7						48.02
300	0.62	99.8						34.87
325	0.63	99.4						19.60
350	0.93	99.1						7.53
375	1.34	98.5	100					
400	1.77	97.9	100					
425	2.41	98.6	94.0		5.97			
450	3.09	99.0	92.5		6.45	1.02		
475	3.64	98.5	90.5		6.87	2.67		
500	5.28	98.1	86.7		8.64	4.65		
525	7.26	97.6	91.6		5.31	3.11		
550	10.53	96.2	91.9		4.52	3.54		

Appendix D:

2: Propene oxidation

Table 2.1.2: Silica supported 3.5 Wt % Vanadium oxide catalyst.

			Selectivities (%)					
Temp (C)	**Conver. (%)**	**Carbon balance**	**CO_2**	**Meth.**	**Acrol.**	**Acrylic acid**	**CO**	**Acet.**
175	0							
200	0.01	99.9						100
225	0.14	99.8						100
250	0.24	99.6						100
275	0.45	99.4	41.6					58.36
300	0.66	99.1	45.0					54.97
325	0.96	99.4	66.1					33.93
350	1.35	98.7	71.3			12.65		16.02
375	1.50	98.6	70.0			13.40		16.64
400	2.04	98.1	68.3		19.55	12.20		
425	2.81	97.4	60.7		27.08	12.20		
450	3.98	96.7	61.8		20.84	17.38		
475	6.67	94.7	67.1		15.74	17.21		
500	9.77	94.5	84.2		8.69	7.13		
525	15.81	94.6	91.2		4.78	3.67		
550	17.89	91.5	89.6		5.26	5.11		

Appendix D:

2: Propene oxidation.

Table 2.1.3: Silica supported 5 Wt % Vanadium oxide catalyst.

			Selectivities (%)					
Temp (C)	**Conver. (%)**	**Carbon balance**	**CO_2**	**Meth.**	**Acrol.**	**Acrylic acid**	**CO**	**Acet.**
200	0							
225	0.17	99.9						100
250	0.16	99.8						100
275	0.60	99.7	44.3					55.74
300	0.65	99.7	67.2					32.84
325	0.84	99.5	81.7					18.26
350	1.04	99.1	89.6					10.45
375	1.17	98.6	94.0					6.01
400	1.58	98.9	100					
425	1.80	98.4	93.6		5.14	1.25		
450	2.46	98.7	85.7		10.58	3.69		
475	3.00	99.1	78.3		14.26	7.48		
500	7.21	97.6	87.8		10.77	1.42		
525	14.93	95.1	93.1		4.32	2.55		
550	16.97	94.6	90.2		5.68	4.08		

Appendix D:

2: Propene oxidation

Table 2.1.4: Silica supported 6 Wt % Vanadium oxide catalyst.

			Selectivities (%)					
Temp (C)	**Conver. (%)**	**Carbon balance**	**CO_2**	**Meth.**	**Acrol.**	**Acrylic acid**	**CO**	**Acet.**
225	0							
250	0.02	100.0	0					100
275	0.59	99.4	0					100
300	0.76	99.3	49.6					50.43
325	0.92	99.2	61.9					37.87
350	1.21	98.9	80.6					19.58
375	1.52	98.6	87.9					12.12
400	2.00	98.1	100.0					
425	2.53	97.8	84.6		7.21	8.23		
450	3.11	97.8	83.1		9.70	7.23		
475	4.35	98.3	85.3		11.13	3.59		
500	6.89	100.4	92.1		6.34	1.54		
525	12.87	99.6	93.0		2.93	4.04		
550	13.12	96.0	90.0		4.48	5.38		

Appendix D:

2: Propene oxidation

Table 2.1.5: Silica supported 7 Wt % Vanadium oxide catalyst.

			Selectivities (%)					
Temp (C)	**Conver. (%)**	**Carbon balance**	**CO_2**	**Meth.**	**Acrol.**	**Acrylic acid**	**CO**	**Acet.**
200	0							
225	0.01	100.0						100
250	0.01	99.9						87.51
275	0.03	99.8						51.45
300	0.05	99.9						42.25
325	0.19	99.6						20.41
350	0.49	99.4						8.63
375	0.95	98.7	100					
400	1.42	99.0	100					
425	2.05	98.4	91.1		4.19	4.71		
450	3.06	98.1	87.1		9.67	3.25		
475	6.65	98.3	90.2		7.38	2.44		
500	10.77	97.8	93.0		4.88	2.17		
525	12.88	97.4	92.1		3.79	4.12		
550	12.45	96.7	91.7		3.57	4.76		

Appendix D:

2: Propene oxidation

Table 2.1.6: Silica supported 10 Wt % Vanadium oxide catalyst.

			Selectivities (%)					
Temp (C)	**Conver. (%)**	**Carbon balance**	**CO_2**	**Meth.**	**Acrol.**	**Acrylic acid**	**CO**	**Acet.**
200	0							
225	0.01	99.9						100
250	0.08	99.9						100
275	0.14	99.4	47.3					52.71
300	0.67	99.4	68.2					31.76
325	0.68	99.0	85.0					14.98
350	1.03	98.1	89.2			10.78		
375	1.99	98.1	77.2		9.41	13.34		
400	2.01	97.9	77.6		10.41	12.04		
425	2.39	98.3	82.9		8.57	8.57		
450	2.42	99.0	89.1		7.79	3.07		
475	3.10	100.2	94.1		3.90	2.00		
500	5.04	100.7	91.0		4.90	4.14		
525	10.33	94.8	90.1		6.32	3.59		
550	13.84	94.5	90.2		6.59	3.23		

Appendix D:

2: Propene oxidation

Table 2.1.7: Silica supported 15 Wt % Vanadium oxide catalyst.

			Selectivities (%)					
Temp (C)	**Conver. (%)**	**Carbon balance**	**CO_2**	**Meth.**	**Acrol.**	**Acrylic acid**	**CO**	**Acet.**
200	0							
225	0.01	100.0						100
250	0.01	100.1	9.8					90.21
275	0.02	99.7	49.0					51.02
300	0.05	99.6	61.6					38.45
325	0.24	99.3	80.8					19.16
350	0.49	99.1	87.5					12.47
375	1.30	98.6	92.9					7.10
400	1.59	98.7	100					
425	2.16	98.5	88.5		6.74	4.80		
450	3.06	99.0	89.6		4.82	5.61		
475	3.45	98.5	93.8		3.75	2.47		
500	5.87	98.1	94.1		2.94	2.96		
525	6.65	97.7	92.0		4.17	3.87		
550	10.98	95.2	92.3		6.24	1.44		

Appendix D

2: Propene oxidation

2.2: Silica supported Molybdenum catalysts.

Table 2.2.1: Silica supported 2.5 Wt % molybdenum oxide catalyst.

			Selectivities (%)					
Temp (C)	**Conver. (%)**	**Carbon balance**	**CO_2**	**Meth.**	**Acrol.**	**Acrylic acid**	**CO**	**Eth.**
250	0							
275	0.22	100.0	100					
300	0.39	99.8	100					
325	0.65	98.9	100					
350	0.84	99.5	100					
375	1.64	99.6	100					
400	2.41	99.2	86.0		13.96			
425	3.00	99.3	79.9		20.15			
450	4.70	98.4	83.2		15.20	1.57		
475	5.08	97.9	89.4		8.25	2.40		
500	7.49	98.2	90.7		7.83	1.44		
525	8.88	99.1	96.2		3.26	0.57		
550	10.99	97.1	97.4		2.25	0.35		
575	12.48	95.6	97.9		1.23	0.83		

Appendix D

2: Propene oxidation

Table 2.2.2: Silica supported 3.5 Wt % molybdenum oxide catalyst.

			Selectivities (%)					
Temp (C)	**Conver. (%)**	**Carbon balance**	**CO_2**	**Meth.**	**Acrol.**	**Acrylic acid**	**CO**	**Eth.**
250	0							
275	0.14	100.0	100					
300	0.41	98.7	100					
325	0.54	99.8	100					
350	1.22	99.4	100					
375	1.71	99.2	100					
400	2.20	99.5	86.4		13.58			
425	2.66	98.6	82.0		16.85	1.20		
450	3.03	99.1	86.0		12.51	1.54		
475	3.67	98.7	88.7		10.40	0.87		
500	4.95	98.1	92.8		6.41	0.81		
525	7.55	97.6	95.0		4.55	0.45		
550	11.21	98.0	96.9		2.67	0.46		
575	14.73	96.4	96.9	0.26	2.23	0.63		

Appendix D

2: Propene oxidation

Table 2.2.3: Silica supported 5 Wt % molybdenum oxide catalyst.

			Selectivities (%)					
Temp (C)	**Conver. (%)**	**Carbon balance**	**CO_2**	**Meth.**	**Acrol.**	**Acrylic acid**	**CO**	**Eth.**
225	0							
250	0.10	100.0	100					
275	0.19	99.8	100					
300	0.22	99.6	100					
325	0.55	99.9	100					
350	0.61	99.1	100					
375	0.93	99.2	85.7		14.29			
400	1.59	99.5	79.8		20.16			
425	2.92	98.7	84.4		14.82	0.80		
450	4.42	97.9	85.9		13.38	0.74		
475	5.27	97.6	93.1		6.45	0.46		
500	7.94	98.2	97.7		2.13	0.16		
525	9.15	97.4	99.2		0.70	0.06		
550	12.57	96.1	99.6	0.10	0.34			

Appendix D

2: Propene oxidation

Table 2.2.4: Silica supported 6 Wt % molybdenum oxide catalyst.

			Selectivities (%)					
Temp (C)	**Conver. (%)**	**Carbon balance**	**CO_2**	**Meth.**	**Acrol.**	**Acrylic acid**	**CO**	**Eth.**
225	0							
250	0.27	100.0	100					
275	0.66	99.8	100					
300	1.15	100.1	100					
325	1.41	100.5	100					
350	1.55	99.8	100					
375	1.81	99.6	86.4		13.59			
400	2.14	99.4	84.2		15.28	0.52		
425	2.39	99.4	86.7		12.54	0.81		
450	4.28	98.2	92.1		7.40	0.51		
475	6.78	99.0	93.5		6.21	0.27		
500	7.56	98.7	98.1		1.48	0.45		
525	9.49	97.3	99.1		0.75	0.15		
550	11.88	96.8	99.6		0.41			

Appendix D

2: Propene oxidation

Table 2.2.5: Silica supported 6.9 Wt % molybdenum oxide catalyst.

			Selectivities (%)					
Temp (C)	**Conver. (%)**	**Carbon balance**	**CO_2**	**Meth.**	**Acrol.**	**Acrylic acid**	**CO**	**Eth.**
250	0							
275	0.21	100	100					
300	0.35	99.8	100					
325	0.46	99.7	100					
350	0.52	99.4	100					
375	1.70	99.5	100					
400	2.87	98.9	89.9		10.07			
425	4.61	98.2	87.4		12.20	0.41		
450	5.08	98.4	91.1		7.85	1.04		
475	5.21	98.7	92.6		6.42	0.95		
500	7.35	97.8	95.0		4.09	0.89		
525	7.96	98.1	96.3		2.46	1.20		
550	8.79	97.6	97.0		2.17	0.85		
575	13.84	95.9	97.9	0.55	1.12	0.47		

Appendix D

2: Propene oxidation

Table 2.2.6: Silica supported 10 Wt % molybdenum oxide catalyst.

			Selectivities (%)					
Temp (C)	**Conver. (%)**	**Carbon balance**	**CO_2**	**Meth.**	**Acrol.**	**Acrylic acid**	**CO**	**Eth.**
250	0							
275	0.04	100.0	100					
300	0.24	99.8	100					
325	0.50	99.5	100					
350	0.69	99.3	100					
375	0.76	99.3	85.4		14.64			
400	1.04	99.2	78.9		21.06			
425	1.64	99.0	78.6		19.92	1.44		
450	2.25	99.3	82.8		15.71	1.48		
475	4.54	99.2	88.5		10.33	1.11		
500	8.11	99.9	94.0		5.37	0.66		
525	11.41	101.9	96.5		3.09	0.40		
550	13.53	102.7	97.0		1.56	0.41		0.06
575	14.42	100.9	94.6	0.06	3.34	1.88		0.14

Appendix D

2: Propene oxidation.

Table 2.2.7: Silica supported 15 Wt % molybdenum oxide catalyst.

			Selectivities (%)					
Temp (C)	**Conver. (%)**	**Carbon balance**	**CO_2**	**Meth.**	**Acrol.**	**Acrylic acid**	**CO**	**Eth.**
250	0	99.9						
275	0.01	99.8	100					
300	0.24	99.6	100					
325	0.30	99.1	100					
350	0.58	99.2	100					
375	0.84	99.4	100					
400	1.53	98.6	89.8		10.24			
425	2.21	98.4	86.8		11.89	1.29		
450	3.37	98.9	90.0		9.10	0.87		
475	4.12	99.1	90.1		8.76	0.52		
500	5.65	98.2	92.7		6.87	0.47		
525	7.24	98.7	95.7		3.57	0.69		
550	8.50	98.3	98.0		1.64	0.33		
575	10.09	97.5	97.8		1.49	0.67		

Appendix D

2: Propene oxidation.

2.3: Silica and blank empty reaction tube.

Table 2.3.1: Silica blank.

			Selectivities (%)					
Temp (C)	**Conver. (%)**	**Carbon balance**	**CO_2**	**Meth.**	**Acrol.**	**Acrylic acid**	**CO**	**Eth.**
250	0	100.0						
275	0.58	99.4	100					
300	0.70	99.4	56.0		44.0			
325	0.97	99.5	82.4		17.58			
350	2.56	98.6	90.8		9.18			
375	5.00	97.8	94.7		5.32			
400	6.74	99.3	97.7		2.30			
425	9.05	102.0	98.8		1.20			
450	11.87	105.2	99.7		0.34			

Appendix D

2: Propene oxidation

Table 2.3.2: Blank empty reaction tube.

			Selectivities (%)					
Temp (C)	**Conver. (%)**	**Carbon balance**	**CO_2**	**Meth.**	**Acrol.**	**Acrylic acid**	**CO**	**Eth.**
225	0							
250	0.01	100.0	100					
275	0.01	99.8	100					
300	0.02	100.2	100					
325	0.04	100.0	100					
350	0.06	100.0	100					
375	0.07	99.8	65.1		34.93			
400	0.07	99.3	75.8		24.16			
425	0.25	99.4	84.8		15.23			
450	0.58	98.1	84.8		15.21			
475	1.74	97.9	89.8		9.37	0.78		
500	4.84	99.3	97.0		2.76	0.25		
525	6.17	98.8	98.6		1.30	0.11		
550	8.22	99.7	99.3		0.63	0.05		

Appendix D

2: Propene oxidation.

2.4: Boron nitride supported vanadium oxide catalysts.

Table 2.4.1: Boron nitride blank.

			Selectivities (%)					
Temp (C)	**Conver. (%)**	**Carbon balance**	**CO_2**	**Meth.**	**Acrol.**	**Acrylic acid**	**CO**	**Eth.**
225	0							
250	0.01	100.0	100					
275	0.12	99.9	100					
300	0.58	99.5	79.9		20.10			
325	0.52	99.6	78.0		22.03			
350	1.10	99.4	73.2		26.76			
375	1.31	99.6	69.5		30.46			
400	1.89	10.2	66.7		32.11	1.20		
425	4.54	99.5	67.7		31.30	1.02		
450	7.52	98.7	70.8		28.28	0.89		
475	9.43	98.7	74.9		24.41	0.68		
500	11.92	97.5	77.3		22.07	0.62		
525	14.01	96.2	67.6	0.11	16.60	0.45	15.2	
550	16.32	95.6	67.6	0.26	15.46	0.39	16.2	

Appendix D

2: Propene oxidation

Table 2.4.2: Boron nitride supported 7 Wt % Vanadium catalyst.

			Selectivities (%)					
Temp (C)	**Conver. (%)**	**Carbon balance**	**CO_2**	**Meth.**	**Acrol.**	**Acrylic acid**	**C_3-C_2 Oxyg.**	**Acet.**
225	0							
250	0.01	100.0						100
275	0.26	99.8						100
300	0.52	99.5						100
325	0.68	99.4	63.7		20.10			16.21
350	1.03	99.1	73.6		26.42			
375	1.39	98.9	64.8		29.89	5.34		
400	2.53	98.2	67.5		26.28	6.24		
425	6.32	96.0	79.0		15.79	5.21		
450	10.19	94.9	81.8		14.46	3.44	0.26	
475	12.30	93.8	82.6		14.02	3.9	0.27	
500	17.37	93.1	85.6		11.64	2.56	0.21	
525	20.41	92.9	84.9		12.56	2.23	0.27	
550	23.49	90.7	82.4		14.30	2.50	0.53	
575	27.15	90.0	78.6		15.73	3.55	1.38	

Appendix D

2: Propene oxidation

Table 2.4.3: Boron nitride supported 21 Wt % Vanadium catalyst.

			Selectivities (%)					
Temp (C)	**Conver. (%)**	**Carbon balance**	**CO_2**	**Meth.**	**Acrol.**	**Acrylic acid**	**CO**	**Eth.**
250	0							
275	0.01	100.0	100.0					
300	0.15	100.2	56.1		43.92			
325	0.28	99.8	58.5		41.50			
350	0.84	99.3	63.8		36.16			
375	1.75	98.5	59.9		32.81	7.31		
400	2.43	98.5	49.2		41.23	9.55		
425	4.36	97.9	55.9		29.58	14.51		
450	6.14	97.3	69.4		19.81	10.79		
475	8.55	96.6	75.6		16.85	7.55		
500	12.41	95.2	85.5		10.48	4.01		
525	18.70	94.9	90.2		6.87	2.92		
550	20.25	95.6	91.9		5.47	2.60		
575	21.23	91.02	92.5		5.39	2.14		

Appendix D

2: Propene oxidation

Table 2.4.4: Boron nitride supported 35 Wt % Vanadium catalyst.

			Selectivities (%)					
Temp (C)	**Conver. (%)**	**Carbon balance**	**CO_2**	**Meth.**	**Acrol.**	**Acrylic acid**	**CO**	**Eth.**
250	0							
275	0.01	100.0	100.0					
300	0.05	99.8	60.4		39.57			
325	0.38	99.6	55.6		44.42			
350	0.85	99.7	56.4		43.57			
375	1.15	99.1	53.2		40.25	6.54		
400	1.96	98.7	50.2		37.46	12.77		
425	3.30	99.4	48.3		41.19	10.52		
450	6.61	99.2	62.9		26.34	10.76		
475	10.94	98.6	74.8		18.24	6.98		
500	12.69	98.5	82.7		12.20	5.14		
525	13.59	97.9	87.7		8.68	3.66		
550	14.13	95.8	89.6		7.56	2.89		
575	16.25	95.2	91.9		5.99	2.14		

Appendix D

3: Propane oxidation with co-fed water

3.1 Silica supported molybdenum catalysts.

Table 3.1.1: Silica supported 2.5 Wt % molybdenum catalyst.

			Selectivities (%)					
Temp (C)	**Conver. (%)**	**Carbon balance**	**CO_2**	**Meth.**	**Acrol.**	**Acrylic acid**	**CO**	**Eth.**
250	0							
275	0.04	100.0	100					
300	0.45	99.9	100					
325	0.39	99.7	100					
350	0.55	99.5	100					
375	0.72	99.4	100					
400	1.37	99.0	100					
425	1.57	99.0	100					
450	2.00	98.8	100					
475	2.27	99.1	99.3		0.70			
500	2.71	99.3	99.1	0.39	0.47			
525	3.26	99.7	98.4	0.94	0.63			
550	3.71	100.1	94.2	4.70	1.07			
575	7.78	102.3	83.8	13.63	1.88	0.66		

Appendix D

3: Propane oxidation with co-fed water

Table 3.1.2: Silica supported 5 Wt % molybdenum catalyst.

			Selectivities (%)					
Temp (C)	**Conver. (%)**	**Carbon balance**	**CO_2**	**Meth.**	**Acrol.**	**Acrylic acid**	**CO**	**Eth.**
125	0							
150	0.12	100.0	100					
175	0.07	99.9	100					
200	0.30	99.9	100					
225	0.46	99.9	100					
250	1.12	99.8	100					
275	2.93	100.0	100					
300	6.61	100.0	100					
325	8.13	102.8	100					
350	9.96	104.1	100					
375	9.57	104.4	100					
400	9.37	103.7	100					
425	7.59	102.5	100					
450	7.39	101.0	100					
475	7.65	100.3	99.9		0.13			
500	7.83	100.5	99.8		0.21			

Appendix D

3: Propane oxidation with co-fed water

Table 3.1.3: Silica supported 15 Wt % molybdenum catalyst

			Selectivities (%)					
Temp (C)	**Conver. (%)**	**Carbon balance**	**CO_2**	**Meth.**	**Acrol.**	**Acrylic acid**	**CO**	**C_3.**
200	0							
225	0.09	100.0	100					
250	0.17	99.9	100					
275	0.24	99.9	100					
300	0.43	99.8	100					
325	0.65	99.6	100					
350	0.76	99.4	100					
375	1.00	99.3	100					
400	1.29	99.1	100					
425	1.58	98.9	100					
450	1.64	98.6	100					
475	1.81	98.6	100					
500	2.72	98.4	92.7	4.01	3.24			
525	3.42	97.6	72.2	19.63	8.14			
550	4.92	97.3	58.2	4.91	11.06	1.66	22.9	1.29
575	7.90	100.2	24.6	33.52	3.79	1.12	35.4	1.55

Appendix D

3: Propane oxidation with co-fed water

3.2: Silica supported vanadium catalysts.

Table 3.2.1: Silica supported 3.5 Wt % vanadium catalyst.

			Selectivities (%)					
Temp (C)	**Conver. (%)**	**Carbon balance**	**CO_2**	**Meth.**	**Acrol.**	**Acrylic acid**	**CO**	**Eth.**
175	0							
200	0.02	100.0	100					
225	0.31	9.7	100					
250	1.09	99.1	100					
275	1.86	98.8	100					
300	2.22	98.5	100					
325	2.46	98.5	100					
350	3.28	99.1	100					
375	4.71	10.5	100					
400	9.14	102.7	100					
425	13.83	103.7	100					

Appendix D

3: Propane oxidation with co-fed water.

Table 3.2.2: Silica supported 5 Wt % vanadium catalyst.

			Selectivities (%)					
Temp (C)	**Conver. (%)**	**Carbon balance**	**CO_2**	**Meth.**	**Acrol.**	**Acrylic acid**	**CO**	**Eth.**
225	0							
250	0.18	99.8	100					
275	0.37	99.7	100					
300	0.60	99.5	100					
325	1.20	99.0	100					
350	1.43	98.9	100					
375	1.81	98.8	100					
400	2.46	98.6	100					
425	2.88	98.9	99.3		0.66			
450	6.89	102.0	46.3		0.11		53.6	
475	8.56	99.2	48.0	0.04	0.10		51.9	

Appendix D

3: Propane oxidation with co-fed water.

Table 3.2.3: Silica supported 15 Wt % vanadium catalyst.

			Selectivities (%)					
Temp (C)	**Conver. (%)**	**Carbon balance**	**CO_2**	**Meth.**	**Acrol.**	**Acrylic acid**	**CO**	**C_3.**
200	0							
225	0.16	100.0	100					
250	0.26	99.9	100					
275	0.50	99.7	100					
300	0.58	99.5	100					
325	0.75	99.4	100					
350	1.38	99.3	100					
375	1.45	98.7	100					
400	1.71	98.6	100					
425	2.19	98.5	100					
450	2.72	98.0	100					
475	2.88	97.6	95.9	1.63	2.45			
500	4.07	97.5	94.0	2.39	3.58			
525	5.26	96.6	88.1	4.02	6.03	0.94		0.81
550	7.39	95.8	80.3	6.23	9.35	2.46		1.64
575	12.56	95.8	95.5	1.38	2.07	0.88		0.15

Appendix D

3: Propane oxidation with co-fed water

3.3: Boron nitride supported vanadium catalysts.

Table 3.3.1: Boron nitride blank.

			Selectivities (%)					
Temp (C)	**Conver. (%)**	**Carbon balance**	**CO_2**	**Meth.**	**Acrol.**	**Acrylic acid**	**CO**	**C_3.**
325	0							
350	0.05	100.0	100					
375	0.10	99.9	100					
400	0.26	99.8	100					
425	0.38	99.6	100					
450	0.67	99.4	100					
475	1.01	99.1	100					
500	1.17	98.0	91.1		8.94			
525	2.20	98.7	59.7	29.25	9.84			1.16
550	3.53	100.7	39.7	45.47	10.11	1.17		3.50

Appendix D

3: Propane oxidation with co-fed water.

Table 3.3.2: Boron nitride supported 7 Wt % Vanadium catalyst.

			Selectivities (%)					
Temp (C)	**Conver. (%)**	**Carbon balance**	**CO_2**	**Meth.**	**Acrol.**	**Acrylic acid**	**CO**	**C_3.**
325	0							
350	0.04	100.0	100					
375	0.08	99.9	100					
400	0.14	99.9	100					
425	0.31	99.7	100					
450	0.58	99.5	100					
475	0.96	99.1	100					
500	1.63	98.5	59.0	28.15	12.83			
525	1.94	98.4	44.4	41.62	14.01			
550	3.83	97.5	34.9	47.17	13.55	1.58		2.77
575	6.12	99.6	20.5	60.61	5.15	1.79	40.3	1.64
600	8.39	100.6	23.2	41.82	3.88	1.06	27.3	2.75

Appendix D

3: Propane oxidation with co-fed water.

Table 3.3.3: Boron nitride supported 21 Wt % Vanadium catalyst.

			Selectivities (%)					
Temp (C)	**Conver. (%)**	**Carbon balance**	**CO_2**	**Meth.**	**Acrol.**	**Acrylic acid**	**CO**	**C_3.**
275	0							
300	0.10	99.9	100					
325	0.51	99.5	100					
350	0.75	99.3	100					
375	0.83	99.2	100					
400	1.18	98.9	100					
425	2.12	98.3	94.3		5.67			
450	2.87	98.1	87.6	2.79	9.57			
475	3.46	97.6	83.2	9.09	7.74			
500	4.95	97.5	51.5	9.45	2.86	0.53	35.0	0.68
525	6.20	99.2	48.8	27.61	3.62	1.45	17.8	0.68
550	8.07	99.6	46.4	35.17	2.73	1.08	13.8	1.08

Appendix D

3: Propane oxidation with co-fed water.

Table 3.3.4: Boron nitride supported 35 Wt % Vanadium catalyst.

			Selectivities (%)					
Temp (C)	**Conver. (%)**	**Carbon balance**	**CO_2**	**Meth.**	**Acrol.**	**Acrylic acid**	**CO**	**C_3.**
325	0							
350	0.06	100.0	100					
375	0.11	99.9	100					
400	0.35	99.7	100					
425	0.70	99.3	100					
450	1.07	99.0	100					
475	1.59	98.6	85.3	6.54	8.20			
500	2.13	98.4	63.7	17.26	15.70			3.38
525	3.64	98.9	27.5	13.12	4.87	0.96	51.1	2.43
550	5.86	10.3	19.7	22.14	3.36	2.31	51.5	1.00
575	8.25	99.8	15.0	28.89	2.25	2.12	49.9	1.88

Appendix D

4: Methane oxidation

4.1: Silica supported molybdenum catalysts.

Table 4.1.1: Silica supported 3.5 Wt % Mo catalyst.

Temp. (C)	Convers. (%)	Carbon Bal. (%)	CO_2 Select. (%)	CO Select. (%)	Ethane Select (%)
525	0	100.0			
550	0.13	99.9	100		
575	0.15	100.1	100		
600	0.59	99.5	100		
625	1.36	98.7	100		
650	1.63	98.6	100		
675	2.19	98.3	100		

Appendix D

4: Methane oxidation

Table 4.1.2: Silica supported 6 Wt % Mo catalyst.

Temp. (C)	Convers. (%)	Carbon Bal. (%)	CO_2 Select. (%)	CO Select. (%)	Ethane Select (%)
425	0	100.0			
450	0.14	99.9	100		
475	0.24	99.8	10		
500	0.45	99.9	100		
525	0.66	99.7	100		
550	0.96	99.4	100		
575	1.35	98.9	100		
600	1.50	99.2	100		
625	2.04	97.9	100		
650	2.81	98.2	100		
675	3.98	97.6	100		

Appendix D

4: Methane oxidation

Table 4.1.3: Silica supported 10 Wt % Mo catalyst.

Temp. (C)	Convers. (%)	Carbon Bal. (%)	CO_2 Select. (%)	CO Select. (%)	Ethane Select (%)
475	0.10	99.9			
500	0.66	99.4	100		
525	0.97	99.1	100		
550	1.26	98.8	100		
575	1.46	98.6	100		
600	1.68	98.4	100		
625	2.39	97.0	100		
650	2.67	97.7	100		
675	5.09	96.1	100		

Appendix D

4: Methane oxidation

4.2: Silica supported vanadium catalysts.

Table 4.2.1: Silica supported 3.5 Wt % V catalyst.

Temp. (C)	Convers. (%)	Carbon Bal. (%)	CO_2 Select. (%)	CO Select. (%)	Ethane Select (%)
350	0	100.0			
375	0.04	100.0	100		
400	0.20	99.9	100		
425	0.51	99.7	100		
450	1.32	99.3	100		
475	2.50	99.0	100		
500	3.98	99.5	100		
525	5.99	100.3	100		
550	9.19	103.9	100		
575	19.61	104.5	100		
600	34.42	103.8	100		

Appendix D

4: Methane oxidation

Table 4.2.2: Silica supported 6 Wt % V catalyst.

Temp. (C)	Convers. (%)	Carbon Bal. (%)	CO_2 Select. (%)	CO Select. (%)	Ethane Select (%)
400	0	100.0			
425	0.07	99.8	100		
450	0.20	99.9	100		
475	0.34	99.7	100		
500	0.50	99.5	100		
525	0.91	99.7	100		
550	1.41	99.4	100		
575	2.23	99.1	100		
600	4.22	97.8	100		
625	6.31	97.1	100		

Appendix D

4: Methane oxidation

Table 4.2.3: Silica supported 10 Wt % V catalyst.

Temp. (C)	Convers. (%)	Carbon Bal. (%)	CO_2 Select. (%)	CO Select. (%)	Ethane Select (%)
425	0	100.0			
450	0.09	100.0	100		
475	0.19	100.0	100		
500	0.77	99.6	100		
525	1.00	99.5	100		
550	1.42	99.5	100		
575	1.67	99.7	100		
600	2.13	100.1	100		
625	2.60	101.7	100		
650	3.18	103.3	100		

Appendix D

4: Methane oxidation

4.3: Silica and blank reaction tube.

Table 4.3.1: Silica

Temp. (C)	**Convers. (%)**	**Carbon Bal. (%)**	**CO_2 Select. (%)**	**CO Select. (%)**	**Ethane Select (%)**
525	0				
550	0.09	100.0	100		
575	0.43	99.6	100		
600	0.65	99.4	100		
625	1.40	98.3	100		

Appendix D

4: Methane oxidation

Table 4.3.2: Blank reaction tube.

Temp. (C)	Convers. (%)	Carbon Bal. (%)	CO_2 Select. (%)	CO Select. (%)	Ethane Select (%)
450	0	100.0			
475	0.01	100.3	100		
500	0.40	100.1	100		
525	0.53	99.7	100		
550	0.78	99.5	100		
575	0.74	99.7	100		
600	1.34	99.2	100		
625	2.38	98.3	100		
650	2.69	98.1	100		
675	3.55	97.6	100		

Appendix D

4: Methane oxidation

4.4: Boron nitride supported vanadium catalysts.

Table 4.4.1: Boron nitride.

Temp. (C)	Convers. (%)	Carbon Bal. (%)	CO_2 Select. (%)	CO Select. (%)	Ethane Select (%)
500	0	100			
525	0.14	99.9	100		
550	0.32	99.7	100		
575	1.05	99.0	100		
600	1.18	98.9	100		
625	1.41	98.7	100		
650	3.38	98.8	100		

Appendix D

4: Methane oxidation

Table 4.4.2: Boron nitride supported 7 Wt % V catalyst.

Temp. (C)	Convers. (%)	Carbon Bal. (%)	CO_2 Select. (%)	CO Select. (%)	Ethane Select (%)
475	0	100.0			
500	0.04	99.8	100		
525	0.05	99.9	100		
550	0.36	99.7	100		
575	0.66	99.5	100		
600	1.11	98.9	100		
625	3.15	98.2	100		

Appendix D

4: Methane oxidation

Table 4.4.3: Boron nitride supported 21 Wt % V catalyst.

Temp. (C)	Convers. (%)	Carbon Bal. (%)	CO_2 Select. (%)	CO Select. (%)	Ethane Select (%)
450	0	100.0			
475	0.14	99.9	100		
500	0.06	100.0	100		
525	0.33	99.7	100		
550	0.79	99.3	100		
575	1.08	99.0	100		
600	26.1	98.0	38.4	59.7	4.59
625	36.9	97.3	42.3	56.9	1.82

Appendix D

4: Methane oxidation

Table 4.4.4: Boron nitride supported 35 Wt % V catalyst.

Temp. (C)	Convers. (%)	Carbon Bal. (%)	CO_2 Select. (%)	CO Select. (%)	Ethane Select (%)
400	0	100.0			
425	0.15	99.9	100		
450	0.19	99.9	100		
475	0.43	99.6	100		
500	0.46	99.9	100		
525	0.39	99.8	100		
550	0.57	99.5	100		
575	0.72	99.7	100		
600	0.79	99.6	100		
625	1.06	99.1	100		
650	1.26	99.0	100		

Appendix D

5: Ethane oxidation

5.1 Silica supported molybdenum catalysts.

Table 5.1.1: Silica supported 2.5 Wt % Mo catalyst.

Temp (C)	Conv. (%)	C. Balan. (%)	CO_2 Sel. (%)	CO Sel. (%)	Meth. Sel (%)	Ethene Sel. (%)
300	0	100				
325	0.01	100.0	100			
350	0.10	100.0	100			
375	0.02	100.0	100			
400	0.15	99.9	100			
425	0.07	100.0	100			
450	0.24	99.9	100			
475	0.39	99.8	100			
500	0.70	99.7	100			
525	0.90	99.4	60.6			39.45
550	1.90	99.4	40.8			59.23
575	5.17	98.8	15.1		0.54	84.37
600	28.7	97.9	7.2	7.9	2.00	82.86

Appendix D

5: Ethane oxidation

Table 5.1.2: Silica supported 5 Wt % Mo catalyst.

Temp (C)	Conv. (%)	C. Balan. (%)	CO_2 Sel. (%)	CO Sel. (%)	Meth. Sel (%)	Ethene Sel. (%)
250	0	100				
275	0.10	99.9	100			
300	0.31	99.7	100			
325	0.42	99.8	100			
350	1.29	100.1	100			
375	17.10	107.6	100			
400	17.69	107.2	100			

Appendix D

5: Ethane oxidation

Table 5.1.3: Silica supported 6.9 Wt % Mo catalyst.

Temp (C)	Conv. (%)	C. Balan. (%)	CO_2 Sel. (%)	CO Sel. (%)	Meth. Sel (%)	Ethene Sel. (%)
275	0	100				
300	0.09	100.0	100			
325	0.07	100.1	100			
350	0.41	100.1	100			
375	0.81	100.2	100			
400	1.04	100.4	100			
425	1.61	100.8	100			
450	2.48	101.1	100			
475	3.01	101.2	100			
500	3.49	101.1	100			
525	3.61	99.6	96.9			3.15
550	3.94	99.1	83.0			17.03
575	8.46	98.0	32.1	6.6	0.61	60.63
600	38.74	102.1	13.6	16.0	3.08	67.36

Appendix D

5: Ethane oxidation

Table 5.1.4: Silica supported 10 Wt % Mo catalyst.

Temp (C)	Conv. (%)	C. Balan. (%)	CO_2 Sel. (%)	CO Sel. (%)	Meth. Sel (%)	Ethene Sel. (%)
375	0	100.0				
400	0.12	99.9	100			
425	0.61	99.4	100			
450	0.96	99.1	100			
475	1.08	99.0	59.0			41.0
500	1.38	99.0	32.7			67.3
525	2.25	98.7	25.3			75.7
550	4.58	97.9	17.8		0.63	81.6
575	12.79	97.0	10.8		0.98	88.2

Appendix D

5: Ethane oxidation

Table 5.1.5: Blank reaction tube.

Temp (C)	Conv. (%)	C. Balan. (%)	CO_2 Sel. (%)	CO Sel. (%)	Meth. Sel (%)	Ethene Sel. (%)
325	0	100				
350	0.09	99.9	100			
375	0.05	100.0	100			
400	0.23	99.8	100			
425	0.44	99.6	100			
450	0.97	99.7	20.2			79.8
475	4.46	99.1	8.3		0.62	91.1
500	5.35	98.3	8.7		0.62	90.7
525	33.05	100.1	8.3	4.3	2.56	84.8
550	33.33	99.2	7.8	3.9	2.59	85.8

Appendix D

5: Ethane oxidation

5.2: Boron nitride supported vanadium catalysts.

Table 5.2.1: Boron nitride.

Temp (C)	Conv. (%)	C. Balan. (%)	CO_2 Sel. (%)	CO Sel. (%)	Meth. Sel (%)	Ethene Sel. (%)
375	0	100				
400	0.06	100.0	100			
425	0.10	99.8	100			
450	0.17	99.7	100			
475	0.16	99.9	100			
500	0.21	101.1	100			
525	0.24	99.4	100			
550	0.28	99.6	100			
575	3.90	98.2	67.4	7.1		25.5
600	14.30	97.9	16.9	20.4	1.25	61.5

Appendix D

5: Ethane oxidation

Table 5.2.2: Boron nitride supported 7 Wt % V catalyst.

Temp (C)	Conv. (%)	C. Balan. (%)	CO_2 Sel. (%)	CO Sel. (%)	Meth. Sel (%)	Ethene Sel. (%)
350	0	100				
375	0.04	100.0	100			
400	0.05	99.9	100			
425	0.06	99.8	100			
450	0.32	99.8	100			
475	1.03	99.2	100			
500	1.26	98.7	100			
525	1.90	98.6	14.2			85.8
550	2.25	98.7	9.8			90.2
575	5.63	97.8	9.4	4.1	0.48	86.0
600	21.82	97.1	17.7	25.6	4.91	51.8

Appendix D

5: Ethane oxidation

Table 5.2.3: Boron nitride supported 21 Wt % V catalyst.

Temp (C)	Conv. (%)	C. Balan. (%)	CO_2 Sel. (%)	CO Sel. (%)	Meth. Sel (%)	Ethene Sel. (%)
325	0	100				
350	0.24	99.8	100			
375	0.20	100.0	100			
400	0.11	10.2	100			
425	0.15	100.3	100			
450	0.39	100.2	100			
475	0.81	99.8	100			
500	1.83	99.8	100			
525	2.43	100.0	37.0			63.0
550	4.89	100.5	8.1		0.90	91.0
575	34.68	100.2	8.0		6.13	85.9

Appendix D

5: Ethane oxidation

Table 5.2.4: Boron nitride supported 35 Wt % V catalyst.

Temp (C)	Conv. (%)	C. Balan. (%)	CO_2 Sel. (%)	CO Sel. (%)	Meth. Sel (%)	Ethene Sel. (%)
350	0	100				
375	0.06	100.0	100			
400	0.14	100.0	100			
425	0.28	99.9	100			
450	0.41	99.8	100			
475	0.58	99.6	100			
500	1.20	99.0	100			
525	1.98	98.3	100			
550	4.95	98.3	8.9			91.09
575	19.94	93.4	6.5			93.50